

# **MACHINABILITY STUDIES ON 17-4 PH STAINLESS STEEL UNDER CRYOGENIC COOLING ENVIRONMENT**

Thesis

Submitted in partial fulfillment of the requirements for the degree of

**DOCTOR OF PHILOSOPHY**

by

**POTTA SIVAIAH**



DEPARTMENT OF MECHANICAL ENGINEERING  
NATIONAL INSTITUTE OF TECHNOLOGY KARNATAKA  
SURATHKAL, MANGALORE-575025

JULY, 2017

# DECLARATION

I hereby declare that the Research Thesis entitled “**Machinability studies on 17-4 PH stainless steel under cryogenic cooling environment**” which is being submitted to the **National Institute of Technology Karnataka, Surathkal** in partial fulfillment of the requirements for the award of the degree of **Doctor of Philosophy in Mechanical Engineering** is a *bonafide report of the research work carried out by me*. The material contained in this Research Thesis has not been submitted to any other Universities or Institutes for the award of any degree.

Register Number: **148039ME14F21**

Name of the Research Scholar: **POTTA SIVAIAH**

Signature of the Research Scholar:

Department of Mechanical Engineering

Place: NITK-Surathkal

Date:

# C E R T I F I C A T E

This is to certify that the Research Thesis entitled “**Machinability studies on 17-4 PH stainless steel under cryogenic cooling environment**” submitted by **Mr. Potta Sivaiah (Register Number: ME14F21)** as the record of the research work carried out by him, *is accepted as the Research Thesis submission* in partial fulfillment of the requirements for the award of the degree of **Doctor of Philosophy**.

Research Guide

**Dr. D. Chakradhar**

Assistant Professor

Department of Mechanical Engineering

**Chairman-DRPC**

Date:

*Dedicated to ...*

*My beloved parents  
and family members...*

*&*

*All of my Teachers and Colleagues  
who taught and encouraged me  
with positive thoughts...*

## ACKNOWLEDGEMENT

I am indebted to my supervisor **Dr. D. Chakradhar**, Assistant Professor, Department of Mechanical Engineering, National Institute of Technology Karnataka, Surathkal, for his excellent guidance and support throughout the research work. His constant encouragement, help and review of the entire work during the course of the investigation are invaluable.

I wish to thank Research Progress Assessment Committee members **Dr. M. R. Ramesh**, Assistant Professor, Department of Mechanical Engineering and **Dr. Narasimhadhan A. V.**, Assistant Professor, Department of Electronics and Communication Engineering for their unbiased appreciation and criticism all through this research work.

I wish to express my sincere gratitude to **Prof. G. C Mohan Kumar**, **Prof. Prasad Krishna** and **Prof. K. V Gangadharan**, for their valuable suggestions to do this research work.

I am immensely grateful to **Prof. Narendranath S**, Professor and Head, Department of Mechanical Engineering for extending the Departmental facilities, which ensured the satisfactory progress of my research work.

I would like to thank all the teaching and non-teaching staff members of the Department of Mechanical Engineering, of NITK Surathkal for their continuous help and support throughout the research work.

I wish to express my thanks to Prof. K. Narayan Prabhu, Professor of Metallurgical and Materials Department for permitting me to use the scanning electron microscope for characterization of specimen and I also express my gratitude to Dr. Uday Bhat, Associate Professor, Department of Metallurgical and Materials for

allowing me to use optical microscope instrument. I also thank Ms. Rashmi Banjan of Department of Metallurgical and Materials, for her support in connection with use of Scanning electron microscope.

I would like to thank CMTI Bangalore for research support during all years of my research. Especially, I would like to thank to Mr. Prakash Vinod, Head, Department of Precision Engineering for his encouragement. I also like to thank Mr. Basavarajappa for his support in connection with use of confocal microscope.

I owe my deepest gratitude to supporting staff of Department of Mechanical Engineering, Mr. Alexander D'Souza, Mr. Harish Chandra, Mr. Jaya Devadiga, Mr. Verghese, Mr. Pradeep and Mr. Sudhakar for their help during conducting experiments.

I thank the Director and the administration of NITK Surathkal for permitting me to pursue my research work at the Institute.

I would like to thank Dr. M. Pradeep Kumar, Associate professor, Department of Mechanical Engineering, Anna University, Chennai for allowing me to conduct trail experiments on cryogenic machining.

I would like to thank to my co-researchers and friends Mr. Venkatesh, Mr. Vinay verghese, Mr. Sachin, Mr. Bala Narasimha, Mr. Ajay Kumar, Mr. Keshav Rao, Mr. Balaji Mr. Naveen Kumar, Mr. Ramana Reddy, Mr. Veeresh Naik, Mr. Nithin Kumar for their kind help, encouragement for successful completion of this research work.

I would like to thank Dr. Manivannan, Research scholar, Anna University for their kind help and suggestions during trail experimental work.

I would like to thank Mangalore Chemicals and Fertilizers (MCF) Mangalore for supplying cryogenic coolant for my entire research work.

I am indebted to all my friends of Department of Mechanical Engineering and other Departments of NITK Surathkal for their constant help and encouragement during the entire this research work.

I would also like to share the happiest moment of my life with my respected parents. Their blessing, guidance and endeavour kept my moral high throughout the research work. I feel happy to express my sincere appreciation to all my family members, for their understanding, care, support and encouragement.

The list goes on and there are many others I should mention. There are people who have helped me all the way and provided me support when I didn't even realize I needed it, or needed it now, or needed it constantly. Listing all of them would fill a book itself, so I merely will have to limit myself to a few words: I THANK YOU ALL.....!

*(Potta Sivaiah)*

## ABSTRACT

17-4 precipitated hardened stainless steel (PH SS) is widely used in various areas including nuclear reactor components, marine constructions, jet engine parts, aircraft fittings, missile fittings, oil field valve parts and rotors of the centrifugal compressors owing to excellent properties like high corrosion resistance, high strength and good ductility. Productivity improvement while machining of 17-4 PH SS is a difficult work due to the limitation of higher cutting conditions. 17-4 PH SS material is treated as difficult to cut material due to formation of built up edges (BUE) on the cutting tool during machining and difficulty in chip control, which causes for poor surface quality as well as increases the number of tools required for machining. One of the methods to overcome above mentioned problems is to use of conventional coolants. But, in the recent years, environmental conscious regulations have become stringent in terms of disposal of chemically contaminated conventional coolants from the health and environmental safe prospective. Because of these reasons, nowadays, metal cutting industries are looking towards new sustainable machining method to reach the target set by the environmentally conscious regulations in terms of usage and disposal of chemical contaminant conventional coolants without sacrificing the productivity. Hence, the present work, focused on cryogenic machining which is recently developed eco-friendly as well as efficient cooling technology.

The present work is divided into three phases while machining of 17-4 PH SS. In the first phase, experiments were conducted based on the one factor at a time approach to study the individual effect of process parameters like cutting velocity, feed rate and depth of cut on performance characteristics like cutting temperature, tool flank wear, material removal rate (MRR), chip morphology and surface integrity (surface topography, surface finish, microhardness, white layer thickness) under various cooling environments like cryogenic (liquid nitrogen), minimum quantity lubrication (MQL), wet machining and dry conditions. It was found that as the cutting velocity, feed rate and depth of cut



increases, response like cutting temperature, flank wear and MRR were increased respectively under all the cooling environments. Whereas, in the case of surface roughness, decreasing trend was observed at the cutting velocity variation and increasing trend was found for feed rate and depth of cut variations conditions respectively. In overall, it was also evident from the experimental results that cryogenic machining significantly improved the machining performance and product performance all the cutting conditions. From result, it was found that cryogenic machining is selected as a best feasible machining method for 17-4 PH SS and it was selected for next phases of the work.

On the other way machining efficiency, quality of the product and machining cost highly depending on the selection of optimum machining conditions. In the second phase, Taguchi L<sub>9</sub> orthogonal array experimental design has been used for optimization of cutting conditions for single and multiple objective responses under the cryogenic cooling environment. Taguchi method was used for single response optimization and ANOVA was used to find the most influenced process parameters on each response. Gray relational analysis (GRA) and Technique for Order Preference by Similarity to Ideal Solution (TOPSIS) optimization techniques have been applied for multi response optimization, best multi optimization tool which suits for the current study have been selected through conformation tests. From the conformation test results, it was observed that Taguchi determined optimum cutting conditions significantly improved the turning performance characteristic during machining of 17-4 PH SS. Whereas, in the case of multi response optimization condition, GRA technique substantially improved the turning performance characteristic when compared to the TOPSIS technique.

In the third phase, correlation models were developed for modeling of cryogenic turning process by finding out the relation between the input process parameters and output responses using Response Surface Methodology (RSM) for cost effective research methodology. In additions to this, interaction effects of process parameters on turning performance characteristics were studied using 3D surface plots. From the modeling

conformation test results, it was observed that close agreement was found between the actual and predicted values. From interaction plots of surface roughness, it was observed that the high level of cutting velocity and low levels of feed rate and depth of cut could be contributed to generate lower surface roughness respectively. Whereas, from interaction plots of flank wear and MRR, it was found that the highest levels of process parameters could produce high flank wear and maximum MRR respectively.

**Keywords:** *17-4 PH SS, Sustainable machining, Environmental friendly machining, Cryogenic machining, MQL, Tool wear, Material removal rate, Chip morphology, Surface, integrity, Taguchi, optimization, Grey Relational Analysis, TOPSIS, Response Surface Methodology*

## CONTENTS

<i>Declaration</i>	
<i>Certificate</i>	
<i>Acknowledgements</i>	
<i>Abstract</i>	
<i>Contents</i>	<i>i</i>
<i>List of Figures</i>	<i>vii</i>
<i>List of Tables</i>	<i>xix</i>
<i>List of Symbols and Abbreviations</i>	<i>xvi</i>
<b>CHAPTER 1-INTRODUCTION</b>	<b>1</b>
1.1 HEAT GENERATION IN METAL CUTTING	1
1.2 EFFECT OF HIGH MACHINING ZONE TEMPERATURES	2
1.3 FACTORS INFLUENCING THE CUTTING TEMPERATURES	2
1.3.1 Workpiece and tool material	2
1.3.2 Process parameters	3
1.3.3 Tool geometry	3
1.3.4 Cutting coolants	3
1.4 COOLING TECHNIQUES FOR REDUCTION OF CUTTING TEMPERATURES	3
1.5 DIFFICULT TO CUT MATERIALS	7
1.6 CRYOGENIC COOLING	8
1.7 NEED FOR THE PRESENT STUDY	10
1.8 THESIS OUTLINE	11
<b>CHAPTER 2- LITERATURE REVIEW</b>	<b>13</b>
2.1 INTRODUCTION	13

2.2	CLASSIFICATION OF DIFFICULT TO CUT MATERIALS	13
2.3	MQL MACHINING OF DIFFICULT TO CUT MATERIALS	15
2.4	CRYOGENIC MACHINING OF DIFFICULT TO CUT MATERIALS	17
2.4.1	Origin of cryogenic material processing	17
2.4.2	Cryogenic cooling approach in machining	17
2.4.2.1	Cryogenic precooling of workpiece	17
2.4.2.2	Indirect cryogenic cooling	19
2.4.2.3	Cryogenic treatment	22
2.4.2.3	Cryogenic spray cooling	25
2.4.3	Effect of cryogenic jet cooling on cutting temperature, tool wear, surface roughness, cutting forces, coefficient of friction and chip morphology	26
2.4.4	Effect of cryogenic machining on surface integrity	35
2.5	OPTIMIZATION AND MODELING TECHNIQUES UNDER DIFFERENT COOLING ENVIRONMENTS	40
2.5.1	Single objective optimization using Taguchi technique	40
2.5.2	Multi objective optimization using GRA and TOPSIS	42
2.5.3	Optimization and modeling of machining process parameter using response surface methodology (RSM)	46
2.6	SUMMARY OF THE LITERATURE REVIEW ON CRYOGENIC MACHINING	54
2.7	MOTIVATION FROM LITERATURE REVIEW	54
1.9	OBJECTIVES OF THE PRESENT STUDY	56
	<b>CHAPTER 3-EXPERIMENTAL WORK</b>	<b>57</b>
3.1	WORK MATERIAL	57
3.2	DIFFERENT COOLING ENVIRONMENTS AND EXPERIMENTAL SETUPS	58

3.2.1	Cryogenic machining	58
3.2.2	Construction of cryogenic machining setup	59
3.2.3	MQL machining	61
3.2.4	Wet and dry machining	61
3.3	EXPERIMENTAL CONDITIONS	61
3.4	METHODOLOGY AND EXPERIMENTAL DESIGN	62
3.4.1	Methodology	62
3.4.2	EXPERIMENTAL DESIGNS	64
3.4.2.1	Taguchi orthogonal array (OA) design	64
3.4.2.2	One factor at a time approach (OFATA)	65
3.4.2.3	Response surface methodology (RSM)	65
3.5	MEASUREMENT OF PERFORMANCE CHARACTERISTICS	66
3.5.1	Cutting temperature	66
3.5.2	Surface roughness	67
3.5.2	Surface topography	68
3.5.3	Tool wear	69
3.5.4	Metal removal rate	69
3.5.5	Scanning electron microscope	70
3.5.7	Microhardness	71
3.5.8	White layer analysis	72
3.6	SUMMARY	72
	<b>CHAPTER 4 - ONE FACTOR AT A TIME APPROACH</b>	<b>73</b>
4.1	INTRODUCTION	73
4.2	EXPERIMENTAL PLAN	73
4.3	EFFECT OF COOLING ENVIRONMENT AND PROCESS PARAMETERS ON CUTTING TEMPERATURE	74

4.3.1	Effect of cooling environment and cutting velocity on cutting temperature	75
4.3.2	Effect of cooling environment and feed rate on cutting temperature	75
4.3.3	Effect of cooling environment and depth of cut on cutting temperature	76
4.4	EFFECT OF COOLING ENVIRONMENT AND PROCESS PARAMETERS ON TOOL FLANK WEAR	77
4.4.1	Effect of cooling environment and cutting velocity on flank wear	78
4.4.2	Effect of cooling environment and feed rate on flank wear	80
4.4.3	Effect of cooling environment and depth of cut on flank wear	82
4.5	EFFECT OF COOLING ENVIRONMENT AND PROCESS PARAMETERS ON MRR	85
4.6	EFFECT OF COOLING ENVIRONMENT AND PROCESS PARAMETERS ON CHIP MORPHOLOGY	86
4.6.1	Effect of cooling environment and cutting velocity on chip morphology	86
4.6.2	Effect of cooling environment and feed rate on chip morphology	89
4.6.3	Effect of cooling environment and depth of cut on chip morphology	92
4.7.1	Effect of cooling environment and cutting velocity on surface roughness	95
4.7.2	Effect of cooling environment and feed rate on surface roughness	98
4.7.3	Effect of cooling environment and depth of cut on surface roughness	100
4.8	EFFECT OF COOLING ENVIRONMENT AND PROCESS PARAMETERS ON SURFACE TOPOGRAPHY	101
4.8.1	Effect of cooling environment and cutting velocity on surface topography	101
4.8.2	Effect of cooling environment and feed rate on surface topography	104
4.8.3	Effect of cooling environment and depth of cut on surface topography	106

4.9	EFFECT OF MACHINING ENVIRONMENT AND PROCESS PARAMETERS ON MICROHARDNESS	108
4.10	EFFECT OF MACHINING ENVIRONMENT AND PROCESS PARAMETERS ON WHITE LAYER THICKNESS (WLT)	109
4.11	SUMMARY	113
	<b>CHAPTER-5-OPTIMIZATION OF CRYOGENIC TURNING PROCESS</b>	<b>115</b>
5.1	INTRODUCTION	115
5.2	EXPERIMENTAL PLAN	115
5.3	TAGUCHI TECHNIQUE (SINGLE OBJECTIVE OPTIMIZATION)	116
5.3.1	Selection of optimum cutting conditions	117
5.3.1.1	Surface roughness	117
5.3.1.2	Flank wear	118
5.3.1.3	Material removal rate (MRR)	119
5.3.2	Confirmation test	120
5.3.3	ANOVA results for surface roughness, flank wear and MRR	123
5.4	MULTI OBJECTIVE OPTIMIZATION TECHNIQUES	125
5.4.1	Taguchi based Grey relational analysis	125
5.4.1.1	Confirmation experiments	130
5.4.1.2	Analysis of variance (ANOVA)	131
5.4.2	Taguchi coupled technique for order preference by similarity to ideal solution (TOPSIS) method	132
5.4.2.1	Conformation test	137
5.5	COMPARISON OF CONFORMATION RESULTS OF TGRA AND TAGUCHI COUPLED TOPSIS TECHNIQUES	138
5.5.1	Taguchi based Grey relational analysis	138
5.5.2	Taguchi couple TOPSIS	138
5.6	SUMMARY	140

<b>CHAPTER 6 - MODELING OF CRYOGENIC TURNING PROCESS</b>	142
6.1 INTRODUCTION	142
6.2 EXPERIMENTATION	142
6.3 RESPONSE SURFACE METHODOLOGY (RSM)	144
6.4 RESULT AND DISCUSSIONS	145
6.4.1 Analysis of surface roughness (Ra)	145
6.4.1.1 Interaction effect of variables on surface roughness	150
6.4.2 Analysis of tool flank wear	151
6.4.2.1 Interaction effect of process variables on flank wear	156
6.4.3 Analysis of Material removal rate (MRR)	157
6.4.3.1 Interaction effect on MRR	162
6.5 CONFORMATION TEST FOR MODELING	164
6.6 SUMMARY	164
<b>CHAPTER 7 - CONCLUSIONS AND SCOPE OF FUTURE WORK</b>	166
7.1 CONCLUSIONS	166
7.2 SCOPE OF FUTURE WORK	168
REFERENCE	169
TECHNICAL PAPERS PUBLISHED	
BIO-DATA	



## LIST OF FIGURES

FIGURE NO.	DESCRIPTION	PAGE NO.
Figure 1. 1	Regions of heat generation zones in metal cutting.	1
Figure 1. 2	Different wear mechanisms (Kaynak et al., 2013).	4
Figure 1. 3	Different cooling techniques to reduce heat generation in metal cutting.	4
Figure 1. 4	Sustainable manufacturing techniques for cleaner production	6
Figure 1. 5	Characteristics of sustainable machining (Chetan et al., 2015).	6
Figure 1. 6	Nitrogen phase diagram (Pušavec et al., 2009).	9
Figure 1. 7	Comparison of productivity and manufacturing cost with cryogenic and emulsion cooling techniques (Hong and Broomer, 2000).	10
Figure 2. 1	Classification of difficult-to-machine materials (Shokrani et al., 2012).	13
Figure 2. 2	various tool failure mechanisms and their principle location on the worn tool	15
Figure 2. 3	Cryogenic precooling of workpiece (Hong and Ding, 2001).	18
Figure 2. 4	Application of LN <sub>2</sub> to tool back (Hong and Ding, 2001).	19
Figure 2. 5	(a) Tool cap (b) LN <sub>2</sub> reservoir (Wang and Rajurkar, 2000).	20
Figure 2. 6	(a) MHX (b) heat exchanger module (c) fabricated tool holder	21
Figure 2. 7	Schematic view of a cryogenic treatment process applied in a controlled manner (Akincioğlu et al., 2015).	22
Figure 2. 8	Sequentially temperature variation of cryogenic treatment process (Akincioğlu et al., 2015).	23
Figure 2. 9	Schematic diagram of LN <sub>2</sub> nozzle system (Hong and Ding, 2001).	25
Figure 2. 10	Details of modified tool holder for LN <sub>2</sub> cooling (Khan and Ahmed, 2008).	27

Figure 2. 11	Three different positions for applying liquid nitrogen cutting fluid a: on the tool face along the principal cutting edge, b: perpendicular to the principal cutting edge, c: from the bottom through the gap between the tool flank and the workpiece.	28
Figure 2. 12	Modified cutting tool for LN <sub>2</sub> supply at rake and flank face	29
Figure 2. 13	Effect of LN <sub>2</sub> on (a) Main cutting force (b) Surface roughness (c) Tool flank wear at varying cutting velocities and constant feed rate, depth of cut of 0.159 mm/rev, 1 mm respectively (Dhananchezian et al., 2011).	30
Figure 2. 14	Liquid nitrogen delivery nozzle (Venugopal et al., 2007b).	30
Figure 2. 15	LN <sub>2</sub> supply with SECO tool holder (Birmingham et al., 2011).	31
Figure 2. 16	Experimental setup for conventionally applied flood emulsion cooling (strategy A) and carbon dioxide snow cooling (strategy B) (MacHai and Biermann, 2011)	32
Figure 2. 17	Experimentally obtained white layer thickness (Umbrello et al., 2012).	37
Figure 2. 18	White layer in dry (a) an cryogenic machining (b): at $v = 75$ m/min, hardness = $61 \pm 1$ and chamfered tool (Umbrello et al., 2012).	37
Figure 2. 19	Surface topography and roughness of machined components a) Dry, b) MQL and c) Cryogenic at $v = 120$ m/min (Kaynak, 2014).	37
Figure 2. 20	Hardness measurements beneath the machined surface (profile), machined	39
Figure 3. 1	Microstructure and major elemental analysis of 17-4 PH SS workpiece	58
Figure 3. 2	Cryogenic machining experimental setup.	59
Figure 3. 3	Schematic view of cryogenic liquid nitrogen machining setup.	60
Figure 3. 4	Modified cap for TA 55 cryocan.	60
Figure 3. 5	MQL machining experimental setup.	61
Figure 3. 6	Machining zone at different environments (a) Cryogenic (b) MQL (c) Wet (d) Dry	62
Figure 3. 7	(a) PSBNR 2020 K12 Tool holder (b) AlTiN PVD coated cutting insert.	61

Figure 3. 8	Flow chart of the present work.	64
Figure 3. 9	Infrared thermometer.	67
Figure 3. 10	Surface roughness tester.	67
Figure 3. 11	Laser optical confocal microscope.	69
Figure 3. 12	Optical microscope.	69
Figure 3. 13	Weighing scale.	70
Figure 3. 14	Scanning electron microscopy.	71
Figure 3. 15	Microhardness tester.	71
Figure 4. 1	Effect of (a) Cutting velocity (b) Feed rate and (c) Depth of cut on cutting temperature under different cutting environments by keeping all other variables as constant at their respective mean levels.	74
Figure 4. 2	Effect of (a) Cutting velocity (b) Feed rate and (c) Depth of cut on flank wear under different cutting environments by keeping all other variables as constant at their respective mean levels.	77
Figure 4. 3	SEM images of tool flank wear at $v = 25$ m/min, $f = 0.143$ mm/rev and $d = 1$ mm under different cooling environments (a) Cryogenic (b) MQL (c) Wet (d) Dry	79
Figure 4. 4	SEM images of tool flank wear at $v = 132$ m/min, $f = 0.143$ mm/rev and $d = 1$ mm under different cooling environments (a) Cryogenic (b) MQL (c) Wet (d) Dry.	80
Figure 4. 5	SEM images of tool flank wear at $v = 55$ m/min, $f = 0.048$ mm/rev and $d = 1$ mm under different cooling environments (a) Cryogenic (b) MQL (c) Wet (d) Dry	81
Figure 4. 6	SEM images of tool flank wear at $v = 55$ m/min, $f = 0.238$ mm/rev and $d = 1$ mm under different cooling environments (a) Cryogenic (b) MQL (c) Wet (d) Dry	82
Figure 4. 7	SEM images of tool flank wear at $v = 78.5$ m/min, $f = 0.143$ mm/rev and $d = 0.2$ mm under different cooling environments (a) Cryogenic (b) MQL (c) Wet (d) Dry.	84
Figure 4. 8	SEM images of tool flank wear at $v = 78.5$ m/min, $f = 0.143$ mm/rev and $d = 1.4$ mm under different cooling environments (a) Cryogenic (b) MQL (c) Wet (d) Dry.	84

Figure 4. 9	Effect of (a) Cutting velocity (b) Feed rate and (c) Depth of cut on MRR under different cutting environments by keeping all other variables as constant at their mean levels.	85
Figure 4. 10	Form of chips generated at $v = 25$ m/min, $f = 0.143$ mm/rev and $d = 1$ mm under different cooling environments (a) Cryogenic (b) MQL (c) Wet (d) Dry.	88
Figure 4. 11	Form of chips at $v = 132$ m/min, $f = 0.143$ mm/rev and $d = 1$ mm under different cooling environments (a) Cryogenic (b) MQL (c) Wet (d) Dry.	88
Figure 4. 12	Microscopic images of chips at $v = 132$ m/min, $f = 0.143$ mm/rev and $d = 1$ mm under different cooling environments (a) Cryogenic (b) MQL (c) Wet (d) Dry.	89
Figure 4. 13	Form of chips generated at $v = 55$ m/min, $f = 0.048$ mm/rev and $d = 1$ mm under different cooling environments (a) Cryogenic (b) MQL (c) Wet (d) Dry.	90
Figure 4. 14	Form of chips generated at $v = 55$ m/min, $f = 0.238$ mm/rev and $d = 1$ mm under different cooling environments (a) Cryogenic (b) MQL (c) Wet (d) Dry.	91
Figure 4. 15	Microscopic images of chips at $v = 55$ m/min, $f = 0.238$ mm/rev and $d = 1$ mm under different cooling environments (a) Cryogenic (b) MQL (c) Wet (d) Dry.	91
Figure 4. 16	Chip forms generated at $v = 78.5$ m/min, $f = 0.143$ mm/rev and $d = 0.2$ mm under different cooling environments (a) Cryogenic (b) MQL (c) Wet (d) Dry.	93
Figure 4. 17	Chip forms generated at $v = 78.5$ m/min, $f = 0.143$ mm/rev and $d = 1.4$ mm under different cooling environments (a) Cryogenic (b) MQL (c) Wet (d) Dry.	93
Figure 4. 18	Effect of (a) Cutting velocity (b) Feed rate and (c) Depth of cut on surface roughness under different cutting environments by keeping all other variables as constant at their mean levels.	95
Figure 4. 19	Microscopic images of chips at $v = 78.5$ m/min, $f = 0.143$ mm/rev and $d = 1.4$ mm under different cooling environments (a) Cryogenic (b) MQL (c) Wet (d) Dry.	94
Figure 4. 20	SEM images of machined surfaces at $v = 25$ m/min, $f = 0.143$ mm/rev and $d = 1$ mm under different cooling environments (a) Cryogenic (b) MQL (c) Wet (d) Dry.	97

Figure 4. 21	SEM images of machined surfaces at $v = 132$ m/min, $f = 0.143$ mm/rev and $d = 1$ mm under different cooling environments (a) Cryogenic (b) MQL (c) Wet (d) Dry.	97
Figure 4. 22	SEM images of surface morphology at $v = 55$ m/min, $f = 0.048$ mm/rev and $d = 1$ mm under different cooling environments (a) Cryogenic (b) MQL (c) Wet (d) Dry.	99
Figure 4. 23	SEM images of surface morphology at $v = 55$ m/min, $f = 0.238$ mm/rev and $d = 1$ mm under different cooling environments (a) Cryogenic (b) MQL (c) Wet (d) Dry.	100
Figure 4. 24	SEM images of surface morphology at $v = 55$ m/min, $f = 0.143$ mm/rev and $d = 0.2$ mm under different cooling environments (a) Cryogenic (b) MQL (c) Wet (d) Dry.	102
Figure 4. 25	SEM images of surface morphology at $v = 55$ m/min, $f = 0.143$ mm/rev and $d = 1.4$ mm under different cooling environments (a) Cryogenic (b) MQL (c) Wet (d) Dry.	102
Figure 4. 26	SEM images of surface topography at $v = 25$ m/min, $f = 0.143$ mm/rev and $d = 1$ mm under different cooling environments (a) Cryogenic (b) MQL (c) Wet (d) Dry	103
Figure 4. 27	SEM images of surface topography at $v = 132$ m/min, $f = 0.143$ mm/rev and $d = 1$ mm under different cooling environments (a) Cryogenic (b) MQL (c) Wet (d) Dry.	104
Figure 4. 28	3D images of surface topography at $v = 55$ m/min, $f = 0.048$ mm/rev and $d = 1$ mm under different cooling environments (a) Cryogenic (b) MQL (c) Wet (d) Dry.	105
Figure 4. 29	3D images of surface topography at $v = 55$ m/min, $f = 0.238$ mm/rev and $d = 1$ mm under different cooling environments (a) Cryogenic (b) MQL (c) Wet (d) Dry.	106
Figure 4. 30	3D surface topography at $v = 78.5$ m/min, $f = 0.143$ mm/rev and $d = 0.2$ mm under different cooling environments (a) Cryogenic (b) MQL (c) Wet (d) Dry.	107
Figure 4. 31	3D surface topography at $v = 78.5$ m/min, $f = 0.143$ mm/rev and $d = 1$ mm under different cooling environments (a) Cryogenic (b) MQL (c) Wet (d) Dry	107
Figure 4. 32	Method of sample preparation and measurement of microhardness.	108
Figure 4. 33	Subsurface microhardness profiles of machined samples at various machining conditions.	108
Figure 4. 34	Cross-sectional microstructure after (a) cryogenic and (b) MQL (c) Wet (d) Dry machining at $v = 132$ m/min, $f = 0.143$ mm/rev	

	and $d = 1$ mm.	110
Figure 4. 35	Effect of cooling environment on white layer thickness at $v = 132$ m/min, $f=0.143$ mm/rev and $d = 1$ mm.	110
Figure 4. 36	SEM images of white layer thickness at $v = 132$ m/min, $f=0.143$ mm/rev and $d = 1$ mm under different cooling environments (a) Dry (b) Wet (c) MQL (d) Cryogenic.	111
Figure 4. 37	EDAX analysis of 17-4 PH SS (a) At polished surface (b) At white layer surface.	112
Figure 5. 1	Mean S/N ratio of surface roughness.	118
Figure 5. 2	Mean S/N ratio of tool flank wear.	119
Figure 5. 3	Mean S/N ratio of MRR.	120
Figure 5. 4	SEM images of the machined surface at (a) Initial parameter settings at $v = 85$ m/min, $f = 0.143$ mm/rev, $d = 0.6$ mm and MQL environment ( $v_2 - f_2 - d_2$ ) (b) Taguchi optimum settings at $v = 132$ m/min, $f = 0.048$ mm/rev, $d = 0.6$ mm ( $v_3 - f_1 - d_2$ ).	123
Figure 5. 5	SEM images of the tool flank wear at (a) Initial parameter settings at $v = 85$ m/min, $f = 0.143$ mm/rev, $d = 0.6$ mm ( $v_2 - f_2 - d_2$ ) (b) Taguchi optimum settings at $v = 25$ m/min, $f = 0.048$ mm/rev, $d = 0.2$ mm ( $v_1 - f_1 - d_1$ ).	123
Figure 5. 6	Means of S/N ratios of grey relation grades.	130
Figure 5. 7	Means of S/N ratios of closeness efficient.	136
Figure 6. 1	Normal probability plot for surface roughness.	149
Figure 6. 2	Plot of residual Vs. predicted for surface roughness.	149
Figure 6. 3	3D surface interaction plot in feed rate and cutting velocity for Surface roughness.	150
Figure 6. 4	3D surface interaction plot in depth of cut and cutting velocity for surface roughness.	151
Figure 6. 5	Normal probability plot for flank wear.	155
Figure 6. 6	Plot of residual Vs. predicted for flank wear.	155
Figure 6. 7	3D surface interaction plot in depth of cut and cutting velocity for flank wear.	156

Figure 6. 8	3D surface interaction plot in depth of cut and feed rate for flank wear.	157
Figure 6. 9	Normal probability plot for MRR.	161
Figure 6. 10	Plot of residual Vs. predicted for MRR.	161
Figure 6. 11	3D surface interaction plot in feed rate and cutting velocity for MRR.	162
Figure 6. 12	3D surface interaction plot in depth of cut and cutting velocity for MRR.	163
Figure 6. 13	3D surface interaction plot in depth of cut and feed rate for MRR.	163

## LIST OF TABLES

TABLE NO.	DESCRIPTION	PAGE NO.
Table 1. 1	Cutting fluid consumption and their associate costs.	5
Table 2. 1	Contributions of earlier researchers on difficult to cut materials during turning with cryogenic jet cooling method.	50
Table 2. 2	Literature report available on optimization and techniques during turning of different materials under environments.	52
Table 3. 1	Chemical composition of 17-4 PH stainless steel.	58
Table 3. 2	Mechanical properties of 17-4 PH stainless steel.	58
Table 3. 3	Experimental conditions.	63
Table 3. 4	Taguchi L <sub>9</sub> orthogonal array design.	65
Table 3. 5	One factor at a time approach experimental design.	66
Table 3. 6	RSM based L <sub>20</sub> central composite design (CCD).	68
Table 4. 1	Cryogenic turning process parameters and their levels for OFATA.	74
Table 5. 1	Cryogenic turning process parameters and their levels for optimization study.	116
Table 5. 2	Plan of experiments, experimental results and their calculated S/N ratios.	117
Table 5. 3	Mean S/N ratio response table for surface roughness.	118
Table 5. 4	Mean S/N ratio response table for tool flank wear.	119
Table 5. 5	Mean S/N ratio response table for MRR.	120
Table 5. 6	Conformation test results for surface roughness.	122
Table 5. 7	Conformation test results for tool flank wear.	122
Table 5. 8	Conformation test results for MRR.	122



Table 5. 9	ANOVA of S/N ratio of surface roughness.	124
Table 5. 10	ANOVA of S/N ratios of flank wear.	124
Table 5. 11	ANOVA of S/N ratio of MRR.	125
Table 5. 12	Performance characteristics GRC, GRG, S/N ratio and its order.	128
Table 5. 13	S/N Response table for grey relational grade.	129
Table 5. 14	Results of cutting performance at conformation test.	131
Table 5. 15	ANOVA of grey relational grade	132
Table 5. 16	Normalized data, weighted normalized data, separation measures.	133
Table 5. 17	Closeness coefficients and S/N ratio.	136
Table 5. 18	Response table for S/N ratios of closeness coefficient.	136
Table 5. 19	Conformation test results for optimization.	137
Table 5. 20	Comparison of conformation results of TGRA and TOPSIS techniques.	139
Table 6. 1	Process parameters and their levels.	142
Table 6. 2	RSM experimental design (L <sub>20</sub> ) and results.	143
Table 6. 3	ANOVA for response surface quadratic model (Response: Ra).	147
Table 6. 4	ANOVA for response surface reduced quadratic model (Response: Ra).	148
Table 6. 5	ANOVA for response surface quadratic model (Response: Flank wear)	153
Table 6. 6	ANOVA for response surface reduced quadratic model (Response: Vb).	154
Table 6. 7	ANOVA for response surface quadratic model (Response: MRR).	159
Table 6. 8	ANOVA for response surface reduced quadratic model (Response: MRR).	160
Table 6. 9	Conformation test results for modeling.	164

## LIST OF SYMBOLS AND ABBREVIATIONS

COSHH	: Control of Substances Hazardous to Health
MWF	: Metal Working Fluids
TRGS	: Technical Code of Practice for Hazardous Substances
NIOSH	: The National Institute for Occupational Safety and Health
OHSAS	: Occupational Health and Safety Assessment Series
PH SS	: Precipitated Hardenable Stainless Steel
LN <sub>2</sub>	: Liquid Nitrogen
OFATA	: One Factor At a Time Approach
R <sub>a</sub>	: Average Surface Roughness
V <sub>b</sub>	: Flank Wear
MRR	: Material Removal Rate
SEM	: Scanning Electron Microscope
XRD	: X-Ray Diffraction
MQL	: Minimum Quantity Lubrication
BUE	: Built-Up-Edge
WLT	: White Layer Thickness
EDS	: Energy Dispersive X-Ray Spectroscopy
TGRA	: Taguchi based Gray Relational Analysis
TOPSIS	: Technique for Order Preference by Similarity to Ideal Solution
ANOVA	: Analysis Of Variance
RSM	: Response Surface Methodology
CCD	: Central Composite Design

ANOVA	: Analysis of variance
GRA	: Gray Relational Analysis
CRMQL	: Cryo Minimum Quantity Lubrication
MADM	: Multi attribute Decision Methods
ELECTRE	: Elimination and Choice Translating Reality
AHP	: Analytic Hierarchy Process
PROMOTHEE	: Preference Ranking Organization Method for Enrichment Evaluation
GA	: Genetic Algorithm
PSO	: Particle Swarm Optimization
EDM	: Electric Discharge Machining
AJM	: Abrasive Jet Machining
DCT	: Deep Cryogenic Treatment
IC	: Integrated Circuit
$v$	: Cutting velocity
$f$	: Feed rate
$d$	: Depth of cut
$R^2$	: Determination Coefficient
DOF	: Degree of Freedom

## CHAPTER 1

### INTRODUCTION

#### 1.1 HEAT GENERATION IN METAL CUTTING

In metal cutting processes, machining is one of the most useful metals shaping process. Many industries are using difficult-to-cut materials; therefore it is necessary to improve the productivity of products from these materials without compromising the quality with reduced environmental impact and cost. Many non conventional machining processes (Li et al., 2015; Liu et al., 2015) were used to machine difficult to cut materials but these have limitation in its productivity owing to lower material removal rate (MRR) and high machining cost. Generally conventional turning process offers higher speeds and feed rates to improve the productivity but generates more machining zone temperatures (Sharma et al., 2009). Figure 1.1 shows the different heat generation zones during metal cutting process. There are three cutting generation zones during machining namely primary zone, secondary zone and tertiary zone respectively.

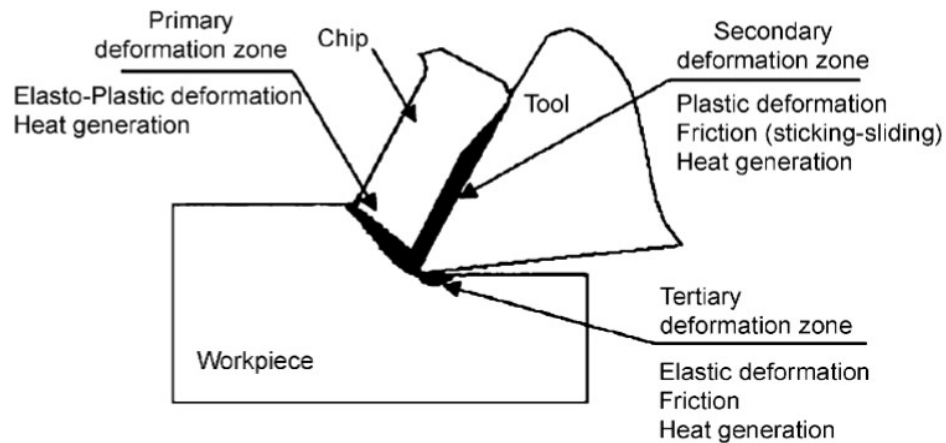


**Figure 1.1** Regions of heat generation zones in metal cutting

(Abukhshim et al., 2006).

Primary heat zone is due to the shearing and plastic deformation of metal. Secondary heat zone is due to the tool-chip sliding contact and secondary deformation. Tertiary heat zone is due to the rubbing action between the tool and workpiece. During machining, at high cutting conditions severe plastic deformation occurs at the primary zone and develops more friction at the secondary zone due to the sliding contact between the tool and workpiece causes more heat generation at the machining zone. It was reported that the approximate heat dissipation by the chip, tool and workpiece was 70 %, 20 % and 10 % respectively (Shaw, 1984).

## **1.2 EFFECT OF HIGH MACHINING ZONE TEMPERATURES**

As the machining zone temperatures rises more thermal stresses act on the cutting tool, these leads to thermal softening of cutting tool resulting in failure of tool (Zhao et al., 2002). The tool-chip interface temperatures significantly affect the tool life. Tool failure is contributed due to the adhesion, thermal damage (plastic deformation, thermal diffusion and chemical reaction), mechanical damage (abrasion, chipping, fracture and fatigue) as shown in Figure 1.2. The higher cutting zone temperatures show significant effect on turning performance characteristics like poor quality of the machined surface, low tool life, poor dimensional accuracy and non beneficial subsurface characteristics. As tool wear increases, tool geometry damages causes generation of more chatters results in more tool wear marks on the machined surface hence poor dimensional accuracy (Dhar et al., 2001). Also, more tool wear badly affects the surface integrity characteristics (Kaynak et al., 2014).

## **1.3 FACTORS INFLUENCING THE CUTTING TEMPERATURES**

### **1.3.1 Workpiece and tool material**

Workpiece and tool material mechanical, thermal properties significantly affect the machining zone temperatures. As the tool and workpiece material hardness increases then cutting zone temperatures rise more during machining and vice versa. Likewise, as the thermal conductivity of tool and workpiece material increases then cutting zone temperatures decreases and vice versa.

### **1.3.2 Process parameters**

In turning operation, the process parameters like cutting velocity, feed rate and depth of cut significantly affect the cutting temperatures. The cutting temperature rises with a rise in aforementioned cutting parameters (Shaw, 1984).

### **1.3.3 Tool geometry**

Tool geometry substantially affects the machining zone temperatures. As the negative rake angle rises then the tool contact area increases correspondingly results in rise in cutting zone temperatures. Likewise, the cutting temperatures increases with the rise in approx angle because chip thickness increases for the same feed rate and depth of cut. Similarly, the cutting zone temperatures increases with increase in tool nose radius (MacHai and Biermann, 2011; Manivel and Gandhinathan, 2016; Kirby et al., 2006).

### **1.3.4 Cutting coolants**

Cutting fluids significantly control the machining zone temperatures but the level of control of temperatures completely depends on the cutting conditions levels. Effectiveness of cutting temperature control decreases while the cutting conditions levels increases (Dhananchezian et al., 2011).

## **1.4 COOLING TECHNIQUES FOR REDUCTION OF CUTTING TEMPERATURES**

Reducing the machining zone temperature in tiny amount will leads to improved tool life. MRR is one of the deciding factors for the machining cost. MRR increases then more generation of friction and heat at the machining zone this leads to shortening of tool life hence machining cost increases (Kalyan and Choudhury, 2008). To overcome this problem, many researchers have attempted several cooling techniques to cool the machining zone temperatures as shown in Figure 1.3. For many years, machining industries are using conventional fluid cooling at the machining zone to overcome the temperature raises (Baradie, 1996a). However it was found that flood cooling technique not able to reduce the cutting temperature at tool-chip interface at higher cutting speeds (Shaw et al., 1951; Cassin and Boothroyd, 1965).

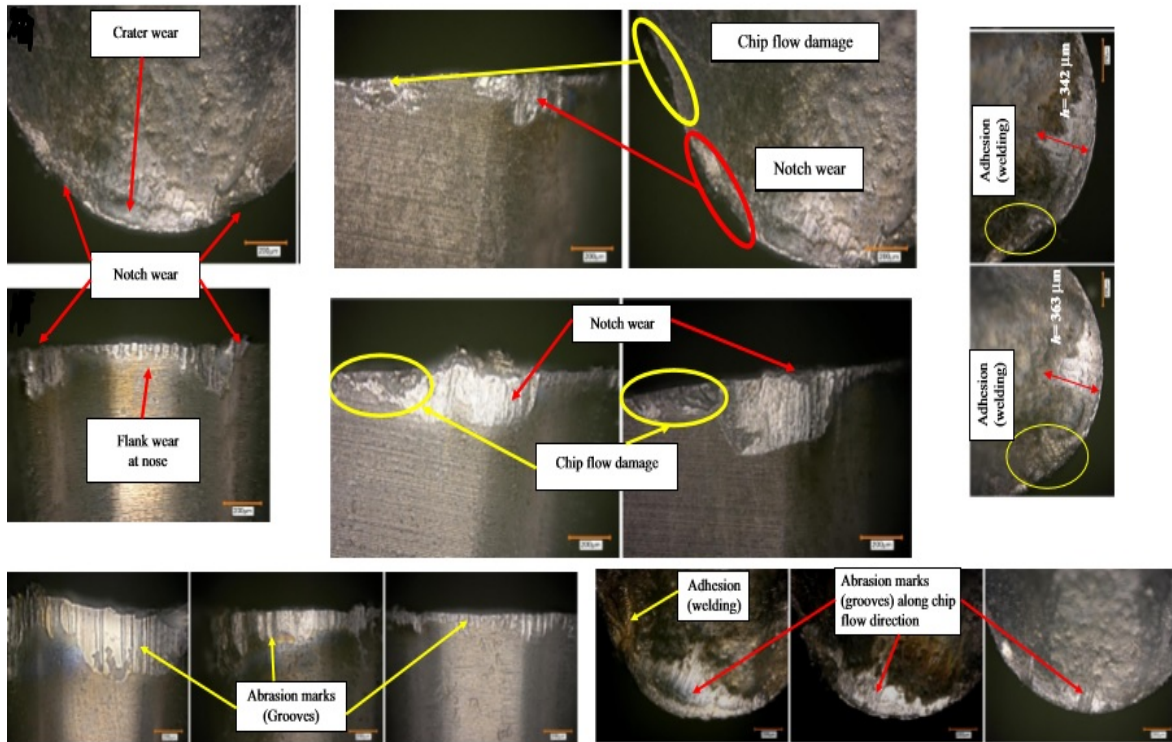


Figure 1. 2 Different wear mechanisms (Kaynak et al., 2013).

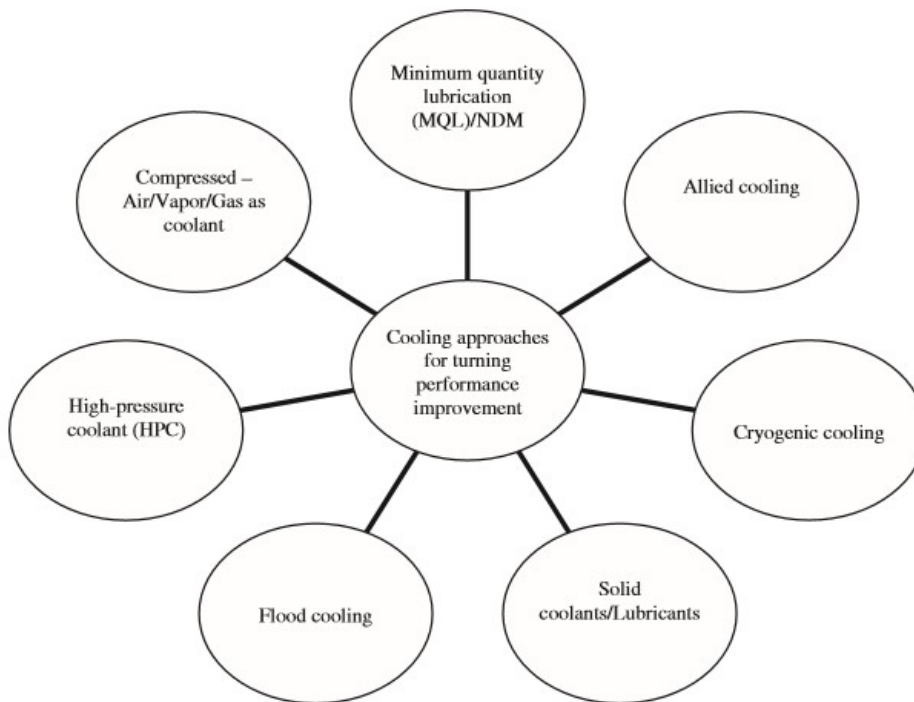


Figure 1. 3 Different cooling techniques to reduce heat generation in metal cutting.

and conventional cutting fluids are chemical contaminants causes several health, environmental problems and additional disposal cost (Baradie, 1996b). It has been reported that approximately 1 million workers are exposed to coolant in U.S (Shaw, 1984; Chetan et al., 2015). Table 1.1 shows the yearly consumption of cutting fluid and their associate costs in various countries and regions.

**Table 1. 1** Cutting fluid consumption and their associate costs.

<b>Country name</b>	<b>Cutting fluid consumption</b>	<b>Purchasing and disposing cost</b>	<b>Reference</b>
United states	100 million gallons per year	48 billion dollars a year	(Feng and Hattori, 2000)
Germany	75,500 tons a year	1 billion German Mark	(Klocke and Eisenblätter, 1998)
Japan		71billion Japanese Yen a year (in this 42 billion Yen purchasing cost)	(Feng and Hattori, 2000)
the European Union alone	320 million tons		(Lawal et al., 2012)
The Asia-Pacific region	891,330 tons		(Lahiri N.D.)
Turkey	272,48200litres		(Shokrani et al., 2012)

It is expected that the annual usage of metal working fluids (MWFs) across the world is a grand total of 640 million gallons (Brockhoff and Walter, 1998). It is predicted that the associated costs related to cutting fluids are in the range of 20-30 % of the total manufacturing costs while machining of hard-to-cut group materials (Pusavec et al., 2010). Usage of cutting fluids additionally includes the maintenance and disposal cost and it can be up to 2 to 4 times of their purchase price (Chetan et al., 2015). This issue has been supported through the introduction of environmentally conscious regulations such as the Control of Substances Hazardous



to Health (COSHH) in U.K and the Technical Code of Practice for Hazardous Substances (TRGS) in Germany (Shokrani et al., 2012), The National Institute for Occupational Safety and Health (NIOSH) and ISO 14001 (Marksberry, 2007), OHSAS 18001 Occupational Health and Safety Assessment Series and many international global standards like ISO 9000,14000,14001 (Rao, 2011) restricted the metal cutting industries in terms of usage and disposal of conventional cutting fluids due to the health hazardous and environmental pollution impact. Because of these drawbacks, recently researchers have concentrated on different sustainable manufacturing processes as shown in Figure 1.4. The characteristics of the sustainable machining process are shown in Figure 1.5.

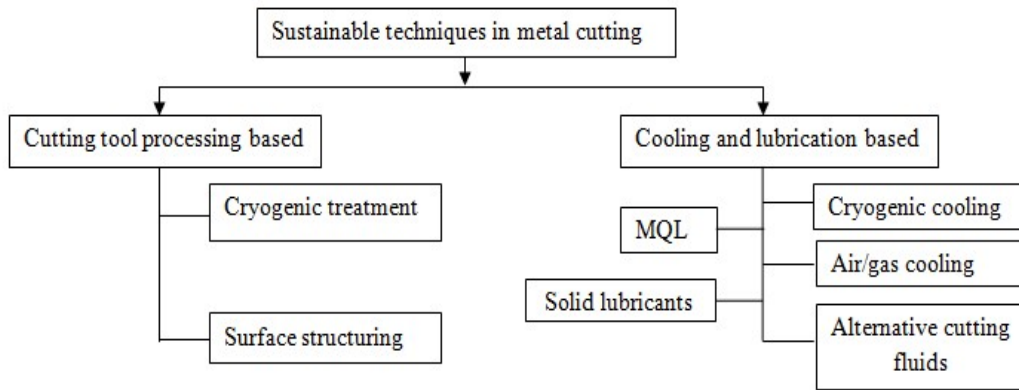


**Figure 1. 4** Sustainable manufacturing techniques for cleaner production (Chetan et al., 2015).

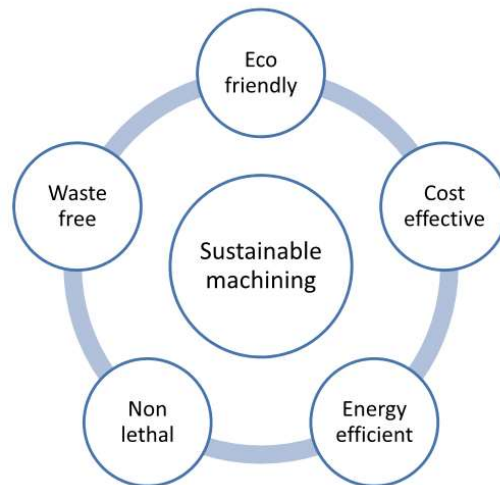


**Figure 1. 5** Characteristics of sustainable machining (Chetan et al., 2015).

MQL is one of alternative method i.e., supplying the coolant at the tool-chip interface at 50-500 ml/hr. Consumption of cutting fluid in MQL was 10000 times lesser than the conventional cooling method (Dhar et al., 2006). Aoyama et al. (2008) have reported that MQL machining is not feasible for industrial machining conditions because it fails to remove the chips at the cutting zone and creates health problems to the machinist due to the presence of oil mist at working environment. Chetan et al. (2015) reviewed the different sustainable machining techniques and discussed the advantages and disadvantages of different sustainable machining techniques. It was reported that air/gas cooling technique requires special cooling equipment as well as air/gas coolants inactive in controlling the machining zone temperatures during machining of super alloys. Likewise, solid lubrication cooling technique is a costly due to involvement of more production cost for solid lubricants and requirement of special equipments for supplying the solid lubricants. Alternative coolants like vegetable oil and ionic liquids are biodegradable but these are costly when these applied in flood cooling technique. Also, vegetable fluids have very poor thermal stability results in not able to control the machining zone temperatures.

### **1.5 DIFFICULT TO CUT MATERIALS**

Difficult-to-machine materials are referred to the materials which produce excessive tool wear, heat and/or cutting forces, difficulties in chip formation and/or poor surface quality during machining operations. These effects are due to the high strength, corrosive resistance, high hardness and low thermal conductivity. Because of these attractive properties these have applications in the field of industries like aerospace, chemical, nuclear, marine etc., (Shokrani et al., 2012).

Among all the difficult to cut materials, the demand for the steel materials have been increasing due to various applications like gears, helicopter camshaft gears, shafts bushes, hub units, dies, punches, nuts, bolts, jet engine mountings, fuel injector nozzles and turbine blades etc., (Chinchanikar and Choudhury, 2015). Especially applications of precipitated hardened stainless steel materials have many applications due to their peculiar mechanical properties. These steels can with stand their strength

up to 315 °C temperatures due to reason this material has been used to produce the actuator parts used for modern fighter aircrafts (Kumar et al., 2013).

Nowadays, the demand for high corrosion resistance and high strength materials has been increasing more in many industries. 17-4 PH SS is one of the high corrosion resistance and high strength material due to the major presence of 17 % chromium and 4 % nickel in its chemical constituents. Because of these favorable properties, this material is having many applications in aerospace, nuclear, chemical and marine fields (Kochmański and Nowacki, 2006). Machining of this kind of material under the dry environment leads to poor surface quality and more machining cost (Mohanty et al., 2015).

## **1.6 CRYOGENIC COOLING**

‘Cryogenic’ means use of metals at low temperatures below -150 °C. Cryogenic machining is an environmental friendly process and it was introduced in 1969 by Uehara and Kumagai. Commonly used potential cryogenic coolants in machining are liquid nitrogen (LN<sub>2</sub>) and liquid carbon dioxide (LCO<sub>2</sub>). LCO<sub>2</sub> creates oxygen deficiency problems for the operator at the working environment during machining because it is heavier than air and could cause CO<sub>2</sub> accumulation. Hence, in the present study, the external cryogenic cooling method was used with LN<sub>2</sub>. LN<sub>2</sub> is lighter than air and no accumulation of LN<sub>2</sub> occurs at the shop floor. Figure 1.6 depicts the phase diagram of nitrogen and triple point of nitrogen occurs at 12.463 Pa atmospheric pressure and temperature of 63.15 K. The melting and boiling points for the nitrogen are 63.3 K and 77.4 K respectively (-210 °C and -196 °C). Therefore liquid nitrogen causes for low temperatures where it delivered. 78 % of human inhale consists of nitrogen and liquid nitrogen can easily evaporate therefore no environmental pollution effect, it could avoid disposal cost, chip cleaning cost and health problems.

Many researchers have used the LN<sub>2</sub> as a cutting fluid to reduce the machining zone temperatures. LN<sub>2</sub> substantially reduces the temperatures at tool-chip interface during machining and produces a much lower friction coefficient (Hong et al., 2002). In

metal cutting applications, cutting forces has a vital impact on the generation of cutting temperatures and surface finish.

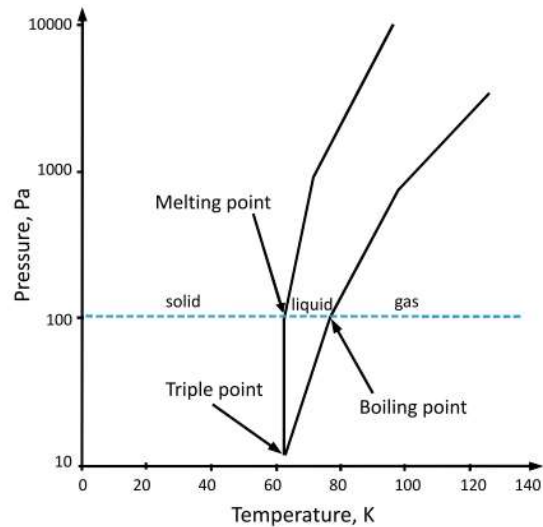


**Figure 1. 6** Nitrogen phase diagram (Pušavec et al., 2009).

Dhananchezian et al. (2011) used cryogenic spray cooling method in machining of AISI 304 material and observed 16 % reduction in cutting forces compared to flood machining due to the cushioning effect provided by the liquid nitrogen at the tool-workpart contact. Gupta et al. (2015) conducted experiments on AISI 1040 Steel in turning and observed low cutting forces, tool wear and surface rough in cryogenic machining. Bordin et al. (2015) observed low tool wear and low surface roughness in cryogenic machining compared to dry machining during machining of titanium alloy. Klocke et al. (2013) observed lower tool wear, lower cutting forces, reduced surface roughness and improved chip morphology in cryogenic machining compared wet, minimum quantity lubrication (MQL) machining conditions due to substantial reduction of the cutting temperatures. Hence, cryogenic machining increases the productivity and quality of the product in machining of gamma titanium aluminides compared to the other wet, MQL machining. Hong and Broomer (2000) carried out economical and ecological study in cryogenic turning of AISI 304 grade material and concluded that cryogenic machining is more profitable and helps to reach greater productivity compared to emulsion cooling, without health and environmental

concerns. Figure 1.7 depicts the comparison of productivity and manufacturing cost with cryogenic and emulsion cooling techniques.

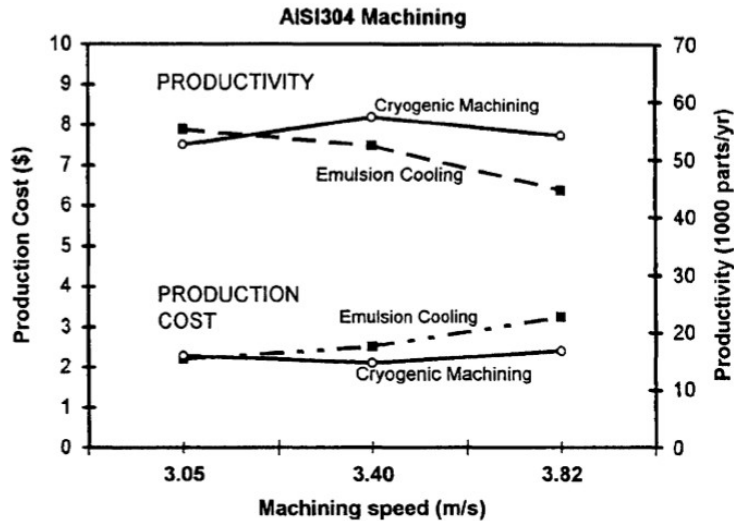


**Figure 1. 7** Comparison of productivity and manufacturing cost with cryogenic and emulsion cooling techniques (Hong and Broomer, 2000).

### 1.7 NEED FOR THE PRESENT STUDY

Tool wear is the natural phenomena observed during machining process and it has more impact on the product performance. Nowadays, metal cutting industries demanding improved productivity but it requires higher cutting conditions. However, machining at higher cutting conditions develops more tool wear resulting in poor product performance. Machinability of 17-4 PH stainless steel is poor because of difficult control of chip, more built-up-edge formation on tool and more abrasive wear, which causes for poor surface quality as well as increases number of tools required (Mohanty et al., 2015). Metal cutting industries have restrictions in usage and disposal of conventional coolants due to strict environmental conscious regulations in prospective of health and environmental issues (Baradie, 1996b; Hong and Broomer, 2000). Nowadays, for metal cutting industries, coupling of these environmental regulations into a management system is one of the major strategic challenges. For these reasons, many industries looking for an alternatives cooling techniques which can avoid the low productivity, health and environmental damage problems.

Cryogenic machining is an efficient, eco-friendly manufacturing process. However, few researchers have worked with various kinds of hard to cut materials like smart materials, super alloys and steels by using LN<sub>2</sub> as a coolant. In the literature not much work was reported on the surface integrity characteristics. 17-4 PH SS have many applications in various emerging fields, so there is a necessity to carry out the extensive experimental investigation on it. Hence, selection of suitable machining technique for machining of 17-4 PH SS need to be identified for improving the product performance. Still, no report was found in the literature on feasibility checking of cryogenic, MQL, wet and dry cooling environments for turning of 17-4 PH SS. In the present thesis an attempt was made to select the feasible machining technique for machining 17-4 PH SS. It is expected that cryogenic machining produces the products with high fatigue strength for improving the product life.

## **1.8 THESIS OUTLINE**

To select the feasible machining technique for machining 17-4 PH SS, the present thesis has been divided into seven chapters as follows:

**CHAPTER 1** explains the basics in metal cutting, temperature issues, factors influencing the temperatures in turning process, various cooling method to overcome the high temperatures in metal cutting, difficult to cut materials, various problems in different sustainable machining processes, cryogenic machining, need of a present work and outline of the thesis.

**CHAPTER 2** discusses the different kinds of cryogenic machining methods, their advantages and disadvantages, literature on effect of cryogenic spray cooling method on different performance characteristics during machining of various kinds of difficult to cut materials in different manufacturing processes, literature on optimization and modeling under different cooling environments, scope and objectives of the present work.

**CHAPTER 3** gives the details about the workpiece material, cutting tools, tool holder, different experimental designs, methodology, experimental setups used in the

present work and different equipments used for measuring the different turning performance characteristics and their procedure. In the thesis results like cutting temperature, tool flank wear, MRR, chip morphology and surface integrity (surface topography, surface finish, microhardness and white layer thickness (WLT)) were considered as turning performance characteristics.

**CHAPTER 4** shows studies on the effect of turning process parameters and cooling environment on turning performance characteristics during machining of 17-4 PH SS. In this chapter, experiments were conducted based on the one factor at a time approach (OFATA) by taking cutting velocity, feed rate and depth of cut as controllable parameters under the cryogenic, MQL, wet and dry machining environments respectively.

**CHAPTER 5** focuses on determination of optimum process parameters for single as well as multi objective responses under the cryogenic environment. Tool flank wear, surface roughness and MRR were considered as responses and experiments were done according to the  $L_9$  orthogonal array. Single objective optimization was done using Taguchi method and AVOVA was carried out to find the most influenced process parameter on responses. Multi objective optimization was done using Taguchi coupled GRA and Taguchi coupled TOPSIS methods and selected the best multi objective optimization technique for the current problem.

**CHAPTER 6** presents the mathematical models developed for the each response using RSM under the cryogenic environment. In this chapter, experiments were conducted based on the face centered central composite design ( $L_{20}$ ) and responses considered were tool flank wear, surface roughness and MRR.

**CHAPTER 7** gives the summary of conclusion from the total work carried out in this research work and future scope of the work.

## CHAPTER 2

### LITERATURE REVIEW

#### 2.1 INTRODUCTION

This chapter explains the literature on various difficult to cut materials and their machining under various sustainable cooling techniques especially with cryogenic coolants. Also, detailed explains the literature on various optimization and modeling techniques and their effect on machining performance while machining of various classes of difficult to cut materials.

#### 2.2 CLASSIFICATION OF DIFFICULT TO CUT MATERIALS

From the literature, it was observed that there is no standardized format given to classify the difficult to cut materials. The definitions of the difficult to cut materials still a vogue. Shokrani et al. (2012) have done review on various kinds of materials and classified the difficult to cut materials into three types as shown in Figure 2.1, namely hard materials, ductile materials and non homogeneous materials.

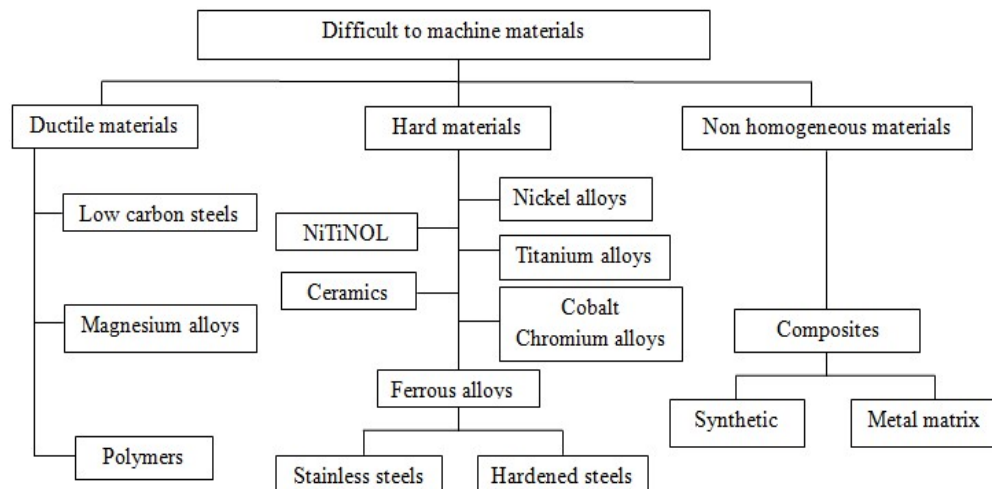


**Figure 2. 1** Classification of difficult-to-machine materials (Shokrani et al., 2012).



These materials were treated as difficult to cut materials by considering the different mechanical and thermal properties. These properties includes high hardness, poor thermal conductivity, high strength and high ductility (Ezugwu et al., 2003; Zhang et al., 2012; Chinchankar and Choudhury, 2015). Materials which produce more tool wear, cutting force and difficulties in chip formation during machining are classified as difficult to cut materials. The excessive generation of cutting zone temperatures at the machining zone is one of the phenomena in machining of difficult to cut materials (Shokrani et al., 2012).

Machining of these materials associated high manufacturing cost and low productivity due to high machining zone temperatures and difficult of chip removal. Use of cutting fluids is one of the solutions to control the machining zone temperatures. The rate of temperature reduction range at the machining zone varies depending on the type of cooling method used. Therefore, proper selection of cooling method is required to better control of machining temperature as well as performance characteristics like tool life, chip morphology, cutting force, dimensional accuracy and surface integrity. Conventional cooling methods are not feasible for machining of difficult to cut materials at higher cutting conditions and there are many disadvantages with it. However, dry machining and hot machining fails at higher cutting conditions. Mohanty et al. (2015) have conducted machinability studies on 17-4 PH SS under the dry condition and more adhesion wear and poor quality of machined surface were found. The different tool failure mechanisms and their principle location on the worn tool as shown in Figure 2.2.

Productivity enhancement along with the health and environmental damage free is a challenge for metal cutting manufacturing industries due to stringent environmental regulations. Nowadays, for metal cutting industries, coupling of these environmental regulations into a management system is one of the major strategic challenges. For these reasons, many industries looking for alternative cooling techniques which can avoid low productivity, health and environmental damage problems. The researchers concentrated

on various environmental conscious machining processes as discussed in previous chapter and their disadvantages were discussed.

In the present thesis, two environmental conscious machining processes like MQL and cryogenic were investigated as given below and experimental results were compared with conventional and dry machining environments respectively.

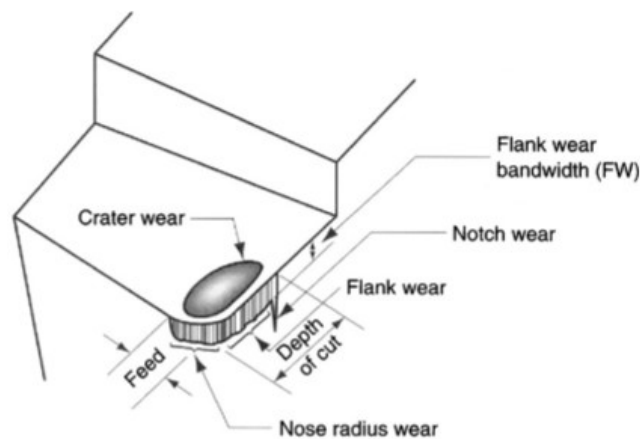


**Figure 2. 2** Various tool failure mechanisms and their principle location on the worn tool (Groover, 2007).

### 2.3 MQL MACHINING OF DIFFICULT TO CUT MATERIALS

In MQL machining, small quantity lubrication (50-450 ml/hr) is supplied along with compressed air, resulting in MQL mist is generated at the machining zone. In MQL, cutting zone temperature reduction is mainly due to the convection of the compressed air and partially evaporation of cutting oil (Ezugwu, 2005). Various researchers have applied the MQL during machining of difficult to cut materials to the machining zone at different manufacturing processes. Kuzu et al. (2015) conducted experimental study on compacted graphite iron material under the dry and MQL cutting conditions. They have observed that MQL machining substantially reduced the  $V_b$ ,  $R_a$  and  $F_c$  by 10 %, 25 % and 5 % respectively over the wet machining. They found that the reason of turning performance improvement in MQL was due to the substantial decrease of a coefficient of

friction between contact asperities. Amini et al. (2014) in the first stage of their work, they determined optimum MQL process parameters in terms of flow rate, nozzle position and nozzle effective distance from the machining zone for conducting the experiments on AISI 4142 material. Afterward, the  $V_b$ ,  $R_a$  and  $F_c$  studies were done under the MQL and dry environments. They have observed significant improvement in the turning performance under the MQL condition due to the control of built up edge formation at the cutting tool. Chinchankar and Choudhury (2014) obtained superior tool life in MQL environment over the dry environment due to the better lubrication effect. Sohrabpoor et al. (2014) carried out the experiments on AISI 4340 material under the MQL, wet, dry and air coolant conditions and investigated the  $V_b$  and  $R_a$  respectively. In their study, they supplied the MQL at both flank, rake faces of the tool and they found that MQL machining provided favorable results compared to other conditions due to the substantial decrement of cutting zone temperature. Kouam et al. (2015) achieved advantageous turning performance results in MQL machining while machining of 7075-T6 aluminum alloy over the dry machining. Sarikaya et al. (2016) have performed the experimental investigation on the  $V_b$  and  $R_a$  in machining of Hayness 25 super alloy under the dry, wet and MQL machining. They applied the MQL mist at the rake face of the cutting insert. They found that cutting temperature significantly reduced at the cutting zone in MQL cooling condition and improved turning results were obtained over the dry and wet machining respectively. Khan et al. (2009) used vegetable based coolant as a MQL coolant in machining of low alloy steel AISI 9310 and investigated the  $R_a$  and  $V_b$  under the MQL, dry and wet machining conditions. They found that among all the cooling conditions, MQL improved the turning performance due to the significant reduction of machining zone temperatures enables advantageous tool-chip contact nature. Sharma and Sidhu (2014) achieved the reduced cutting temperature and low  $R_a$  in MQL environment over the dry condition in turning of AISI D2 steel. MQL is one of the eco friendly manufacturing processes. The drawback of MQL is it fails to control the machining zone temperatures at the industrial cutting conditions (Attanasio et al., 2006; Obikawa et al.,

2006). Nevertheless, still MQL presents coolant mist at the machining surroundings, affects the operator health (Aoyama et al., 2008).

## **2.4 CRYOGENIC MACHINING OF DIFFICULT TO CUT MATERIALS**

### **2.4.1 Origin of cryogenic material processing**

During 2<sup>nd</sup> world war, scientists were found that wear resistance increases when the metal frozen to lower temperature. The research and standard organizations defines the cryogenic processing is the frozen of metals below -150 °C (Jawahir et al., 2016). The company name called Cryo Tech (Detrit, MT, USA) introduced the term cryogenic processing in the year 1966, later on, the term cryogenic machining was first introduced by Uehara in 1969 and they found 200 % improvement in the tool life (Uehara and Kumagai, 1969). Cryogenic coolants have different applications in the fields of aerospace industry, manufacturing industry, health, electronics and automotive industry (Yildiz and Nalbant, 2008).

### **2.4.2 Cryogenic cooling approach in machining**

Cryogenic cooling approaches have been classified into 4 types

1. Cryogenic precooling of workpiece
2. Indirect cryogenic cooling
3. Cryogenic treatment of tool
4. Cryogenic spray cooling/Cryogenic jet cooling

#### **2.4.2.1 Cryogenic precooling of workpiece**

In this method, workpiece cooled with cryogenic coolants in an enclosed bath or general flooding. The intension of this method is to covert the properties of material from ductile to brittle nature, because brittle materials gives discontinuous chips i.e., chip breakability improves (Hong and Ding, 2001). Productivity in machining processes significantly

affected by the type of chip formation during machining and it was proved by Jawahir (Jawahir, 1988). Control of chip accumulation and chip breakability at the machining zone will improve the machining performance. Hong and Ding (2001) have used two test methods during machining of AISI 1008 low carbon steel. In their first method, they have used test setup as shown in Figure 2.3 for workpiece cooling purpose. They have observed significant chip embrittlement with LN<sub>2</sub> cooling. Ahmed et al. (2007) have found enhanced chip breakability with LN<sub>2</sub> cooling of newly generated surfaces in machining of AISI 4340 material.

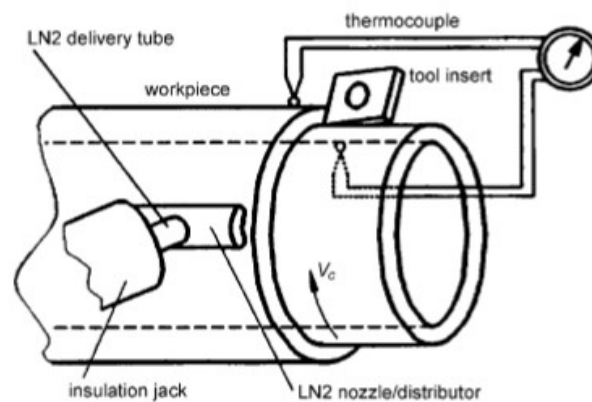


**Figure 2. 3** Cryogenic precooling of workpiece (Hong and Ding, 2001).

Uehara and Kumagai (1968, 1970) have cooled the workpiece surface with LN<sub>2</sub> injected through single nozzle (1968) and two nozzles (1970) and they found that chip breakability can be increased regardless of cryogenic cooling method but drastic increase in material hardness was observed when double nozzle setup used resulting in increased cutting force compared to wet machining. Ding and Hong (1998) studied the chip breakability of cryogenically cooled AISI1008 low carbon steel workpiece and achieved improved chip breaking capabilities at medium cutting speeds.

However, this method is limited to academic purpose only due to impractical in the industry. This method is uneconomical due to consumption of high LN<sub>2</sub>. Also, this method over cools the workpiece results in increased cutting forces and abrasion wear during machining which are not favorable for improvement of process performance.

### 2.4.2.2 Indirect cryogenic cooling

In this method, there is no direct contact between the machining zone and LN<sub>2</sub> but it cools the tool cutting tip in indirect way like keeping the LN<sub>2</sub> cooling storage chamber near the tool tip edge or face of the tool. In this method, heat at the machining zone is removed by conduction way. Various researchers have used different indirect cooling systems for improving turning performance characteristics. Hong and Ding (2001) have used a indirect cooling setup for cooling the tool tip as depicted in Figure 2.4. In their setup, they have provided LN<sub>2</sub> chamber between the tool insert and shim to control the tool back face.

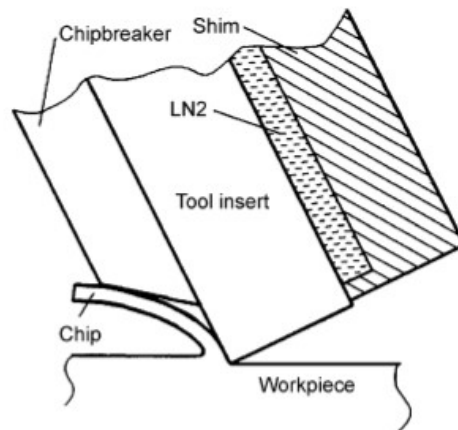


**Figure 2. 4** Application of LN<sub>2</sub> to tool back (Hong and Ding, 2001).

Wang and Rajurkar (2000) have developed the new LN<sub>2</sub> cooling system as shown in Figure 2.5 to cool the cutting insert. This cooling system consists of metal cap designed in such a way that LN<sub>2</sub> comes in close contact with the cutting edge. The cover has two taps on its top surface. The tap close to the cutting insert tip is used as the inlet for the liquid nitrogen and the other tap is used as the outlet. Wang et al (2000) have been conducted experiments on polycrystalline cubic boron nitrid PCBN tool, titanium alloys, Inconel alloys, and tantalum with cemented carbide tools with liquid nitrogen as a cutting fluid. They found low tool wear and surface roughness with the developed system

compared to dry machining. The increased wear resistance with LN<sub>2</sub> cooling attributed to favorable results in their work.

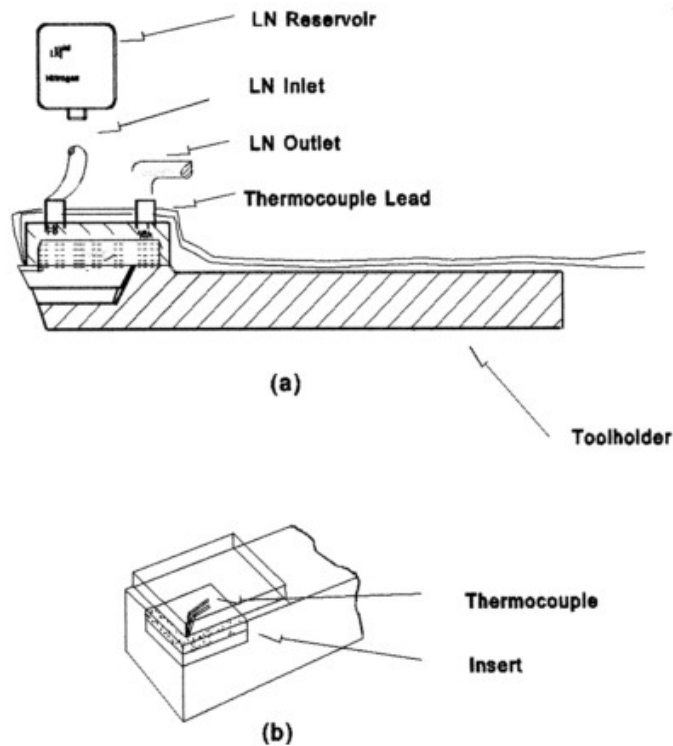


**Figure 2. 5** (a) Tool cap (b) LN<sub>2</sub> reservoir (Wang and Rajurkar, 2000).

Rozzi et al. (2011) developed a new indirect cooling system depicts in Figure 2.6 in which cryogenic fluid passes through a micro channel heat exchanger (MHX) that is mounted below the cutting tool insert which cools the cutting tool and avoid the workpiece. They have conducted experiments on AISI 416 stainless steel in turning process. Average flank wear, maximum flank wear and notch wear were calculated. They found that the use of a cryogenic working fluid can significantly improve tool life at all cutting speeds over flood cooling technique. Also, they have developed predictive thermal model of cutting tool-chip interface temperature for flood cooling and the indirect cooling approaches. Finally, they concluded that reasonable agreement was obtained between the predictive model developed for tool life and the experimental results.

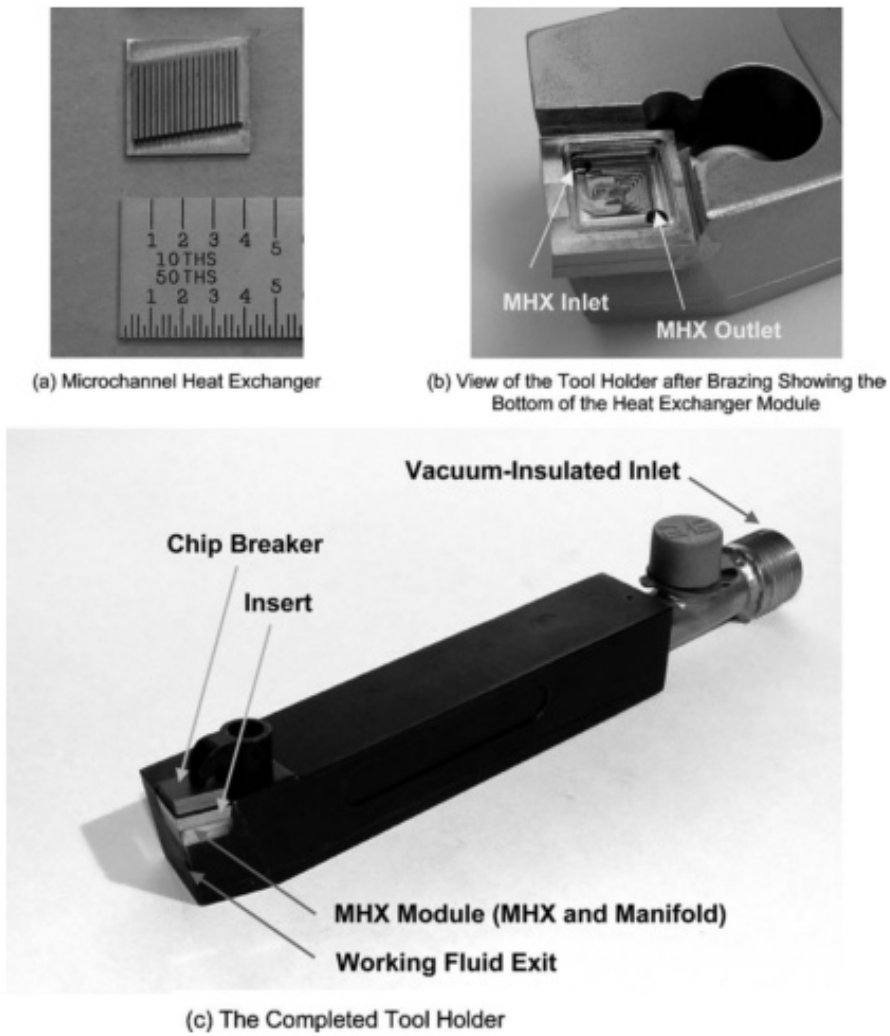


Figure 2. 6 (a) MHX (b) heat exchanger module (c) fabricated tool holder  
(Rozzi et al., 2011).

In Indirect cryogenic cooling method, workpiece does not contact with LN<sub>2</sub>. Therefore, overcooling effect is completely eliminated in this method results in no rise of cutting force, hence, this method could improve the performance of the process. However, the drawback of this method is effectiveness of LN<sub>2</sub> cooling highly depends on the thermal conductivity of tool material, insert thickness, distance from the high temperature source to LN<sub>2</sub> source and area of contact of cutting insert with LN<sub>2</sub> cooling chamber respectively (Yildiz and Nalbant, 2008).



### 2.4.2.3 Cryogenic treatment

It is similar to the heat treatment process but it is done at low temperatures. In this process, cutting tools are frozen gradually with help of gases like nitrogen, helium, neon and oxygen in a control unit as shown in Figure 2.7 (Balasubramanian et al., 2012; Candane et al., 2013).

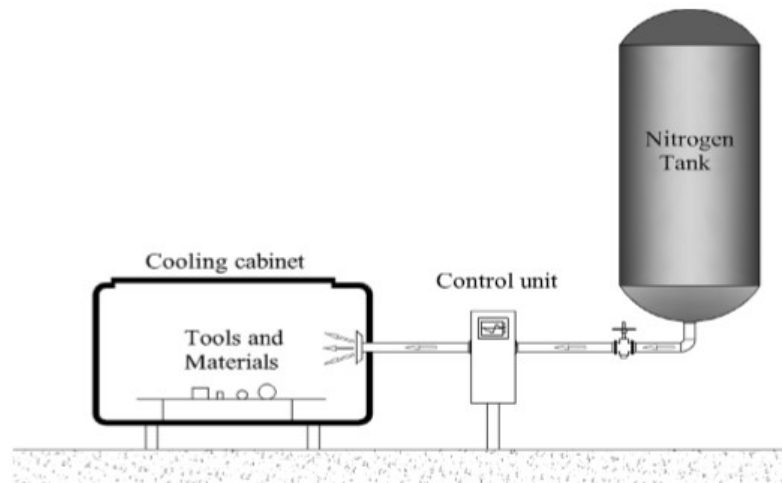


**Figure 2. 7** Schematic view of a cryogenic treatment process applied in a controlled manner (Akincioğlu et al., 2015).

This method is applied for different products like cutting tool, brake discs, tool steel, alloy steel, polymers, composites, race car engines for performance improvement (Das et al., 2009; Reddy et al., 2009; Indumathi et al., 1999; Gill and Singh, 2013). In this process, samples are cool down between  $-80\text{ }^{\circ}\text{C}$  to  $-196\text{ }^{\circ}\text{C}$  for some time and bring back to room temperature following tempering as shown in Figure 2.8 (Senthilkumar and Rajendran, 2011; Podgornik et al., 2009). There are two types of cryogenic heat treatment processes namely shallow cryogenic treatment and deep cryogenic treatment process. In shallow cryogenic treatment process, samples are frozen to temperature range of  $-80\text{ }^{\circ}\text{C}$  to  $-140\text{ }^{\circ}\text{C}$ , whereas, sample cooling range in cryogenic treatment process was  $-140\text{ }^{\circ}\text{C}$  to  $-196\text{ }^{\circ}\text{C}$ . The important controllable parameters in cryogenic treatment process are soaking period, soaking temperature, cooling speed and tempering process (Thakur et al., 2008; Baldissera and Delprete, 2008). Particularly, in cryogenic treatment

of tools, these factors play a crucial role in the performance behavior of tools in terms of wear resistance, toughness and hardness due to conversion of tool material from austenite to martensite, carbide distribution and formation of new carbides. Soaking period controls the conversion of tool material from austenite to martensite, carbide distribution and formation of new carbides (Baldissera and Delprete, 2008; Gill et al., 2010).

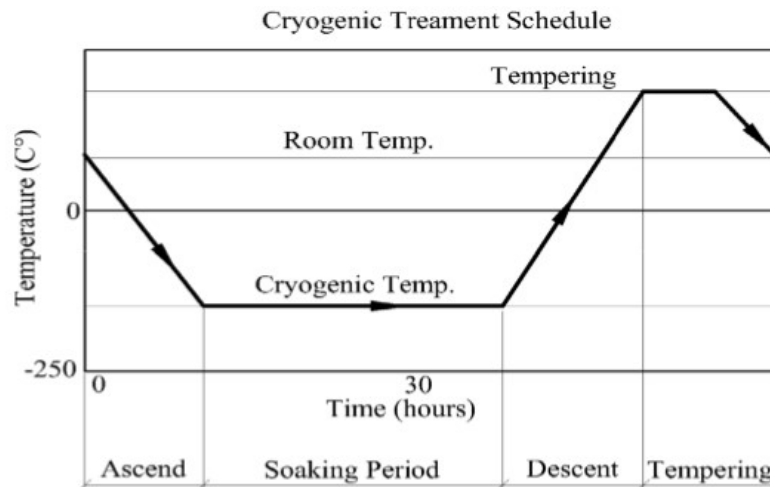


**Figure 2. 8** Sequentially temperature variation of cryogenic treatment process (Akincioğlu et al., 2015).

Different researchers have used different soaking temperatures for improving the tool performance and they found that -184 °C as optimum cryogenic treatment temperature (Akincioğlu et al., 2015). Tempering process in cryogenic treatment is to eliminate the internal stress formed during excessive cooling (Bensely et al., 2012; Gill et al., 2012). Generally, tools are holding for 1.5 to 2 h at 150 °C to 200 °C in tempering process (Dogra et al., 2011; Xuan et al., 2008; Firouzdor et al., 2008). The primary target of this method is to increase the hardness and wear resistance of the tool results in reduced tool wear, low surface roughness and low cutting forces. Candane et al. (2013) observed fine carbide particles after two consecutive tempering treatment of AISI T4 material.

Various researchers have applied the cryogenic treated tools for improving the performance characteristics in turning process. Reddy et al. (2009) have performed deep cryogenic (LN<sub>2</sub>) treatment on multilayer CVD coated cemented carbide inserts at a

cooling temperatures of  $-176\text{ }^{\circ}\text{C}$  at the rate of  $2\text{ }^{\circ}\text{C}$  per minute, holding the temperature at  $-176\text{ }^{\circ}\text{C}$  for 24 hours, then later raising the temperature back to room temperature at the rate of  $2\text{ }^{\circ}\text{C}$  per min. After this, turning experiments were carried out on AISI 1040 medium carbon steel using cryogenically treated tool and untreated tools. They found that  $V_b$ ,  $F_c$  and  $R_a$  value were substantially reduced with cryogenically untreated tools when compared to cryogenically untreated tools. They reported that reason for results improvement is increase of wear resistance of cryogenically untreated tools. Thornton et al. (2013) investigated the effect of deep cryogenic treatment (93 K) of H13A cobalt-bonded tungsten carbide cutting inserts on the surface and sub-surface wear development during wet machining of AISI 1045 steel and results were compared with untreated tools. They found improved tool life with cryogenic treated tool over the untreated tool. He et al. (2014) studied the effect of deep cryogenic treatment (DCT) of TiAlN coated YT15 tungsten carbide inserts on cutting forces, cutting temperature, surface qualities and tool life in dry turning of AISI 5140 steel and compared these results with untreated inserts. They have conducted the experiments at various cutting speeds and constant depth of cut, feed rate respectively. They observed that the maximum reduction found in cutting force, cutting temperature and surface roughness was 27%, 7.7% and 28.5% respectively with DCT inserts compared to untreated insert. Strano et al. (2015) studied the effect of deep cryogenically treated PVD coated TiAlN layer WC inserts on average flank, surface roughness, different forces, coefficient of friction ( $\mu$ ) and morphology in CNC rough turning of titanium alloy at low and high speeds and results have been compared with un DCT tools. It was observed that cryogenically treated tools improved the productivity even at higher cutting speeds over the untreated tools. Thakur et al. (2012) observed improved turning performance characteristics results with WC-Co (K20) tungsten carbide post treated cryogenic treatment while machining of Inconel 718 material. Thakur et al. (2014) investigated the effect of various treatments methods namely cryogenic treatment and controlled heating and oil quenching of cemented tungsten carbide (WC-Co, K20) tools. Machining studies was done on Inconel 718 with treated tools and investigated the turning performance characteristics. They found 110 to

150 % improvement in tool life with treated tools due to the improved wear resistance of tool over the untreated tools. However, the initial cost investment required is high in this method. Also, cryogenic treated tool performance varies from one machining process to another.

### 2.4.2.3 Cryogenic spray cooling

In this method, cutting zone temperatures reduces with help of cryogenic coolants particularly at the tool-workpiece interface. General flooding of cryogenic coolants at the machining zone causes for more production cost. Also, flood cooling with cryogenic coolant leads to unwanted cooling areas results in increase of cutting force (Kalyan and Choudhury, 2008). These drawbacks can be reduced with help of cryogenic jet cooling. In cryogenic jet cooling, cryogenic coolant is supplied at the exact cutting area where heat will develop using micro nozzles. Hong and Ding (2001) have developed a LN<sub>2</sub> cooling system with micro nozzles as shown in Figure 2.9. In this cooling system, one nozzle is used to cool the flank face of the tool and another nozzle for rake face cooling.

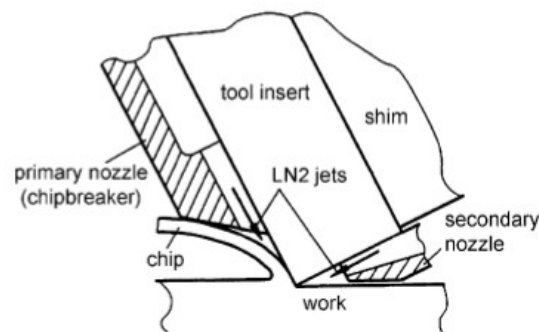


**Figure 2. 9** Schematic diagram of LN<sub>2</sub> nozzle system (Hong and Ding, 2001).

This method has many advantages like no unwanted cooling area, reduced cooling power wastage, localized cooling at the machining zone causes reduction of cutting zone temperatures, less formation of BUE on the tool, increasing tool hardness, decreased tool wear and improved chip breakability. In this method, LN<sub>2</sub> consumption is very low and it

is measured as approximately 0.625 l/min for rake nozzle whereas for flank nozzle it is 0.53 l/min and for both rake and flank nozzle it a 0.814 l/min. So, this method can reduce the manufacturing cost and increases the productivity greatly (Hong, 1995). Because of these benefits, many researchers have used this method for performance improvement in various manufacturing processes. In this method, the way of LN<sub>2</sub> supply with micro nozzles can significantly affects the process performance. Hong (2006) conducted experiments on five different pairs of surface and concluded that regardless of the type of pair, LN<sub>2</sub> generates hydrodynamic film which provided the lubrication effect. Hong et al. (2002) reported that the application of LN<sub>2</sub> with high pressure causes the penetration of LN<sub>2</sub> at the contact zone of asperities, resulting in low friction due to the micro-scale hydrostatic resultant force. LN<sub>2</sub> provides the lower cutting temperature which changes the nature of contact from sticky to sliding; resulting in reduced effective shear strength to shear off the material. Spraying of LN<sub>2</sub> at the tool-workpiece zone allows the soaking of the cutting tool with LN<sub>2</sub>, resulting in increased hardness of the tool hence low tool wear and maintaining good surface integrity characteristics. Hong (2006) found the lubrication mechanisms offered by the LN<sub>2</sub> while disk-flat contact tests of AISI 1018 and Ti-6Al-4V materials under the different combinations of LN<sub>2</sub> cooling methods. Finally he claimed that quantity of friction coefficients is depends on the material properties and method LN<sub>2</sub> supply. Hong and Ding (2001) used LN<sub>2</sub> amid the machining zone in machining of Ti-6Al-4V and found lower cutting force and coefficient of friction contrasted with dry machining. This effect is mainly on account of cushioning effect of LN<sub>2</sub> amid interface surfaces. Very few researchers have supplied the LN<sub>2</sub> to the machining zone using novel methods.

#### **2.4.3 Effect of cryogenic jet cooling on cutting temperature, tool wear, surface roughness, cutting forces, coefficient of friction and chip morphology**

Jun (2005) used patented nozzle delivery system (supply head system) for novel supply of the LN<sub>2</sub> at both the rake and flank faces simultaneously and compared the coefficient of friction with dry, emulsion and LN<sub>2</sub> jet cooling of tool chip interface with one nozzle

(tool rake face cooling) respectively. He observed that LN<sub>2</sub> cooling with one nozzle reduced the coefficient of friction 0.3 for Ti-6Al-4V alloy and 0.4 for AISI 1018 material respectively over the dry or emulsion cooling. Whereas, LN<sub>2</sub> cooling with two nozzles reduced the coefficient of friction for AISI 1018 material as 0.35 and 0.27 for Ti-6Al-4V alloy compared to dry or emulsion cooling. From the results, it has been concluded that the friction coefficient is depends on the LN<sub>2</sub> delivery approach, especially nozzle design and nozzle location. Khan and Ahmed (2008) analyzed the tool life while conducting the experiments on AISI 304 stainless steel in turning operation with TiC coated inserts under the conventional and cryogenic cooling conditions. For conventional experimentation, a mixer of Kutwell 40 soluble oil and water was used as the coolant in the ratio of 5:95. For cryogenic experimentation, LN<sub>2</sub> was supplied through a modified tool holder to cool down the cutting insert as shown in Figure 2.10. They observed four times improvement in the tool life in cryogenic machining over the conventional cooling method and also claimed that LN<sub>2</sub> cooling is effective at higher speed and feed rate conditions due to reduced abrasion and attrition wear.

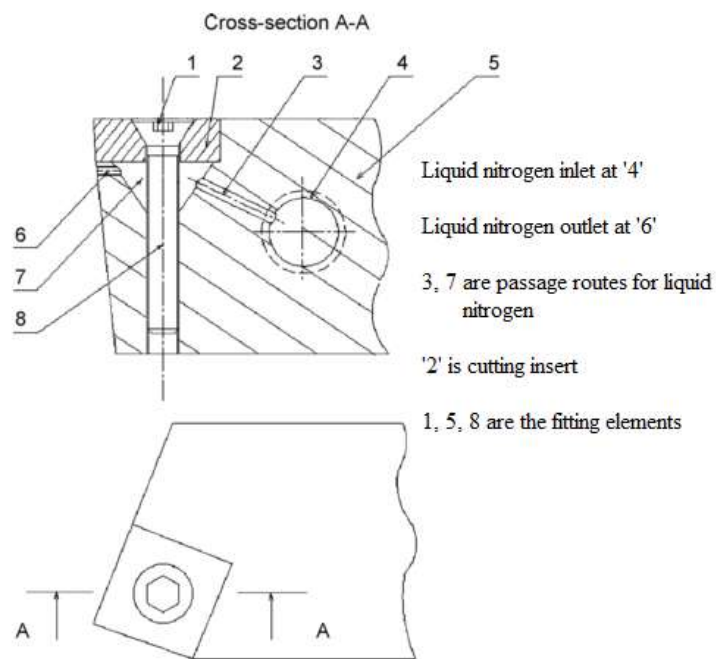


**Figure 2. 10** Details of modified tool holder for LN<sub>2</sub> cooling (Khan and Ahmed, 2008).

In another work, Khan et al. (2010) used a special device was developed to supply the LN<sub>2</sub> at the machining zone in convenient way to the machining zone and studied the flank wear and surface roughness at three different positions with LN<sub>2</sub> cooling while machining AISI 304 as shown in Figure 2.11 and results were compared with dry machining. They found that at all the three positions with LN<sub>2</sub> cooling improved the results greatly compared dry machining. They also found that the position of the nozzle at the machining did not affect the workpiece surface but tool life varies. Among all the positions with LN<sub>2</sub> cooling, they found four times increment in the tool life with position 'c' over the dry machining.

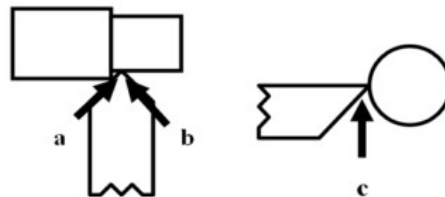


**Figure 2. 11** Three different positions for applying liquid nitrogen cutting fluid a: on the tool face along the principal cutting edge, b: perpendicular to the principal cutting edge, c: from the bottom through the gap between the tool flank and the workpiece (Khan et al., 2010).

Dhananchezian et al. (2011) utilized modified cutting tool for supplying the LN<sub>2</sub> at the machining zone with a pressure of 3 bar in turning of AISI 304 material. They have conducted the experiments at varying cutting velocity condition and keeping other parameters constant using PVD TiAlN coated carbide insert. Modified cutting tool consists of a two holes, one at flank face (Ø1mmx 2 mm) and another at the rake face (Ø2mmx 2.5mm) as shown in Figure 2.12. They have observed that the respective maximum reductions found in cutting temperature, cutting force, surface roughness was 51 %, 16 % and 34 % over the wet environment as shown in Figure 2.13. Similarly, they have conducted experiments on Ti- 6Al-4V and aluminium 6061-T6 alloy with modified cutting tool and found significant improvement in the turning performance characteristics

with LN<sub>2</sub> cooling over conventional cooling (Dhananchezian and Kumar, 2010; Dhananchezian and Pradeep Kumar, 2011).

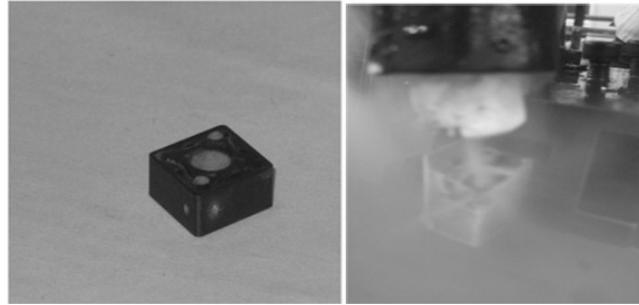


**Figure 2. 12** Modified cutting tool for LN<sub>2</sub> supply at rake and flank face (Dhananchezian et al., 2011).

Jerold and Kumar (2012) they supplied the LCO<sub>2</sub> at the machining with a flow rate of 3 g/s during turning of AISI 316 stainless steel and observed superior results as a function of surface roughness, tool wear, chip morphology and cutting temperature over wet and dry machining. Similarly, they carried out experimental investigation on Ti-6Al-4V, AISI 1045 materials by supply of coolants at the machining zone at different cutting speed, feed rates under cryogenic coolants, dry and wet cooling conditions. They found better turning performance characteristics compared to dry and wet machining conditions (Jerold and Kumar, 2013; Dilip Jerold and Pradeep Kumar, 2011; Dilip Jerold and Pradeep Kumar, 2012). Venugopal et al. (2007a;2007b) Supplied the LN<sub>2</sub> through the specially designed nozzle as shown in Figure 2.14 at both rake and flank face cooling of the cutting insert. Improved tool life was observed in turning of Ti-6Al-4V alloy using LN<sub>2</sub> cryogenic machining due to the increase of tool hardness at lower temperature over the dry and wet machining. Bermingham et al. (2011) have utilized Seco jet stream<sup>TM</sup> tool holder for supplying the LN<sub>2</sub> at the rake of the tool and secondary copper nozzle for flank face cooling respectively as shown in Figure 2.15 and investigated the tool life, cutting force and chip morphology during turning of Ti-6Al-4V alloy and results were compared with dry machining respectively. In cryogenic machining, it was observed greater tool life at higher feed rates and lower depth of cut cutting condition respectively.



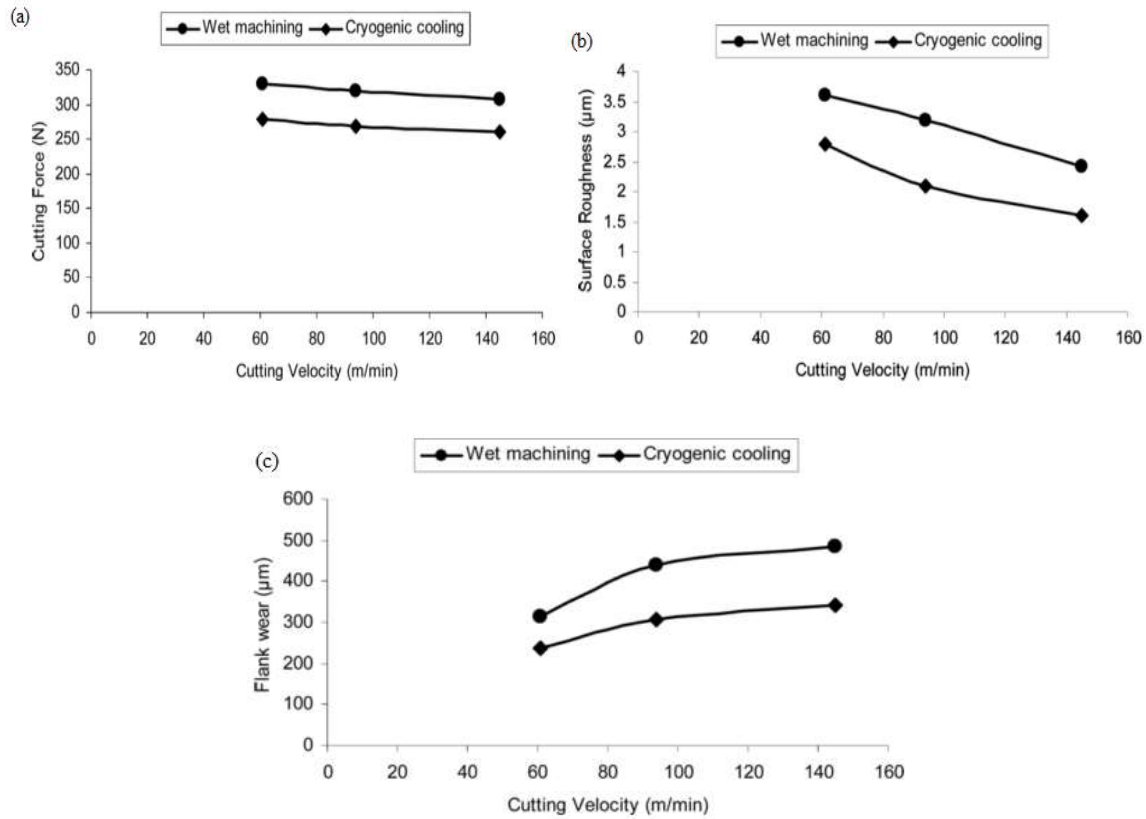


**Figure 2. 13** Effect of  $\text{LN}_2$  on (a) Main cutting force (b) Surface roughness (c) Tool flank wear at varying cutting velocities and constant feed rate, depth of cut of 0.159 mm/rev, 1 mm respectively (Dhananchezian et al., 2011).



**Figure 2. 14** Liquid nitrogen delivery nozzle (Venugopal et al., 2007b).

Also, it has been observed thicker chips and reduced shear band angle was found in cryogenic machining due to the effective cooling at the cutting zone. Paul et al. (2001) supplied the  $\text{LN}_2$  at the flank and rake face of the tool using a specially design nozzle and

studied its effect on tool wear and surface finish in turning of AISI 1060 steel with two different cutting inserts. From the results, it was found that better performance characteristics were observed in cryogenic machining over the dry and conventional cooling conditions. They reported that the beneficial results are attributed due the effective control of cutting zone temperatures, increase of tool hardness and advantageous tool-chip interface.



**Figure 2. 15** LN<sub>2</sub> supply with SECO tool holder (Bermingham et al., 2011).

In another work, at same cooling conditions, Paul and Chattopadhyay (2006) carried out experiments on AISI 1040, AISI E4340C, AISI 4140, AISI 4320 with two composite carbide inserts and studied the performance characteristics like tool wear, cutting force, cutting temperature, chip reduction coefficient, dimensional accuracy and chip morphology. They found better results in cryogenic machining for all grades of steels over the dry and wet machining conditions. Kumar and Choudhury (2008) have used a specially designed nozzle for spraying of LN<sub>2</sub> at the machining while machining of SS 202 material. They studied the effect of cutting speed, feed rate and depth of cut individually on cutting force and tool flank wear under the cryogenic and dry environments. They observed low cutting force and flank wear in cryogenic machining at all the cutting parameter levels over the dry machining due to effective control of machining zone temperatures. MacHai and Biermann (2011) studied the effect of carbon dioxide snow as a coolant on flank wear, notch wear for turning Ti–10V–2Fe–3Al with two types of cemented carbide tool with rake angles 10°, 15° and results have been compared with emulsion flood cooling. In their work, they sprayed the coolant at the

cutting edge through the integrated holder to the cooling system as shown in Figure 2.16. The Results showed that cryogenic machining increased the tool life, cutting force and controlled the burr formation even at high cutting speeds over the emulsion cooling. Yap et al. (2013) LN<sub>2</sub> jet was directed with a pressure of 0.0345 MPa to the interface between the tool-workpiece while cutting of Ti-5Al-4V-0.6Mo-0.4Fe (Ti54) material in turning. They found reduction of cutting forces, coefficient of friction and surface roughness in cryogenic machining compared to dry machining.

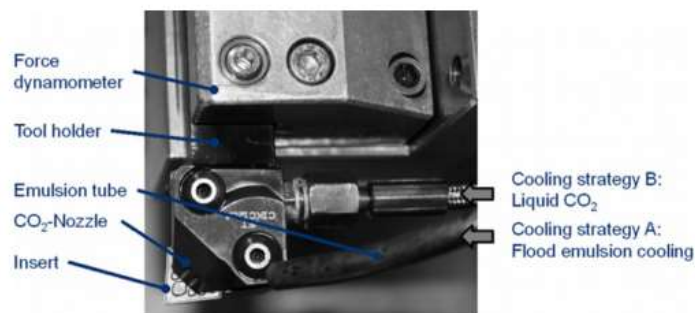


**Figure 2. 16** Experimental setup for conventionally applied flood emulsion cooling (strategy A) and carbon dioxide snow cooling (strategy B) (MacHai and Biermann, 2011)

Klocke et al. (2013) supplied LN<sub>2</sub> at the rake face of the tool using external nozzle and carried out the experiments by keeping the cutting time as constant. Also, in MQL machining, they have used vegetable oil as coolant, whereas, in wet machining they used emulsion coolant in the ratio of 6:94. They have observed better performance results in cryogenic machining of gamma titanium aluminides ( $\gamma$ -TiAl) compared dry, wet and MQL machining conditions because of significant reduction of the cutting temperatures. Raza et al. (2014) performed the experiments under six different environments namely dry, wet, MQL, cryogenic, cryo-MQL and cooled air in turning of Ti-6Al-4V alloy. In all cooling methods, they applied the coolants at the machining zone using external nozzle. They have used LN<sub>2</sub> for cryogenic cooling, rapeseed vegetable oil for MQL cooling, a combined vegetable and LN<sub>2</sub> for cryo-MQL (CRMQL) respectively. They

claimed that MQL and CRMQL reduced the tool wear and surface roughness greatly at lower cutting conditions whereas at higher cutting conditions, cryogenic machining is more suitable due to low tool wear. They found low BUE formation on the in cryogenic machining over other cooling environments at higher cutting conditions. Kaynak (2014) supplied the LN<sub>2</sub> at the machining zone using one and two external nozzle with a flow rate of approximately 10 g/s while machining of additive manufactured Inconel 718 with uncoated carbide insert. He conducted experiments at two varying cutting velocities under cryogenic, MQL and dry condition respectively. It has been found that cryogenic machining gave better results in terms of cutting temperature, surface roughness, cutting force and chip morphology over MQL and dry machining. He also concluded that cutting force and power consumption are significantly influenced by the number of nozzle used to supply the LN<sub>2</sub>. Bordin et al. (2015) supplied the LN<sub>2</sub> with two external copper nozzles at the both rake and flank faces of the tool at an angle of 45° during machining of additive manufactured (AM) Ti-6Al-4V alloy. They obtained the improved tool life and surface finish in cryogenic machining over dry machining. In another work, Bordin et al. (2016) have studied the V<sub>b</sub>, R<sub>a</sub> and chip morphology while machining of additive manufactured Ti-6Al-4V alloy under the cryogenic, wet and dry machining conditions. It has been found that advantage results were obtained in cryogenic machining as a function of tool wear and chip morphology at all the machining parameters over the wet and dry environments. However, reduced surface roughness was obtained merely at the higher cutting conditions compared to dry and wet environments.

In the recent years, few researchers have supplied the cryogenic coolants at the machining zone using external nozzle and various machinability studies were done during machining of different kinds of difficult to cut materials. Sartori et al. (2017) have worked on two different micro structure variant Ti-6Al-4V alloys produced by the two different additive manufacturing methods under the dry and cryogenic conditions. They have claimed that cryogenic machining significantly controlled the adhesion wear due to lower temperatures provided by the LN<sub>2</sub> compared to dry environment. Pereira et al. (2016) have investigated the various kinds and combinations of environmental

friendly machining processes in machining of AISI 304 material. It was claimed that dry machining is not suitable solution due to high tool wear rate, but the combination of cryo-MQL technique has improved the machining performance greatly compared to stand alone MQL, dry and cryogenic machining conditions. Chetan et al. (2015) have investigated the effect of various sustainable cooling environments namely cryogenic, MQL and dry on turning performance particularly as a function of chip thickness,  $V_b$ ,  $R_a$ , chip contact length and chip morphology in turning of Nimonic 90 alloy. It has been observed that both cryogenic and MQL machining environments gave superior performance at higher cutting velocities. Improved chip breakability was observed using  $LN_2$  at machining zone while machining of low carbon steel (Hong et al., 1999). Dhar and Kamruzzaman (2007) have performed the turning experiments on AISI 4037 in  $LN_2$  spray cooling environment and advantages results were obtained in terms of cutting temperature, surface roughness, tool wear and dimensional accuracy over dry machining due to the changes in the tool-chip contact nature. Dhar et al. (2002) used two different tool geometries namely SNMG 120408-26 TTS and SNMM 120408 TTS for machining AISI4140 material under cryogenic, dry and wet machining environments. They found significant improvement in the machinability characteristics under cryogenic cooling with SNMM 120408 TTS. Cryogenic machining improved the turning performance characteristics at higher cutting speeds in machining of Inconel 718 compared to wet and minimum quantity lubrication (MQL) machining conditions (Kaynak, 2014). Schoop et al. (2015) have conducted turning experiments on porous tungsten material under the cryogenic, dry machining environments and observed significant improvement in the cryogenic environment with regard to tool wear and surface integrity characteristics due to significant reductions in the machining zone temperatures. Yap et al. (2013) have done the turning experiments on titanium based alloy by utilizing  $LN_2$  as a coolant and observed positive results in terms of surface roughness, cutting force and friction coefficient over the dry machining. Sun et al. (2015) have researched on Ti-4Al-6V under the compressed cryogenic air environment and noticed better results contrasted with dry turning. Gupta et al. (2015) have done the turning experiments on AISI 1040

steel by impinging the LN<sub>2</sub> at the rake face of the tool and observed reduction in tool wear, cutting temperature and cutting force in relative to the dry machining. Dinesh et al. (2016) have investigated the effect of different non-textured and linearly textured tungsten carbide cutting inserts on machinability characteristics like tool wear, cutting forces, surface roughness, microhardness and cutting temperature in turning of ZK60 magnesium alloy under the LN<sub>2</sub> environment. Significant improvement was observed in the machinability characteristics with the textured tools due to the simultaneous effect of formation of thin lubrication film between the tool-chip and micro pool lubrication. Various authors (Bermingham et al., 2011; Dilip Jerold and Pradeep Kumar, 2011; Klocke et al., 2013) have analyzed the chip morphology in various machining conditions and improved chip breakability was observed using cryogenic coolants due to effective control of chip temperatures. Bordin et al. (2016) concluded that the cryogenic machining significantly reduced the chip thickness compared to wet and dry machining conditions due to the improved chip segmentation mechanism at low cutting zone temperatures.

#### **2.4.4 Effect of cryogenic machining on surface integrity**

While machining, final product fatigue strength significantly affected by surface integrity characteristics. The major surface integrity characteristics includes surface finish, surface topography, microstructure, microhardness, white layer/depth of affected layer, residual stresses and phase transformation. Product life increases with low surface roughness, good surface topography, low white layer formation, low residual stresses and high microhardness in the machined surface. The surface roughness studies were done extensively under the cryogenic machining as mentioned in the above discussions. It has been observed that improved surface finish was obtained in cryogenic environment during machining of various kinds of materials such as titanium alloys, nickel based alloys and different grades of steels. Few authors have examined the impact of machining environment on surface integrity characteristics. Poulachon et al. (2005) correlated white layer formation with the tool wear in hard turning and concluded that

white layer thickness increases with increase in tool wear. They gave another conclusion that white layer is not an advantageous and have the negative impact on surface wear resistance. Umbrello and Filice (2009) have performed the experimental investigation on AISI 52100 in dry orthogonal cutting condition and concluded that white layer thickness increases when both speed and feed rate increases due relative cutting temperature variations. However, very few attempts have been made on measurement of white layer, microhardness, surface topography and residual stresses under the cryogenic machining.

However, very few attempts have been made in measurement of white layer under the cryogenic machining. Umbrello et al. (2012) studied role of LN<sub>2</sub> on surface integrity characteristics while orthogonal cutting of AISI 52100 and found that substantial reduction of cutting temperature greatly enables the changes in the machined workpiece microstructure causes the improvement in the product quality characteristics compared to the dry machining. It was also found minimum white layer thickness in cryogenic machining compared to dry machining during machining of AISI 52100 as shown in Figure 2.17. The reported reason is that it crosses the austenitizing temperature in dry machining due to more temperature generation resulting in thermal softening of material and subsequent quenching with LN<sub>2</sub> cooling within tiny time. Because of lacking time, it cannot revert into the martensite stage. In their work, they observed white layer in the SEM as shown in Figure 2.18 and it found it as featureless structure. Rotella et al. (2013) provided LN<sub>2</sub> cooling at both rake and flank faces of the tool using two external nozzles. They have observed improved surface integrity performance characteristics as function of microhardness and phase transformation in cryogenic machining because of decrease of grain size in microstructure compared to dry, MQL machining during turning of titanium alloy. Schoop et al. (2016) have studied the effect of turning cutting conditions and machining environment on performance characteristics particularly function of surface integrity in machining of porous tungsten material under the external cryogenic environment. In their study, they sprayed the LN<sub>2</sub> at the machining zone and results showed that cryogenic machining have improved the surface integrity due to increased hardness of cutting tool. Kaynak (2014) performed experiments on Inconel 718 material

under the dry, MQL and cryogenic machining environments at varying cutting speed conditions and obtained low peak valley height on the machined surface in cryogenic machining over the dry and MQL machining environments as shown in Figure 2.19. It has been found that good surface topography in cryogenic machining is attributed due to the less thermal distortion and less tool wear. Dinesh et al. (2015) observed similar results during machining of ZK60 magnesium alloys.

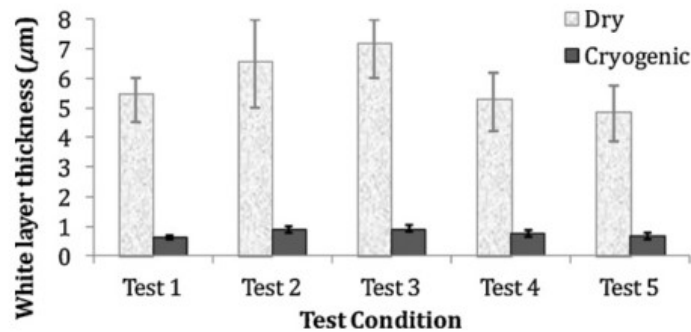


**Figure 2. 17** Experimentally obtained white layer thickness (Umbrello et al., 2012).

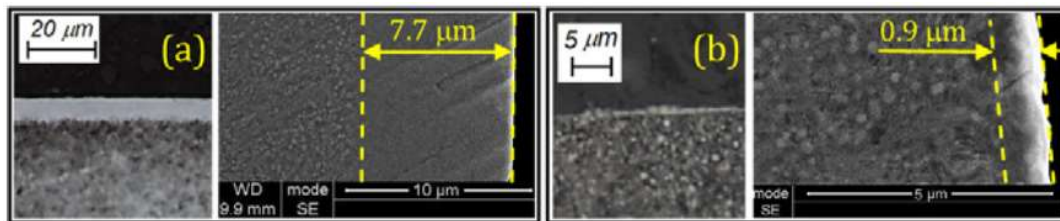


**Figure 2. 18** White layer in dry (a) and cryogenic machining (b): at  $v = 75$  m/min, hardness=  $61 \pm 1$  and chamfered tool (Umbrello et al., 2012).

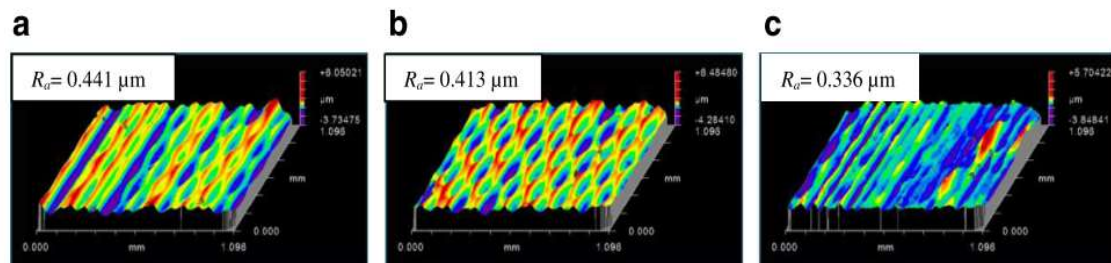


**Figure 2. 19** Surface topography and roughness of machined components a) Dry, b) MQL and c) Cryogenic at  $v = 120$  m/min (Kaynak, 2014).



Kaynak et al. (2014) reviewed the various surface integrity characteristics under the different machining environments and observed that, among all, cryogenic machining significantly improved the product quality and performance. They also investigated the effect of cryogenic coolant on the surface integrity characteristics like surface roughness and surface topography during machining of AISI 304L and found similar results. Kaynak et al. (2014) have conducted the experiments on NiTi shape memory alloy under the dry and cryogenic environments at varying cutting speeds and investigated the different surface integrity characteristics in terms of microhardness, depth of affected layer, transformation temperature, transformation response and latent heat for transformation. They observed positive subsurface alteration in cryogenic machining over dry machining due to the significant reductions in the machining zone temperatures. Bruschi et al. (2016) have investigated the turning performance characteristics as a function of coefficient of friction,  $V_b$ ,  $R_a$ , microhardness and residual stresses under the cryogenic, dry machining environments during machining of additive manufactured Ti-6Al-4V alloy. They have observed significant improvements in results except surface roughness under the cryogenic machining. The quantity and type of residual stresses formed in product during machining significant affects the life of the product greatly. During machining, higher cutting temperatures causes for development of residual stresses in the product. In general, after machining, there are two types of stresses presents namely compressive stresses and tensile stresses respectively. Compressive stresses are favorable to the machined product whereas presences of tensile stresses are not acceptable, because these will develop due to the higher cutting temperatures. There are different factors which affect the quantity and type of residual stresses in turning process such as tool geometry, cutting parameters and cutting environment. Among all, cooling conditions plays a very significant role on residual stresses because cooling conditions enables reductions in cutting temperature. Limited researchers have studied the residual stresses during machining of difficult to cut materials under the cryogenic cooling environment. Pusavec et al. (2011) have used two external nozzles to direct the  $LN_2$  at rake and flank faces respectively during machining of Inconel 718 material under

dry, cryogenic, MQL and cryo+MQL machining conditions. It has been showed that cryo+MQL machining combination facilitated better surface integrity characteristics in terms of surface hardness, surface roughness and residual stress compared to other cooling combinations due to better cooling and lubrication. They also found that increase in microhardness in cryogenic machining is attributed due to the decrease of grain size in the microstructure as depicted in Figure 2.20. Kenda et al. (2011) have obtained similar results while machining of Inconel 718. Pu et al. (2012) had conducted experiments on AZ31B Mg alloy with two different cutting edge radius tools under the dry and external cryogenic machining environments. They studied the different surface integrity characteristics like surface roughness, residual stresses, feature less surface layer, microhardness and phase transformation. They found better surface integrity characteristics in cryogenic machining over the dry machining. Also, it was claimed that use of large edge radius tools along with cryogenic cooling environments improved the functional performance of the product due to large and deep compressive stresses compared with dry machining.

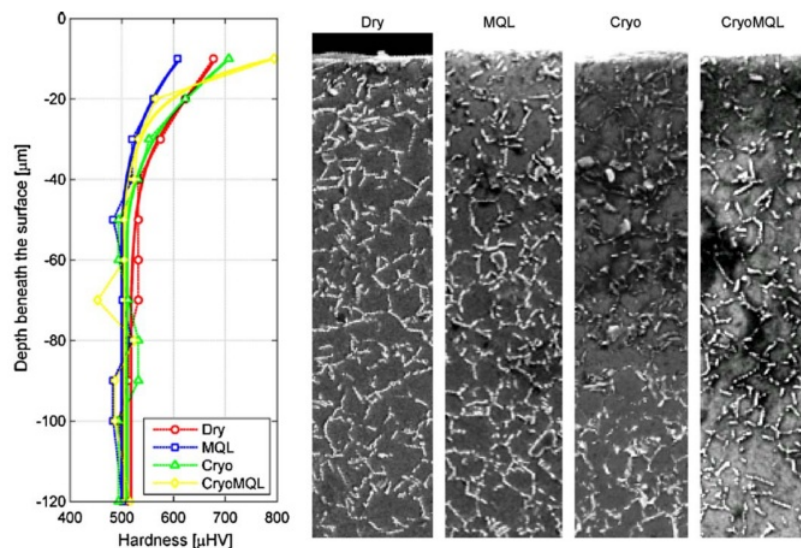


**Figure 2. 20** Hardness measurements beneath the machined surface (profile), machined under different cooling lubrication conditions and their correlation with the metallographic structure of the material beneath the surface (Pusavec et al., 2011).

## 2.5 OPTIMIZATION AND MODELING TECHNIQUES UNDER DIFFERENT

### COOLING ENVIRONMENTS

#### 2.5.1 Single objective optimization using Taguchi technique

Selection of optimum process cutting conditions helps to improve the performance of any manufacturing process. In any process or product design, Taguchi technique is one of the robust designs which have been used for determination of optimum process parameter settings. Many researchers have used Taguchi method for optimizing the single objective in machining applications.

Sahoo and Pradhan (2013) observed superior turning performance characteristics like  $R_a$  and  $V_b$  while turning of Al/SiC<sub>p</sub> metal matrix composite using Taguchi methodology with tungsten carbide inserts. From the tool wear analysis, it was found to be abrasion and adhesions were most dominated wear mechanisms. ANOVA results found that  $R_a$  and  $V_b$  were extremely influenced by spindle speed and feed rate respectively. Also, mathematical regression models were developed for responses and found minimum error amid the predicted and experimental results. Negrete (2013) observed reduced energy consumption and  $R_a$  of turning process using Taguchi method in machining of AISI 6061 T6 material. Philip Selvaraj et al. (2014) reported that during turning of nitrogen alloyed duplex steel, substantial improvements in quality characteristics like tool wear, cutting forces and surface roughness were observed using Taguchi predicted optimum parameters settings. Senthilkumar et al. (2016) have used Taguchi method and achieved a reduction of 53.86 %, 15.95 % for  $V_b$  and  $R_a$  respectively while machining of hardened alloy steel material. From ANOVA, it has been observed that cutting insert shape is the most affected process parameter on turning performance characteristics. Dureja et al. (2014) optimized the turning process in machining of AISI D3 steel by applying the Taguchi method. In their study tool wear and surface roughness were treated as responses. Sarikaya and Gullu (2014) investigated on AISI 1050 steel material under the MQL environment using Taguchi and RSM analysis and positive results were obtained. Debnath et al. (2016) have used Taguchi technique for optimizing the MQL

fluid flow rate and cutting parameters in turning of mild steel and better results were obtained in  $R_a$  and  $V_b$  at the optimum conditions. Also conducted ANOVA and feed rate, cutting speed were found to be more affecting process parameter on  $R_a$  and  $V_b$  respectively. Manivel and Gandhinathan (2016) in their study tool nose radius, depth of cut, feed rate and cutting speed were considered as hard turning process controllable parameters in machining of austempered ductile iron (grade 3) material and  $R_a$  and  $V_b$  were treated as responses. They applied Taguchi optimization analysis and obtained significant improvement in output responses. Gupta et al. (2015) used Taguchi optimization technique and determined the optimum cutting parameters while turning of EN24 steel. In their study, experiments were carried out on EN24 alloy steel during turning with uncoated tungsten carbide insert tool using Taguchi  $L_9$  orthogonal array in order to optimize the cutting parameters. Process parameters like cutting speed, feed rate and different cooling conditions (i.e. dry, wet and liquid nitrogen used as a coolant) were considered as input turning process parameters and tool wear (crater and flank wear) was considered as output response. Thakur et al. (2010) studied the impact of cutting parameters (type of tool, speed, feed rate and depth of cut) on tool life and work hardening during high speed turning of Inconel 718. They have done the ANOVA analysis for tool wear. They found that cutting speed, feed, and type of tool were the most significant deciding parameters on tool wear and postcryogenic-treated tool improved the performance in terms of tool life and work hardening. Also, they concluded that postcryogenic-treated tool reduced the cutting force from 10%-15% compared to untreated tools and 7% decrease in residual stress compared to the untreated tool. Asiltürk and Akkuş (2011) considered the cutting speed, feed rate and depth of cut as controllable process parameters and improved the surface quality of the AISI 4140 turned product with coated WC insert by employing the Taguchi methodology. Also performed ANOVA and revealed that feed rate is the most significant process parameter on the surface quality. Fetecau and Stan (2012) used Taguchi methodology and improved the turning performance in machining of polytetrafluoroethylene composite material. Davim (2003) employed ANOVA to know the effect of turning process parameters

cutting time, feed rate and depth of cut on surface roughness, cutting power and tool wear in machining of A356/20SiC<sub>p</sub>/T6 type MMC. It has been found that cutting speed has the highest effect on the cutting power and tool wear, feed rate has the most influence on surface roughness. He also developed regression models and good correlation was observed amid the predicted and experimental results with minimum error. Singh and Kumar (2006) yielded the better improvement in the turning process using Taguchi optimum parameters in machining of EN24 steel material and found that cutting forces were significantly affected by depth of cut parameter. Kirby et al. (2006) considered the tool nose radius, depth of cut, feed rate and cutting speed as process parameters in turning of 6061-T6 aluminum alloy and output response is taken as surface roughness. Taguchi method was used to predict the optimum parameters and it was conformed that surface roughness was reduced at the optimum parameters. It has been observed that surface roughness is highest influenced by nose radius and feed rate respectively. Hwang and Lee (2010) observed enhancement in the machinability characteristics were observed in turning of AISI 1045 using Taguchi method under wet and MQL environments. Sarıkaya et al. (2016) have applied single objective optimization Taguchi technique and obtained optimum process parameters in terms of cooling type, cutting speed and feed rate respectively for attaining low R<sub>a</sub> and low V<sub>b</sub> in turning of Hayness 25 super alloy. Gaitonde et al. (2008) conducted experiments on brass material using K10 carbide tool based on Taguchi's L<sub>9</sub> orthogonal array under the MQL environment. From ANOVA it was identified that feed rate is the most influenced process parameter on R<sub>a</sub> and F<sub>c</sub>.

### **2.5.2 Multi objective optimization using GRA and TOPSIS**

One of the methods to improve the performance characteristics of any process is to work at the optimum cutting conditions. Selection of optimum cutting conditions for single response problems is easy. Nowadays, all industry requirements are improved multi response performance characteristics and selection of optimum cutting conditions for multi response optimization is a difficult task (Aggarwal et al., 2008). Therefore, many

researchers have been used many meta-heuristic optimization techniques like GA (Khandey et al., 2017), PSO (Munish Kumar Gupta et al., 2015), SA (Hu et al., 2016) for solving the multi objective problems. But these techniques requires high-end mathematical/statistics back ground knowledge, computer coding knowledge and takes long computing time, owing to these reasons these are complex to execute by individuals and little practical use (Rajyalakshmi and Ramaiah, 2013). Likewise, there are multiple attribute decision making methods (MADMs) such as Grey, ELECTRE I, II, VIKOR, AHP, PROMOTHEE, TOPSIS and Fuzzy TOPSIS for solving uncertainty data multi-objective problems. Among all MADM techniques, Grey relational analysis (GRA) and TOPSIS analysis were frequently used in the selection of optimum machining conditions for various machining operations due their ease with usage.

Many researchers have improved the different process performance characteristics using TGRA. Lin (2015) carried out experiments on S45C steel bar according to the L<sub>9</sub> orthogonal design and optimized the dry turning process using Taguchi based grey relational analysis (TGRA). In his study parameters like cutting speed, feed rate and depth of cut were treated as controllable input parameters and tool life, cutting force and surface roughness were taken as output responses. It has been found that optimum process parameters determined by TGRA increased the tool life by 150 %, reduced the cutting force and surface roughness by 58 % and 122 % respectively. Tzeng et al. (2008) performed experiments on SKD11 tool steel based on L<sub>9</sub> orthogonal design to optimize the wet turning performance characteristics like average roughness, maximum roughness and roundness using TGRA. Cutting speed, feed rate, depth of cut and cutting fluid ratios were taken as controllable process parameters. Through conformation test it was found that significant improvement in the turning performance characteristics was observed with TGRA. Sarikaya and Gullu (2015) employed TGRA for optimizing the turning process in machining of hard to cut Hayness 25 material under minimum quantity lubrication (MQL) environment. They have considered L<sub>9</sub> experimental design to carryout experimental work, tool wear and surface roughness were considered as quality

characteristics and 34.9 % improvement in the grey relational grade was observed. Ranganathan and Senthilvelan (2011) attempted TGRA for optimizing the hot turning performance qualities while machining of SS 316. It was found that TGRA increases the tool life and MRR by 13.5 % and 99 % respectively and reduces the surface roughness by 16 %. From the ANOVA, it was determined that feed rate is the most dominant parameter on the hot turning performance. Ramanujam et al. (2011) employed TGRA to optimize the dry turning process of MMC (A356/10/SiC<sub>p</sub>) material. Cutting speed, feed rate and depth of cut were considered as process parameters and specific power, surface roughness were taken as output responses respectively. The confirmation experiment was carried out using TGRA determined optimum cutting conditions and significant improvement was found in turning performances characteristics were observed. Goel et al. (2015) employed Taguchi based grey relational analysis to optimize the turning process of mono-crystalline germanium material under wet environment with single point cutting tool. Top rake angle, tool overhang, depth of cut, tool feed rate, and rotational speed of the workpiece were considered as process parameters. Surface roughness profile error and waviness error were taken as target responses, improvement in turning performances characteristics were obtained through the conformation test. From the analysis of variance (ANOVA) it has been concluded that feed rate is the most influenced process parameter of turning performance characteristics. Senthilkumar et al. (2014) obtained reduced tool flank wear by 92.67 %, surface roughness by 0.67 % with an increase in MRR by 7.28 % in high speed turning of hardened alloy steels using optimal process parameters obtained by weighted grey relational analysis. Kibria et al. (2013) has been conducted experiments on alumina (Al<sub>2</sub>O<sub>3</sub>) ceramic material in Nd:YAG laser micro-turning operation and 30 % reduction of surface roughness and 48 % reduction of micro turning depth deviation have been observed using grey relational analysis. Abhang and Hameedullah (2011) applied TGRA to the dry turning of EN-31 steel and through conformation test it was perceived that 16.06 % improvement in surface finish and 27.30 % reduction in chip thickness were noted. Siddiquee et al. (2013) determined optimum micro-countersinking process parameters like rake angle, feed and speed using

Grey relational analysis coupled with principal component analysis. In their study out-of-roundness and eccentricity of the countersunk hole were considered as output responses. From ANOVA it has been found that interaction between feed and speed has the most influence on micro-countersinking process. Manna (2013) employed Taguchi based grey relational analysis to optimize the thrust force and surface roughness in drilling of LM6Mg15SiC-Al-MMC composite material and there was improvement of 69.3 % on thrust force and 180.4 % on surface roughness were observed. Siva et al. (2015) employed TGRA to optimize multiple response of dimensional stability, wear resistance, and hardness for deep cryogenic treatment (DCT) process parameters for 100Cr6 bearing and the cooling rate, soaking temperature, soaking time and tempering temperature were considered as process parameter steel. They observed that at the optimum cryotreated condition 13.77, 49.02 and 19.35 % improvement in dimensional stability, wear resistance and hardness respectively. Also performed ANOVA and found that soaking temperature influence most in deep cryogenic treatment process. Kumar and Kumar (2014) applied Grey relational analysis to determine the optimum cryogenically cooled electric discharge machining (EDM) process parameters. process parameters includes electrode environment (conventional electrode and cryogenically cooled electrode), discharge current, pulse on time, gap voltage on the other side material removal rate, electrode wear, and surface roughness were considered as multiple responses in machining of Al-SiC<sub>p</sub> metal matrix composite. Cryogenic cooled electrode, the current is 9 A, the pulse on time 100 ms and the gap voltage 65 V were determined as the optimum process parameters.

Several researchers have used Technique for Order Preference by Similarity to Ideal Solution (TOPSIS) in material selection for a given engineering application (Rao and Davim, 2008), IC packing application (Wang et al., 2016), site selection evaluation (Sánchez-Lozano et al., 2014), selection of modern machining methods (Cortés Sáenz et al., 2015), robot selection for a given industrial application (Rao et al., 2011) and evaluation of aggregate risk in green manufacturing



(Sivapirakasam et al., 2011), optimum concrete mixture selection for civil application ( Baris Simsik and Tayfun Uygunoglu, 2016). Very few researchers have been attempted the TOPSIS method for multi objective optimization in machining application. Yuvaraj and Kumar (2014) optimized the multi objectives in AJM during machining of AA5083-H32 material by using Taguchi coupled TOPSIS method and achieved improved performance results. Manivannan and Kumar (2016) have applied Taguchi coupled TOPSIS method to optimize the micro EDM drilling process parameters in machining of AISI 304 under the cryogenic cooling environment and obtained improved results. Singh et al. (2011) obtained the optimum cutting conditions in the dry turning of GFRP composite material and obtained advantages various surface roughness quality characteristics using TOPSIS. Ramesh et al. (2016) applied different optimization techniques like GRA, TOPSIS and RSM for optimizing the turning process while machining of magnesium alloy AZ91D under the dry environment and found improved results using all optimization techniques. Wu (2015) concluded that any individual MADM method is not accurate and different MADM methods gives different solutions for particular engineering problem. So the best way to find the best result concerning to the problem is to compare the results by applying the different MADM methods and select the suitable MADM method for that problem.

### **2.5.3 Optimization and modeling of machining process parameter using response surface methodology (RSM)**

Many researchers have used RSM for prediction and optimization of various kinds of processes during cutting of different kind of materials. Aggarwal et al. (2008) investigation involves the effect cutting process parameters and cutting environment on power consumption in turning of AISI P-20 tool steel using RSM. It was revealed that cryogenic environment contributed more influence on power consumption. They also compared optimum results which were obtained from Taguchi, RSM methods respectively and concluded that RSM have edge over the Taguchi method. Gupta et al. (2015) considered side cutting edge angle, cutting speed and feed rate were

taken as turning process parameters and studied its effect on tool-chip contact length, tool wear, surface roughness and cutting force using RSM during machining of titanium (grade 2) alloy under MQL environment. They also found the optimum process parameter using RSM desirability analysis. In another work, Gupta et al. (2016) carried out experiments under the nanofluid based MQL environment by considering approach angle, feed rate and cutting speed as process parameters and responses as cutting force, surface roughness, tool wear and cutting temperature respectively in turning of titanium alloy. They used RSM to explain the effect of process parameters on responses and they claimed that cutting speed significantly affects the turning responses. They found improved turning performance characteristics at approach angle  $84^\circ$ . Makadia and Nanavati (2013) have studied the optimization and modeling of turning process in machining of AISI 410 steel using RSM. It was observed that RSM developed model predicted the surface roughness with an accuracy of 6 % and also found that surface roughness is most influenced by feed rate. Asiltürk et al. (2016) conducted experiments on Co28Cr6Mo ASTM F 1537 steel (medical material) in turning process and RSM was used for their investigation. In their study, they treated  $R_a$  and  $R_z$  as quality characteristics and nose radius, depth of cut, feed rate and cutting speed as process parameters respectively. ANOVA results showed that nose radius parameter has the most influence on surface quality characteristics. They found that the RSM developed models predicted the results with minimum error and suggested use to similar type of application. Bouacha et al. (2010) developed the relationship between the input process parameters (depth of cut, feed rate and cutting speed) and output responses (cutting force and surface roughness) for turning process in machining of AISI 52100 steel using RSM. Also from ANOVA investigation, it was found that surface roughness is highly sensitive to feed rate whereas cutting force is most influenced by depth of cut respectively. Bouacha et al. (2014) analyzed the effect of process parameters like cutting time, depth of cut, feed rate and cutting speed on hard turning performance characteristics (material removal rate, cutting forces, tool wear and surface roughness) using RSM in machining of AISI 52100 bearing steel and also established relation between the input

and output responses. Mandal et al. (2011) carried out the experimental investigation on tool wear by taking into account of depth of cut, feed rate and cutting speed as process parameters in turning of EN 24 steel with developed cutting tools using RSM. It has been concluded that the developed RSM model well predicted the responses within the range of given process parameters. Also, found that tool wear is highly sensitive to the cutting speed using ANOVA investigation. Similarly, Mandal et al. (2013) used RSM for prediction and optimization of surface roughness in turning of AISI 4340 steel. It was concluded that improved surface roughness was obtained at higher cutting speed. Mandal et al. (2012) developed Zirconia Toughened Alumina (ZTA) inserts and established the relation between the input parameters (depth of cut, feed rate and cutting speed) and output responses (cutting forces). Also they obtained minimum cutting forces using desirability analysis. Bhushan (2013) achieved low power consumption and low tool wear in turning of 7075 Al alloy + 15 % SiC (20-40 mm) composite material using RSM. Also, they predicted the responses by developing the relationship amid the responses and process parameters. Palanikumar (2008) have used Taguchi method, RSM respectively for optimization and modeling of turning of turning process while machining of glass fiber reinforced plastic (GFRP). He considered surface roughness as response and found that surface roughness is most influenced by feed rate. Also, he has used RSM for predicting the surface roughness and fairly close results were obtained compared experimental results. Routara et al. (2009) have studied the optimization, modeling and analyses of surface roughness in end milling using RSM in machining of three different materials namely aluminium, brass and mild steel. Seeman et al. (2010) developed the machinability evaluation model using RSM in turning of homogenized 20% SiC<sub>p</sub>-LM25 Al metal matrix composite (MMC) and well agreement was observed between the input and output variables. In their study, tool flank wear and surface roughness were optimized using desirability analysis. ANOVA results showed that at lower cutting levels of cutting speed, feed rate and depth of cut causes low tool wear. Whereas, low surface roughness was observed at high cutting speed, low feed rate and depth of cut respectively. Aouici et al. (2011) conducted the modeling and optimization studies in

hard turning process during machining of AISI H11 hardened steel using RSM. In their study, process parameters were considered as depth of cut, feed rate and cutting speed and responses as tool wear and surface roughness respectively. They also employed ANOVA and found that the most influenced process parameters are cutting time and feed rate on tool wear and surface roughness respectively. Palanikumar and Karthikeyan (2006) applied RSM for experimental investigation, optimization and modeling of turning process in machining of LM25 Al+SiC particulate composites. It was found that feed rate and percentage of SiC particulates were most dominant parameters for surface roughness. In their study results showed that significant improvement was observed in turning process using RSM desirability analysis. Chauhan and Dass (2012) in their study, RSM investigation was explored on cutting force and surface roughness in turning of titanium (grade 5) material by considering process parameters as approach angle of the tool, depth of cut, feed rate and cutting velocity respectively. Results showed that surface roughness was increased with an increase in cutting speed and feed rate respectively, whereas it was decreased when the approach angle decreases. In the case of cutting force was decreased with decrease in cutting speed and depth of cut respectively, whereas it was increased with increase in approach angle. Also, carried out the modeling studies and good fit was observed between the experimental and predicted results. Priyadarshi and Sharma (2015) investigated the effect of turning cutting conditions and SiC-Gr composition on cutting force and surface roughness using RSM in machining of Al-6061-SiC-Gr hybrid nanocomposites material. From the results, it was found that results were most influenced by feed rate. They also performed optimization and modeling studies, positive outcomes were observed. Jeyakumar et al. (2013) applied RSM and assessed the tool wear, surface roughness and cutting forces in end milling process during machining of Al6061/SiC composite. Table 2.1 summarized the effect of cryogenic spray/jet cooling environment on turning performance characteristics while machining of various difficult to cut. Table 2.2 summarizes the literature available on GRA, TOPSIS and RSM optimization techniques in turning of various materials under different machining environments.

**Table 2. 1** Contributions of earlier researchers on difficult to cut materials during turning with cryogenic jet cooling method.

S.No.	Author (year)	Material	Turning performance characteristics											
			T	V <sub>b</sub>	F <sub>c</sub>	CM	μ	R <sub>a</sub>	ST	H <sub>v</sub>	PT	R	WL	
1	Kumar and Choudhury (2008)	SS 202		√	√									
2	Hong and Ding (2001)	AISI 1008	√	√	√	√	√							
3	Hong et al. (2002)	Ti-6Al-4V, AISI 1018					√							
4	Hong et al. (2001)	Ti-6Al-4V			√		√							
5	Jun (2005)	Ti-6Al-4V, AISI I018					√	√						
6	Khan and Ahmed (2008)	AISI 304		√										
7	Khan et al. (2010)	AISI 304		√				√						
8	Dhananchezian et al. (2011)	AISI 304	√	√	√			√						
9	Dhananchezian and Kumar (2010;2011)	Ti- 6Al-4V, Al 6061-T6 alloy	√	√	√			√						
10	Jerold and Kumar (2011;2012;2013)	AISI 316, Ti-6Al-4V, AISI 1045	√	√	√	√		√						
11	Venugopal et al. (2007a;2007b)	Ti-6Al-4V alloy		√										
12	Bermingham et al. (2011)	Ti-6Al-4V alloy		√	√	√								
13	Paul et al. (2001)	AISI 1060		√				√						
14	Paul and Chattopadhyay (2006)	AISI1040, AISI1060, AISI E4340C, AISI 4140, AISI 4320	√	√	√	√								
15	MacHai and Biermann (2011)	Ti-10V-2Fe-3Al		√	√	√								
16	Yap et al. (2013)	Ti54			√		√	√						
17	Klocke et al. (2013)	γ-TiAl		√	√	√		√						
18	Raza et al. (2014)	Ti-6Al-4V alloy		√				√						
19	Kaynak (2014)	Inconel 718	√	√	√	√								
20	Bordin et al. (2015)	AM Ti-6Al-4V alloy		√		√		√						

21	Bordin et al. (2016)	AM Ti-6Al-4V alloy		√		√		√						
22	Sartori et al. (2017)	AM Ti-6Al-4V alloy		√										
23	Pereira et al. (2016)	AISI 304		√	√			√	√	√				
24	Chetan et al. (2015)	Nimonic 90 alloy		√		√		√						
25	Hong et al. (1999)	AISI 1008	√			√								
26	Dhar and Kamruzzaman (2007)	AISI 4037	√	√				√						
27	Dhar et al. (2001)	AISI 1040 and E4340C steels	√	√				√						
28	Schoop et al. (2015)	porous tungsten material		√				√						
29	Yap et al. (2013)	Ti-5Al-4V-0.6Mo-0.4Fe				√		√	√					
30	Sun et al. (2015)	Ti-4Al-6V	√	√	√									
31	Gupta et al. (2015)	AISI 1040	√	√	√			√						
32	Dinesh et al. (2016)	ZK60 magnesium alloy	√	√	√			√	√		√			
33	Umbrello et al. (2012)	AISI 52100						√			√	√	√	√
34	Rotella et al. (2013)	Ti-4Al-6V						√			√	√		
35	Schoop et al. (2016)	porous tungsten	√			√	√	√						
36	Kaynak (2014)	Inconel 718	√	√			√	√	√					
37	Dinesh et al. (2015)	ZK60 magnesium alloy	√			√					√			
38	Kaynak et al. (2014)	AISI 304L						√	√					
39	Kaynak et al. (2014)	NiTi									√	√		√
40	Bruschi et al. (2016)	Ti-6Al-4V alloy		√				√			√		√	
41	Pusavec et al. (2011)	Inconel 718						√			√	√	√	
42	Pu et al. (2012)	AZ31B Mg alloy						√			√	√	√	√
43	Kenda et al., (2011)	Inconel 718						√			√	√	√	

R<sub>a</sub> = Surface roughness; T = Cutting temperature; F = Cutting force; TW = Tool wear; CM = Chip morphology; μ = Coefficient of friction; R = Residual stresses; PT = Phase transformation; ST = Surface Topography; HV = Microhardness; WL = White layer thickness

**Table 2. 2** Literature report available on optimization and techniques during turning of different materials under environments.

S.No.	Author (s) and year	Material	Machining environment	Optimization technique used	Turning performance characteristics					
					V <sub>b</sub>	R <sub>a</sub>	F	MRR	P	R
1	Sahoo and Pradhan (2013)	Al/SiC <sub>p</sub> MMC	Dry	Taguchi	√	√				
2	Negrete (2013)	AISI 6061 T6 material	Dry	Taguchi		√			√	
3	Philip Selvaraj et al. (2014)	duplex steel	Dry	Taguchi	√	√	√			
4	Senthilkumar et al. (2016)	Hardened alloy steel	Dry	Taguchi	√	√				
5	Dureja et al. (2014)	AISI D3 steel	Dry	Taguchi	√	√				
6	Sarikaya and Gullu (2014)	AISI 1050 steel	MQL	Taguchi		√				
7	Debnath et al. (2016)	mild steel	MQL	Taguchi	√	√				
8	Manivel and Gandhinathan (2016)	Austempered ductile iron (grade 3)	Dry	Taguchi	√	√				
9	Gupta et al. (2015)	EN24 alloy steel	Dry, Wet, Cryogenic	Taguchi	√					
10	Thakur et al. (2010)	Inconel 718	MQL	Taguchi	√		√			
11	Asiltürk and Akkuş (2011)	AISI 4140	Dry	Taguchi		√				
12	Fetecau and Stan (2012)	Polytetrafluoroethylene composite material	Dry	Taguchi		√	√			
13	Davim (2003)	A356/20SiC <sub>p</sub> /T6 type MMC	Dry	Taguchi		√	√		√	
14	Singh and Kumar (2006)	EN24	Dry	Taguchi			√			
15	Kirby et al. (2006)	6061-T6	Dry	Taguchi		√				
16	Hwang and Lee (2010)	AISI 1045	Wet, MQL	Taguchi		√	√			
17	Sarikaya et al. (2016)	Hayness 25	Dry, MQL	Taguchi	√	√				
18	Gaitonde et al. (2008)	brass	MQL	Taguchi		√	√			
19	Lin (2015)	S45C steel	Dry	GRA	√	√	√			
20	Tzeng et al. (2008)	SKD11 tool steel	Dry	GRA		√				√
21	Sarikaya and Gullu (2015)	Hayness 25	MQL	GRA	√	√				

22	Ranganathan and Senthilvelan (2011)	SS 316	TAM	GRA	√	√		√		
23	Ramanujam et al. (2011)	A356/10/SiC <sub>p</sub> MMC	Dry	GRA		√			√	
24	Goel et al. (2015)	mono-crystalline germanium material	Dry	GRA		√				
25	Senthilkumar et al. (2014)	hardened alloy steels	Dry	GRA	√	√		√		
26	Abhang and Hameedullah (2011)	EN-31 steel	Dry	GRA		√				
27	Singh et al. (2011)	GFRP composite	Dry	TOPSIS		√				
28	Ramesh et al.(2016)	AZ91D	Dry	TOPSIS	√	√				
29	Aggarwal et al. (2008)	AISI P-20 tool steel	Dry, wet, Cryogenic	RSM					√	
30	Gupta et al. (2015;2016)	Titanium (grade 2)	MQL	RSM	√	√	√			
31	Makadia and Nanavati (2013)	AISI 410 steel	Dry	RSM		√				
32	Asiltürk et al. (2016)	Co28Cr6Mo ASTM F 1537 steel	Dry	RSM		√				
33	Bouacha et al. (2010;2014)	AISI 52100 steel	Dry	RSM	√	√	√	√		
34	Mandal et al. (2011)	EN 24	Dry	RSM	√					
35	Mandal et al. (2012;2013)	AISI 4340 steel	Dry	RSM		√	√			
36	Bhushan (2013)	7075 Al alloy+ 15 % SiC MMC	Dry	RSM	√				√	
37	Palanikumar (2008)	Glass fiber reinforced plastic (GFRP)	Dry	RSM		√				
38	Seeman et al. (2010)	20% SiC <sub>p</sub> -LM25 Al MMC	Dry	RSM	√	√				
39	Aouici et al. (2011)	AISI H11	Dry	RSM	√	√				
40	Palanikumar and Karthikeyan (2006)	LM25 Al+SiC MMC	Dry	RSM		√				
41	Chauhan and Dass (2012)	Titanium (grade 5)	Dry	RSM		√	√			
42	Priyadarshi and Sharma (2015)	Al-6061-SiC-Gr MMC	Dry	RSM		√	√			

$V_b$  = Tool wear;  $R_a$  = surface roughness; F = cutting forces; MRR = Material Removal Rate; P = Power; R = Roundness



## **2.6 SUMMARY OF THE LITERATURE REVIEW ON CRYOGENIC MACHINING**

- The conventional flood cooling technique not able to reduce the cutting temperature at tool-chip interface at higher cutting conditions and also these are chemical contaminants causes several health, environmental problems and additional disposal cost.
- Dry machining inactive in controlling the BUE on the cutting tool leads to poor product performance and high manufacturing cost.
- MQL is one of the eco friendly manufacturing processes. But MQL fails to control the machining zone temperatures at the industrial cutting conditions. Nevertheless, still MQL presents coolant mist at the machining surroundings, affects the operator health.
- Cryogenic machining approaches significantly improved the turning performance characteristics like cutting temperature, tool wear, cutting forces, chip morphology and surface integrity characteristics (surface roughness, surface topography, white layer thickness, residual stresses, microhardness and phase transformation) over the dry, wet and MQL machining conditions.
- Cryogenic precooling of workpiece method is limited to academic purpose only due to impractical in the industry. This method is uneconomical due to consumption of high LN<sub>2</sub>. Also, this method over cools the workpiece results in increased cutting forces and abrasion wear during machining which are not favorable for improvement of process performance.
- In indirect cryogenic cooling method, the effectiveness of LN<sub>2</sub> cooling highly depends on the thermal conductivity of tool material, insert thickness, distance from the high temperature source to LN<sub>2</sub> source and area of contact of cutting insert with LN<sub>2</sub> cooling chamber respectively.
- The initial cost investment required is high in cryogenic treatment process. Also, cryogenic treated tool performance varies from one machining process to another.

## **2.7 MOTIVATION FROM LITERATURE REVIEW**

Nowadays, the trend has been increasing towards the environmental damage free manufacturing processes due to severe environmental conscious regulations. Cryogenic assisting machining is an emerging manufacturing process because of non-toxic and environmentally clean process.

From the literature, it was found that cryogenic spray cooling/cryogenic external jet cooling method has many advantages like less coolant consumption, no unwanted cooling area, reduced cooling power wastage; localized cooling at the machining zone causes reduction of cutting zone temperatures. In the literature, many researchers have employed this method to machine different kinds of difficult to cut materials and observed better performance characteristics when compared to dry, wet and MQL machining conditions. Hence, the present study focused on the external cryogenic cooling method with LN<sub>2</sub> as coolant. From the literature, it was also found that method of supply of LN<sub>2</sub> at the machining zone significantly influences the turning performance characteristics greatly. In the current work, a low cost external cryogenic jet cooling setup has been developed to spray the LN<sub>2</sub> between the tool-workpiece interfaces.

However, few researchers have worked with various kinds of hard to cut materials like smart materials, super alloys and steels by using external cryogenic jet cooling method with LN<sub>2</sub> as a coolant. 17-4 PH SS is one which is widely used in various areas including nuclear reactor components, marine constructions, jet engine parts, aircraft fittings, missile fittings, oil field valve parts and rotors of the centrifugal compressors owing to excellent properties like high corrosion resistance, high strength and good ductility. 17-4 PH SS have many key applications; therefore, critical research has to be carried out on the surface integrity characteristics to improve the product life of the 17-4 PH SS. From the literature, no effort has been made to examine the effect of cutting conditions on turning performance characteristics in machining of 17-4 PH SS under the MQL, wet, dry and external jet cryogenic cooling environments. Therefore, the current work target is to explore the effect of external LN<sub>2</sub> jet cooling on cutting temperature, tool flank wear, MRR, chip morphology and surface integrity (surface topography, surface finish, microhardness and white layer thickness (WLT)) during machining of 17-4 PH SS and comparison of these findings with MQL, wet and dry machining conditions.

It is essential to determine the optimum cutting conditions and development of correlation models between the input process parameters and output responses to improve the productivity with low manufacturing cost. In the literature, no attempt has been made on modeling and optimization of turning process while machining of 17-4 PH SS under the cryogenic cooling environments.

## 2.8 OBJECTIVES OF THE PRESENT STUDY

The objectives of the present work are as follows

1. To develop the cryogenic machining setup.
2. To study the effect of liquid nitrogen on cutting temperature, tool flank wear, chip morphology, surface integrity and results will be compare with dry, wet, MQL machining environments while machining 17-4 PH stainless steel.
3. To determine the optimum cutting conditions for single response optimization for achieving better turning performance characteristics using the Taguchi technique.
4. To determine the optimum cutting conditions for multi response optimization for achieving better turning performance characteristics using Gray Relational Analysis (GRA) and Technique for Order Preference by Similarity to Ideal Solution (TOPSIS) techniques.
5. To develop a correlation models between process parameters and responses by using RSM.

Methodology followed for addressing the each objective as follows

1. Cryogenic setup was developed
2. One factor at a time approach experimental design has been used to investigate the turning performance characteristics under the cryogenic, MQL, wet and dry machining conditions.
3. Taguchi  $L_9$  orthogonal array experimental design has been used for optimization of cutting conditions for single and multiple objective responses under the cryogenic cooling environment. Taguchi method was used for single response optimization and ANOVA was used to find the most influenced process parameter on each response.
4. Taguchi coupled GRA and Taguchi coupled TOPSIS optimization techniques have been applied for multi response optimization, best multi optimization tool which suits for the current study have been selected based conformation test results.
5. Experiments were conducted based on response surface methodology (RSM) based face centered central composite design ( $L_{20}$ ) and development of correlation models between the input process parameters and output responses has been done.

## CHAPTER 3

### EXPERIMENTAL WORK

This chapter gives the details about experimental setups used to conduct experiments on 17-4 PH SS workpiece material, experimental details considered in the present work and different equipments used for measuring the different turning performance characteristics and their procedure. In the current work, performance characteristics like cutting temperature, tool flank wear, MRR, chip morphology and surface integrity (surface topography, surface finish, microhardness and white layer thickness (WLT)) were considered as turning performance characteristics.

#### 3.1 WORK MATERIAL

17-4 PH SS has many emerging applications in the field of aerospace industry, nuclear industry, chemical industry and marine industry owing to peculiar properties like high corrosion resistance, high ductility and high strength (Kochmański and Nowacki, 2006; Mohanty et al., 2015). The major chemical composition and microstructure of 17-4 PH SS is depicted in Figure 3.1. Machined samples were mirror polished with help of emery papers of different grades, diamond powders paste and ferric chloride (10 g FeCl<sub>3</sub> + 30 ml HCl +120 ml H<sub>2</sub>O) etchant was used for revealing the microstructure of 17-4 PH SS. Scanning electron microscope (SEM) has been used for evaluation of microstructure. Energy Dispersive X-ray spectroscopy (EDAX) has been used for evaluation of elemental composition of 17-4 PH SS. Table 3.1 and Table 3.2 show the chemical composition of 17-4 PH SS and mechanical properties respectively. These attractive properties make this material as an alternative to the high cost titanium material towards the aerospace industry (Chien and Tsai, 2003). Machinability characteristics of 17-4 PH SS material lack with poor surface quality and more built up edge (BUE) formation in the cemented carbide cutting inserts due to high cutting temperatures in dry cutting (Mohanty et al., 2015). Workpiece material was procured from the Sachin steel centre, Mumbai. Whereas, cutting tools were procured from Kennametal, Bangalore.

**Table 3. 1** Chemical composition of 17-4 PH stainless steel.

Element	Ni	Cr	Cu	Mn	Si	C	P	S	Nb	Fe
(%)	3.54	16.17	3.17	0.74	0.36	0.04	0.02	0.01	0.21	Balan
	6	9	7	4	0	2	8	1	0	ce

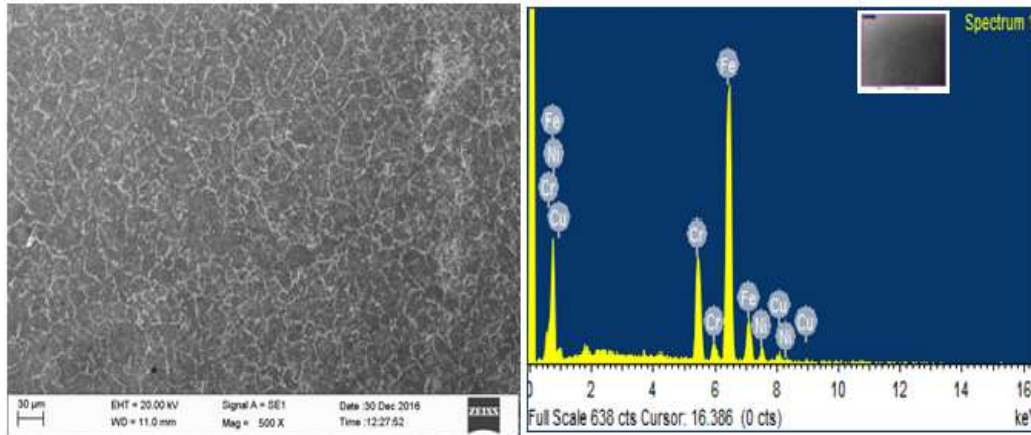


**Figure 3. 1** Microstructure and major elemental analysis of 17-4 PH SS workpiece material.

**Table 3. 2** Mechanical properties of 17-4 PH stainless steel.

Ultimate tensile strength (MPa)	Yield strength (MPa)	Elastic modulus (GPa)	Hardness (HRC)	Density (g/cm <sup>3</sup> )	Melting point (°C)	Thermal conductivity (W/m K)
1018	992	199	30	7.79	1300	17.9

## 3.2 DIFFERENT COOLING ENVIRONMENTS AND EXPERIMENTAL SETUPS

### 3.2.1 Cryogenic machining

In the current work, for cryogenic machining, a low cost external cryogenic jet cooling setup has been developed to spray the LN<sub>2</sub> between the tool-workpiece interfaces as shown in Figure 3.2. In this setup, LN<sub>2</sub> (at -196 °C) is stored in an ‘IOCL’ made ‘TA-55’ cryocan, stored LN<sub>2</sub> was pressurized with a compressed air to

obtain the jet of LN<sub>2</sub> through the nozzle. The schematic diagram of the external cryogenic cooling setup is shown in Figure 3.3.

### 3.2.2 Construction of cryogenic machining setup

The developed cryogenic cooling system consists of the following components namely 'TA55' model cryocan, compressor, modified stainless steel cap, flow regulator, pneumatic hose, pressure relief valve, braided stainless steel hose, and nozzle respectively.

Modified stainless steel cap was fabricated to close the cryocan at the top as shown in Figure 3.4. The modified cap design consists of two holes at the top of the cap and inserted two stainless steel pipes of same diameter of 8 mm in those two holes respectively. Among two stainless steel pipes, one is used to supply the compressed air into the cryocan with help of pneumatic hose and other is for LN<sub>2</sub> outlet respectively. A flexible braided stainless steel was used to transfer the LN<sub>2</sub> from the liquid nitrogen outlet from the cryocan to machining zone with help of a nozzle. A pressure relief valve is connected to the outlet pipe of the cryocan, this can avoid the excessive pressure inside the tank. A flow regulator valve is used to control the flow rate.

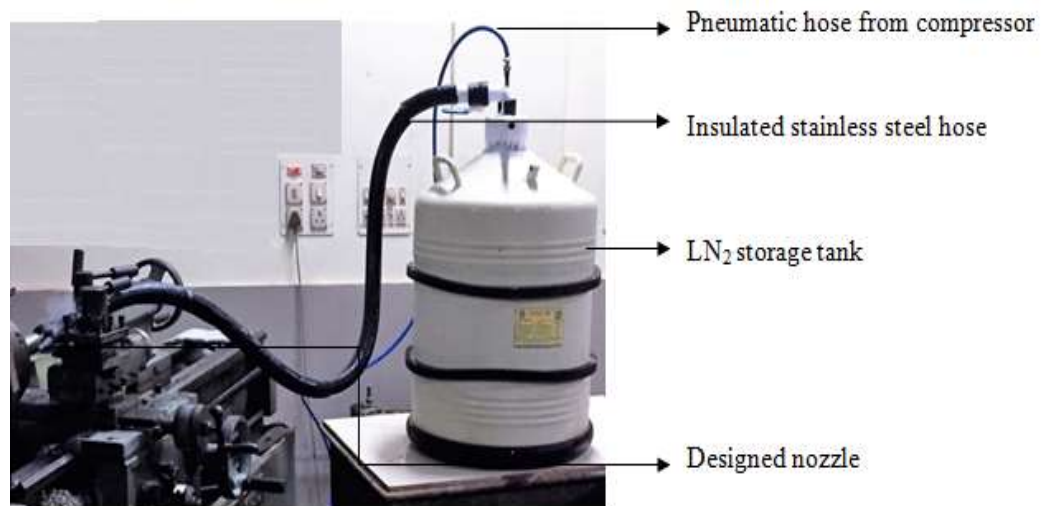


**Figure 3. 2** Cryogenic machining experimental setup.

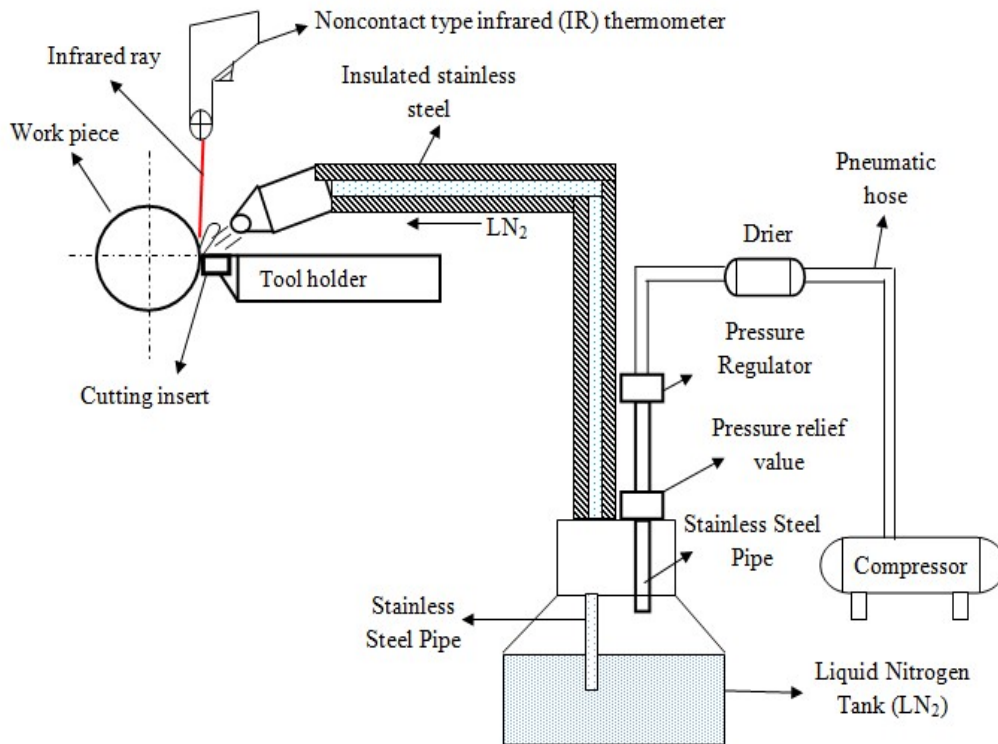


**Figure 3. 3** Schematic view of cryogenic liquid nitrogen machining setup.

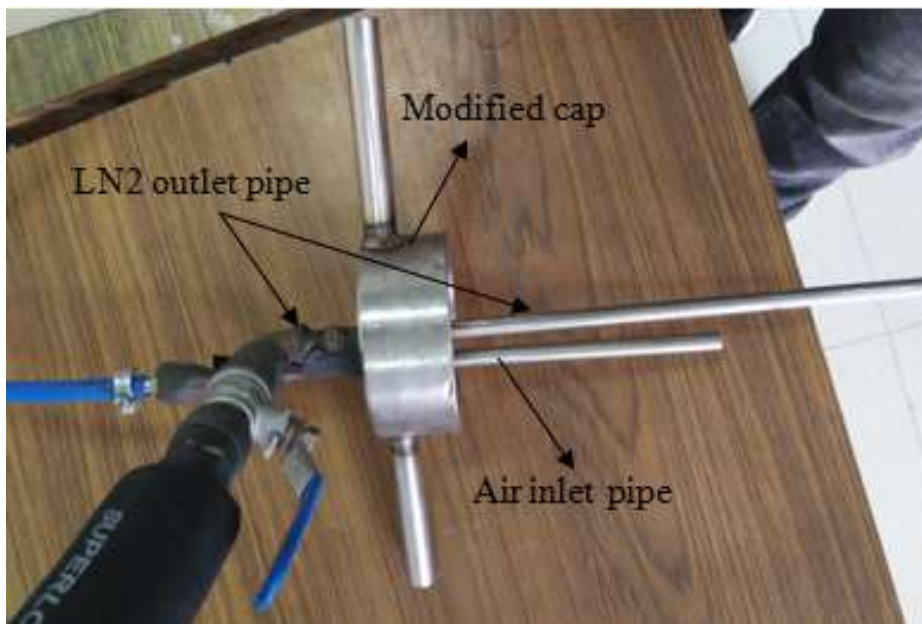


**Figure 3. 4** Modified cap for TA 55 cryocan.

### 3.2.3 MQL machining

Dropco make air oil mist lubricator of a model - 'DAOML - 2/ PS / FS/1' MQL machining setup has been used to supply the coolant air mist at the machining zone as shown in Figure 3.5.



Figure 3. 5 MQL machining experimental setup.

### 3.2.4 Wet and dry machining

In wet machining, emulsion type cutting fluid was used and which was obtained by mixing the water with soluble oil in 1:20 ratio. In dry machining, no coolant was supplied at the machining zone. The machining zone images at the different environments are depicted in Figure 3.6.

## 3.3 EXPERIMENTAL CONDITIONS

Turning experiments were performed on 17-4 PH SS round bars by using 'KIRLOSKAR' make lathe machine. This lathe consists of eight spindle speeds, maximum of 1200 rpm and with 32 feed tables. Table 3.3 shows the experimental conditions considered in the present thesis. Figure 3.7 shows the tool holder and cutting insert images have been used in the current work.



Figure 3. 7 (a) PSBNR 2020 K12 Tool holder (b) AlTiN PVD coated cutting insert.



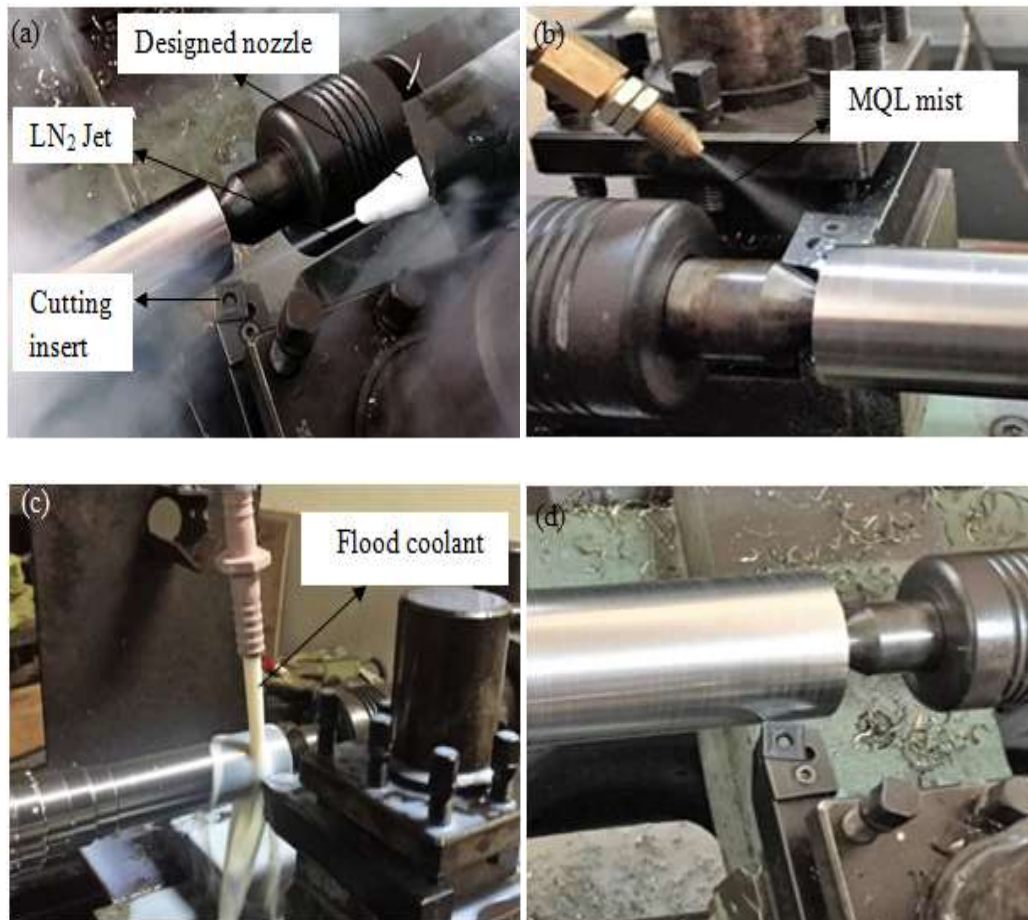


**Figure 3. 6** Machining zone at different environments (a) Cryogenic (b) MQL (c) Wet (d) Dry.

### 3.4 METHODOLOGY AND EXPERIMENTAL DESIGN

#### 3.4.1 Methodology

The methodology followed for the entire thesis as shown in Figure 3.8. The experiments have been conducted based on one factor at a time approach (OFATA) approach to know the effect of each process parameter on difference turning performance characteristics. For single and multi objective optimization, experiments were conducted based on Taguchi L<sub>9</sub> OA design. Face centered central composite rotatable design (CCRD) L<sub>20</sub> has been considered for RSM design analysis.

**Table 3. 3** Experimental conditions.

Workpiece material and dimensions	17-4 PH SS round bar, ( $\varnothing$ 35 mm x 150 mm)
Workpiece chemical composition	(Ni-3.546 %, Cr-16.179 %, Cu-3.177 %, Mn-0.744 %, Si-0.360 %, C-0.042 %, P-0.028 %, S-0.011 %, Nb+Ta-0.356 % and Fe-Balance)
Cutting inserts	AlTiN PVD coated KC5010 tungsten coated carbide inserts (An ISO designation of SNMG120408 MP), Kennametal made
Tool holder	ISO specification of PSBNR 2020 K12
Working insert tool geometry	Inclination angle: $-6^{\circ}$ , rake angle: $-6^{\circ}$ , clearance angle: $6^{\circ}$ , Nose radius: 0.8 mm, major cutting edge angle: $75^{\circ}$
Environments and coolants used	Cryogenic cooling (LN <sub>2</sub> ), Dry (no coolant), MQL and Wet (castrol-cooledge SL oil) emulsion based flood coolant at 1:20 soluble oil),
Cutting fluid supply	Cryogenic cooling - compressed air: $4 \text{ kg/cm}^2$ , flow rate: 0.45 kg/min (through external nozzle);
	MQL cooling - compressed air: $4 \text{ kg/cm}^2$ , flow rate: 70 ml/h (through external nozzle);
	wet cooling - flow rate: 6 l/min (through external nozzle)
Nozzle diameters used to spray coolant for different environments	cryogenics and MQL – $\varnothing$ 1 mm, Wet – $\varnothing$ 10 mm

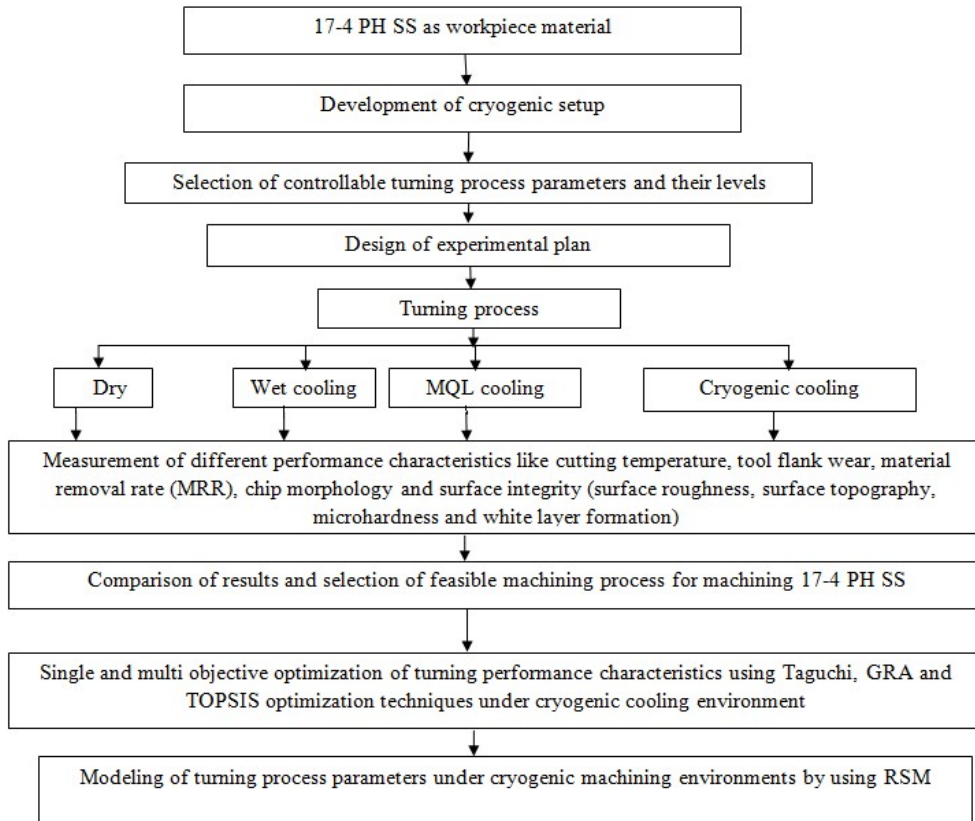


**Figure 3. 6** Flow chart of the present work.

### 3.4.2 EXPERIMENTAL DESIGNS

#### 3.4.2.1 Taguchi orthogonal array (OA) design

Taguchi orthogonal array (OA) design has been used for performing experiments for optimization studies. because it reduces the effort and experimental cost (Montgomery, 1987). The minimum number of experimental runs in the OA is given by equation (3.1). Minimum number of experiments runs required ( $N_{min}$ )

$$(N_{min}) = (L - 1) * F + 1 \quad (3.1)$$

Where, F = number of controllable factors and L = number of levels taken for each controllable factor. Hence, according to Taguchi design concept  $L_9$  orthogonal array as shown in Table 3.4 has been selected for studying the ANOVA, ANOM and multi

objective optimization problem using optimization techniques like GRA and TOPSIS. Experimental design and Taguchi analysis was done using Minitab 17.0 software tool and the means of mean plot, means of S/N ratio plots and analysis of variance (ANOVA) results were obtained and presented in the forth coming discussions.

**Table 3. 4** Taguchi L9 orthogonal array design.

Exp. run	Controllable process parameters		
	Cutting velocity ( $v$ )	Feed rate ( $f$ )	Depth of cut ( $d$ )
1	1	1	1
2	1	2	2
3	1	3	3
4	2	1	2
5	2	2	3
6	2	3	1
7	3	1	3
8	3	2	1
9	3	3	2

#### 3.4.2.2 One factor at a time approach (OFATA)

One factor at a time approach experimental design was considered to know the effect of each control process parameter on machining performance characteristics in which one control factor varied at one time and other controllable factors were keep it constant at their respective average levels. In the literature, several researchers have used OFATA experimental design in their works (Sharma et al., 2015; Manjaiah et al., 2016; Manna, 2013). Table 3.5 shows the OFATA design indicating  $v_3$ ,  $f_3$  and  $d_3$  as mean levels of the cutting velocity ( $v$ ), feed rate ( $f$ ) and depth of cut ( $d$ ) respectively.

#### 3.4.2.3 Response surface methodology (RSM)

RSM will helpful in the industrial processes where several process parameters influence on the process response or quality. It is a statistical and mathematical technique useful for developing, improving and optimization of any processes. In the

present work, central composite design (CCD) was employed by taking into account of three factors and three factors in each factor as shown in Table 3.6. In RSM, second order polynomial model is the most widely using due to flexibility and easy estimation of process parameter estimation. Flexibility in the sense it involves more forms of function for estimating the true function.

**Table 3. 5** One factor at a time approach experimental design.

Exp. run	Controllable process parameters		
	Cutting velocity ( $v$ )	Feed rate ( $f$ )	Depth of cut ( $d$ )
1	$v1$	$f3$	$d3$
2	$v2$	$f3$	$d3$
3	$v3$	$f3$	$d3$
4	$v4$	$f3$	$d3$
5	$v5$	$f3$	$d3$
6	$v3$	$f1$	$d3$
7	$v3$	$f2$	$d3$
8	$v3$	$f3$	$d3$
9	$v3$	$f4$	$d3$
10	$v3$	$f5$	$d3$
11	$v3$	$f3$	$d1$
12	$v3$	$f3$	$d2$
13	$v3$	$f3$	$d3$
14	$v3$	$f3$	$d4$
15	$v3$	$f3$	$d5$

### 3.5 MEASUREMENT OF PERFORMANCE CHARACTERISTICS

#### 3.5.1 Cutting temperature

The temperature at the machining zone was measured by using a calibrated infrared thermometer of model 'Center 350' as shown in Figure 3.9. During temperature measurement, chips at the machining zone as well as coolants were interrupted the

laser beam of the thermometer before reaching the machining zone, so the temperature measurements may not represent the actual values. But these values were considered for the comparison of different environmental conditions only.



**Figure 3. 7** Infrared thermometer.

### 3.5.2 Surface roughness

In the present investigation, average surface roughness ( $R_a$ ) was considered as surface roughness parameters under all machining environments and ‘Mutatoyo SJ301’ surface tester has been used to measure it. Five measurements were taken for  $R_a$  of the each machined sample with a cut off length ( $\lambda_c$ ) of 4 mm and average was taken as actual values. Figure 3.10 shows the Mutatoyo surface roughness tester.

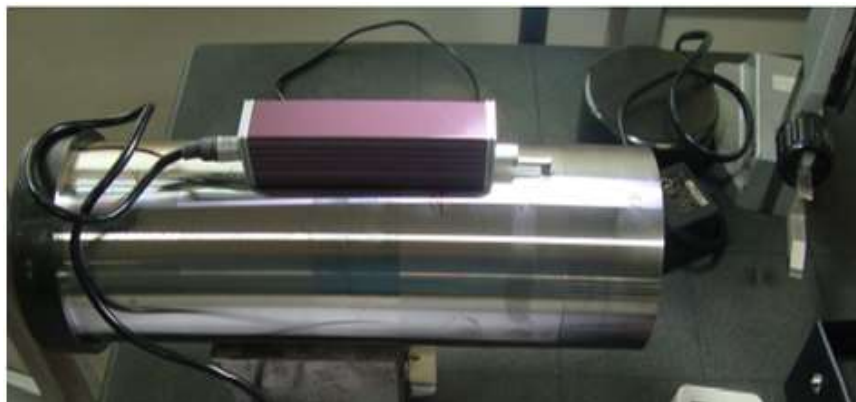


**Figure 3. 8** Surface roughness tester.

**Table 3. 6** RSM based L20 central composite design (CCD).

<b>Std. order</b>	<b>Exp. Run</b>	<b>Cutting velocity (<math>v</math>)</b>	<b>Feed rate (<math>f</math>)</b>	<b>Depth of cut (<math>d</math>)</b>
5	1	-1	-1	1
3	2	-1	1	-1
17	3	0	0	0
14	4	0	0	1
16	5	0	0	0
4	6	1	1	-1
2	7	1	-1	-1
15	8	0	0	0
8	9	1	1	1
20	10	0	0	0
6	11	1	-1	1
12	12	0	1	0
10	13	1	0	0
11	14	0	-1	0
18	15	0	0	0
7	16	-1	1	1
19	17	0	0	0
9	18	-1	0	0
13	19	0	0	-1
1	20	-1	-1	-1

### **3.5.2 Surface topography**

LESTOLS4100 model Confocal laser 3D surface tester has been used to obtain 3D Surface topography images of machined surfaces under all cooling environments. A measuring length of 2.6 mm machined surface was considered for the surface topography investigation. LESTOLS4100 model Confocal laser 3D surface tester is shown in Figure 3.11.

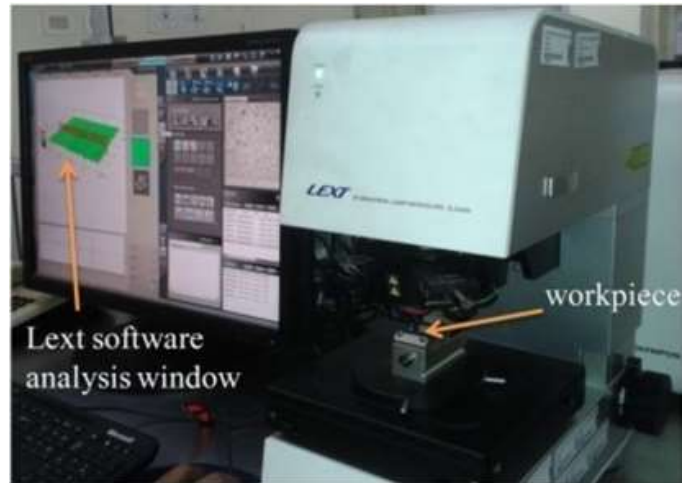


**Figure 3. 9** Laser optical confocal microscope.

### **3.5.3 Tool wear**

Tool wear was observed for a constant machining time of 4 minutes under all machining environments. Tool wear measurement was done by using ‘Zeiss’ optical microscope of model ‘AXIOLAB A1’ as shown in Figure 3.12.



**Figure 3. 10** Optical microscope.

### **3.5.4 Metal removal rate**

Contech made CA 3102 model weighing scale has been used to measure the weight of the workpiece before and after machining as shown in Figure 3.13. Each specimen was weighed using a digital weighing balance having an accuracy of 0.001 gram and



maximum weighing capacity of 3.2 kg. The MRR has been determined using the weight loss method and computed from Eqn. 3.2.

$$MRR = \frac{(W_i - W_f)}{t} \quad (3.2)$$

Where,

$W_i$  = Initial weight of the workpiece before machining (g),

$W_f$  = Final weight of the workpiece after machining (g),

$t$  = Total machining time (4 min).



**Figure 3. 11** Weighing scale.

### 3.5.5 Scanning electron microscope

Analysis of surface defects, tool wear, chip morphology, microstructure and subsurface characteristics were carried out by using 'JEOL-JSM-6380LA' Scanning electron microscope (SEM). The resolution of this equipment is 30 KV. The SEM images were taken at different magnifications for extensive analysis. 'Oxford' made 'X-ACT' type Energy Dispersive X-ray spectroscopy (EDAX) has been used for elemental composition of machined samples. Figure 3.14 depicts the 'JEOL-JSM-6380LA' model SEM.



**Figure 3. 12** Scanning electron microscopy.

### **3.5.7 Microhardness**

‘Fanuc pobocut  $\alpha$ -OiB’ model wire electric discharge machining machine has been used to cut the machined samples into semi circular shape for surface integrity characterization. Afterwards, various grades of silicon papers and diamond paste have been used for polishing to obtain mirror finished across the machined surface. OMNI TECHMVH-S-AUTO type Vickers hardness tester has been used for measuring microhardness of the cross section of the machined surfaces under the various cooling environments as shown in Figure 3.15. Each microhardness test was conducted by five times and average value is considered as microhardness value.



**Figure 3. 13** Microhardness tester.

### **3.5.8 White layer analysis**

For white layer analysis, cross sectional machined samples were polished with various grades of silicon papers and applied diamond paste to obtain mirror finished. Afterwards, (10 g FeCl<sub>3</sub> + 30 ml HCl +120 ml H<sub>2</sub>O) etchant was applied on the polished cross sectional machined samples and then SEM was utilized to investigate the white layer formation at various machining conditions. For each experiment, five measurements were taken along the white layer formation and average of five readings is considered as the white layer thickness.

### **3.6 SUMMARY**

This chapter explained about the 17-4 PH SS material and its mechanical properties, different experimental setups like cryogenic, MQL, wet and dry machining, different experimental designs like Taguchi orthogonal array, one factor at a time approach and response surface methodology, details of the equipments was used for measuring different turning performance characteristics and its measurement procedure.

## CHAPTER 4

### ONE FACTOR AT A TIME APPROACH

#### 4.1 INTRODUCTION

This chapter explains the individual effect of process parameters like cutting velocity, feed rate and depth of cut and cooling environment on cutting temperature, tool flank wear ( $V_b$ ), MRR, chip morphology and surface integrity (surface topography, surface finish, microhardness and white layer thickness) at various cooling environments. SEM and optical microscope images have been used to analyze the tool wear mechanism, surface defect analysis, chip morphology and white layer thickness.

#### 4.2 EXPERIMENTAL PLAN

In the present chapter, one factor at a time approach (OFATA) experimental design has been used to know the effect of each control process parameter on machining performance characteristics in which one control factor was varied at one time and other controllable factors were kept constant at their respective average level. Different controllable process parameters and their levels considered for conducting experiments are shown in Table 4.1. The selections of range of parameters were based on the preliminary experiments conducted. Turning experiments were performed on  $\varnothing$  35 mm diameter 17-4 PH SS round bars by using 'KIRLOSKAR' make lathe machine. In the chapter, cutting temperature, tool flank wear ( $V_b$ ), MRR, chip morphology and surface integrity (surface topography, surface finish ( $R_a$ ), microhardness and white layer thickness) were considered as investigative machinability characteristics under the cryogenic (liquid nitrogen), minimum quantity lubrication (MQL), wet and dry environments.

**Table 4. 1** Cryogenic turning process parameters and their levels for OFATA.

Symbol	Process parameters	Units	Levels				
			1	2	3	4	5
$V$	Cutting speed	m/min	25	35	55	85	132
$F$	Feed rate	mm/rev	0.048	0.096	0.143	0.191	0.238
$D$	Depth of cut	mm	0.2	0.6	1	1.2	1.4

### 4.3 EFFECT OF COOLING ENVIRONMENT AND PROCESS PARAMETERS ON CUTTING TEMPERATURE

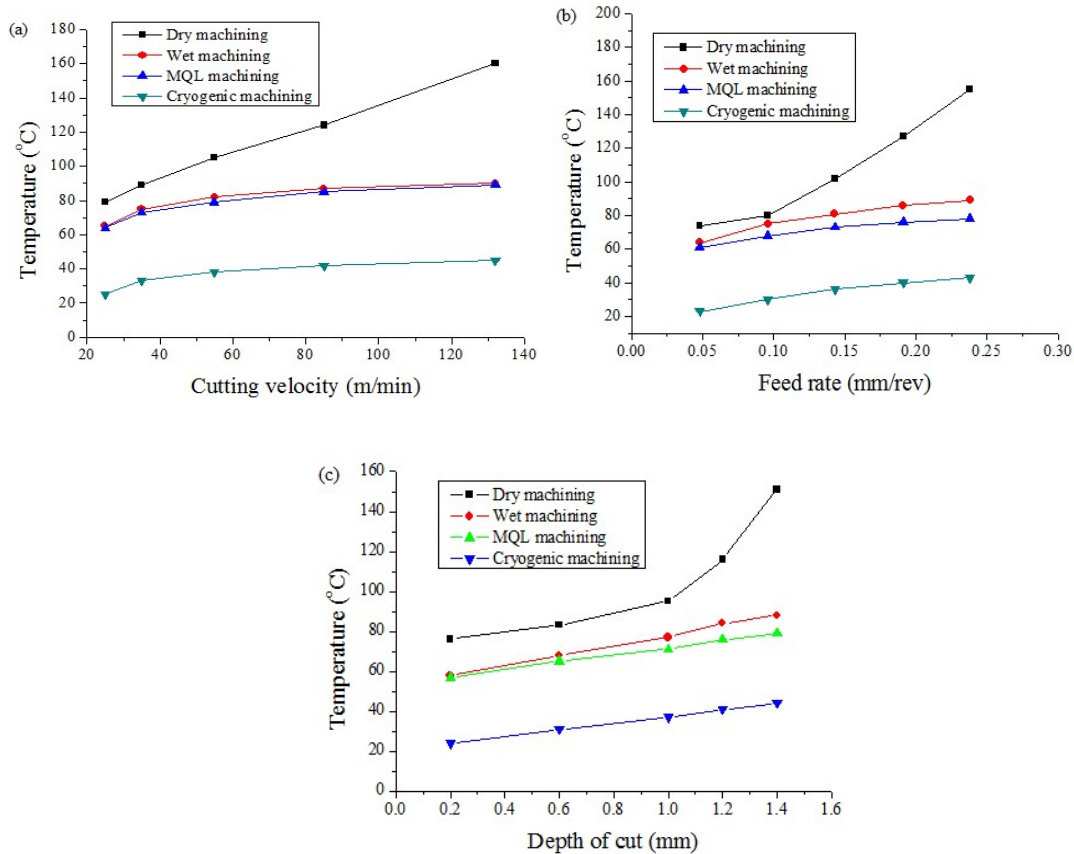


**Figure 4. 1** Effect of (a) Cutting velocity (b) Feed rate and (c) Depth of cut on cutting temperature under different cutting environments by keeping all other variables as constant at their respective mean levels.

#### **4.3.1 Effect of cooling environment and cutting velocity on cutting temperature**

Figure 4.1 (a) represents the cutting temperatures obtained at the machining zone at the varying cutting velocity condition under the different cooling environments. From the Figure 4.1 (a), it was pragmatic that as cutting velocity increases the temperature at the machining zone increases in all environments. This might be due to the development of more friction between the tool and workpiece which causes more heat generation resulting in increased cutting temperature. Among all the cooling environments, cryogenic machining condition reduced the cutting temperatures significantly as shown in Figure 4.1 (a). It can be seen from the Figure 4.1 (a) that at a low cutting velocity of 25 m/min, the obtained machining zone temperature in cryogenic, MQL, wet and dry machining was 25, 64, 65 and 79 °C respectively. At this condition, the temperature reduction found in cryogenic machining was 68 %, 62 % and 61 % respectively over dry, wet and MQL machining conditions. Similarly, at a higher cutting velocity of 132 m/min, the respective cutting temperature reductions found in cryogenic machining was 72 %, 50 % and 49 % compared to dry, wet and MQL machining. From the Figure 4.1 (a), it can be observed that the cutting temperature in dry machining increases sharply with the rise in cutting velocity due to rise in the friction between the contact asperities. Whereas in both wet and MQL machining, almost similar results were found, this might be due to the low friction which is a result from the both coolants lubrication effects during machining. The reason for temperature reduction in cryogenic machining was due to the spraying of LN<sub>2</sub> at the machining zone causes substantial reduction of machining zone temperatures; this indicates that generation of low friction between the tool and workpiece. In overall, the respective temperature reduction range found in cryogenic machining over the dry, wet and MQL machining was 63-72 %, 50-62 % and 49-61 %, respectively, while the rise of cutting velocity from 25 m/min to 132 m/min.

#### **4.3.2 Effect of cooling environment and feed rate on cutting temperature**

As shown in Figure 4.1 (b), as the feed rate increases, cutting temperature at the machining zone increases. The reason might be as feed rate rises, the friction between

the tool and workpiece increases, which causes the rise of heat generation at the contact asperities, resulting in the generation of more temperature at the machining zone. Figure 4.1 (b) depicts that at a low feed rate of 0.048 mm/rev, the corresponding temperature values for the dry, wet, MQL and cryogenic machining was 74, 64, 61 and 23 °C respectively. At this point, MQL and wet machining conditions have developed almost equal temperatures. At this situation, the cryogenic machining reduced the cutting temperatures by 69 %, 64 % and 62 % respectively over the dry, wet and MQL machining conditions. Likely, the respective temperature drop in cryogenic machining was 72 %, 52 % and 45 % compared to dry, wet and MQL machining conditions at a high feed rate of 0.238 mm/rev. From the obtained results, it was observed that significant machining zone temperature reduction was found in cryogenic machining over the other machining environments. These favorable results are owing to the spraying of low temperature LN<sub>2</sub> at the machining zone led to low machining zone temperatures. These favorable cryogenic results indicate that it reduces the friction between the contact asperities. As a whole, the temperature drop range found in cryogenic machining was 63-72 %, 52-64 % and 45-62 %, respectively compared to dry, wet and MQL machining environmental conditions while an increase of feed rate from 0.048-0.238 mm/rev respectively.

#### **4.3.3 Effect of cooling environment and depth of cut on cutting temperature**

As the depth of cut increases, cutting temperature increases under the all cutting environments as depicted in Figure 4.1 (c). This is result of an increase of rubbing action between the tool and workpiece as a depth of cut increases which causes an increase of cutting temperatures. At a high depth of cut of 1.4 mm, cryogenic machining produced 44 °C at the machining zone, whereas, MQL, wet and dry machining developed 79 °C, 88 °C and 151 °C respectively. At this condition, the cutting temperature reductions found in cryogenic machining was 44 %, 50 % and 71 % respectively compared to MQL, wet and dry machining conditions. At the same point, the temperature reduction found in MQL machining was 10 % and 48 % respectively over the wet and dry machining

conditions. From the Figure 4.1 (c), it was perceived that lower cutting zone temperatures were found in cryogenic machining over other machining environments. This difference in cutting temperature is mainly due to the spraying of low temperature  $LN_2$  at the machining zone causes reduction of friction between the tool-chip interfaces. At a low depth of cut of 0.2 mm, both MQL and wet machining have developed almost equal cutting temperatures. From the results, the overall temperature reductions found in cryogenic machining was in the range of 44- 58 %, 50-59 % and 61- 71 % respectively compared to MQL, wet and dry machining environments.

#### 4.4 EFFECT OF COOLING ENVIRONMENT AND PROCESS PARAMETERS ON TOOL FLANK WEAR

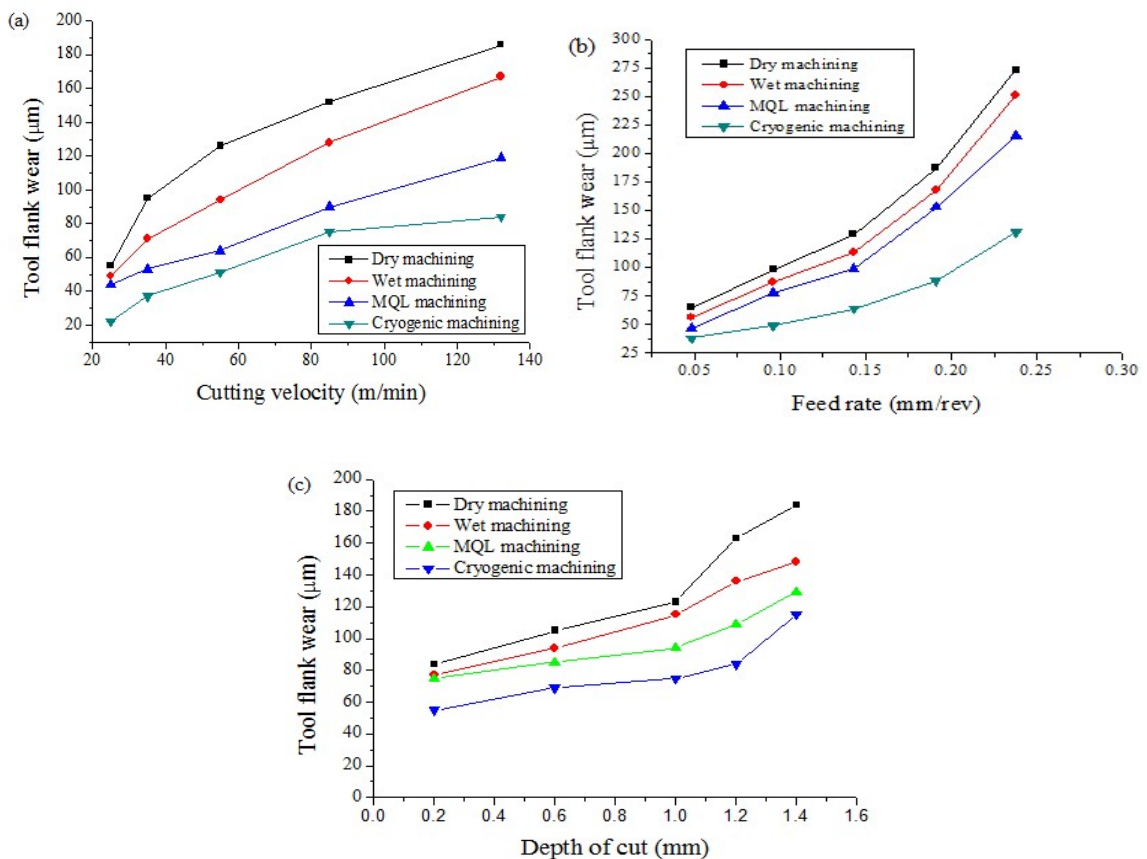


**Figure 4. 2** Effect of (a) Cutting velocity (b) Feed rate and (c) Depth of cut on flank wear under different cutting environments by keeping all other variables as constant at their respective mean levels.



#### 4.4.1 Effect of cooling environment and cutting velocity on flank wear

Flank wear is one of the most important wear to be control because the flank face continuously contacts with the machined material and it raises the cutting forces and it impairs the machined surface (Sornakumar et al., 1993). In the current study, tool flank wear was measured at varying cutting velocities and increasing trend was observed for the flank wear as shown in Figure 4.2 (a). This is because at higher cutting velocity, high cutting temperatures developed within a tiny time. Also, the contact area decreases between the tool and chip interface at high cutting velocity, causing cutting edge very closely exposed to high cutting temperatures leading to thermal softening of the tool material resulting in more tool wear when cutting tool contacts with the workpiece at such conditions. From Figure 4.2 (a), it was observed that at a low cutting velocity of 25 m/min, flank wear was 22  $\mu\text{m}$  in cryogenic machining, whereas, it was 44, 49 and 55  $\mu\text{m}$  for MQL, wet and dry machining respectively. It was found that flank wear reduction in cryogenic machining was 50 % and 55 % and 60 %, respectively compared to MQL, wet and dry machining. This is attributed due to the supply of  $\text{LN}_2$  at the machining zone causing lower cutting temperatures, this leads to less buildup edge formation (BUE) at the tool flank face resulting in increase of tool hardness compared to other machining environments. Similarly, at the same cutting condition, there were 10 % and 20 % reduction of flank wear was found in MQL machining over the wet and dry machining respectively. The reason might be due to the friction reduction between the tool and workpiece interface resulting from the efficient penetration of MQL into the machining zone. Figure 4.3 depicts the different wear mechanisms observed in the machining of 17-4 PH SS at this condition. From the SEM images, it was observed that the formation of BUE, micro grooves on the cutting tool in dry machining conditions. Micro grooves indicate the abrasive marks, whereas, edge chipping and abrasive marks were found in wet machining due to the different tool-chip contact nature. At a low cutting velocity condition, it was observed that major wear mechanisms in the dry environment were adhesion and abrasion, whereas, in wet, MQL and cryogenic environments it was found as abrasion wear mechanism as shown in Figure 4.3. From

the Figure 4.2 (a), it can be seen that at a high cutting velocity of 132 m/min, the obtained flank wear in cryogenic machining was 84  $\mu\text{m}$ , whereas, it was 186, 167 and 119  $\mu\text{m}$  in dry, wet and MQL machining respectively. It was observed that cryogenic machining reduces the flank wear by 55 %, 50 % and 20 % respectively in contrast with dry, wet and MQL machining. Also, reduction of flank wear in MQL machining was found to be 36 % and 29 % compared with dry and wet machining respectively. Figure 4.4 depicts the different wear mechanisms in machining of 17-4 PH SS at the given conditions. At high cutting velocity, adhesion (BUE) and abrasion wear mechanism were found as dominant in dry and wet environments. In MQL environment, wear mechanism is attributed due to fracture, microgrooves and abrasive marks. Wear mechanism found in the cryogenic environment was abrasion only because of spraying of  $\text{LN}_2$  at cutting zone reduces the sticking of workpiece material to the cutting edge, result in less BUE formation on the tool and similar results were found Kaynak et al. (Kaynak et al., 2015) in their study. In overall, the range of reduction of tool flank wear in cryogenic machining was 51-60 %, 41-55 % and 17-50 % respectively over the dry, wet and MQL machining conditions when cutting velocity increases from 25 m/min to 132 m/min.

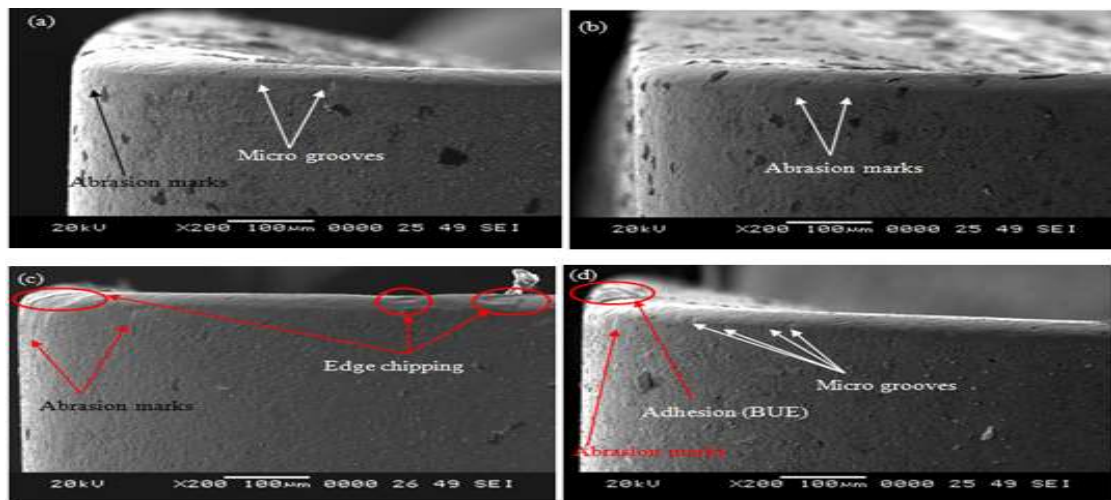


**Figure 4. 3** SEM images of tool flank wear at  $v = 25$  m/min,  $f = 0.143$  mm/rev and  $d = 1$  mm under different cooling environments (a) Cryogenic (b) MQL (c) Wet (d) Dry.

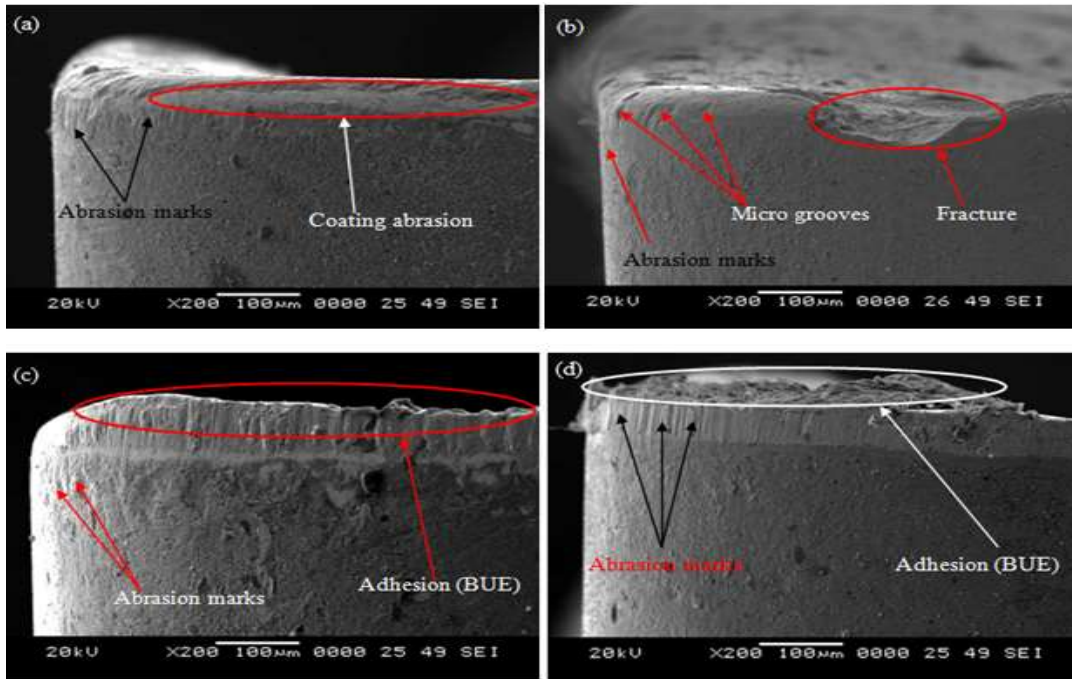


**Figure 4. 4** SEM images of tool flank wear at  $v = 132$  m/min,  $f = 0.143$  mm/rev and  $d = 1$  mm under different cooling environments (a) Cryogenic (b) MQL (c) Wet (d) Dry.

#### 4.4.2 Effect of cooling environment and feed rate on flank wear

From Figure 4.2 (b), it was observed that as feed rate increases, flank wear increases under the all cooling environments. This trend owes to the higher cutting temperatures caused by higher material removal rates at higher feed rates, results in more tool flank wear. It is seen from the Figure 4.2 (b) that at a low feed rate of 0.048 mm/rev, the respective tool flank wear measurements was 65, 56, 47 and 38  $\mu\text{m}$  for dry, wet, MQL and cryogenic machining. At this point, the respective tool flank wear reduction found in cryogenic machining was 42 %, 32 % and 19 % over the dry, wet and MQL machining conditions. However, at this same condition, the respective flank wear reduction in MQL machining was 28 % and 16 % compared to dry and wet machining. The flank wear reductions found at a high feed rate of 0.238 mm/rev was 52 %, 48 % and 39 %, respectively compared to dry, wet and MQL machining as shown in Figure 4.2 (b). At

this condition, 21 % and 14 % reduction of tool flank wear was found in MQL compared to dry and wet machining respectively. This is resulting in the reduction of cutting zone temperatures offered by LN<sub>2</sub> causes less built-up-edge (BUE) on the cutting tool edge. Figure 4.5 and Figure 4.6 depicts the SEM images of tool flank wear obtained at the respective given conditions. It is evident from the SEM analysis that less adhesion wear (BUE) was found in cryogenic machining compared to other machining environments in the respective given conditions. In cryogenic machining, the major tool wear mechanism found was abrasion only, whereas, in other machining environments it was adhesion and abrasion mechanisms. Similar results were obtained in the literature findings (Chetan et al., 2015; Kaynak et al., 2015). In overall, the tool flank wear reductions found in cryogenic machining was in the range of 42-53 %, 32- 48 % and 19-42 % respectively over the dry, wet and MQL machining conditions when the feed rate varies from 0.048 to 0.238 mm/rev.

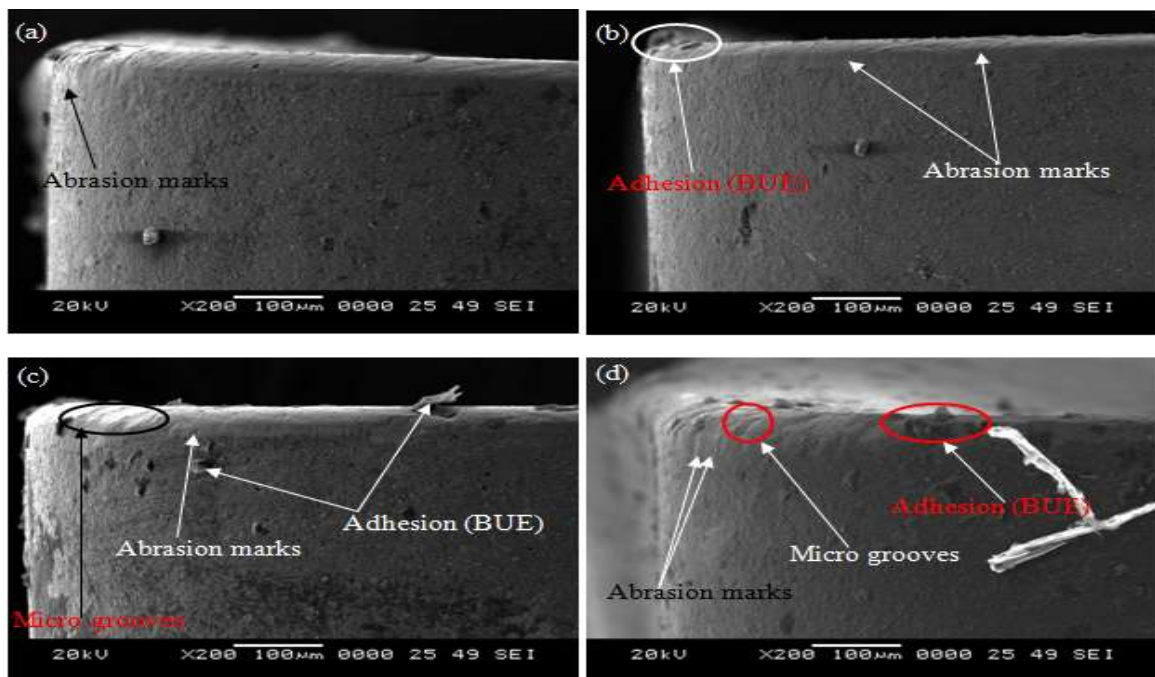


**Figure 4. 5** SEM images of tool flank wear at  $v = 55$  m/min,  $f = 0.048$  mm/rev and  $d = 1$  mm under different cooling environments (a) Cryogenic (b) MQL (c) Wet (d) Dry.

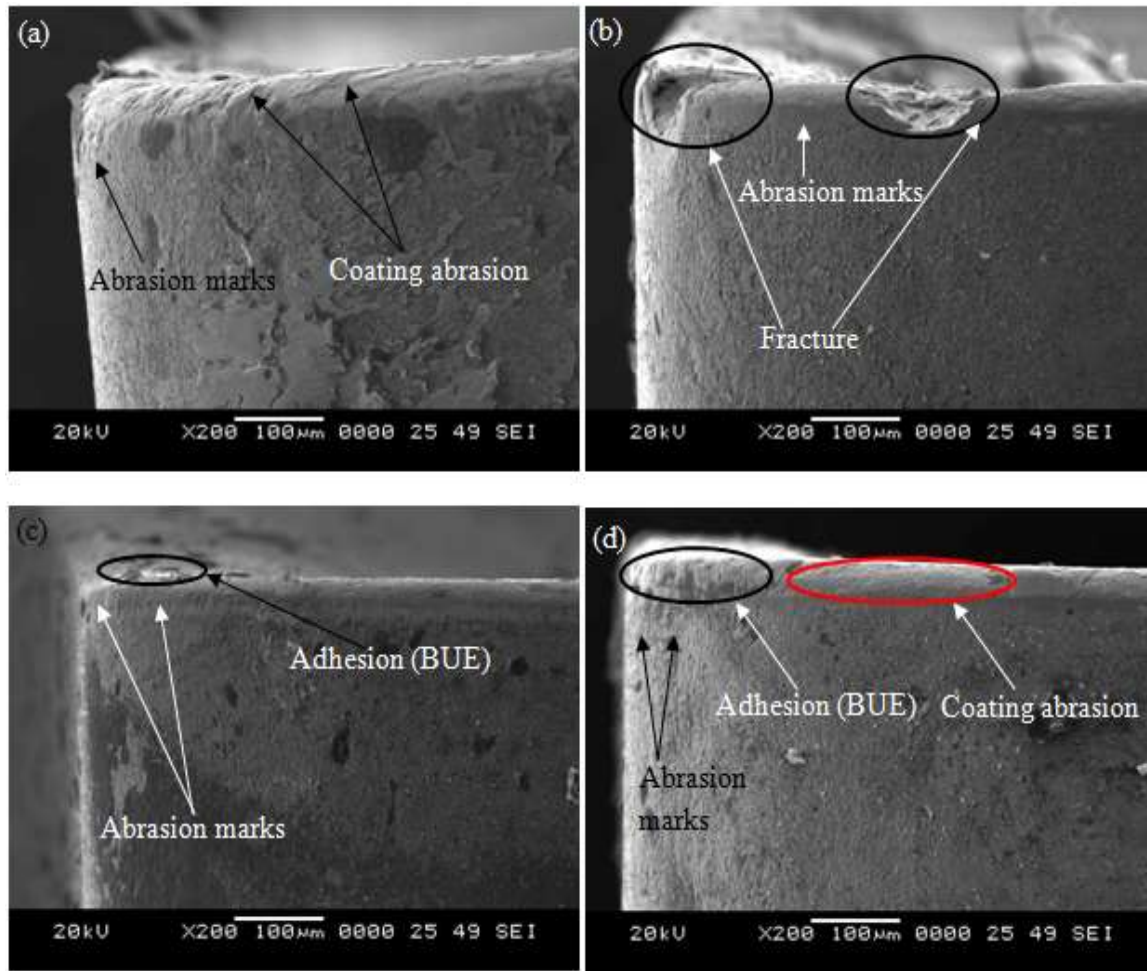
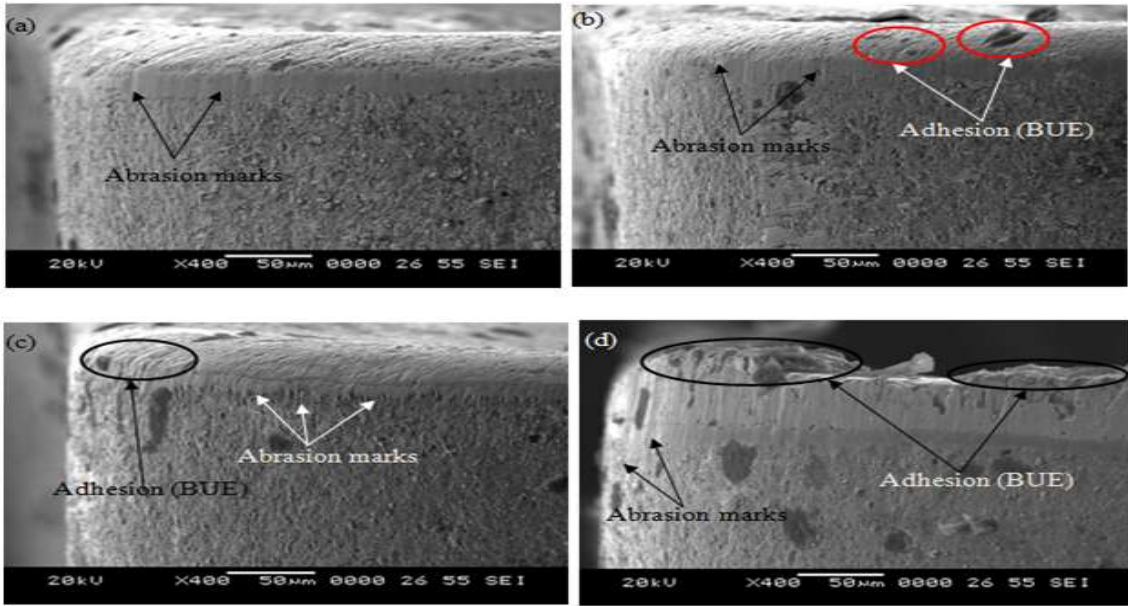


**Figure 4. 6** SEM images of tool flank wear at  $v = 55$  m/min,  $f = 0.238$  mm/rev and  $d = 1$  mm under different cooling environments (a) Cryogenic (b) MQL (c) Wet (d) Dry.

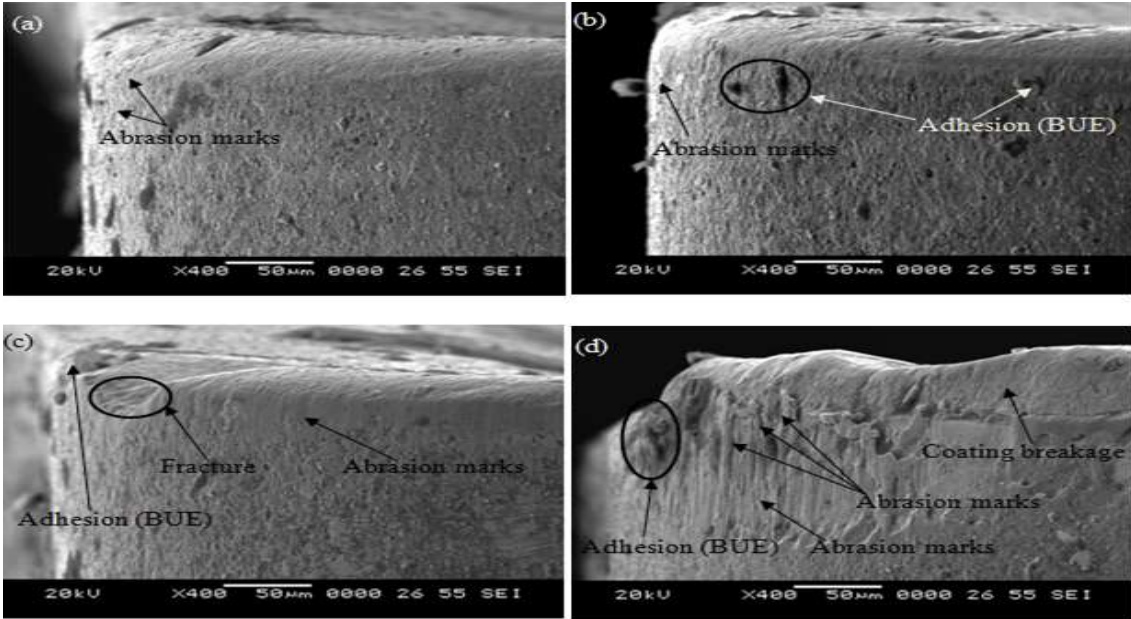
#### 4.4.3 Effect of cooling environment and depth of cut on flank wear

Figure 4.2 (c) depicts that as a depth of cut increases tool flank wear also increases in all the machining environments. This effect is due to more contact between the tool and workpiece at high depth of cuts, causes generation of more friction between the contacting asperities leads to thermal softening of tool resulting in more tool wear. At a low depth of cut of 0.2 mm, the tool flank wear observed was 84, 77, 75 and 55  $\mu\text{m}$  respectively in dry, wet, MQL and cryogenic machining conditions. The flank wear

reductions found in cryogenic machining at this point was 35 %, 29 % and 27 % respectively compared to dry, wet and MQL machining conditions. The flank wear reductions found in MQL machining at this point was 11 % and 3 % respectively over the dry and wet machining conditions. At a high depth of cut of 0.2 mm, the tool flank wear observed was 184, 148, 129 and 115  $\mu\text{m}$  respectively in dry, wet, MQL and cryogenic machining conditions. The flank wear reductions found in cryogenic machining at this point was, 38 %, 22 % and 11 % respectively over dry, wet and MQL machining conditions. At this situation, 33 % and 20 % reductions was found in MQL machining compared to dry and wet machining environments. Compared to other machining environments, the significant reduction of flank wear was found in cryogenic machining depicted in Figure 4.2 (c). This is results in control of adhesion and abrasion wear mechanisms due to the spraying of  $\text{LN}_2$  provide lower cutting temperatures. It is evident from the Figure 4.7 and Figure 4.8 that cryogenic machining developed low flank wear compared to other machining environments. It was also observed from the Figure 4.7 and Figure 4.8 that the major wear mechanism found in cryogenic was abrasion only, whereas, in other machining environments it was adhesion (BUE) and abrasion. In particular, dry machining produced more adhesion and abrasion wears due to the higher cutting temperatures, whereas, failure of tool in MQL was additionally due to fracture mechanism along with abrasion and adhesion wear mechanisms. As shown in Figure 4.2 (c), as the depth of cut increases, the percentage of reduction in flank wear found in cryogenic machining was reduced due to the higher cutting temperatures at the high cutting conditions. as a whole, when the depth of cut varying from 0.2 mm to 1.4 mm, the range of tool wear reductions found in cryogenic machining was 34-48 %, 22-38 % and 11-27 % respectively compared to dry, wet and MQL machining. Similarly, at this varying conditions, the flank wear reductions found in MQL machining was 11-33 % and 3-20 % respectively compared to dry and wet machining conditions. Kalyan Kumar and Choudhury (2008) in their work, found similar results while machining of stainless steel 202 grade.



**Figure 4. 7** SEM images of tool flank wear at  $v = 78.5$  m/min,  $f = 0.143$  mm/rev and  $d = 0.2$  mm under different cooling environments (a) Cryogenic (b) MQL (c) Wet (d) Dry.



**Figure 4. 8** SEM images of tool flank wear at  $v = 78.5$  m/min,  $f = 0.143$  mm/rev and  $d = 1.4$  mm under different cooling environments (a) Cryogenic (b) MQL (c) Wet (d) Dry.

#### 4.5 EFFECT OF COOLING ENVIRONMENT AND PROCESS PARAMETERS ON MRR

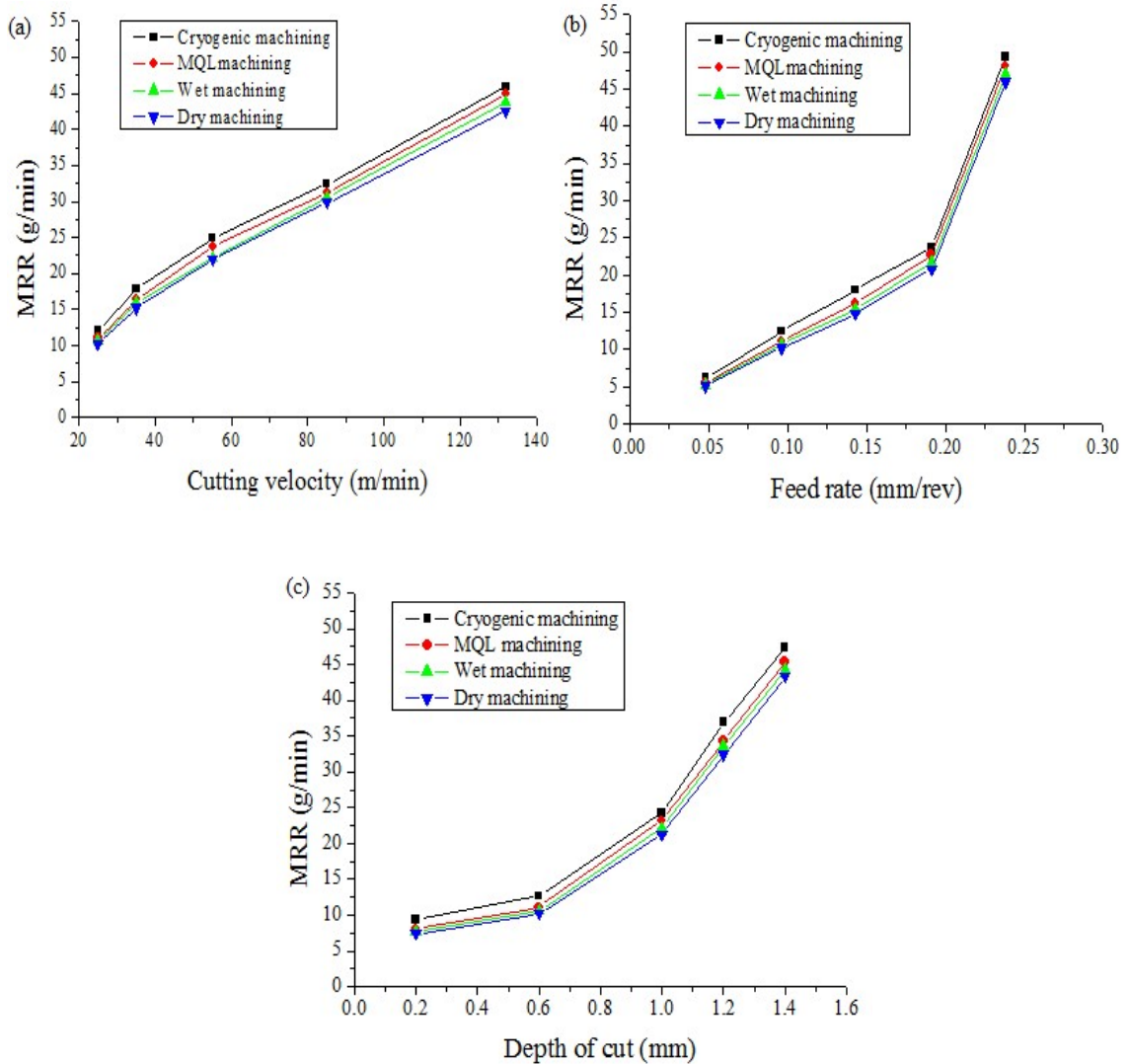


**Figure 4. 9** Effect of (a) Cutting velocity (b) Feed rate and (c) Depth of cut on MRR under different cutting environments by keeping all other variables as constant at their mean levels.

From Figure 4.9 (a)-(c) it is observed that as cutting speed, feed rate and depth of cut increases then MRR also increases respectively. Because MRR has a directly proportional relationship with the cutting velocity, feed rate and depth of cut, thus causes



increase in MRR. This effect is observed due to reduction in chip reduction coefficient resulting higher MRR (Maity and Swain, 2008). When cutting velocity increases from 25 m/min to 132 m/min, cryogenic machining increased the MRR in the range of 7.87 - 17.72 %, 4.89-12.41 % and 2- 9 % respectively over dry, wet and MQL machining respectively as shown in figure 4.9 (a). Whereas, when the feed rate increases from 0.048-0.238 mm/rev, the observed range of rise in MRR in cryogenic machining was 7.36-22.40 %, 5.11-17.69 % and 2.72-12.29 % respectively compared to dry, wet and MQL machining environments as depicted in figure 4.9 (b). In the case of depth of variation from 0.2-1.4 mm, cryogenic machining increased the MRR in the range of 9.38 – 26.52 %, 7-21.65 % and 4.49- 16.38 % respectively over dry, wet and cryogenic machining respectively as shown in figure 4.9 (c). From figures 4.9 (a)-(c), it was observed that cryogenic machining increased the MRR at all the process parameters variation over the dry, wet and MQL machining environments. This effect is due to reduction of tool wear in cryogenic cooling.

#### **4.6 EFFECT OF COOLING ENVIRONMENT AND PROCESS PARAMETERS ON CHIP MORPHOLOGY**

##### **4.6.1 Effect of cooling environment and cutting velocity on chip morphology**

Tool wear and surface quality of machined surface have considerably affected by the forms of chips produced during the machining process. In the current study, favorable chips mean chips which do not encourage the jamming of machining operation and easy flow of chips. Chip morphology obtained at different machining conditions as shown in Figure 4.10 and Figure 4.11. At a low cutting velocity of 25 m/min, cryogenic machining produced the metallic color, thick discontinuous helical or tubular shaped chips with a small diameter which are favorable for the machining operation. Similarly, in wet machining, thick discontinuous helical or tubular shaped chips were obtained, but bluish gray color and bigger diameter than cryogenic machining. Whereas, the chips obtained in MQL machining were a thick metallic color, long continuous spiral shape chips which are difficult to break. But dry machining produced chips were light golden color, thick

long ribbon type which are encouraged to create problem to the manual operator as well as machining operation. Tool-chip contact length significantly influenced by the cutting velocity. As cutting velocity increases, tool-chip contact length decreases, resulting in a reduction in the chip thickness (Gupta et al., 2015). At a high cutting velocity of 132 m/min, metallic color very thin discontinuous long ribbon type chips were found in cryogenic machining which have a complimentary impact on the machining operation. Whereas, all other machining environments have produced thin unfavorable, very long ribbon type chips with different colors. At this point, MQL, wet and dry machining conditions, respectively produced the metallic, bluish gray color and golden color. At all the cutting velocities, the favorable chip shape and size were obtained in the cryogenic machining due to the use of LN<sub>2</sub> at the machining zone, causes lower temperatures at the machining zone, this lead to drop in the plasticity of the material during chip formation as well as ductility and the bending capacity resulting improved chip control (breakability). At a high cutting velocity of 132 m/min, except in cryogenic machining remaining other machining environments, it was observed that jamming of chips at the machining zone during experimentations which causes the generation of scratches on the machined surface resulting in a poor surface finish. Also, this might be the cause for chipping of cutting edge or nose edge of the tool. From the microscopic images of chips, it was seen that more side flow of material was found in dry, wet and MQL machining conditions at the given conditions as shown in Figure 4.12. This is due to the development of high cutting temperatures in dry, wet and MQL machining causes for increased plasticity in the material resulting in more side flow. Whereas, very less side flow of material was found in cryogenic machining and similar results were found in the literature (Chetan et al., 2015). This is resulting from the superior cooling effect of LN<sub>2</sub> led to lower machining temperatures hence less side flow of material. Among all the machining environments, cryogenic machining involves no chip cleaning cost and no hazard from the health and sustainable manufacturing point of view.

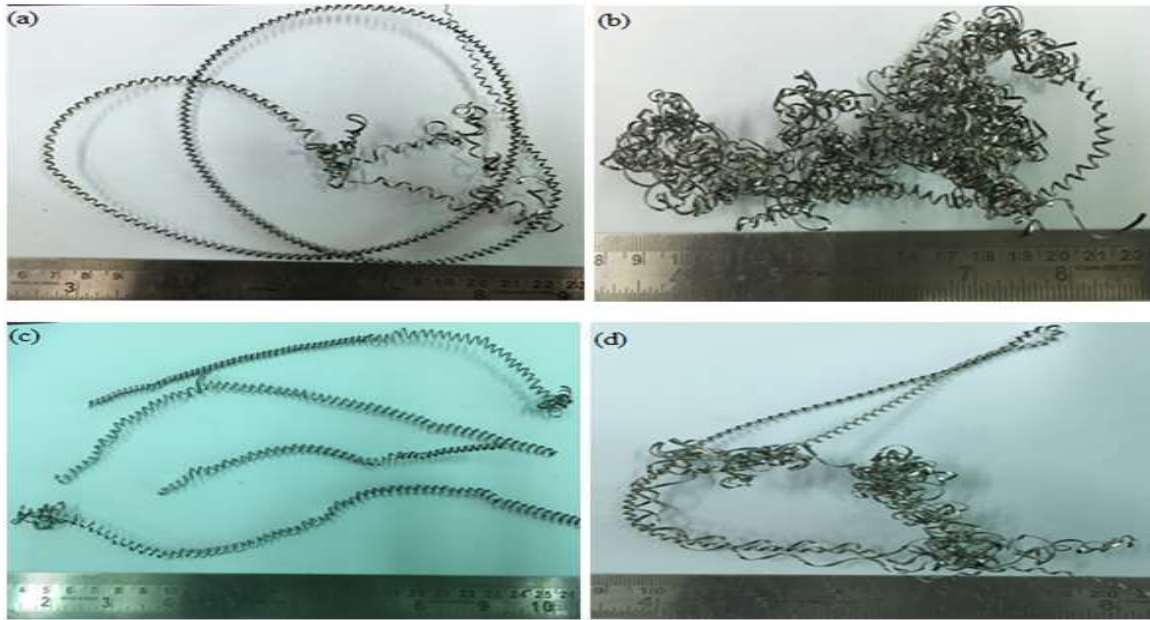


**Figure 4. 10** Form of chips generated at  $v = 25$  m/min,  $f=0.143$  mm/rev and  $d = 1$  mm under different cooling environments (a) Cryogenic (b) MQL (c) Wet (d) Dry.

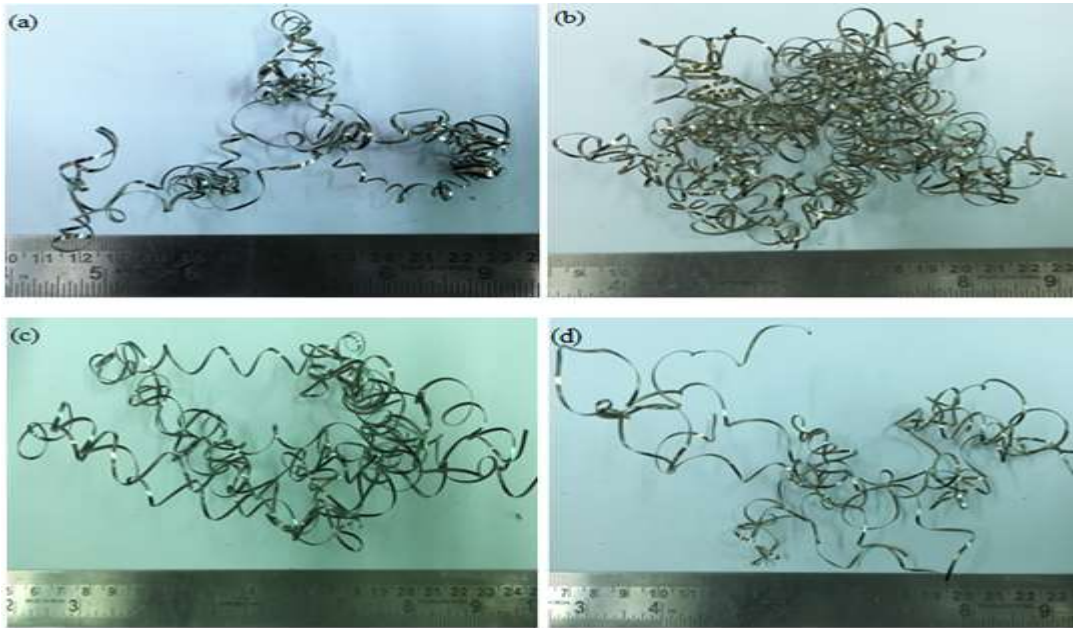


**Figure 4. 11** Form of chips at  $v = 132$  m/min,  $f=0.143$  mm/rev and  $d = 1$  mm under different cooling environments (a) Cryogenic (b) MQL (c) Wet (d) Dry.

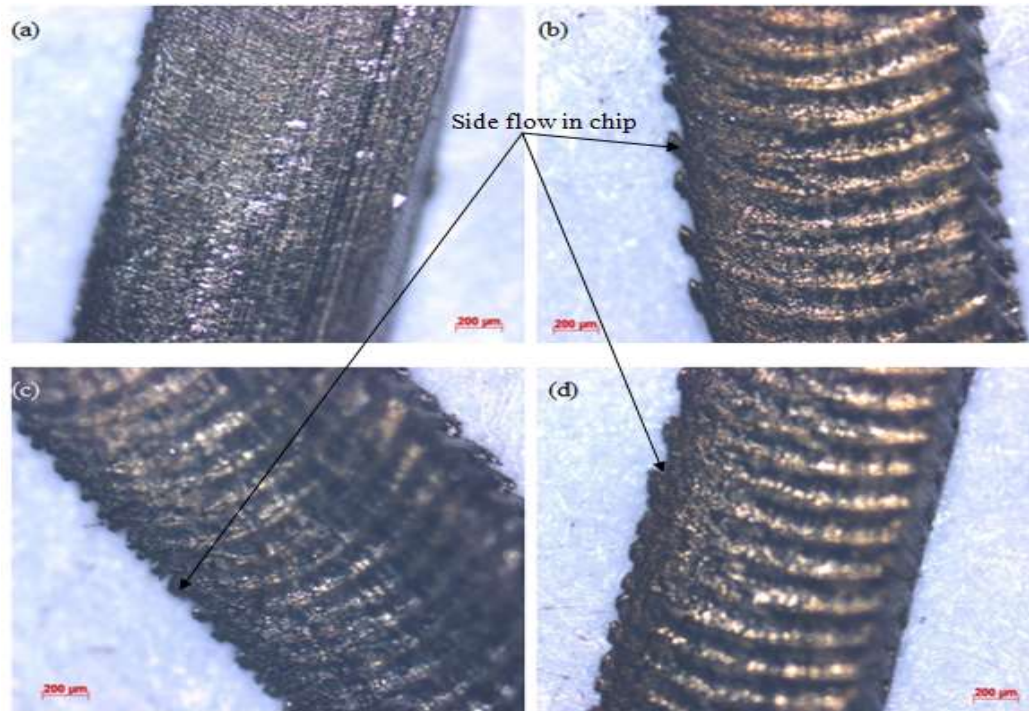


**Figure 4. 12** Microscopic images of chips at  $v = 132$  m/min,  $f = 0.143$  mm/rev and  $d = 1$  mm under different cooling environments (a) Cryogenic (b) MQL (c) Wet (d) Dry.

#### 4.6.2 Effect of cooling environment and feed rate on chip morphology

Form and type of chips produced at varying feed rate conditions as shown in Figure 4.13 and 4.14. During machining, at a low feed rate of 0.048 mm/rev, the chip forms observed were shown in Figure 4.13. The metallic color and continuous long, thin helical shape chips with a small diameter were observed in cryogenic machining. This type of chips was found as favorable chips due to easy chip flow during machining. In the similar fashion, in MQL machining, the observed chips shape was metallic color and continuous long, thin helical shape chips with bigger diameter than chips produced in cryogenic machining. Whereas, bluish color, very continuous long spiral shape chips and light golden color continuous very long ribbon shape chips were found in wet and dry machining respectively. At the low feed rate cutting condition, in cryogenic machining only, favorable chips were found among all machining conditions. At this point,

particularly, dry machining produced most unfavorable and hazardous chips, which cause for the scratching of the machined surface. Chip forms obtained at a high feed rate of 0.238 mm/rev was shown in Figure 4.14. At this point, the shape of the chips as follows. Dry and MQL machining generated light golden color very long continuous thick helical shape chips and very long thick ribbon shape chips respectively which are unfavorable and hazardous to the manual operator. Whereas, in cryogenic machining, most favorable metallic color, very short, thick snarled chips were found and also these are not hazardous to the manual operator. However, wet machining produced discontinuous long light bluish color long thick helical chips, which are favorable during machining. From the Figure 4.13 and 4.14, it was observed that when feed rate increases from 0.048 to 0.238 mm/rev, thick chip thickness increases. However, the chip thickness found in cryogenic machining was less over the other machining conditions as depicted in Figure 4.15. This is owing to the less side flow from the chips which is a result of the lower temperature of LN<sub>2</sub>. Similar type results were found in the literature (Chetan et al., 2015).

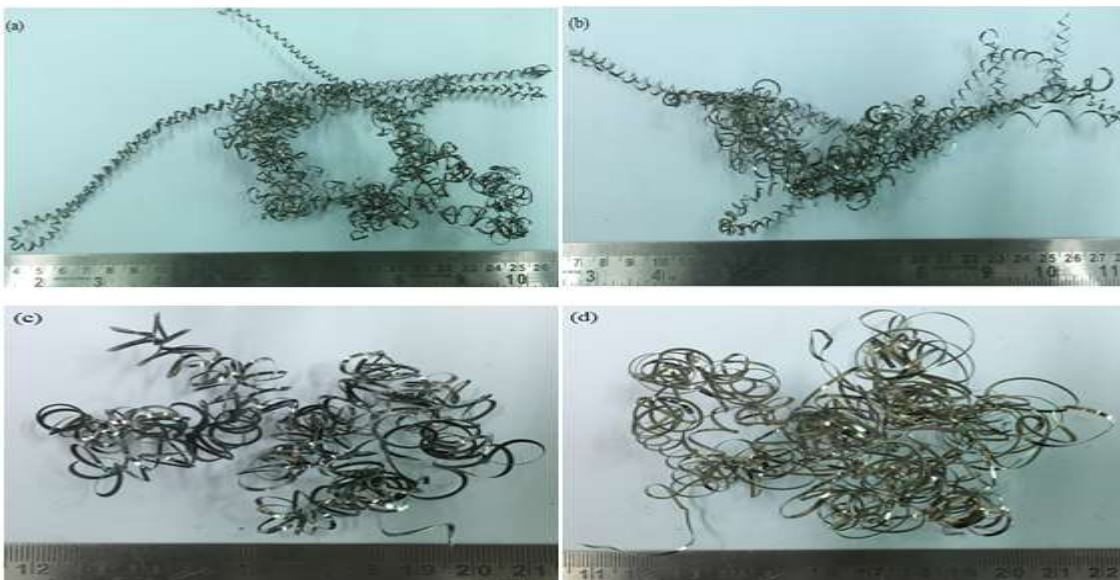


**Figure 4. 13** Form of chips generated at  $v = 55$  m/min,  $f = 0.048$  mm/rev and  $d = 1$  mm under different cooling environments (a) Cryogenic (b) MQL (c) Wet (d) Dry.

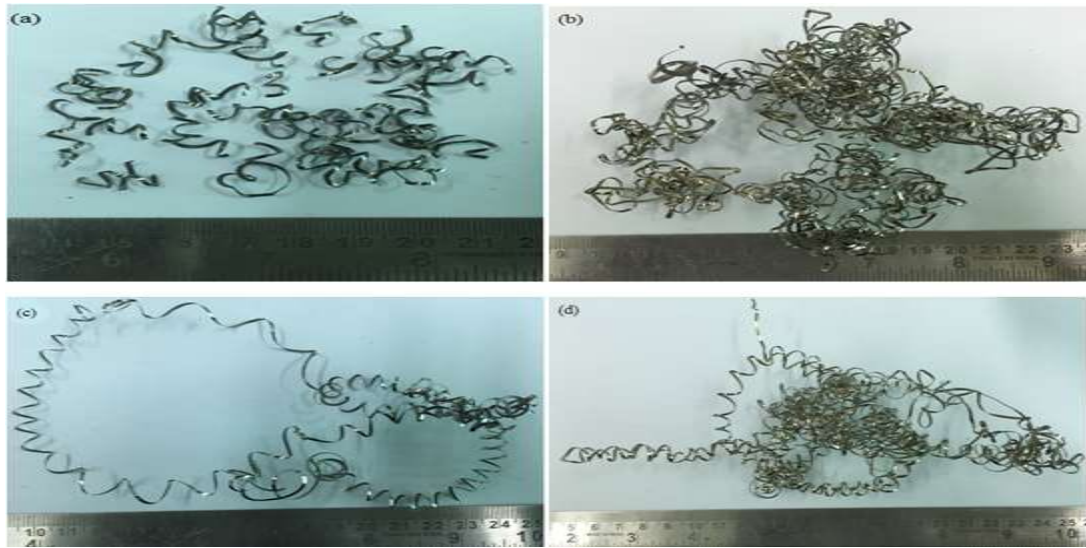


**Figure 4.14** Form of chips generated at  $v = 55$  m/min,  $f = 0.238$  mm/rev and  $d = 1$  mm under different cooling environments (a) Cryogenic (b) MQL (c) Wet (d) Dry.

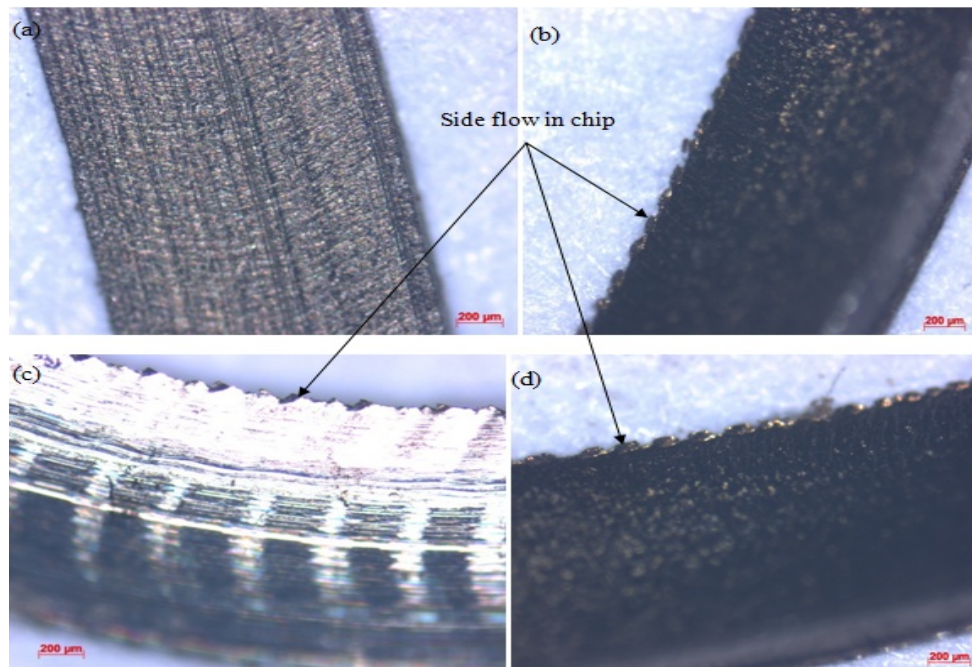


**Figure 4.15** Microscopic images of chips at  $v = 55$  m/min,  $f = 0.238$  mm/rev and  $d = 1$  mm under different cooling environments (a) Cryogenic (b) MQL (c) Wet (d) Dry.

### **4.6.3 Effect of cooling environment and depth of cut on chip morphology**

In all machining environments, when the depth of cut changes from 0.2 mm to 1.4 mm the chip thickness increases is shown in Figure 4.16 and Figure 4.17. It is well known fact that as a depth of cut increases the rate of deformation increases results in more chip thickness. At a low depth of cut of 0.2 mm, the chip observed in dry, wet, MQL and cryogenic machining was long continuous thin ribbon type, long continuous thin helical with a large diameter, long continuous thin helical with a small diameter and discontinuous very thin approximately straight respectively. Except in cryogenic machining other all machining environments have produced unfavorable chips, causes more surface roughness generation. This effect is because of lower cutting temperatures offered by LN<sub>2</sub>, causes better chip breakability in cryogenic machining. At a high depth of cut of 1.4 mm, the form of chips found in dry, wet, MQL and cryogenic machining was very long continuous helical with a large diameter, very long continuous helical with a small diameter, very long continuous thin ribbon type and long discontinuous thin ribbon type respectively. Other than in cryogenic machining, remaining all machining environments has produced unfavorable chips due to high cutting temperatures. At this condition, accumulation of chips was observed at the machining zone in dry, wet and MQL environments during machining, which causes for blocking of penetration of coolants into machining zone, led to high cutting temperatures. At the given conditions the side flow of material observed at different machining environments as depicted in Figure 4.18. It was found that in cryogenic machining less side flow of chip and low thickness chips were observed compared to other machining environments. This is because of spraying of high pressure LN<sub>2</sub> at the machining causes low cutting zone temperatures, less adhesion of chip residuals to the chip in the machining which led to low chip thickness.

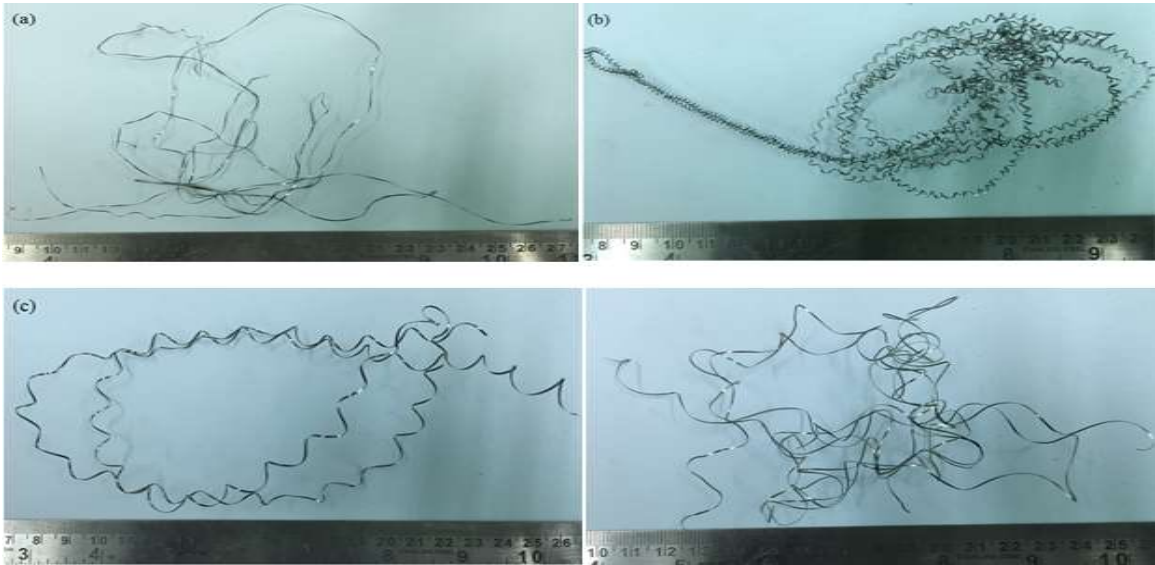


**Figure 4. 16** Chip forms generated at  $v = 78.5$  m/min,  $f = 0.143$  mm/rev and  $d = 0.2$  mm under different cooling environments (a) Cryogenic (b) MQL (c) Wet (d) Dry.

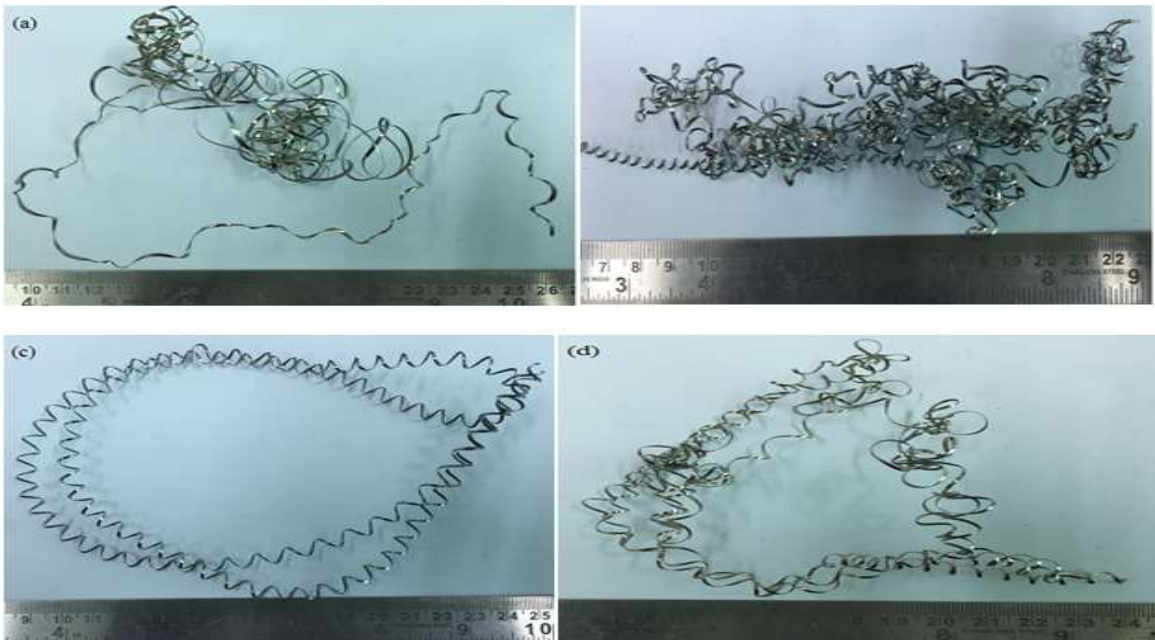


**Figure 4. 17** Chip forms generated at  $v = 78.5$  m/min,  $f = 0.143$  mm/rev and  $d = 1.4$  mm under different cooling environments (a) Cryogenic (b) MQL (c) Wet (d) Dry.



## 4.7 EFFECT OF COOLING ENVIRONMENT AND PROCESS PARAMETERS ON SURFACE ROUGHNESS

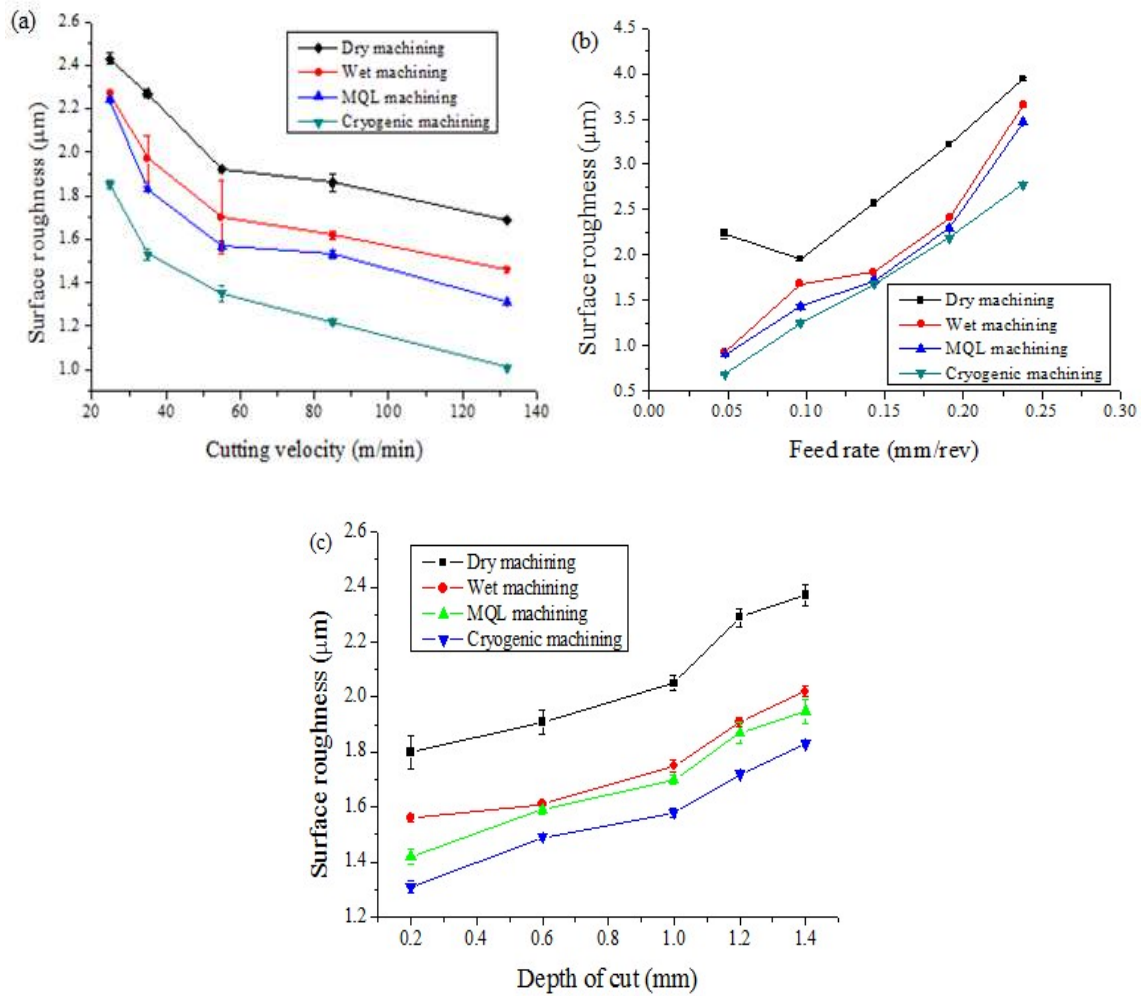
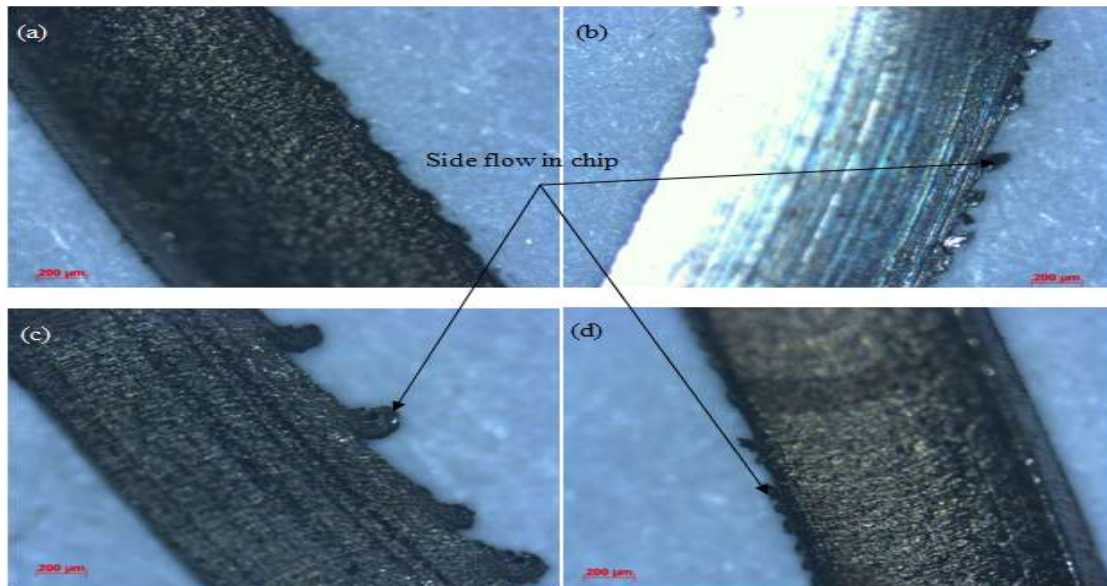


Figure 4. 18 Effect of (a) Cutting velocity (b) Feed rate and (c) Depth of cut on surface roughness under different cutting environments by keeping all other variables as constant at their mean levels.



**Figure 4. 19** Microscopic images of chips at  $v = 78.5$  m/min,  $f = 0.143$  mm/rev and  $d = 1.4$  mm under different cooling environments (a) Cryogenic (b) MQL (c) Wet (d) Dry.

#### 4.7.1 Effect of cooling environment and cutting velocity on surface roughness

In the current study, the average surface roughness value ( $R_a$ ) was considered for representing the surface finish of the machined surfaces because it is most commonly used in manufacturing industries across the world. The effect of cooling environment and cutting velocity on surface roughness as shown in Figure 4.19 (a) and decreasing trend was observed for all the cooling environments. This effect is due to increase of cutting temperatures with an increase in cutting velocity, this causes to thermal softening of workpiece material and more removal of surface discontinuities and flaws at the high cutting velocities resulting in reduced surface roughness (Pawade et al., 2007). At a cutting velocity of 25 m/min, the obtained surface roughness in cryogenic machining was  $1.85 \mu\text{m}$  whereas, it was  $2.43$ ,  $2.27$  and  $2.24 \mu\text{m}$  for dry, wet and MQL machining respectively as depicted in Figure 4.19 (a). At this point, the decrease of surface roughness in cryogenic machining was 24 %, 19 % and 17 %, respectively compared to dry, wet and MQL machining. It was also pragmatic that MQL machining reduced the

surface roughness by 8 % and 1 %, respectively compared to dry and wet machining environments. However, it was noticed that MQL and wet machining were obtained very closer surface roughness values at this cutting velocity. At a high cutting velocity of 132 m/min, the obtained surface roughness values for the respective MQL, wet and dry machining environments was 1.31, 1.46 and 1.69  $\mu\text{m}$ , whereas, for cryogenic machining, it was 1.01  $\mu\text{m}$  as shown in Figure 4.19 (a). At this point, the reduction of surface roughness found in cryogenic machining was 23 %, 31 % and 40 % respectively over the MQL, wet and dry machining environments. Also, in MQL machining 22 % and 10 % reduction of surface roughness was found when compared to dry and wet machining conditions respectively. The surface finish of the machined surface is greatly influenced by the tool flank wear. At all the cutting velocities, cryogenic machining substantially reduced the surface roughness value when compared to other machining environments as shown in Figure 4.19 (a). This results in substantial control of machining zone temperatures with the spraying of  $\text{LN}_2$  at the machining zone, led to lower tool wear, thus the generation of less tool marks and less debris (which come from adhesion wear) on the machined surfaces. It is evident from the Figure 4.20 and Figure 4.21 that less surface defects were found in cryogenic machining, this is ascribed to lower cutting temperatures and retained the tool shape provided by the  $\text{LN}_2$  spray. Whereas, more surface defects like side flow, debris, grooves and adhered micro particles were identified in dry, wet and MQL machining conditions due to the type of tool geometry obtained in the respective machining environments (Refer Figure 4.3 and Figure 4.4). In the present study, the trend of the obtained results is matched with the findings of the literature results (Bordin et al., 2016). Taken as a whole, while the increase of cutting velocity from 25 m/min to 132 m/min, the range of reduction of surface roughness in cryogenic machining was 24-40 %, 19-31 % and 14-23 % respectively over dry, wet and MQL machining. From the health and environmental prospective, dry and cryogenic machining are the feasible solutions for machining 17-4 PH SS. But sustainable manufacturing point of view, cryogenic machining helped to increase the surface finish in contrast with dry machining which leads to improved product performance.

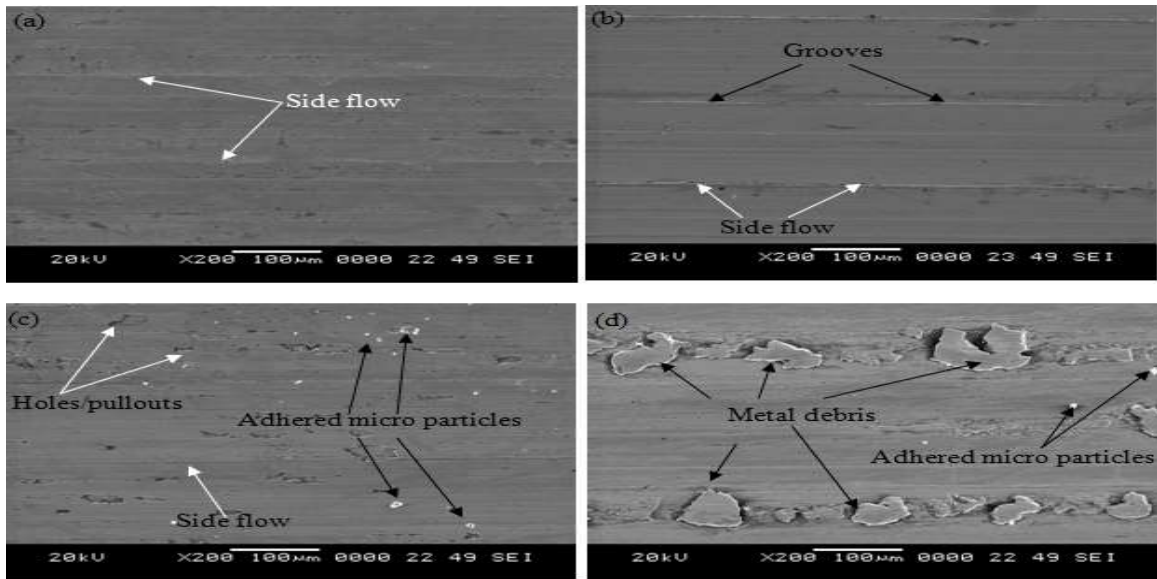


**Figure 4. 20** SEM images of machined surfaces at  $v = 25$  m/min,  $f = 0.143$  mm/rev and  $d = 1$  mm under different cooling environments (a) Cryogenic (b) MQL (c) Wet (d) Dry.

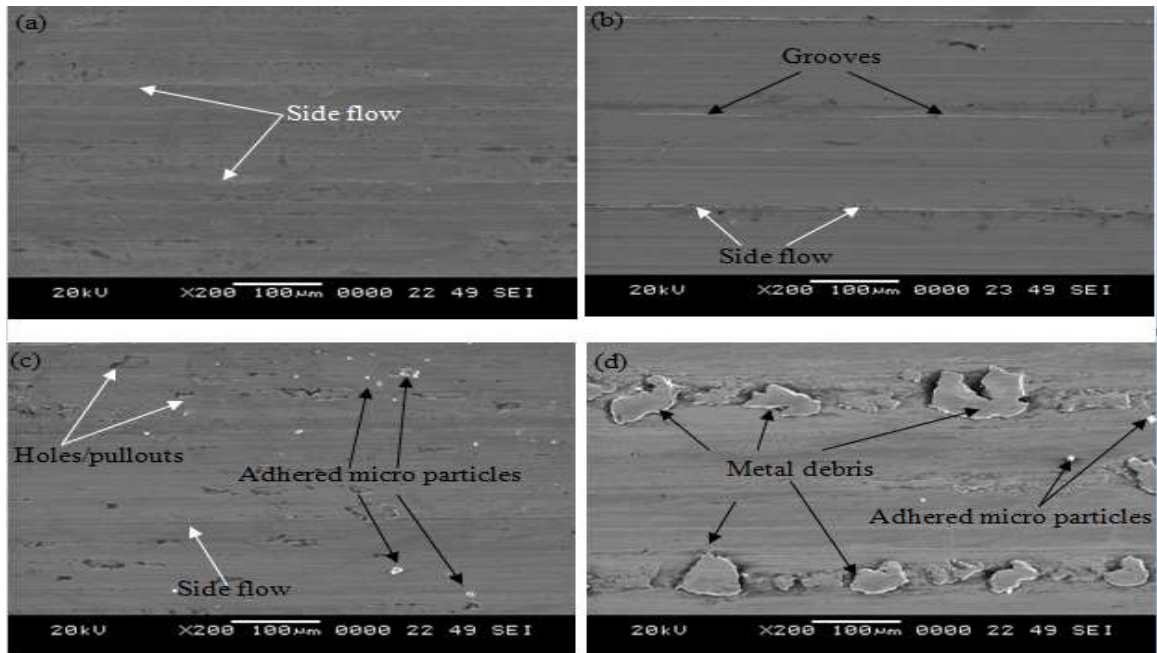


**Figure 4. 21** SEM images of machined surfaces at  $v = 132$  m/min,  $f = 0.143$  mm/rev and  $d = 1$  mm under different cooling environments (a) Cryogenic (b) MQL (c) Wet (d) Dry.

#### 4.7.2 Effect of cooling environment and feed rate on surface roughness

In the present study, an investigation was carried out on the effect of feed rate on average surface roughness and it showed an increasing trend with varying feed rates as depicted in Figure 4.19 (b). It is well known fact that feed rate and surface roughness have a directly propositional relationship. Another reason might be the generation of more tool wear at high feed rates due to more cutting zone temperature resulting in more tool marks on the machined surfaces. At all the feed rates, cryogenic machining generated lower surface roughness values than other cooling environments. The measured surface roughness values found at a low feed rate of 0.048 mm/rev in dry, wet, MQL and cryogenic machining was 2.23, 0.93, 0.91 and 0.69  $\mu\text{m}$  respectively. At a low feed rate of 0.048 mm/rev, the reduction in surface roughness obtained was 69 %, 26 % and 24 % respectively in cryogenic machining over the dry, wet and MQL machining. At this same point, MQL machining also reduced surface roughness by 59 % and 2 % respectively compared dry and wet machining. The reduction of surface roughness in cryogenic machining was due to the less adhesion of workpiece material to the cutting tool (BUE) and retain of cutting tool edge which are a result of the spraying of low temperature  $\text{LN}_2$ . Figure 4.22 depicts the surface morphology obtained on this given condition. From the SEM analysis, it was found that less side flow of material from the tool cutting edge and less adhered chip particles were contributed to low surface roughness in the cryogenic machining. Particularly, the more side flow of material was found in dry machining due to the high cutting temperatures compared to other cooling environments. In the same way, at a high feed rate of 0.238 mm/rev, 29 %, 24 % and 20 % respective reduction of surface roughness were found in cryogenic machining compared to dry, wet and MQL machining as shown in Figure 4.19 (b). Similarly, at this point, MQL machining reduced the surface roughness by 12 % and 5 % over the dry and wet machining respectively. At this point, surface morphology is shown in Figure 4.23. SEM analysis shows that especially dry machining generated more defects like side flow of material and adhered chip particles which are resulting from more tool wear and high cutting temperatures. Whereas, fewer defects were found in other cooling environments, especially very low

defects were observed in cryogenic machining owing low machining zone temperatures and low tool wear. In overall, the range of surface roughness reductions in cryogenic machining was found to be 29-69 %, 7-26 % and 2-24 % respectively compared to dry, wet and MQL machining. Similar results were obtained in the literature (Chetan et al., 2015; Bordin et al., 2016).

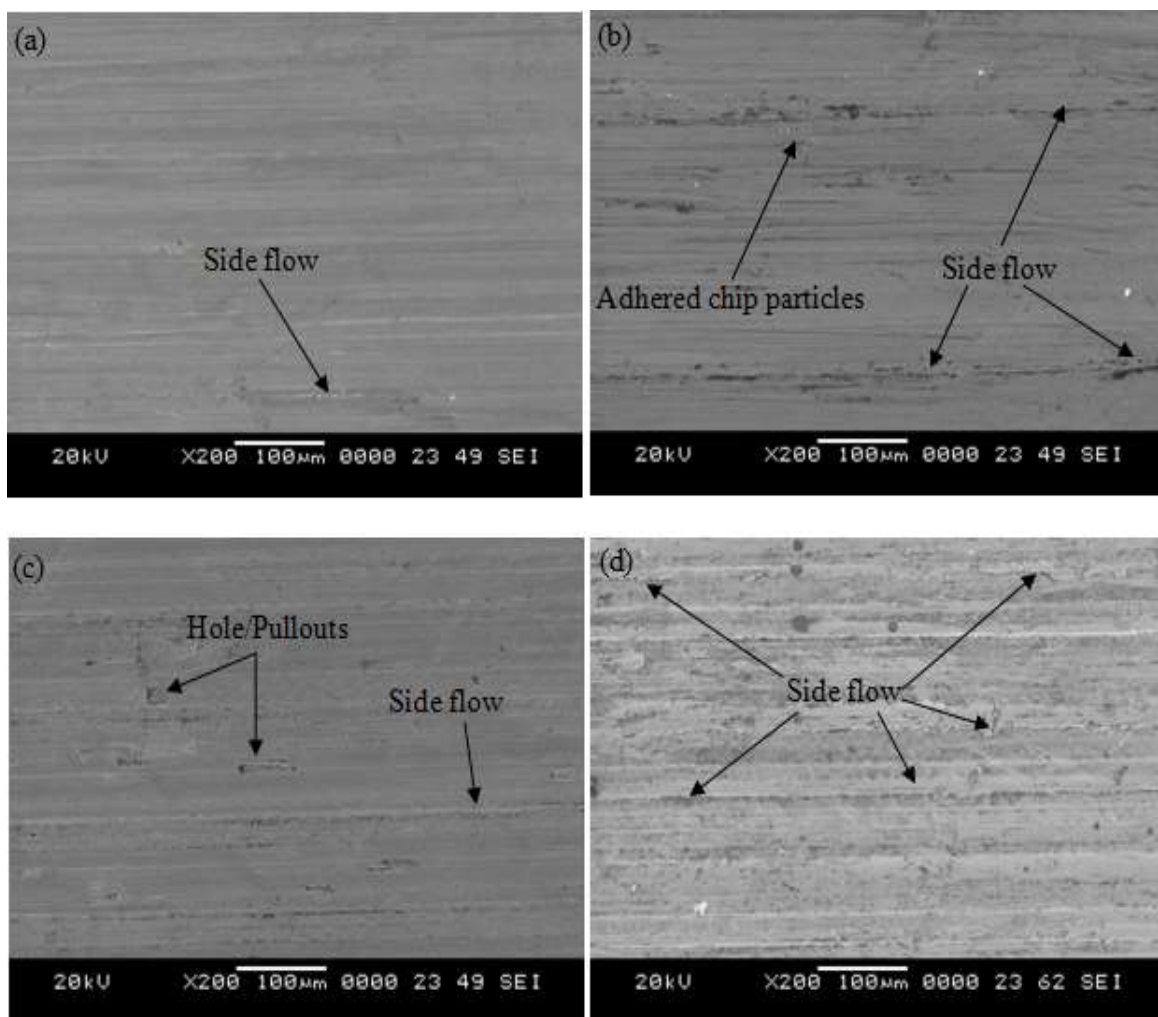


**Figure 4. 22** SEM images of surface morphology at  $v = 55$  m/min,  $f = 0.048$  mm/rev and  $d = 1$  mm under different cooling environments (a) Cryogenic (b) MQL (c) Wet (d) Dry.

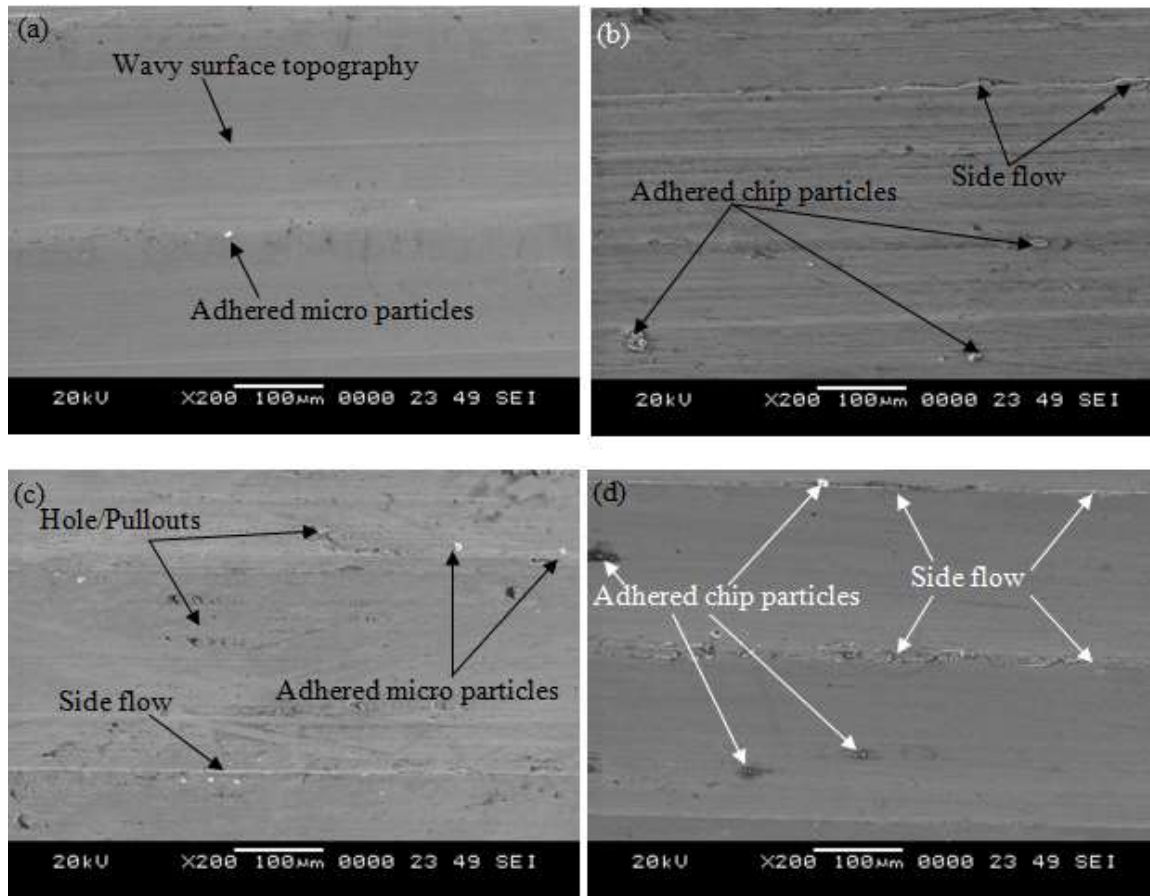


**Figure 4. 23** SEM images of surface morphology at  $v = 55$  m/min,  $f = 0.238$  mm/rev and  $d = 1$  mm under different cooling environments (a) Cryogenic (b) MQL (c) Wet (d) Dry.

#### 4.7.3 Effect of cooling environment and depth of cut on surface roughness

As depicted in Figure 4.19 (c), when the depth of cut increases then increase in surface roughness was found under all the machining environments. This trend is due to the rise of cutting temperature at a high depth of cut causes more tool wear, this leads to more tool wear marks on the machined surface resulting more surface roughness. At a low depth of cut of 0.2 mm, the obtained surface roughness was 1.8, 1.56, 1.42 and 1.31  $\mu\text{m}$  respectively in dry, wet, MQL and cryogenic machining. At this condition, cryogenic machining reduced the surface roughness by 27 %, 16 % and 8 % respectively over the

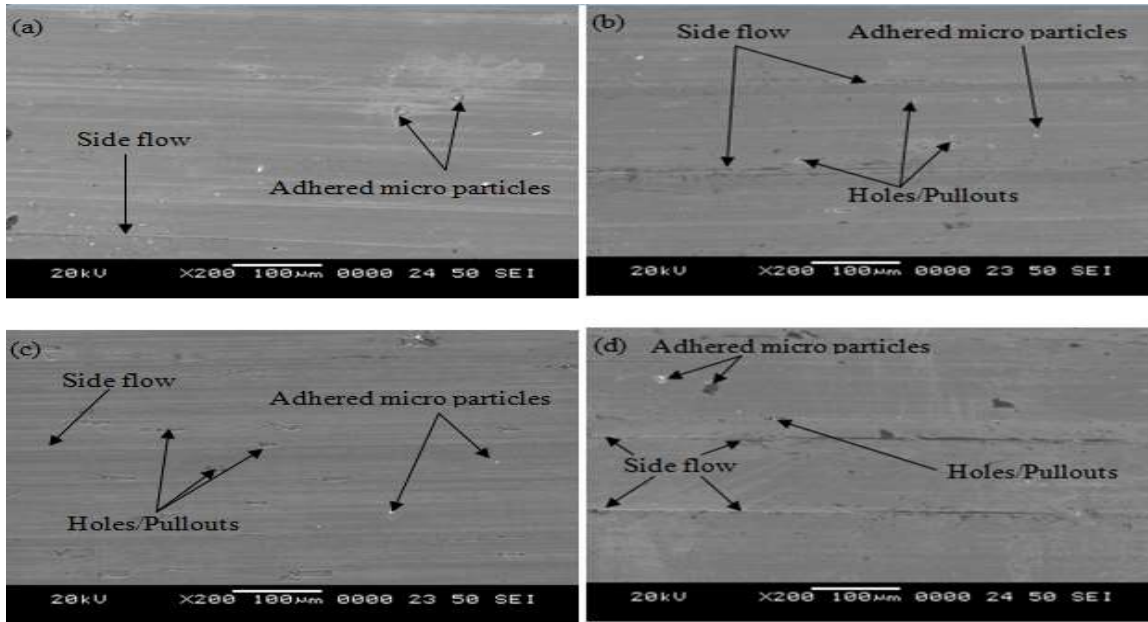
dry, wet and MQL machining. The surface roughness measurements obtained at high depth of cut of 1.4 mm was 2.37, 2.02, 1.95 and 1.83  $\mu\text{m}$  respectively for dry, wet, MQL and cryogenic machining. At this point, cryogenic machining reduced the surface roughness by 23 %, 9 % and 6 % respectively over the dry, wet and MQL machining condition. Similarly, at this condition, the surface roughness reduction found in MQL machining was 18 % and 3 % respectively over the dry and wet machining. At all the depth of cut conditions, cryogenic machining substantially reduced the surface roughness of the machined samples compared to other cutting environments. This is because of lower temperatures offered by the  $\text{LN}_2$  causes of retainment of cutting tool edge led to less tool marks on the machined surfaces results in lower surface roughness. From Figure 4.24 and Figure 4.25, it was found that few surface defects were developed on machined surfaces in cryogenic machining compared to other machining environments. This is due to the efficient control of machining zone temperatures compared to MQL, wet and dry machining environments. In overall, cryogenic machining reduced the surface roughness in the range of 22-27 %, 9-16 % and 6-8 % respectively compared to dry, wet and MQL machining while varying of a depth of cut from 0.2 mm to 1.4 mm respectively. Whereas, the surface roughness reductions found in MQL was 17-21 % and 1-9 % respectively over the dry and wet machining conditions.

#### **4.8 EFFECT OF COOLING ENVIRONMENT AND PROCESS PARAMETERS ON SURFACE TOPOGRAPHY**

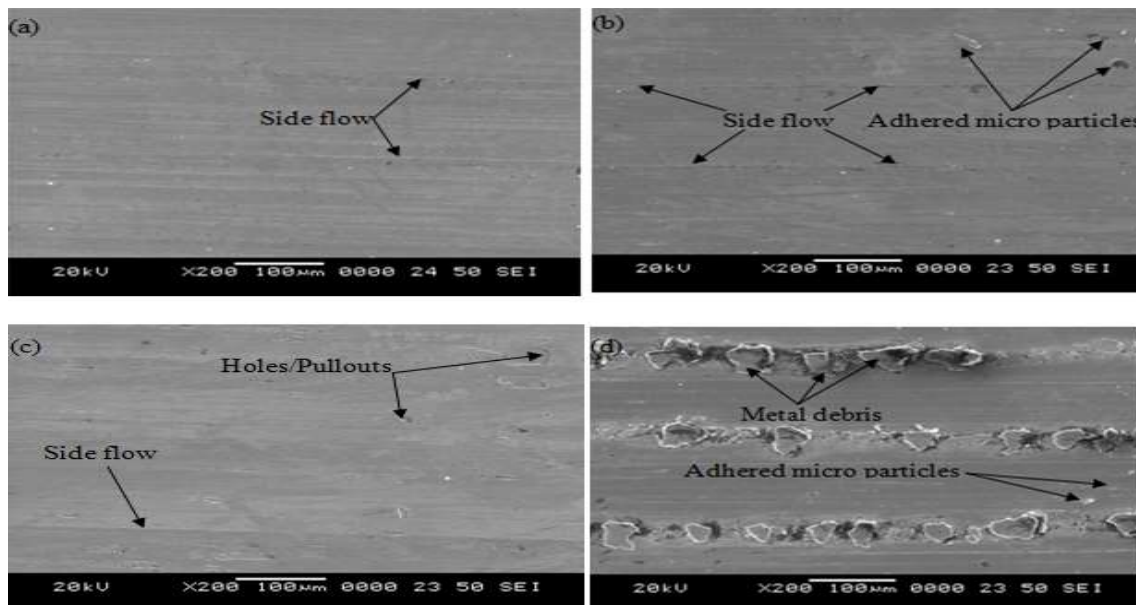
##### **4.8.1 Effect of cooling environment and cutting velocity on surface topography**

Figure 4.26 and Figure 4.27 depict the surface topography obtained in various environmental machining conditions at varying cutting velocity condition. At a low cutting velocity of 25 m/min, cryogenic machining produced the low peak intensity and uniform machined surfaces compared to MQL, wet and dry machining. At a high cutting velocity of 132 m/min, cryogenic machining generated low peak intensity and more uniform surfaces than at a low cutting velocity compared to other machining environments.





**Figure 4. 24** SEM images of surface morphology at  $v = 55$  m/min,  $f = 0.143$  mm/rev and  $d = 0.2$  mm under different cooling environments (a) Cryogenic (b) MQL (c) Wet (d) Dry.



**Figure 4. 25** SEM images of surface morphology at  $v = 55$  m/min,  $f = 0.143$  mm/rev and  $d = 1.4$  mm under different cooling environments (a) Cryogenic (b) MQL (c) Wet (d) Dry.

This is a result from the less tool flank wear (less BUE formation from adhesion wear) observed in the cryogenic machining compared to other cooling environments. Another reason might be the reduction of machining zone temperatures causes less thermal distortion on the cryogenically machined surfaces (Kaynak et al., 2014). In the literature, similar findings were observed (Pereira et al., 2016; Kaynak, 2014; Dinesh et al., 2015). From the Figure 4.26 and Figure 4.27, it was observed that as the cutting velocity increases, the peak intensity of machined surfaces reduces under all the cooling environments. This is due to the increased thermal softening effect at the higher cutting conditions causes fewer surface defects in machined surfaces under all the cooling environments.

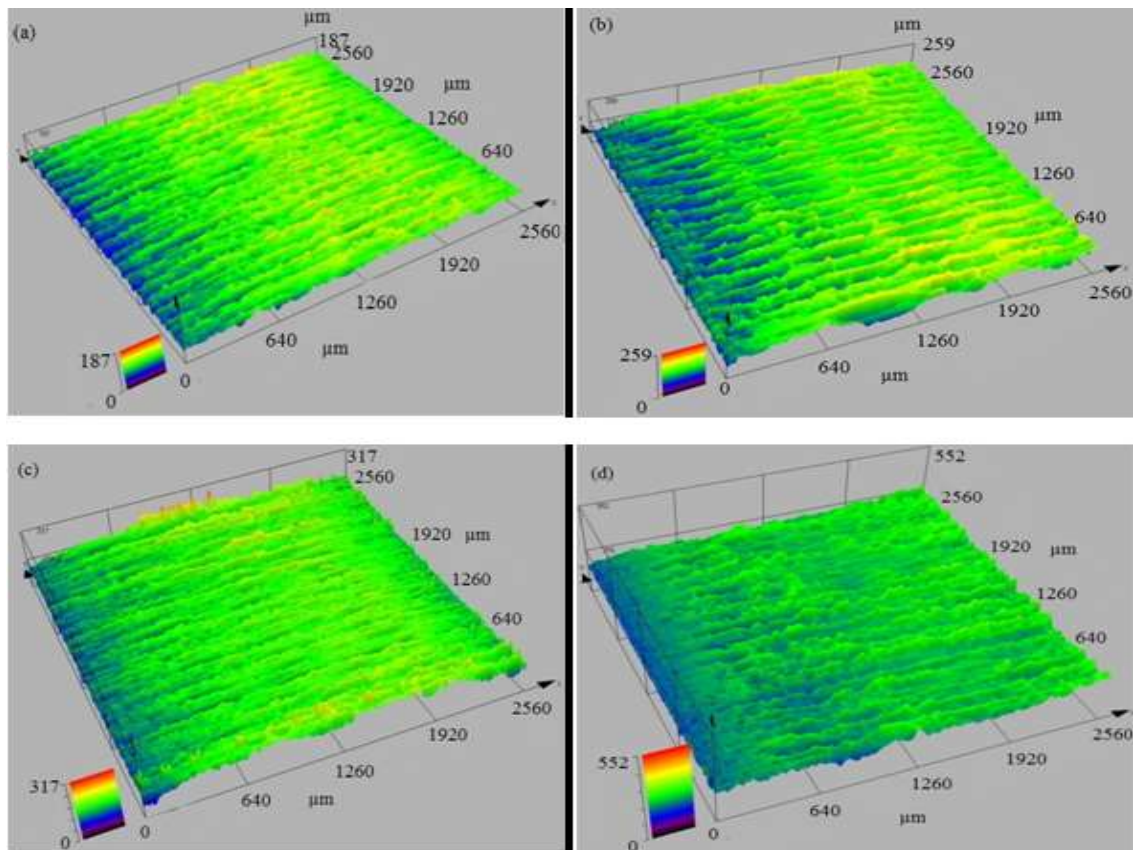


**Figure 4. 26** SEM images of surface topography at  $v = 25$  m/min,  $f=0.143$  mm/rev and  $d = 1$  mm under different cooling environments (a) Cryogenic (b) MQL (c) Wet (d) Dry.

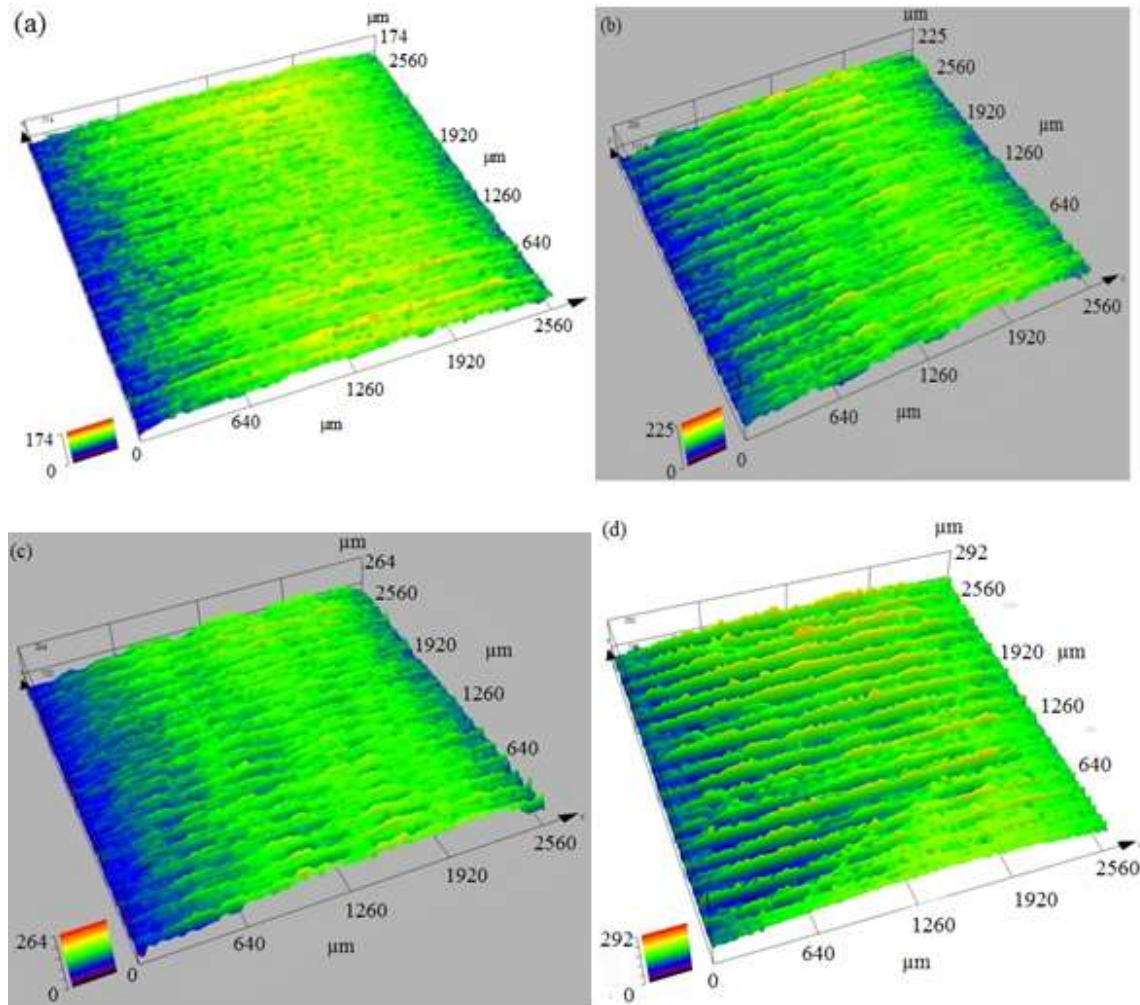
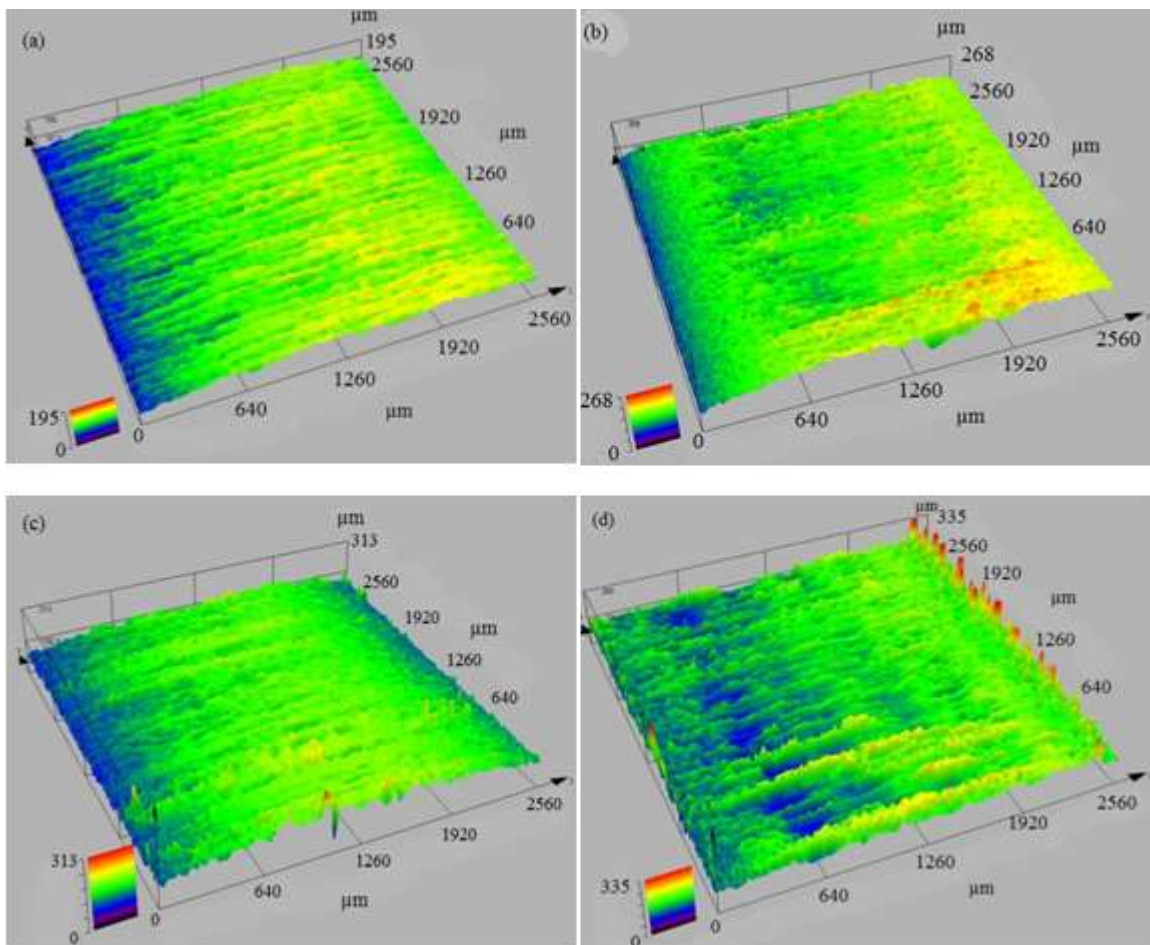


**Figure 4. 27** SEM images of surface topography at  $v = 132$  m/min,  $f = 0.143$  mm/rev and  $d = 1$  mm under different cooling environments (a) Cryogenic (b) MQL (c) Wet (d) Dry.

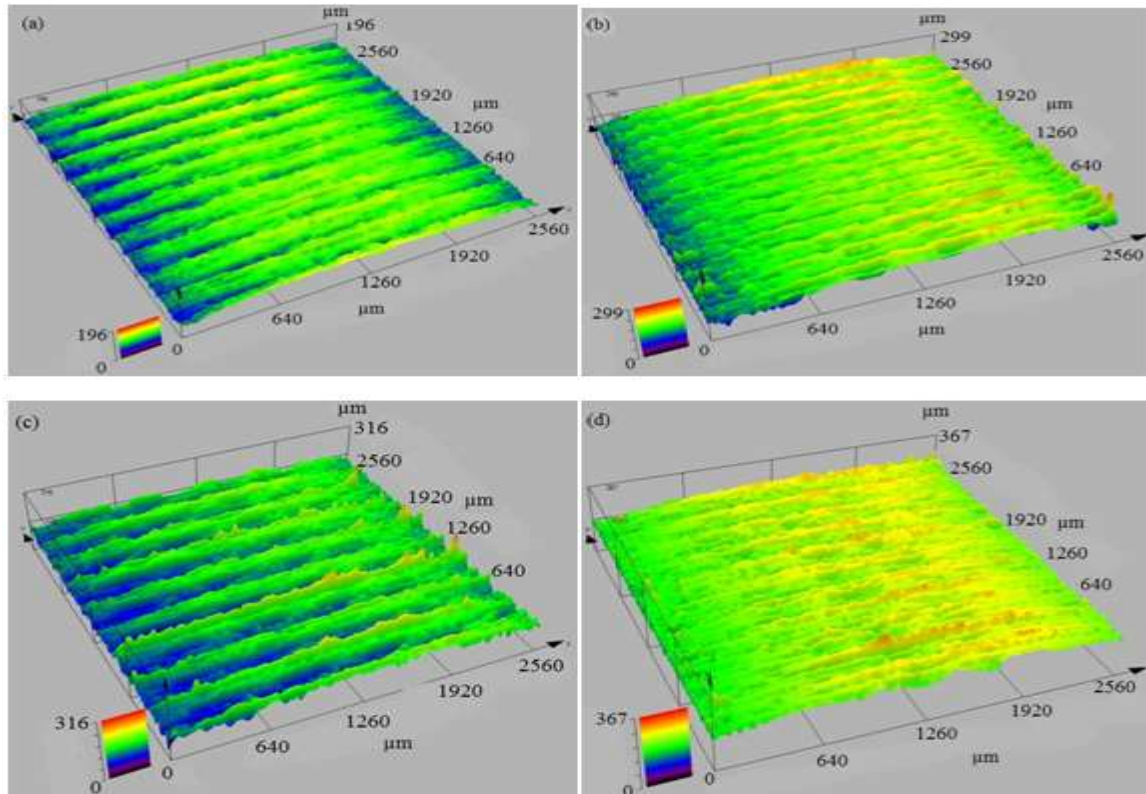
#### 4.8.2 Effect of cooling environment and feed rate on surface topography

Figure 4.28 and Figure 4.29 depict the surface topography of machined surfaces at varying feed rate conditions. From Figure 4.28 and Figure 4.29, it can be noticed that as feed rate increases from 0.048 mm/rev to 0.232 mm/rev, machined surface peak intensity rises. This is because of increased tool wear as feed rate increases. At a low feed rate of 0.048 mm/rev, cryogenic machining produced surface peaks with lower intensity than

other machining environments as depicted in Figure 4.28. In particular, dry machining produced wavier surface and high intensity of surface peaks due to more side flow formation results from high cutting temperature. These results match with the literature results (Kaynak, 2014). At a high feed rate of 0.232 mm/rev, except in cryogenic machining, all other machining environments have generated high intensity peaks and nonuniform wavy surfaces as depicted Figure 4.29. This effect is due to more side flow of material, adhered chip elements and tool wear marks which are results from high cutting temperatures.



**Figure 4. 28** 3D images of surface topography at  $v = 55$  m/min,  $f = 0.048$  mm/rev and  $d = 1$  mm under different cooling environments (a) Cryogenic (b) MQL (c) Wet (d) Dry.



**Figure 4. 29** 3D images of surface topography at  $v = 55$  m/min,  $f = 0.238$  mm/rev and  $d = 1$  mm under different cooling environments (a) Cryogenic (b) MQL (c) Wet (d) Dry.

### 4.8.3 Effect of cooling environment and depth of cut on surface topography

From the Figure 4.30 and Figure 4.31, it was observed that as the depth of cut increases, the peak to valley height of the machined surface increases. This results in increased tool wear at a higher depth of cuts. Cryogenic machining reduced the peak to valley height substantially compared to other machining environments. Whereas, in other machining environments, more peak to valley height was found at all the depth of cuts due to higher cutting temperatures. From the results, it was observed that cryogenic machining produced the favorable surface topography compared to other machining conditions at all the process variable variation conditions. So, cryogenic machining can improve the product performance greatly compared to other machining conditions.

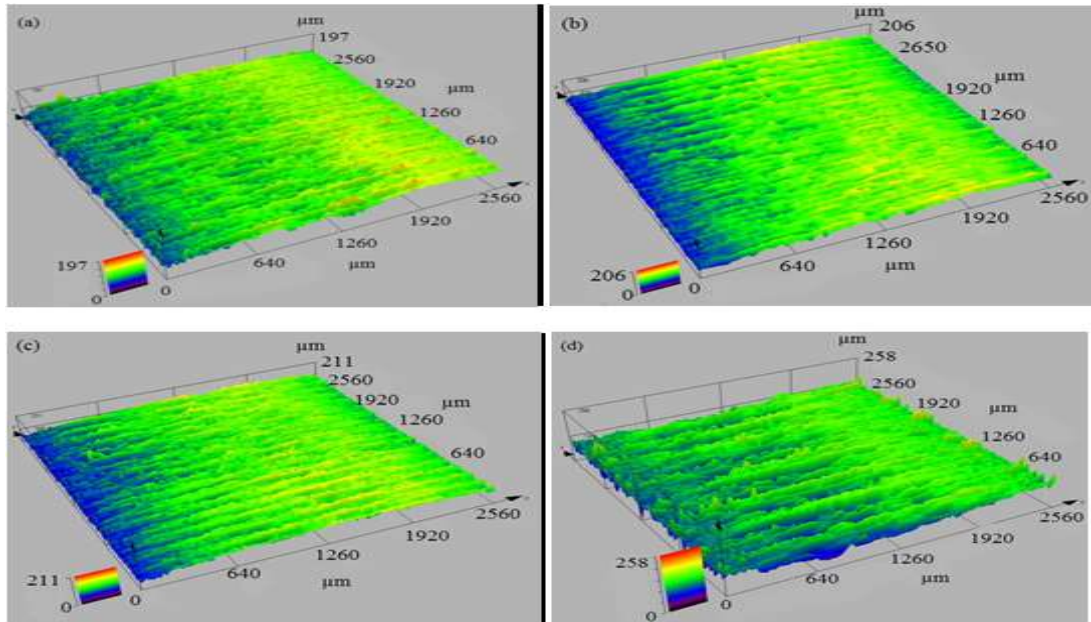


**Figure 4. 30** 3D surface topography at  $v = 78.5$  m/min,  $f = 0.143$  mm/rev and  $d = 0.2$  mm under different cooling environments (a) Cryogenic (b) MQL (c) Wet (d) Dry.

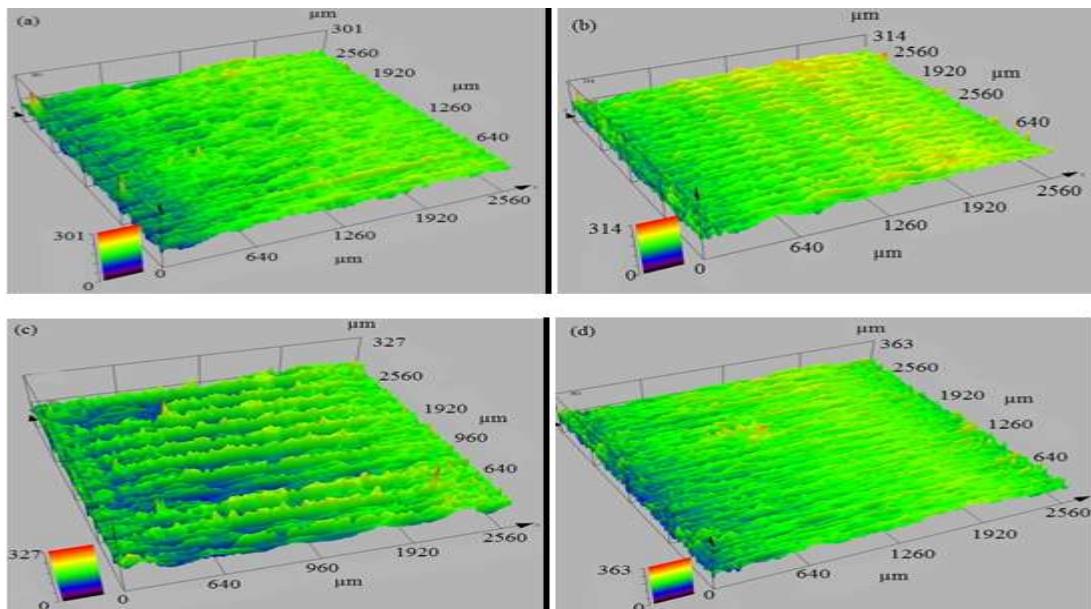


**Figure 4. 31** 3D surface topography at  $v = 78.5$  m/min,  $f = 0.143$  mm/rev and  $d = 1$  mm under different cooling environments (a) Cryogenic (b) MQL (c) Wet (d) Dry

#### 4.9 EFFECT OF MACHINING ENVIRONMENT AND PROCESS PARAMETERS ON MICROHARDNESS

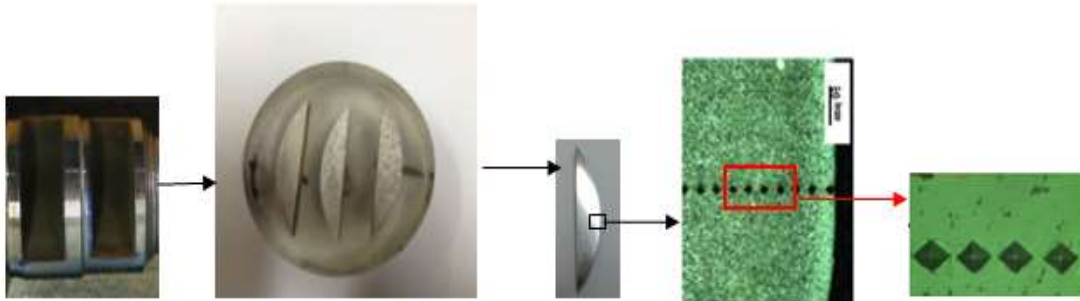


Figure 4. 32 Method of sample preparation and measurement of microhardness.

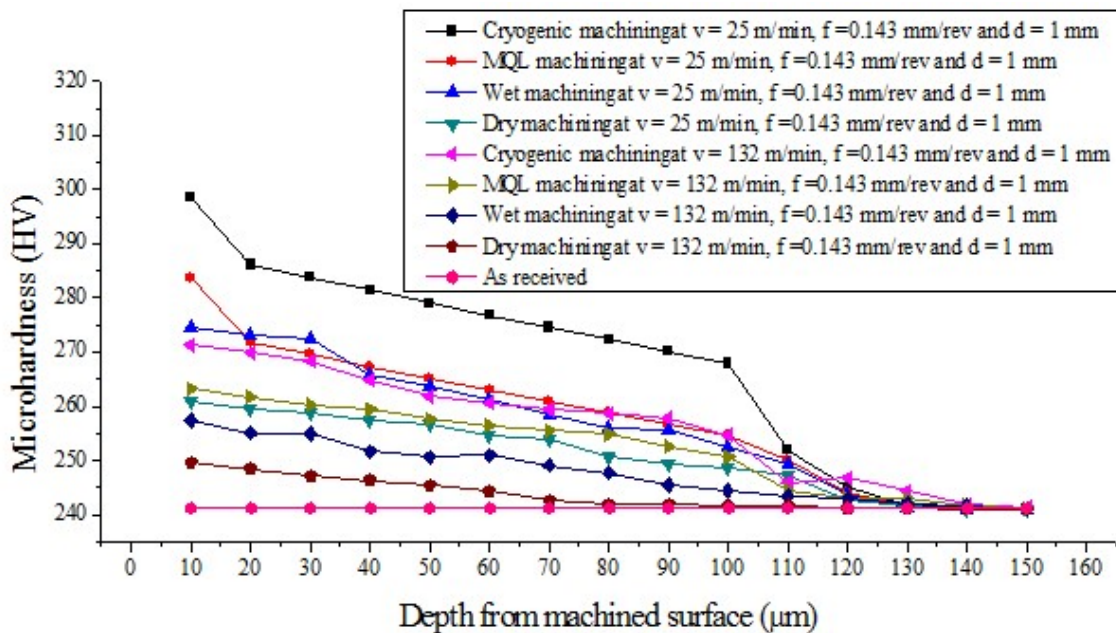


Figure 4. 33 Subsurface microhardness profiles of machined samples at various machining conditions.

In material processing applications, surface and subsurface hardness have an important role because they notably affect the wear resistance and fatigue life of the final product. High wear resistance can be obtained with higher microhardness surfaces. Method of sample preparation for microhardness of the cross sectional machined surface is shown in Figure 4.32. Initially Wire EDM been used to the cut the machined samples into semi

circular shape, Afterwards, various grades of silicon papers and diamond paste have been used for polishing to obtain mirror finished across the machined surface. Figure 4.33 shows the microhardness at the cross-sectional view of the machined surfaces under the different cooling environments at the different cutting conditions. From the machined surface, reference point (0  $\mu\text{m}$ ) was set at a distance of 10  $\mu\text{m}$  due to the limitation in measurement. Measurements were considered at a step of 10  $\mu\text{m}$  until the bulk material microhardness was reached. From Figure 4.33, it was seen that when the depth beneath the machined surface increases, then the microhardness reduces in all the machining environments. Microhardness values at a high cutting velocity of 132 m/min were 261, 275, 284 and 299 HV respectively for dry, wet, MQL and cryogenic machining environments. At this point, the results showed that the rise of microhardness value in cryogenic machining was 13 %, 8 % and 5% respectively contrasted with dry, wet and MQL machining environments. This is due to the grain refinement in the machined material microstructure, which is promoted by  $\text{LN}_2$  as shown in Figure 4.34. However, in cryogenic machining, maximum of 299 HV microhardness was observed at a high feed rate at the given conditions and gradually decreased up to the bulk material microhardness of 241 HV. Hence, cryogenic machining is favorable for increased fatigue life and wear resistance compared to wet machining.

#### **4.10 EFFECT OF MACHINING ENVIRONMENT AND PROCESS PARAMETERS ON WHITE LAYER THICKNESS (WLT)**

Surface wear resistance and fatigue life are the most important required properties for product reliability and these properties are greatly affected by the white layer formation (depth of affected layer) in metal cutting operation. Especially it is a major concern for aerospace and automotive industries (Bosheh and Mativenga, 2006). If the white layer thickness increases, then both subsurface wear resistance and fatigue life decreases due to hard and brittle nature of white layer, so that micro cracks can easily cleave and propagate rapidly. In the literature, the relation between the tool wear and the white layer thickness has been discussed (Umbrello and Filice, 2009; Poulachon et al., 2005). It has



been reported that as tool wear increases, white layer thickness increases. In the current study, high tool wear values were observed at high cutting velocity compared to low cutting velocity.

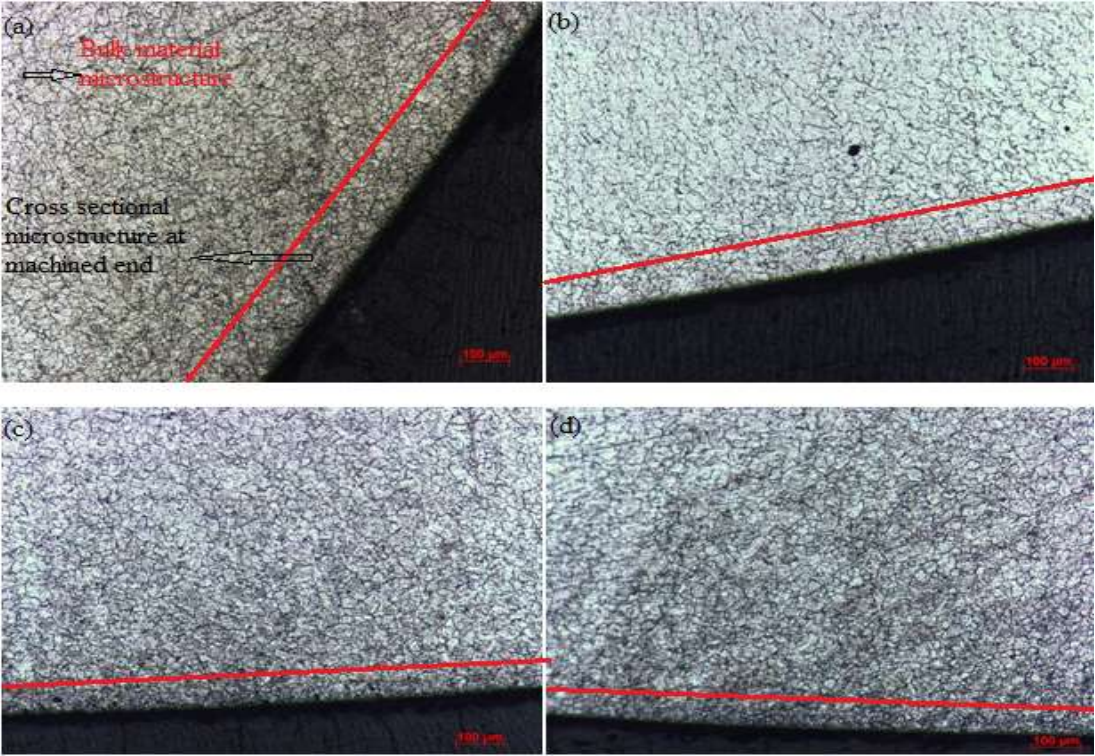


**Figure 4. 34** Cross-sectional microstructure after (a) cryogenic and (b) MQL (c) Wet (d)Dry machining at  $v = 132$  m/min,  $f = 0.143$  mm/rev and  $d = 1$  mm.

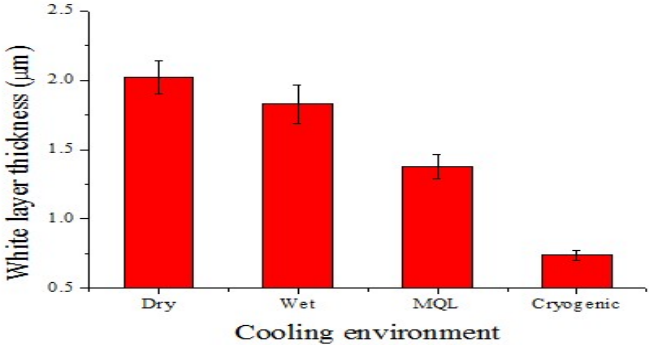


**Figure 4. 35** Effect of cooling environment on white layer thickness at  $v = 132$  m/min,  $f = 0.143$  mm/rev and  $d = 1$  mm.

From Figure 4.35, at the respective given cutting conditions, the observed WLT values for the dry, wet, MQL and cryogenic machining was 2.020, 1.827, 1.376 and 0.737  $\mu\text{m}$  respectively. A similar type of results was found in the literature (Pu et al., 2012; Umbrello et al., 2012) during machining of steel grade material. From the Figure 4.35, it was observed that cryogenic machining produced low WLT compared to other machining environments. It is evident from the Figure 4.36 that WLT produced in cryogenic machining was less compared to other machining environments. This is because of lower cutting temperatures and low tool wear with  $\text{LN}_2$  cooling compared to other cooling environments. Another reason might be due to the reduction of rate of plastic deformation, rapid cooling and quenching mechanisms in cryogenic machining cause for low WLT (Umbrello et al., 2012).

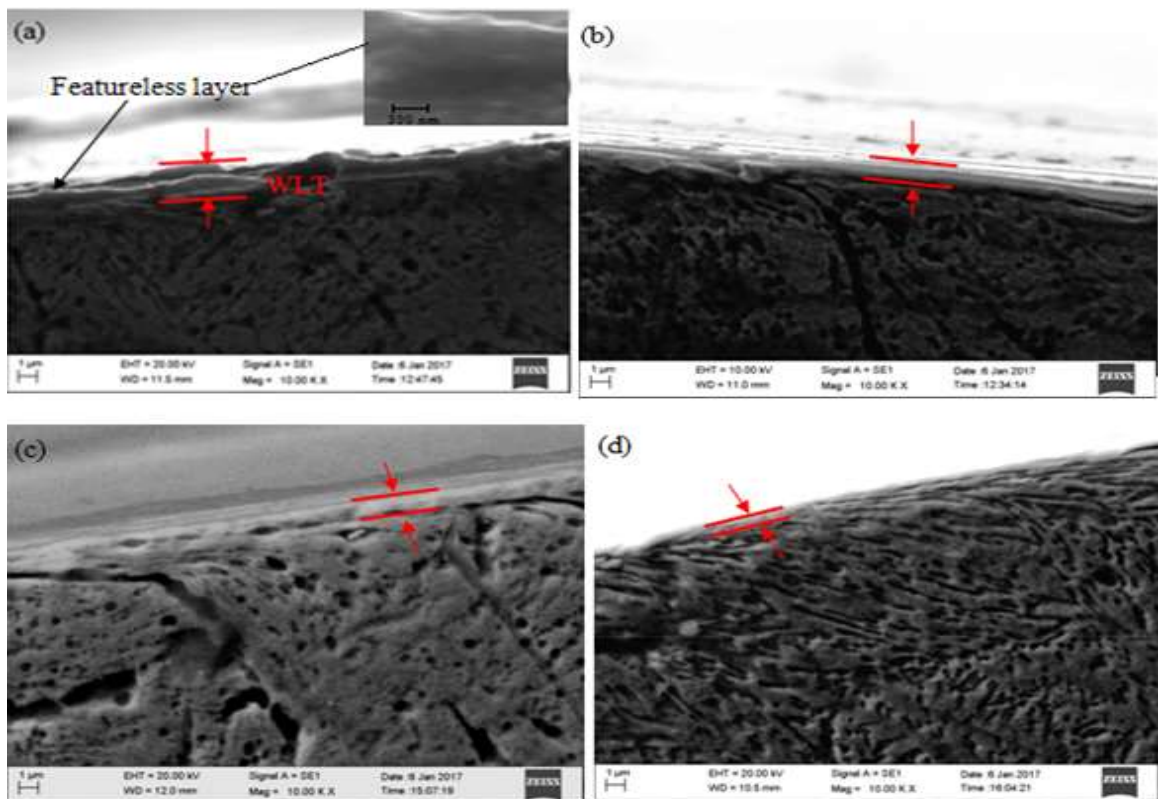


**Figure 4. 36** SEM images of white layer thickness at  $v = 132 \text{ m/min}$ ,  $f = 0.143 \text{ mm/rev}$  and  $d = 1 \text{ mm}$  under different cooling environments (a) Dry (b) Wet (c) MQL (d) Cryogenic.

Figure 4.37 depicts the EDAX analysis at the given condition. From the EDAX analysis, it was found that white layer consists of different chemical composition (presence of foreign elements like C, O and absence of nickel element) compared to the polished surface (bulk material), these changes make the metallurgical changes in the white layer and show different properties. From the results, it has been found that at  $v = 132$  m/min,  $f = 0.143$  mm/rev and  $d = 1$  mm conditions, cryogenic machining reduces the WLT by 63 %, 60 % and 46 % compared to dry, wet and MQL respectively. So, cryogenic machining significantly improves the wear resistance of the product over the other cooling environments.

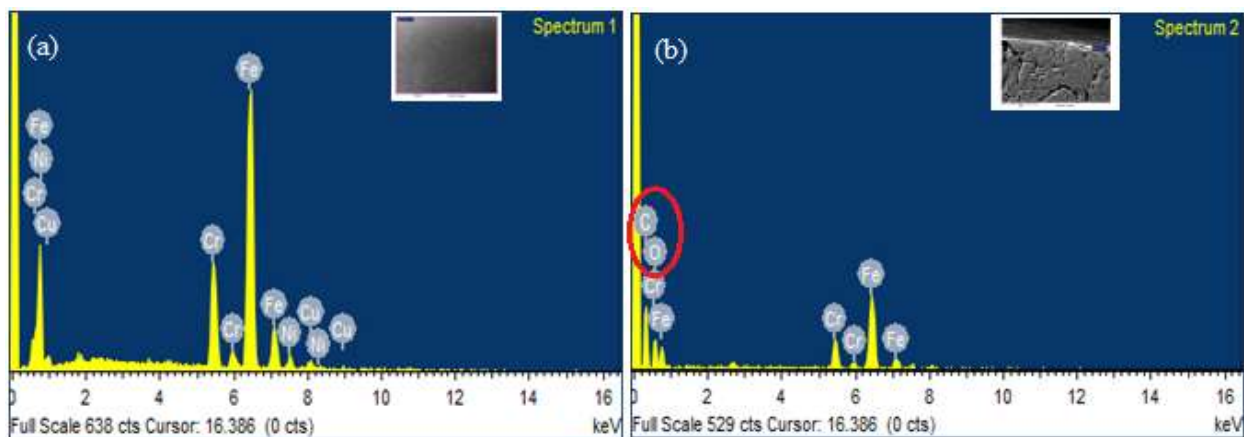


**Figure 4. 37** EDAX analysis of 17-4 PH SS (a) At polished surface (b) At white layer surface

From the operator's health and environmental point of view, wet coolant causes skin decreases and environmental damage. In the same way, for MQL machining there is no environmental pollution, but MQL mist causes inhalation problems to the operator. Whereas, with dry and cryogenic machining no health and environmental pollution because  $LN_2$  quickly evaporates, but dry machining fails to produce quality products and increased productivity, whereas, cryogenic increases both quality and productivity of the product from the sustainable manufacturing point of view. However, in cryogenic machining, proper care has to be taken while handling  $LN_2$ , if skin is exposed to liquid

nitrogen for a longer period, it leads to cold burning. To avoid this, operator should follow safety precautions like use of cryo gloves, cryo apron and cryo face shield while conducting experiments under the cryogenic cooling environment. In overall, at all the parameter settings, cryogenic machining yield better performance characteristics compared to dry, wet and MQL conditions by satisfying the health, environmental and sustainable manufacturing issues. Hence, cryogenic machining is the feasible method for improving the turning performance characteristics in machining of 17-4 PH SS. So, cryogenic machining is chosen for further chapters (optimization and modeling) in this thesis.

#### **4.11 SUMMARY**

In this chapter, influence of process parameters like cutting velocity, feed rate and depth of cut has been studied on cutting temperature, tool flank wear ( $V_b$ ), MRR, chip morphology and surface integrity (surface topography, surface finish ( $R_a$ ), microhardness and white layer thickness) under dry, wet, MQL and cryogenic cooling environments and following results were observed.

- It was observed that as the cutting velocity, feed rate and depth of cut increases, the cutting temperature, flank wear and MRR increased respectively under all the cooling environments. Whereas, in the case of surface roughness, decreasing trend was observed at the cutting velocity increasing condition and increasing trend was found for feed rate and depth of cut increasing conditions respectively. In overall, cryogenic machining attained the positive results in terms of cutting temperature, flank wear and MRR over dry, wet and MQL cooling environments.
- The maximum cutting temperature drop found in cryogenic was 72 %, 64 % and 62 % respectively in contrast to dry, wet and MQL machining conditions
- The maximum tool flank wear reductions observed in cryogenic machining was 60 %, 55 % and 50 % respectively over the dry, wet and MQL machining conditions.

- The maximum surface roughness reduction in cryogenic machining was found to be 69 %, 31 % and 24 %, respectively compared to dry, wet and MQL machining.
- Cryogenic machining increased the MRR to a maximum of 22.40 %, 26.52 % and 21.65 % respectively over dry, wet and MQL machining environments respectively.
- Cryogenic machining produced favorable chip forms with less residual at all the cutting velocities by improving the chip breakability capability compared to other machining environments.
- In overall, cryogenic machining improved the surface and subsurface properties positively, result in improved performance of the product compared to other machining environmental conditions.
- From the health, environmental clean and productivity improvement point of view, cryogenic machining satisfies the requirements compared to dry, wet and MQL machining conditions.

## **CHAPTER-5**

### **OPTIMIZATION OF CRYOGENIC TURNING PROCESS**

#### **5.1 INTRODUCTION**

This chapter discusses the optimization of cutting conditions for single and multiple objective responses under the cryogenic cooling environment. Taguchi method was used for single response optimization and ANOVA was used to find the most influencing process parameter on each response. Taguchi coupled Grey relational analysis (TGRA) and Taguchi coupled TOPSIS optimization techniques have been applied for multi response optimization, best multi optimization tool which suits for the current study have been selected through conformation tests.

#### **5.2 EXPERIMENTAL PLAN**

In this chapter, Taguchi  $L_9$  orthogonal array has been considered to determine the optimum cutting conditions for single and multiple objective responses respectively under the cryogenic cooling environment. List of process parameters and their levels taken in the present chapters are shown in Table 5.1. Output responses considered in the present chapter are tool flank wear ( $V_b$ ), surface finish ( $R_a$ ) and MRR respectively. Experimental results under cryogenic cooling environment were shown in Table 5.2. From literature, it was observed that no optimization technique is better for determining the optimum cutting conditions for multi response optimization. The best way is to apply the several optimization techniques for particular process and select the best optimization technique for that process (Wu and Wu, 2015). Hence, in the present chapter, two multi objective optimization techniques namely Taguchi coupled GRA and Taguchi coupled TOPSIS have been applied and selected the best suited technique for determining the optimum cutting conditions for cryogenic turning process. Taguchi is a powerful single

response optimization technique; hence, it is used for determining the optimum cutting conditions for single response optimization of cryogenic turning process. ANOVA is employed for each response to determine the most influenced process parameter of each response.

**Table 5. 1** Cryogenic turning process parameters and their levels for optimization study.

Symbol	Process parameters	Units	Levels		
			1	2	3
$v$	Cutting velocity	m/min	25	85	132
$f$	Feed rate	mm/rev	0.048	0.143	0.238
$d$	Depth of cut	mm	0.2	0.6	1

### 5.3 TAGUCHI TECHNIQUE (SINGLE OBJECTIVE OPTIMIZATION)

Genichi Taguchi (Taguchi, 1987) used a loss function; it is a difference of experimental value and target value which is again converted into the S/N ratio. S/N ratio defined as the ratio of mean to standard deviation. Taguchi used terms like signal and noise which represents wanted value (mean) for the response and unwanted value (standard deviation) for the response respectively. Based on the requirements of response, Taguchi divided the S/N ratio into three categories namely nominal-the-better, higher-the-better and lower-the-better. In the present study, the quality characteristics like  $R_a$  and  $V_b$  are the lower-the-better requirement whereas MRR is higher-the-better to enhance the machinability. So, equation (5.1) and equation (5.2) have been used to calculate the S/N ratio and results have been shown in Table 5.2. Taguchi analysis was done using Minitab 17.0 software tool, means of S/N ratio plots and analysis of variance (ANOVA) results were obtained and presented in the forth coming discussions.

$$\text{S/N ratio for the smaller the better} = -10 \log \frac{1}{n} \sum (R)^2 \quad (5.1)$$

$$\text{S/N ratio for larger the better} = -10 \log_{10} \frac{1}{n} \sum_{i=1}^n \left( \frac{1}{R^2} \right) \quad (5.2)$$

Where, n = No. of observations

R = Observed data for each response

**Table 5. 2** Plan of experiments, experimental results and their calculated S/N ratios.

Exp. runs	Controllable process parameters			Experimental results			S/N ratios of results		
	$v$	$f$	$d$	$R_a$ ( $\mu\text{m}$ )	$V_b$ ( $\mu\text{m}$ )	MRR (g/min)	$R_a$ (dB)	$V_b$ (dB)	MRR (dB)
1	1	1	1	1.16	25	2.23	-1.28916	-27.9588	6.9661
2	1	2	2	1.40	32	9.21	-2.92256	-30.103	19.2852
3	1	3	3	2.21	106	17.35	-6.88785	-40.5061	24.7860
4	2	1	2	0.99	74	10.89	0.08730	-37.3846	20.7406
5	2	2	3	1.17	85	31.58	-1.36372	-38.5884	29.9882
6	2	3	1	1.87	123	42.78	-5.43683	-41.7981	32.6248
7	3	1	3	0.97	79	21.9	0.26457	-37.9525	26.8089
8	3	2	1	1.08	103	36.52	-0.66848	-40.2567	31.2506
9	3	3	2	1.62	153	68.42	-4.19030	-43.6938	36.7037

### 5.3.1 Selection of optimum cutting conditions

#### 5.3.1.1 Surface roughness

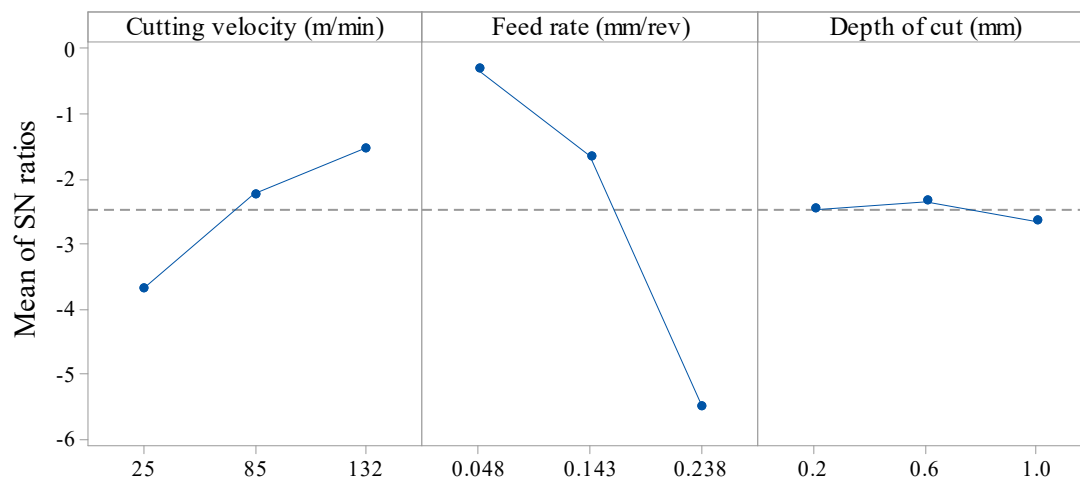
The obtained S/N ratio response table for the  $R_a$  is shown in Table 5.3. Figure 5.1 represents the mean S/N ratio graph obtained in Minitab software tool. Higher S/N ratio represents the minimum variation difference between the desirable output and measured output. From Figure 5.1, it was noticed that the highest mean S/N ratio obtained for  $R_a$  are cutting velocity at 132 m/min, feed rate at 0.048 mm/rev and depth of cut at 0.6 mm respectively. Therefore, the predicted optimum process parameters for obtaining the low



surface roughness using Taguchi method were found as  $v = 132$  m/min,  $f = 0.048$  mm/rev,  $d = 0.6$  mm and corresponding level values were bolded in Table 5.3 for easy understanding from the response table. This predicted optimum combination was represented as  $v_3 - f_1 - d_2$  for surface roughness.

**Table 5. 3** Mean S/N ratio response table for surface roughness.

Symbol	Process parameters	Mean S/N ratio				
		Level 1	Level 2	Level 3	Max-Min	Rank
$v$	Cutting velocity (m/min)	-3.6999	-2.2378	<b>-1.5314</b>	2.1685	2
$f$	Feed rate (mm/rev)	<b>-0.3124</b>	-1.6516	-5.5050	5.1926	1
$d$	Depth of cut (mm)	-2.4648	<b>-2.3419</b>	-2.6623	0.3205	3



Signal-to-noise: Smaller is better (Surface roughness)

**Figure 5. 1** Mean S/N ratio of surface roughness.

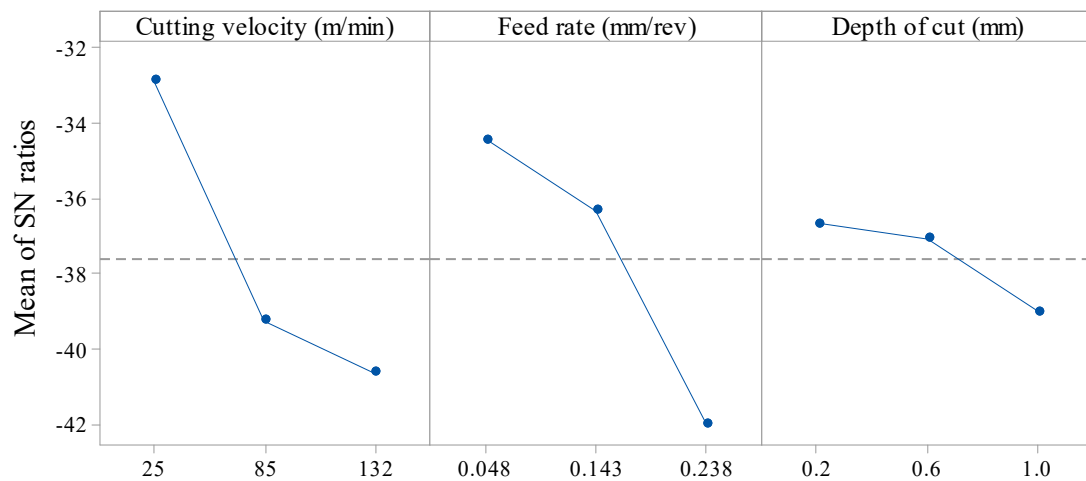
### 5.3.1.2 Flank wear

Table 5.4 shows the obtained S/N ratio response table for the tool flank wear. Means of S/N ratio was represented in the graph as depicted Figure 5.2. From the Figure 5.2, the

estimated optimum process parameters for obtaining the low tool flank was found to be  $v = 25$  m/min,  $f = 0.048$  mm/rev and  $d = 0.2$  mm respectively. This predicted optimum combination was represented as  $v_1-f_1-d_1$  for tool flank wear.

**Table 5. 4** Mean S/N ratio response table for tool flank wear.

Symbol	Process parameters	Mean S/N ratio				
		Level 1	Level 2	Level 3	Max-Min	Rank
$v$	Cutting velocity (m/min)	<b>-32.86</b>	-39.26	-40.63	7.78	1
$f$	Feed rate (mm/rev)	<b>-34.43</b>	-36.32	-42.00	7.57	2
$d$	Depth of cut (mm)	<b>-36.67</b>	-37.06	-39.02	2.34	3



Signal-to-noise: Smaller is better (Flank wear)

**Figure 5. 2** Mean S/N ratio of tool flank wear.

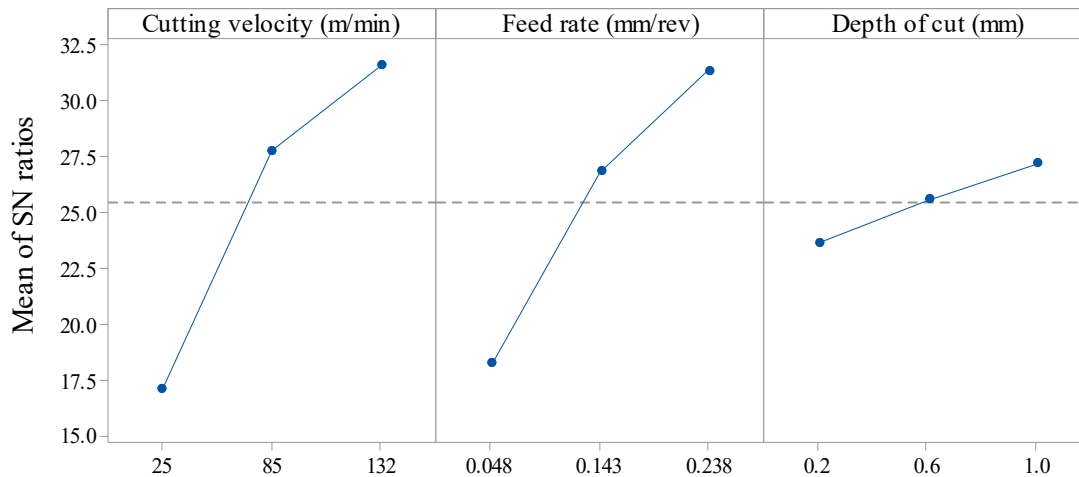
### 5.3.1.3 Material removal rate (MRR)

Table 5.5 shows the obtained S/N ratio response table for the MRR. Figure 5.3 depicts the mean S/N ratio graph MRR. From Figure 5.3, it was noticed that the highest mean S/N ratio obtained for MRR are cutting velocity at 132 m/min, feed rate at 0.048 mm/rev and depth of cut at 0.6 mm respectively, which represents the predicted optimum cutting

conditions and corresponding level values were bolded in Table 5.5 for easy understanding from the S/N response table. This predicted optimum combination was represented as  $v_3 - f_3 - d_3$  for MRR.

**Table 5. 5** Mean S/N ratio response table for MRR.

Symbol	Process parameters	Mean S/N ratio				
		Level 1	Level 2	Level 3	Max-Min	Rank
$v$	Cutting velocity (m/min)	17.01	27.78	<b>31.59</b>	14.58	1
$f$	Feed rate (mm/rev)	18.17	26.84	<b>31.37</b>	13.20	2
$d$	Depth of cut (mm)	23.61	25.58	<b>27.19</b>	3.58	3



*Signal-to-noise: Larger is better (MRR)*

**Figure 5. 3** Mean S/N ratio of MRR.

### 5.3.2 Confirmation test

For validating the Taguchi predicted optimum conditions, conformation tests need to be performed. The predicted S/N ratio ( $\epsilon$ ) was used to predict and verify the response at predicted optimum cutting conditions and it was calculated by using the Eqn. (5.3).

$$\varepsilon_{predicted} = \varepsilon_l + \sum_{i=1}^x (\varepsilon_o - \varepsilon_l) \quad (5.3)$$

Where  $\varepsilon_l$  = Total mean S/N ratio

$\varepsilon_o$  = Mean S/N ratio at optimal level

x = No. of input process parameters

At the Taguchi predicted optimum cutting conditions, the conformation experiments were performed and results were shown in Table 5.6, Table 5.7 and Table 5.8 respectively for  $R_a$ ,  $V_b$  and MRR. The predicted optimum cutting conditions for  $R_a$ ,  $V_b$  and MRR gave an improvement in the performance characteristic results. From the Table 5.6, Table 5.7 and Table 5.8, it was observed that S/N ratios of predicted and optimal cutting condition are very close for all responses. The S/N ratio improvement found at the optimal cutting condition for  $R_a$ ,  $V_b$  and MRR were 0.028 dB, 9.88 dB and 7.77 dB respectively when compared to initial parameter settings ( $v_2$ -  $f_2$  -  $d_2$ ) as shown in Table 5.6, Table 5.7 and Table 5.8. From the conformation experiments, it was found that the Taguchi predicted optimum cutting conditions gave favorable results over the initial parameter conditions. From the Taguchi predicted optimum cutting conditions,  $R_a$ , and  $V_b$  reduction found to be 20.53%, 67.95% respectively compared to initial parameter conditions whereas in the case of MRR 144.67 % increment was observed. Therefore, the Taguchi predicted optimum cuttings were taken as optimum cutting conditions for obtaining the better performance characteristics in machining of 17-4 PH SS under the given conditions. Figure 5.4 and Figure 5.5 shows the SEM images obtained at the initial parameter conditions and Taguchi optimum cutting conditions for  $R_a$  and  $V_b$  respectively. From Figure 5.4 and Figure 5.5, it is evident that Taguchi optimum cuttings conditions produced low  $R_a$  and low  $V_b$ . Philip Selvaraj et al. (2014) found similar results during machining of duplex stainless steel. From the results, it was observed that Taguchi optimization method significantly improved the machinability characteristics of 17-4 PH SS under the given process parameters.

**Table 5. 6** Conformation test results for surface roughness.

	Initial process parameter	Optimal process parameters	
		Prediction	Experiment
Level	$v_2 - f_2 - d_2$	$v_3 - f_1 - d_2$	$v_3 - f_1 - d_2$
Surface roughness ( $\mu\text{m}$ )	1.12	0.828889	0.89
S/N ratio (dB)	-0.984360	0.793649	1.01220
Improvement in S/N ratio (dB)	0.02784		
Percentage reduction of surface roughness	20.53		

**Table 5. 7** Conformation test results for tool flank wear.

	Initial process parameter	Optimal process parameters	
		Prediction	Experiment
Level	$v_2 - f_2 - d_2$	$v_1 - f_1 - d_1$	$v_1 - f_1 - d_1$
Tool wear ( $\mu\text{m}$ )	78	24	25
S/N ratio (dB)	-37.8419	-28.7943	-27.9588
Improvement in S/N ratio (dB)	9.8831		
Percentage reduction of flank wear	67.95		

**Table 5. 8** Conformation test results for MRR.

	Initial process parameter	Optimal process parameters	
		Prediction	Experiment
Level	$v_2 - f_2 - d_2$	$v_3 - f_3 - d_3$	$v_3 - f_3 - d_3$
MRR (g/min)	29.597	55.2111	72.421
S/N ratio (dB)	29.4250	39.2305	37.1973
Improvement in S/N ratio (dB)	7.7723		
Percentage improvement of MRR	144.67		

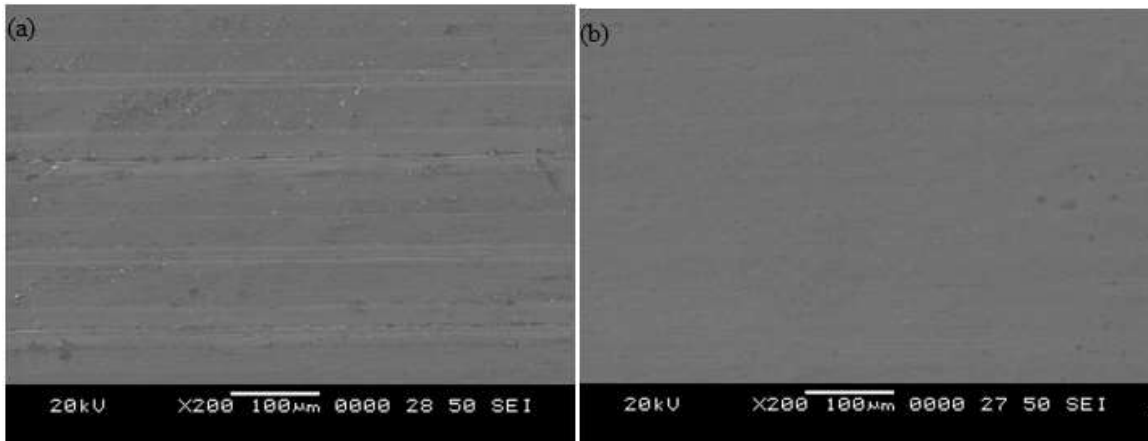


**Figure 5. 4** SEM images of the machined surface at (a) Initial parameter settings at  $v = 85$  m/min,  $f = 0.143$  mm/rev,  $d = 0.6$  mm and MQL environment ( $v_2 - f_2 - d_2$ ) (b) Taguchi optimum settings at  $v = 132$  m/min,  $f = 0.048$  mm/rev,  $d = 0.6$  mm ( $v_3 - f_1 - d_2$ ).

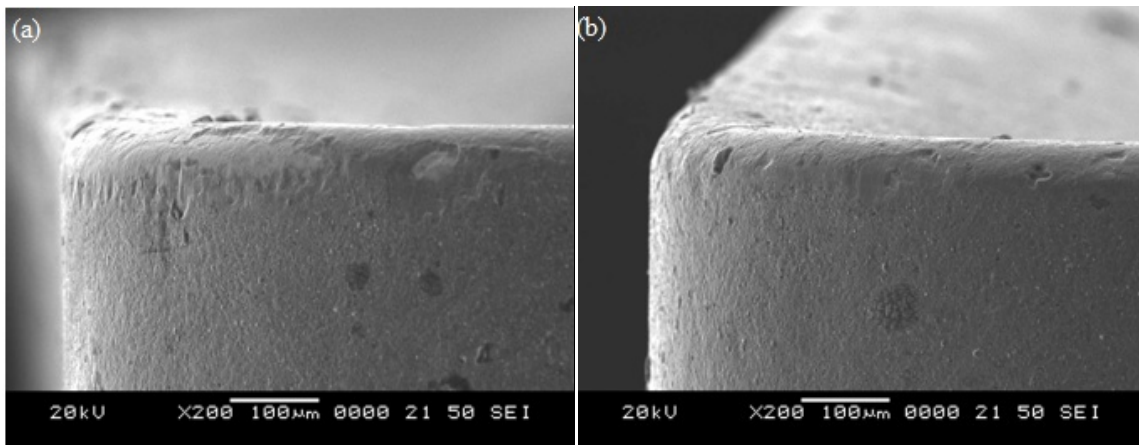


**Figure 5. 5** SEM images of the tool flank wear at (a) Initial parameter settings at  $v = 85$  m/min,  $f = 0.143$  mm/rev,  $d = 0.6$  mm ( $v_2 - f_2 - d_2$ ) (b) Taguchi optimum settings at  $v = 25$  m/min,  $f = 0.048$  mm/rev,  $d = 0.2$  mm ( $v_1 - f_1 - d_1$ ).

### 5.3.3 ANOVA results for surface roughness, flank wear and MRR

The purpose of ANOVA is to know the most influenced cutting parameters which affects the turning performance characteristics. ANOVA results obtained for  $R_a$  and  $V_b$  as shown in Table 5.9 and Table 5.10 respectively. From the Table 5.9, it was found that  $R_a$

is significantly influenced by feed rate followed by cutting velocity and depth of cut respectively. The percentage contribution of feed rate, cutting velocity and depth of cut on  $R_a$  was 84.9 %, 14.29 % and 0.03 % respectively as shown in Table 5.9. Similarly, tool flank wear was mostly influenced by cutting velocity followed by feed rate and depth of cut respectively. The respective percentage contribution of cutting velocity, feed rate and depth of cut on  $V_b$  was 46.87 %, 42.21 % and 4.3 % respectively as shown in Table 5.10. In the case of MRR, it was observed from Table 5.11 that the cutting velocity is the most sensitive parameter on MRR followed by feed rate and depth of cut respectively with respective contribution of 53.88 %, 42.41 % and 3.03 %. From the ANOVA analysis, it was perceived that both  $V_b$  and MRR were significantly affected by cutting velocity whereas it was feed rate for  $R_a$ .

**Table 5. 9** ANOVA of S/N ratio of surface roughness.

Source	DOF	Sum of squares	Mean squares	F	P	% contribution
$v$	2	7.3389	3.6694	28.11	0.034	14.29
$f$	2	43.6048	21.8024	167.00	0.006	84.9
$d$	2	0.1568	0.0784	0.60	0.625	0.03
Residual Error	2	0.2611	0.1306			0.05
Total	8	51.3616				100.00

**Table 5. 10** ANOVA of S/N ratios of flank wear.

Source	DOF	Sum of squares	Mean squares	F	P	% contribution
$v$	2	103.374	51.687	7.08	0.124	46.87
$f$	2	93.115	46.557	6.38	0.136	42.21
$d$	2	9.471	4.735	0.65	0.607	4.3
Residual Error	2	14.606	7.303			6.62
Total	8	220.565				100.00

**Table 5. 11** ANOVA of S/N ratio of MRR.

Source	Degree of freedom	Sum of squares	Mean squares	F	P	% contribution
<i>v</i>	2	342.942	171.471	78.91	0.013	53.88
<i>f</i>	2	269.913	134.957	62.11	0.016	42.41
<i>d</i>	2	19.290	9.645	4.44	0.184	3.03
Residual Error	2	4.346	2.173			0.068
Total	8	636.490				100.00

#### **5.4 MULTI OBJECTIVE OPTIMIZATION TECHNIQUES**

From Table 5.2, multiple responses considered for determining optimum cutting conditions for the multi objective optimization are surface roughness, flank wear and MRR respectively.

##### **5.4.1 Taguchi based Grey relational analysis**

Deg (1982) proposed the grey system theory and has been proven to be useful for dealing with poor, incomplete, and uncertain information. Black in the system represents insufficient information, whereas white in the system represents abundance of information. Thus, a system that contains information that is either incomplete or uncertain is called a grey system. Grey relation is a relation with incomplete information. The multi-response variables are complicated and difficult to solve. The grey system is a statistical technique assisting to solve multi objective optimization problems. It converts the multiple characteristics into single characteristic. Various authors (Manimaran et al., 2013; Kumar and Kumar, 2014; Tang et al., 2014; Sarikaya and Gullu, 2015) followed the following steps in Taguchi based Grey relational analysis.



### ***Step 1: Calculation of Grey relational generation***

Normalization processing step is carried out to nullify the effect of response units and data ranges for comparison. It is a process of normalizing the experimental data in between 0 and 1 based on the type of performance characteristic. Following formulae are used to convert the original data sequence  $D_p^*(q)$  into the normalized sequence between 0 and 1 ( $0 \leq D_p^*(q) \leq 1$ ) are according to the expectancy of the performance characteristics. If the expectancy of performance characteristic is larger-the-better then equation (5.4) can be used to convert the original sequence into the normalized sequence and if the expectancy of performance characteristic is smaller- the-better then equation (5.5) can be used for normalization sequence. In the current study, higher the better was chosen for MRR to improve the productivity and surface roughness and flank wear were chosen for smaller-the-better characteristics. The calculated normalized values are tabulated in the Table 5.12.

Larger - the - better

$$D_p^*(q) = \frac{D_p(q) - \text{Min } D_p(q)}{\text{Max } D_p(q) - \text{Min } D_p(q)} \quad (5.4)$$

Smaller - the - better

$$D_p^*(q) = \frac{\text{Max } D_p(q) - D_p(q)}{\text{Max } D_p(q) - \text{Min } D_p(q)} \quad (5.5)$$

Where,

$D_p^*(q)$  = Sequence after data processing

$D_p(q)$  = Original sequence

$\text{Max } D_p(q)$  = Maximum value of entity 'p'

$\text{Min } D_p(q)$  = Minimum value of entity 'p'

p = Number of characteristics (1, 2, 3)

q = Number of experimental runs (1, 2, ..., 9)

### ***Step 2: Calculation of Grey relational coefficient (GRC)***

The purpose of calculating the Grey relational coefficient is to know the relation between the desirable and real experimental data. The Grey relation coefficients  $\varepsilon_p(q)$  for the all turning performances are calculated using equation (5.6) and listed in the Table 5.12.

$$\varepsilon_p(q) = \frac{\Delta_{Min} + \zeta \Delta_{Max}}{\Delta_{op}(q) + \zeta \Delta_{Max}} \quad (6)$$

Where  $\Delta_{op}(q)$  indicates the absolute difference between current data sequence value ( $D_p^*(q)$ ) and ideal value  $D_p^o(q)$  and  $\zeta$  is the distinguishing coefficient and it is used to alter the variation of the grey relational coefficients and if lower distinguishing coefficient higher will be the distinguishing ability.  $\zeta$  is taken as 0.5 by taking into account of all the process variables are equally weighing (Sarıkaya and Gullu, 2015). Equation (5.7), (5.8) and (5.9) are used to compute the values of  $\Delta_{op}(q)$ ,  $\Delta_{Min}$ ,  $\Delta_{Max}$ .

$$\Delta_{op}(q) = |D_p^o(q) - D_p^*(q)| \quad (5.7)$$

$$\Delta_{Min} = \min_p \min_q \Delta_{op}(q) \quad (5.8)$$

$$\Delta_{Max} = \max_p \max_q \Delta_{op}(q) \quad (5.9)$$

### ***Step 3: Calculation of Grey relational grade (GRG)***

Grey relational grade is useful in evaluating the multiple performance characteristics. Average of all obtained grey relational coefficient gives the grey relation grade. Equation (5.10) is used to compute the grey relation grade ( $\gamma_p(q)$ ) and obtained results and grey relational grade ranks were tabulated in Table 5.12.

$$\gamma_p(q) = \frac{1}{N} \sum_{i=0}^N [\omega_p * \varepsilon_p(q)] = \frac{1}{N} \sum_{i=0}^N \varepsilon_p(q) \quad (5.10)$$

Where N = No. of performance characteristics.

$\omega_p$  = Weightage or importance of each performance characteristics, in this work it is assumed that all the performance characteristics have equal importance, this value should be in between 0 and 1 ( $0 < \omega_i < 1$ ). The larger grey relational grade represents how closer the corresponding experimental response to the ideal value.

**Table 5. 12** Performance characteristics GRC, GRG, S/N ratio and its order.

Exp. No.	Normalized values of Performance characteristics			Grey relational coefficient			Grey relational grade	S/N ratio	Order
	R <sub>a</sub>	V <sub>b</sub>	MRR	R <sub>a</sub>	V <sub>b</sub>	MRR			
				Ideal sequence					
				1	1	1			
1	0.8468	1	0	0.7411	1	0.3333	0.7686	-2.28	1
2	0.6532	0.9453	0.1055	0.404	0.8065	0.3484	0.5348	-5.43	8
3	0	0.3672	0.2284	0.3333	0.5814	0.3839	0.408	-7.78	9
4	0.9839	0.6172	0.1308	0.6684	0.641	0.3984	0.6492	-3.75	4
5	0.8387	0.5313	0.4434	0.7574	0.6098	0.4232	0.5628	-4.99	7
6	0.2742	0.2344	0.6126	0.7664	0.5814	0.4481	0.6063	-4.34	5
7	1	0.5781	0.2972	1	0.3333	0.566	0.6619	-3.58	3
8	0.9113	0.3906	0.5181	0.7411	0.3731	0.5925	0.6061	-4.34	6
9	0.4758	0	1	0.8805	0.3731	1	0.6832	-3.30	2

From the above scientific methodology it has been observed that, multiple response are converted to single response, now it is treated as a single objective optimization problem.

Further Taguchi method was used to optimize the obtained grey relational grade. Hence, higher-the-better quality characteristic is considered for obtaining the S/N ratio for grey relational grade. S/N ratio values of grey relational grade are tabulated in Table 5.12 which is computed from equation (5.11). Minitab 17.0 was used to compute the means of grey relational grade for each level of process parameters and results were tabulated in the Table 5.13. Grey relational grade results for each process parameter namely cutting speed, feed rate and depth of cut at each level has been summarized and depicted in Fig. 5.6.

$$\text{S/N ratio for Larger-the-better} = -10\log_{10}\left(\frac{1}{n}\right)\sum_{i=1}^n\left(\frac{1}{(\gamma_p(q))^2}\right) \quad (5.11)$$

Where n = No. of replications of response (No. of repeated trails),

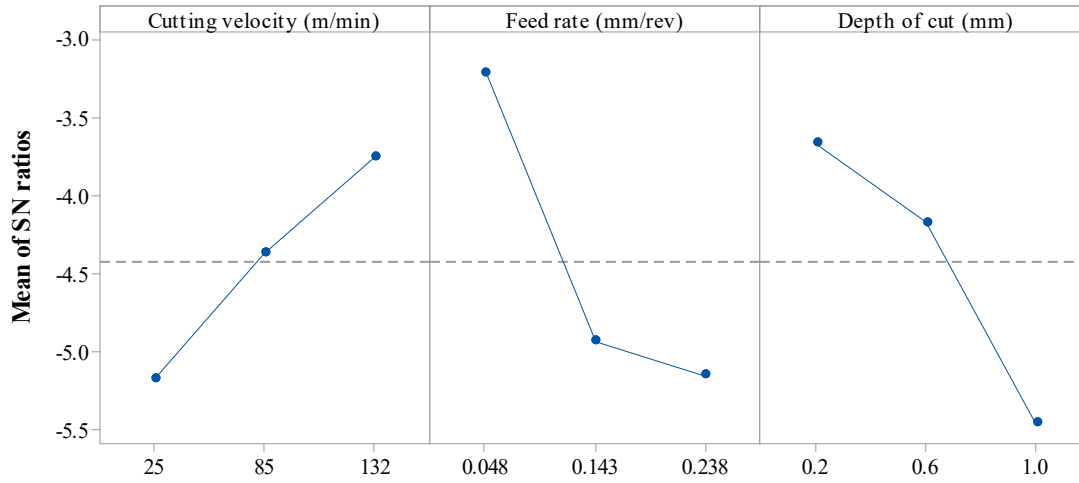
The number of repeated trial was one, since only one relational grade was acquired in each group for this particular calculation of S/N.

$$\gamma_p(q) = \text{Observed response value}$$

From the analysis of means,  $v_3-f_1-d_1$  combination determined as the predicted optimum process parameters. The optimum process parameters levels are cutting velocity at 132 m/min, feed rate at 0.048 mm/rev and depth of cut 0.2 mm respectively.

**Table 5. 13** S/N Response table for grey relational grade.

Symbol	Process Parameters	Grey relational grade				
		Level 1	Level 2	Level 3	Delta	Rank
A	Cutting speed (m/min)	-5.170	--4.364	<b>-3.747</b>	1.422	3
B	Feed rate (mm/rev)	<b>-3.208</b>	-4.926	-5.147	1.940	1
C	Depth of cut (mm)	<b>-3.660</b>	-4.166	-5.455	1.794	2



Signal-to-noise: Larger is better (Gray relational grade)

**Figure 5. 6** Means of S/N ratios of grey relation grades.

#### 5.4.1.1 Confirmation experiments

The confirmation experiments were conducted at the optimum levels to validate the Taguchi based grey relation analysis. The projected grey relational grade  $\gamma_{predicted}$  can be computed using equation (5.12).

$$\gamma_{predicted} = \gamma_m + \sum_{i=1}^k (\gamma_o - \gamma_m) \quad (12)$$

Where,

$\gamma_m$  = Average of total grey relational grade

$\gamma_o$  = the mean of the grey relational grade at the optimal levels

k = Total number of the machining parameters

The estimated grey relational grade for optimum parameters is computed according to equation (5.12) and results was tabulated in the Table 5.14. Confirmation results were compared with the initial parameter settings. Table 5.14 shows the conformation results at the optimal cutting conditions ( $v_3-f_1-d_1$ ) and the initial parameter settings ( $v_2-f_2-d_2$ ).

From Table 5.14, it is observed that surface roughness reduced from 1.08  $\mu\text{m}$  to 0.75  $\mu\text{m}$ , decrease of MRR from 25.123 g/min to 18.721 g/min, tool flank wear decreases from 81  $\mu\text{m}$  to 68  $\mu\text{m}$  and improvement of grey relation grade by 10.63 %. The above results are well in agreement with the results from literature (Ranganathan and Senthilvelan, 2011; Tang et al., 2014; Senthilkumar et al., 2014). The grey relational grade value is further analyzed with analysis of variance to the attain effect of each process parameter on grey relation grade value.

**Table 5. 14** Results of cutting performance at conformation test.

	Initial parameter settings	Optimal process parameters using Taguchi based grey relational analysis	
		Prediction	Experiment
<b>Level</b>	$(v_2-f_2-d_2)$	$(v_3-f_1-d_1)$	$(v_3-f_1-d_1)$
Surface roughness ( $\mu\text{m}$ )	1.08		0.75
Material removal rate (g/min)	25.123		18.721
Tool wear ( $\mu\text{m}$ )	81		68
Grey relational grade	0.6026	0.785989	0.6667
The improvement in GRG= 0.0641 The percentage improvement in GRG =10.63 %			

#### 5.4.1.2 Analysis of variance (ANOVA)

The purpose of ANOVA is to know the most influenced cutting parameters which affects the turning performance characteristics. It involves calculations connected to sum of squares, mean squares and percentage contribution. From the results of ANOVA as shown in Table 5.15 it was found that feed rate has most influence on cryogenic turning performances of 17-4 PH stainless steel which contributed 34.45 %. Goel et al. (2015)

obtained similar results in machining of mono crystalline germanium. It was observed that depth of cut has 26.15 % and cutting speed has 15.54 % contribution on the performance characteristics. If feed rate increases then the contact area between the cutting tool and workpiece increases resulting increased cutting forces during machining. This leads to increased vibrations in the cutting tool and more heat generation resulting increased tool wear, causes more tool marks on the machined surface resulting in more surface roughness (Suresh et al., 2012).

**Table 5. 15** ANOVA of grey relational grade

Source	Degree of freedom	Sum of squares	Mean squares	F	P	% contribution
A	2	3.052	1.526	0.65	0.606	15.54
B	2	6.765	3.383	1.44	0.409	34.45
C	2	5.135	2.568	1.10	0.477	26.15
Residual Error	2	4.686	2.343			23.86
Total	8	19.639				100.00

#### **5.4.2 Taguchi coupled technique for order preference by similarity to ideal solution (TOPSIS) method**

TOPSIS method was introduced by Hwang and Yoon in 1981 (Hwang and Yoon, 1981). This method selects the best alternative which is close to the ideal solution. In the current study, TOPSIS was used to convert the multi responses into a single response with following procedure.

##### ***Step 1:***

TOPSIS is an ideal ranking method; it compares the responses by eliminating the unit differences among the responses using normalization of responses. Normalization values

vary between the 0 and 1. Equation (5.13) is used to normalize the responses and normalized values were listed in Table 5.16.

$$N_{lm} = \frac{K_{lm}}{\sqrt{\sum_{l=1}^p K_{lm}^2}} \quad (5.13)$$

Where,  $l$  = No. of experimental runs ( $l = 1, 2, 3, \dots, 9$ )

$m$  = No. of responses ( $m = 1, 2, 3$ )

$K_{lm}$  = Normalized value of  $l^{\text{th}}$  experimental run allied with  $m^{\text{th}}$  response

$N_{lm}$  = Normalized performance matrix

**Table 5. 16** Normalized data, weighted normalized data, separation measures.

Exp. No.	Normalized data			Weighted normalized data			Separation measures	
	R <sub>a</sub>	V <sub>b</sub>	MRR	R <sub>a</sub>	V <sub>b</sub>	MRR	Q <sup>+</sup>	Q <sup>-</sup>
1	0.267767	0.087855	0.02249	0.0892	0.0293	0.0075	0.2230	0.1703
2	0.323167	0.112455	0.092886	0.1077	0.0375	0.0310	0.2019	0.1566
3	0.510142	0.372506	0.174981	0.1700	0.1242	0.0583	0.2181	0.0749
4	0.228525	0.260051	0.10983	0.0762	0.0867	0.0366	0.2017	0.1350
5	0.270075	0.298708	0.318495	0.0900	0.0996	0.1062	0.1432	0.1499
6	0.431659	0.432247	0.431451	0.1439	0.1441	0.1438	0.1594	0.1432
7	0.223909	0.277622	0.220869	0.0746	0.0925	0.0736	0.1687	0.1449
8	0.2493	0.361963	0.368317	0.0831	0.1206	0.1228	0.1411	0.1558
9	0.37395	0.537674	0.69004	0.1246	0.1792	0.2300	0.1580	0.2271



**Step 2:**

In this step weighted normalized matrix ( $P_{lm}$ ) was obtained by multiplying the normalized values of the responses and decision maker importance given to the individual response (Eqn. 5. 14). In the current study, equal importance was given to the both  $R_a$  and  $V_b$  such that sum of the weights is equal to 1. The obtained  $P_{lm}$  values were shown in Table 5.16.

$$P_{lm} = W_m * N_{lm} \quad (5. 14)$$

Where,  $W_m$  = weight given to the  $m^{\text{th}}$  response ( $m = 1, 2, 3$ )

**Step 3:**

In this step, best and worst alternative close to the ideal solution of the each response has been identified. In the current study both  $R_a$  and  $V_b$  are the minimum requirements and MRR is a maximum requirement for performance improvement.

$$P^+ = \left\{ \sum_l^{\max} P_{lm} / m \in L, \sum_l^{\min} P_{lm} / m \in L' / l = 1, 2, \dots, 9 \right\}$$
$$= \{P_1^+, P_2^+, \dots, P_m^+\}$$

$$P^- = \left\{ \sum_l^{\min} P_{lm} / m \in L, \sum_l^{\max} P_{lm} / m \in L' / l = 1, 2, \dots, 9 \right\}$$
$$= \{P_1^-, P_2^-, \dots, P_m^-\}$$

Where,  $L = (l = 1, 2, \dots, 9)$  // is related with beneficial attributes

$L' = (l = 1, 2, \dots, 9)$  // is related with non-beneficial attributes.

$$P^+ = \text{ideal best solution} = \{0.0746, 0.0293, 0.2300\}$$

$$P^- = \text{ideal worst solution} = \{0.1700, 0.1792, 0.0075\}$$

**Step 4:**

In this step, separation measure was calculated for the best alternative ( $Q^+$ ) and worst alternative ( $Q^-$ ) to know the separation of each alternative to the ideal alternative which is given by Euclidean distance. Equation (5. 15) and Eqn. (5. 16) was used to compute the  $Q^+$  and  $Q^-$  distances and results were shown in Table 5.16 respectively.

$$Q^+ = \sqrt{\sum_{l=1}^9 (P_{lm} - P_m^+)^2} \quad (l = 1, 2, \dots, 9) \quad (5. 15)$$

$$Q^- = \sqrt{\sum_{l=1}^9 (P_{lm} - P_m^-)^2} \quad (5. 16)$$

**Step 5:**

In this step, closeness coefficient ( $R_l$ ) was calculated using Eqn. (5. 17) for the each alternative it indicates the closeness distance of each alternative to the ideal solution. Table 5.17 shows the respective  $R_l$  values for each alternative in  $L_9$  OA design respectively.

$$R_l = \frac{Q^-}{Q^+ + Q^-} \quad (l = 1, 2, \dots, 9) \quad (5. 17)$$

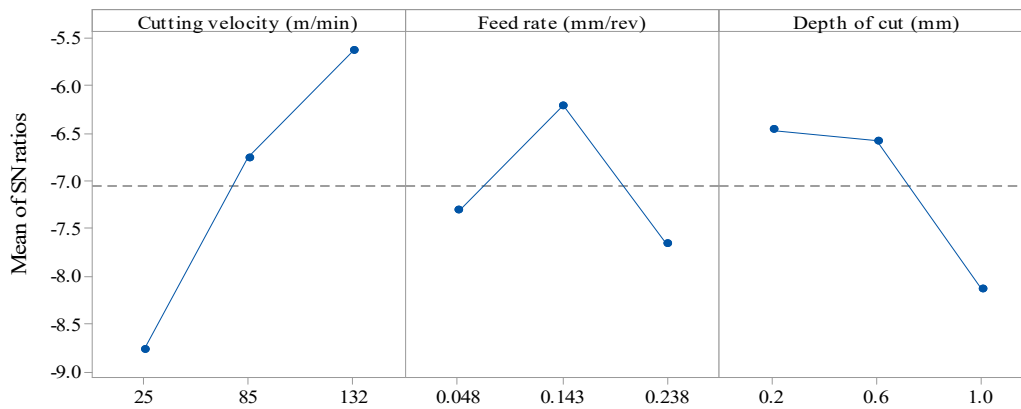
In this step, multiple responses were converted into the single response as closeness coefficient ( $R_l$ ). Now,  $R_l$  treated as the one response and higher the  $R_l$  value indicates the close to the ideal solution because of this reason  $R_l$  is treated as the higher the better characteristic and Taguchi method was used to optimize the  $R_l$  response. In this step, mean S/N ratio response table and mean S/N ratio response plot of  $R_l$  was obtained using Minitab tool 17.0 and results were shown in Table 5.18 and Fig. 5.7 respectively. From Fig. 5.7, the highest mean of respective process parameters of  $R_l$  was taken as Taguchi predicted optimum process parameter settings. The Taguchi predicted optimum settings were identified as  $v = 132$  m/min,  $f = 0.143$  mm/rev and  $d = 0.2$  mm respectively ( $v_3-f_2-d_1$ ).

**Table 5. 17** Closeness coefficients and S/N ratio.

S. No.	Closeness coefficient ( $R_l$ )	S/N ratio
1	0.433037	-7.2695
2	0.436769	-7.19497
3	0.255684	-11.8459
4	0.400884	-7.93963
5	0.511454	-5.82387
6	0.473232	-6.49851
7	0.462021	-6.70677
8	0.524711	-5.6016
9	0.589624	-4.5885

**Table 5. 18** Response table for S/N ratios of closeness coefficient.

Symbol	Process Parameters	closeness coefficient				
		Level 1	Level 2	Level 3	Delta	Rank
$v$	Cutting speed (m/min)	-8.770	-6.754	<b>-5.632</b>	3.138	1
$f$	Feed rate (mm/rev)	-7.305	<b>-6.207</b>	-7.644	1.438	3
$d$	Depth of cut (mm)	<b>-6.457</b>	-6.574	-8.126	1.669	2



Signal-to-noise: Larger is better (Closeness coefficient)

**Figure 5. 7** Means of S/N ratios of closeness efficient.

### 5.4.2.1 Conformation test

Equation (5. 18) was used to compute the predicted closeness coefficient value ( $\Omega_{predicted}$ ) at the Taguchi predicted optimum parameter settings.

$$\Omega_{predicted} = \Omega_l + \sum_{l=1}^m (\Omega_o - \Omega_l) \quad (5. 18)$$

Where,  $\Omega_l$  = Total mean S/N ratio

$\Omega_o$  = Mean S/N ratio at optimal level

m = No. of input process parameters

Conformation experiments were carried out at the Taguchi predicted optimum parameter settings and results were compared to the initial parameter settings ( $v_2-f_2-d_2$ ). The conformation result as seen in Table 5.19 at the predicted optimum parameter setting conditions ( $v_3-f_2-d_1$ ), it was observed that no improvement was found in surface roughness over the initial parameter settings ( $v_2-f_2-d_2$ ). However, at the predicted optimum parameter setting conditions ( $v_3-f_2-d_1$ ) the respective improvements found in flank wear and MRR were 27.16 % and 45.36 %.

**Table 5. 19** Conformation test results for optimization.

Level	Initial parameter settings	Optimal process parameters	
	$(v_2-f_2-d_2)$	Prediction	Experiment
		$(v_3-f_2-d_1)$	$(v_3-f_2-d_1)$
Surface roughness ( $\mu\text{m}$ )	1.08		1.08
Tool wear ( $\mu\text{m}$ )	81		103
MRR (g/min)	25.123		36.52
closeness coefficient	0.469217	0.585108	0.524711
Improvement of closeness coefficient = 0.055494			
Percentage improvement of closeness coefficient = 11.82			

## 5.5 COMPARISON OF CONFORMATION RESULTS OF TGRA AND TAGUCHI COUPLED TOPSIS TECHNIQUES

Table 5.20 summarize the conformation test results at the optimum cutting conditions individually determined by the TGRA and Taguchi couple TOPSIS.

### 5.5.1 Taguchi based Grey relational analysis

The surface roughness reduction found at the TGRA determined optimum cutting parameters ( $v_3-f_2-d_1$ ) was 30.55 % compared to initial parameter settings. This effect is owing to the softening of the area near to the chip-tool interface at higher temperatures. This would cause of removal of surface discontinuities and flaws at the cutting zone (Pawade et al., 2007). In the case of tool flank wear, 25 % reduction was observed at optimum cutting conditions over the initial cutting conditions. However, It was observed that there was 25.48 % reduction in MRR at the optimum cutting parameters because MRR is a function of cutting speed, feed rate and depth of cut thus these causes decrease in MRR.

### 5.5.2 Taguchi couple TOPSIS

From Table 5.20, it was observed that no improvement was found in surface roughness at the Taguchi couple TOPSIS determined optimum cutting conditions ( $v_3-f_2-d_1$ ) over the initial parameter settings ( $v_2-f_2-d_2$ ). Whereas, the observed increment in MRR was 45.36 % over the initial parameter settings. However, flank wear of 27.16 % was found to be increased over the initial parameter settings.

In any manufacturing process, surface finish of the machined component significantly improves the life of the product. Similarly, tool wear directly affects the total manufacturing cost. From Table 5.20, it was observed that both surface roughness and flank wear significantly reduced at the TGRA determined optimum cutting parameters ( $v_3-f_2-d_1$ ) over the Taguchi couple TOPSIS determined optimum cutting conditions

( $v_3-f_2-d_1$ ). However, a slight decrease of MRR (6.402 g) was found at TGRA optimum conditions.

Since, equal importance was given to the three responses in the present work; TGRA technique positively improved the two responses ( $R_a$  and  $V_b$ ) whereas Taguchi couple TOPSIS technique positive improved only one response (MRR). Therefore from the above results, it may be said that significant improvement in the turning performances characteristics were obtained during machining of difficult-to-cut material 17-4 PH stainless steel with the Taguchi based grey relational analysis, hence, in the present work, TGRA technique is more suitable for solving the multi response optimization problem within a given range of process parameters under cryogenic cooling environment.

**Table 5. 20** Comparison of conformation results of TGRA and TOPSIS techniques.

	Initial parameter settings	Optimal process parameters		Percentage change in results at the optimum cutting conditions over initial parameter settings	
		GRA	TOPSIS	GRA	TOPSIS
		( $v_2-f_2-d_2$ )	( $v_3-f_1-d_1$ )	( $v_3-f_1-d_1$ )	( $v_3-f_2-d_1$ )
Surface roughness ( $\mu\text{m}$ )	1.08	0.75	1.08	30.55 % Reduction	0 % No improvement
Tool wear ( $\mu\text{m}$ )	81	68	103	25 % Reduction	27.16 % increment
MRR (g/min)	25.123	18.721	36.52	25.48 % Reduction	45.36 % increment

## 5.6 SUMMARY

In this chapter, experiments were performed based on the Taguchi L<sub>9</sub> orthogonal array design under the cryogenic cooling environment and determined the optimum cutting conditions for single and multiple objective responses under the cryogenic cooling environment. Taguchi method was used for single response optimization and ANOVA was used to find the most influenced process parameter on each response. GRA and TOPSIS optimization techniques have been applied for multi response optimization. Following conclusions were drawn for the experimental results.

- Optimum cutting condition combination for obtaining the low surface roughness was found as  $v = 132$  m/min,  $f = 0.048$  mm/rev and  $d = 0.6$  mm ( $v_3 - f_1 - d_2$ ) using Taguchi method and it was observed that 53.5 %reduction of surface roughness was found at the Taguchi determined optimum cutting condition.
- Taguchi method determined the optimum cutting conditions for obtaining the low flak wear are  $v = 25$  m/min,  $f = 0.048$  mm/rev and  $d = 0.2$  mm ( $v_1- f_1- d_1$ ). Taguchi determined optimum cutting conditions reduced the tool flank wear by 67.95 %.
- The optimum combination of process parameters for attaining maximum MRR was determined as  $v = 132$  m/min,  $f = 0.238$  mm/rev and  $d = 1$  mm ( $v_3- f_3- d_3$ ). This optimum combination significantly improved the MRR by 144.67 % over the initial parameter settings.
- From the ANOVA, it was observed that flank wear and MRR significantly affected by the cutting velocity with a contribution of 46.87 % and 53.88 % respectively, Whereas, surface roughness is highly sensitive to feed rate. From the ANOVA of gray relational grade, it was found that all the responses were significantly affected by feed rate followed by cutting velocity and depth of cut respectively.
- From TGRA, the optimum combination of cutting conditions were determined as  $v = 132$  m/min,  $f = 0.048$  mm/rev and  $d = 0.2$  mm ( $v_3-f_1-d_1$ ). At this condition,

reduction found in surface roughness and flank wear were 30.55 % and 25 % respectively. However, 25.48 % decrease of MRR was obtained.

- The optimum turning parameters were observed at  $v = 132$  m/min,  $f = 0.143$  mm/rev and  $d = 0.2$  mm ( $v_3-f_2-d_1$ ) respectively using Taguchi coupled TOPSIS multi objective optimization method. At this parameter conditions, the observed MRR increase was 45.36 % whereas no reduction was found in surface roughness. However, there was a 27.16 % increase of flank wear was found.
- The advantages results were found in TGRA technique over the Taguchi coupled TOPSIS technique. Hence, in the present work, TGRA technique is more suitable for solving the multi response optimization problem within a given range of process parameters under cryogenic cooling environment.
- Taguchi based grey relational analysis method involved simple mathematical equation and can be applied to solve multi response optimization problems effectively.
- Cryogenic machining effectively reduces the cutting temperatures due LN<sub>2</sub> characteristics; it can be applied to machining of difficult to cut materials and different machining processes to improve the performance characteristics.



## CHAPTER 6

### MODELING OF CRYOGENIC TURNING PROCESS

#### 6.1 INTRODUCTION

In the present chapter, response surface methodology (RSM) has been used for modeling and analyze of responses. This chapter is divided into two phases while machining of 17-4 PH SS under the cryogenic cooling environment. In the first phase, development of correlation models between the input process parameters and output responses has been done. In the second phase, the direct and interaction effects of process parameters on turning performance characteristics were studied.

#### 6.2 EXPERIMENTATION

The process parameters and levels considered for the present work is shown in Table 6.1. In the present work, experiments were performed according to RSM based face centered central composite design and analysis was done using Design Expert software 10. The RSM experimental design ( $L_{20}$ ) and experimental results were shown in Table 6.2.

**Table 6. 1** Process parameters and their levels.

Factor code	Symbol	Process parameters	Units	Level 1	Level 2	Level 3
A	$v$	Cutting velocity	m/min	35 (-1)	83.5 (0)	132 (+1)
B	$f$	Feed rate	mm/rev	0.048 (-1)	0.143 (0)	0.238 (+1)
C	$d$	Depth of cut	mm	0.2 (-1)	0.6 (0)	1 (+1)

**Table 6. 2** RSM experimental design (L<sub>20</sub>) and results.

<b>Exp. No.</b>	<b>Cutting velocity (m/min)</b>	<b>Feed rate (mm/rev)</b>	<b>Depth of cut (mm)</b>	<b>Surface roughness (µm)</b>	<b>Flank wear (µm)</b>	<b>MRR (g/min)</b>
1	35	0.048	1	1.25	37.89	4.59
2	35	0.238	0.2	2.15	79.56	8.4
3	83.5	0.143	0.6	1.33	60.59	18.9
4	83.5	0.143	1	1.87	67.95	30.21
5	83.5	0.143	0.6	1.42	60.84	18.92
6	132	0.238	0.2	1.25	110.32	47.275
7	132	0.048	0.2	0.52	44.23	5.59
8	83.5	0.143	0.6	1.32	60.71	14.85
9	132	0.238	1	1.25	182.64	78.425
10	83.5	0.143	0.6	1.41	59.73	14.94
11	132	0.048	1	0.65	80.48	18.785
12	83.5	0.238	0.6	1.87	107.54	45.68
13	132	0.143	0.6	0.85	95.69	26.55
14	83.5	0.048	0.6	1.21	45.98	10.35
15	83.5	0.143	0.6	1.57	45.82	18.85
16	83.5	0.238	1	2.67	120.36	16.95
17	83.5	0.143	0.6	1.58	60.69	18.78
18	35	0.143	0.6	1.74	84.56	6.43
19	83.5	0.143	0.2	1.43	47.56	8.54
20	35	0.048	0.2	0.64	30.45	1.93

### 6.3 RESPONSE SURFACE METHODOLOGY (RSM)

RSM develops the mathematical equations using a statistical analysis for predicting the relation between the input variable (independent) and output variables (dependent) (Montgomery, 1987). It also explains the direct and interaction effect of process parameters on responses. Equation (6.1) explains the relation between the dependent output and independent input variables.

$$y = f(A, B, C); \quad (6.1)$$

Where, 'y' represents the preferred response which is a function (f) of independent variables A, B and C. Function 'f' was fitted according to the second-order polynomial regression model which is also called as quadratic model represented in equation (6.2).

$$y = \alpha_0 + \sum_{i=1}^3 \alpha_i x_i + \sum_{i=1}^3 \alpha_{ii} x_i^2 + \sum_{i<j}^3 \alpha_{ij} x_i x_j \quad (6.2)$$

Where,  $\alpha_0$  denotes an intercept or a constant and  $\alpha_i$ ,  $\alpha_{ii}$  and  $\alpha_{ij}$  are the corresponding coefficient of linear, quadratic, and cross-product terms respectively.  $x_i$  denotes the coded variables that correspond to the machining parameters studied in the study. Equations (6.3), (6.4) and (6.5) was used to transform the studied machining parameters into coded variables  $x_{ii} = 1, 2, 3$ .

$$x_1 = \frac{A-A_0}{\Delta A} \quad (6.3)$$

$$x_2 = \frac{B-B_0}{\Delta B} \quad (6.4)$$

$$x_3 = \frac{C-C_0}{\Delta C} \quad (6.5)$$

Where, the corresponding coded values of machining parameters A, B and C are  $x_1$ ,  $x_2$  and  $x_3$  respectively. The respective zero levels of machining parameters A, B and C are  $A_0$ ,  $B_0$  and  $C_0$ .  $\Delta A$ ,  $\Delta B$  and  $\Delta C$  denote the intervals of the variation in A, B and C respectively. In the present work, a quadratic model of function (f) has been selected as a fitted model to analyze the surface roughness, tool flank wear and MRR respectively.

## 6.4 RESULT AND DISCUSSIONS

Design expert software 10 Version has been used to analyze and develop the quadratic predicting models for surface roughness, tool flank wear and MRR using the input and output data from the RSM experimental design (Table 6.2). No transformation has been performed on the each response, fit summary of the fit analysis found that quadratic model is statistically significant for all the responses and the same model has been used for the all responses in the present study. The least square method has been used to fit the model containing dependent and independent variables by reducing the residual error measured by the sum of squares between the predicted and actual responses. It involves the determination of regression model coefficients including the intercept.

### 6.4.1 Analysis of surface roughness ( $R_a$ )

The regression model coefficients were determined from the Design expert software and the developed final regression model for the surface roughness is shown in equation (6.6).

Equation in terms of coded factors:

$$R_a = +1.48 - 0.39 A + 0.49 B + 0.17 C - 0.20 AB - 0.12 AC - 0.027 BC - 0.26 A^2 - 0.011 B^2 + 0.099 C^2 \quad (6.6)$$

ANOVA result was used to check the adequacy and significance of the regression model. The adequacy and significance tests were performed for the surface roughness modeling using the ANOVA Table 6.3. The regression model is significant if the value of “P > F” is less than the 0.05. In Table 6.3, the value of “P < 0.0001” indicates that the model is significant which is desirable, it represents the terms present in the model have the significant impact on response. There is only a 0.01% chance that an “F-value” this large could occur due to noise. Values of "Prob > F" less than 0.0500 indicates that the model terms are significant. From ANOVA Table 6.3, it was found that A, B, C, AB, AC and  $A^2$  are significant model terms. All the model terms having “P > F” greater than 0.05 are not significant. In this respect, the model terms BC,  $B^2$  and  $C^2$  were found as an

insignificant terms. Removal of insignificant terms may lead to an improved result. The “lack of fit” was found to be insignificant from Table 6.3, this is desirable and it implies that model is not significant related to the pure error. Table 6.4 represents the ANOVA results analysis after backward elimination of insignificant terms in the model. From Table 6.4, it was observed that model is still significant and the still lack of fit was insignificant, as we want a model that fits.

Additional checks are required to check the adequacy of the model includes the determination of various coefficients of determinations ( $R^2$ ) and examination of residuals (Stephan et al., 1998). These  $R^2$  values have between the 0 and 1. The differences between the predicted and observed responses are the residuals. The examination of residuals is done using the normal probability plots of residuals and plots of residuals versus the predicted responses (Montgomery, 1987). The model is said to be adequate if the points on the normal probability plots of the residuals should form a straight line. The other way is the plots of the residuals versus the predicted response should be structured less that is they should not contain particular obvious patterns. In Table 6.4, The “Pred R-Squared” of 0.9102 is in reasonable agreement with the “Adj R-Squared” of 0.9372. “Adj R-Squared” is useful when comparing the models with a different number of terms. “Adeq Precision” measures the signal to noise ratio. A ratio greater than 4 is desirable. In Table 6.4, the ratio of 27.406 indicates an adequate signal. This model can be used to navigate the design space. Figure 6.1 and Figure 6.2 depicts the normal probability plots of the residuals and plots of residuals versus the predicted response for surface roughness. From Figure 6.1, it was observed that residuals fall on a straight line, it represents that errors are distributed normally. From Figure 6.2, it is seen that the plot of residuals versus the predicted response structured less and not obvious pattern. This indicates that the proposed surface roughness model is adequate for predicting the surface roughness and no violation of independent and constant variation assumption. Hence, the developed predicted model for surface roughness is adequate because it satisfies all adequacy tests. Equation (6.7) and (6.8) indicates the final empirical model for surface roughness in terms of coded and actual factors respectively.

Final equation in terms of coded factors:

$$R_a = +1.50 - 0.39 A + 0.49 B + 0.17 C - 0.20 AB - 0.12 AC - 0.20 A^2 \quad (6.7)$$

Final equation in terms of actual factors:

$$R_a = -0.263 + 0.0164 v + 8.803 f + 0.963 d - 0.043 v f - 0.00644 v d - 0.0000867 v^2 \quad (6.8)$$

**Table 6. 3** ANOVA for response surface quadratic model (Response:  $R_a$ ).

Source	Sum of squares	DOF	Mean square	F-value	p-value prob.>F	
Model	4.94	9	0.55	29.64	< 0.0001	significant
A-Cutting velocity	1.54	1	1.54	83.37	< 0.0001	
B-Feed rate	2.42	1	2.42	130.66	< 0.0001	
C-Depth of cut	0.29	1	0.29	15.60	0.0027	
AB	0.32	1	0.32	17.27	0.0020	
AC	0.12	1	0.12	6.75	0.0266	
BC	0.00605	1	0.00605	0.33	0.5803	
A <sup>2</sup>	0.18	1	0.18	9.76	0.0108	
B <sup>2</sup>	0.0003551	1	0.0003551	0.019	0.8926	
C <sup>2</sup>	0.027	1	0.027	1.44	0.2572	
Residual	0.19	10	0.019			
Lack of Fit	0.12	5	0.024	1.88	0.2522	not significant
Pure Error	0.064	5	0.013			
Cor Total	5.13	19				
Std. Dev.	0.14		R-Squared		0.9639	
Mean	1.40		Adj R-Squared		0.9313	
C.V. %	9.73		Pred R-Squared		0.8296	
PRESS	0.87		Adeq Precision		21.923	

**Table 6. 4** ANOVA for response surface reduced quadratic model (Response:  $R_a$ ).

Source	Sum of squares	DOF	Mean square	F-value	p-value prob.>F	
Model	4.91	6	0.82	48.29	< 0.0001	significant
A-Cutting velocity	1.54	1	1.54	91.19	< 0.0001	
B-Feed rate	2.42	1	2.42	142.93	< 0.0001	
C-Depth of cut	0.29	1	0.29	17.06	0.0012	
AB	0.32	1	0.32	18.89	0.0008	
AC	0.13	1	0.13	7.38	0.0176	
A <sup>2</sup>	0.21	1	0.21	12.29	0.0039	
Residual	0.22	13	0.017			
Lack of Fit	0.16	8	0.019	1.52	0.3359	not significant
Pure Error	0.064	5	0.013			
Cor Total	5.13	19				
Std. Dev.	0.13		R-Squared		0.9571	
Mean	1.40		Adj R-Squared		0.9372	
C.V. %	9.30		Pred R-Squared		0.9102	
PRESS	0.46		Adeq Precision		27.406	

Design-Expert® Software  
Surface roughness

Color points by value of  
Surface roughness:

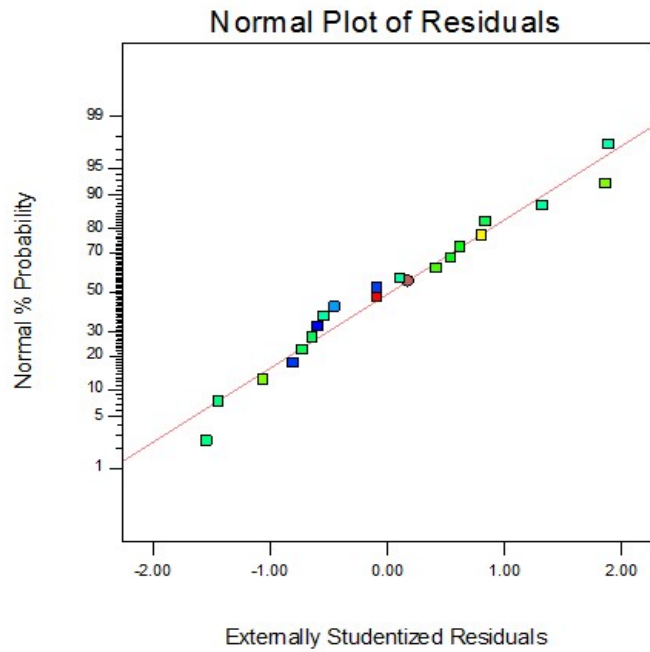


Figure 6. 1 Normal probability plot for surface roughness.

Design-Expert® Software  
Surface roughness

Color points by value of  
Surface roughness:

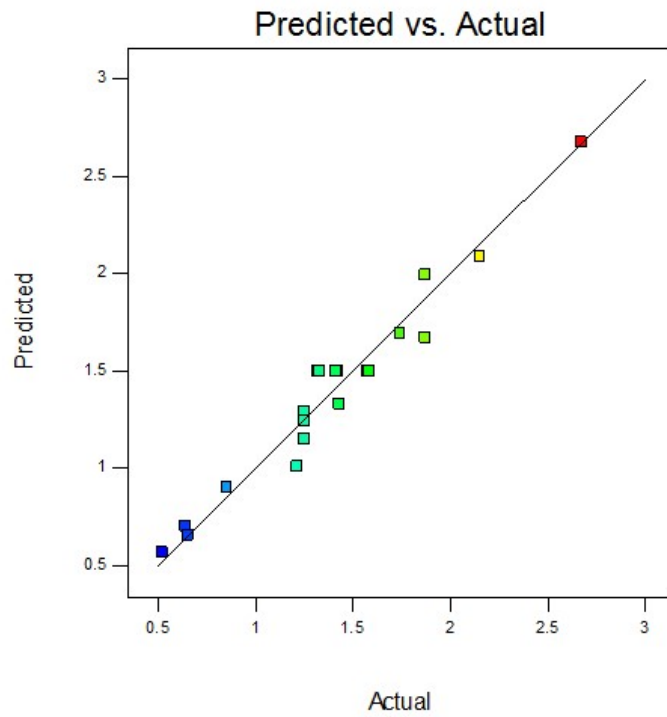
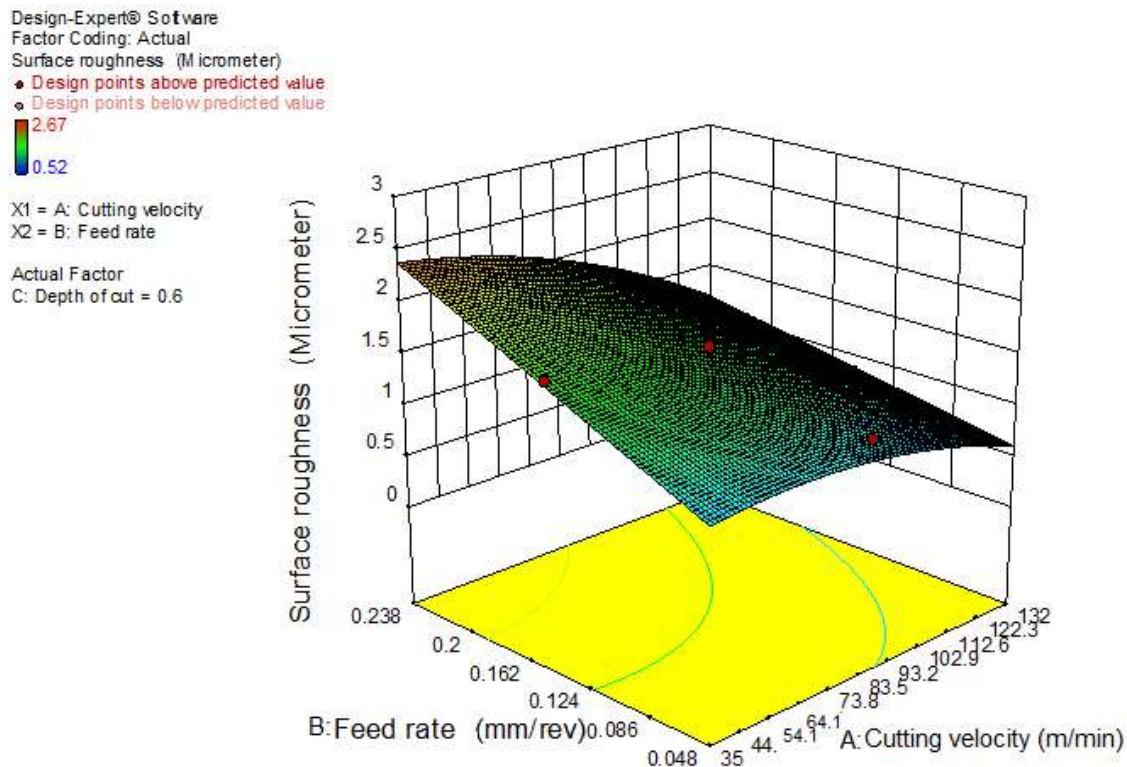


Figure 6. 2 Plot of residual Vs. predicted for surface roughness.



### 6.4.1.1 Interaction effect of variables on surface roughness

Figure 6.3 and Figure 6.4 depicts the 3D-surface plots for surface roughness response. Since the final regression model developed for surface roughness has been proved as an adequate model, the surface plots can be used to predict the surface roughness for different parameter settings. From surface plots, it is also evident that feed rate is the most affecting process parameter on surface roughness. This 3D surface plot result supports the perturbation plot results. From Figure 6.3, it was observed that lowest surface roughness can be obtained at the highest level of cutting velocity and lowest levels of feed rate respectively. From Figure 6.4, lowest level of depth of cut and highest level of cutting velocity could produce low surface roughness respectively.



**Figure 6. 3** 3D surface interaction plot in feed rate and cutting velocity for surface roughness.

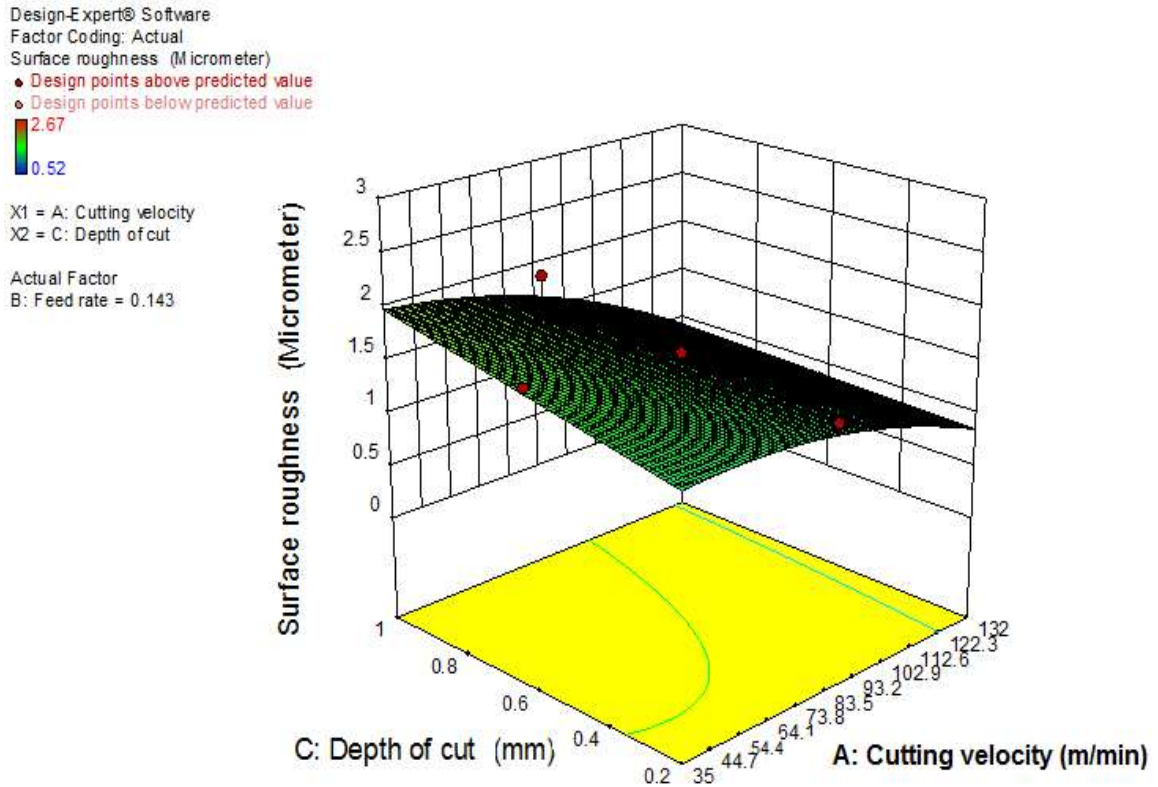


**Figure 6. 4** 3D surface interaction plot in depth of cut and cutting velocity for surface roughness

#### 6.4.2 Analysis of tool flank wear

RSM analysis was conducted for the flank wear and the developed regression model for the flank wear is shown in equation (6.9).

Equation in terms of coded factors:

$$V_b = +61.38 + 16.05 A + 36.14 B + 17.72 C + 4.58 AB + 7.54 AC + 8.68 BC + 23.78 A^2 + 10.42 B^2 - 8.59 C^2 \quad (6.9)$$

Table 6.5 show the ANOVA result for the tool wear and has been used to test the adequacy and significance of the model flank wear model. The model “F-value” of 29.09 implies the model is significant. There is only a 0.01% chance that an F-value this large

could occur due to noise. Values of “Prob > F” less than 0.0500 indicate model terms are significant. In the case of flank wear the model terms A, B, C, AC, BC and A<sup>2</sup> are significant as shown in Table 6.5. Values greater than 0.0500 indicate the model terms are not significant. In Table 6.5, the flank wear models terms AB, B<sup>2</sup> and C<sup>2</sup> were found as insignificant. The insignificant terms in the flank wear model were eliminated using backward elimination method. The “Lack of Fit” is not significant and it is required the model to fit. Table 6.6 represents the ANOVA result for the response surface quadratic model for flank wear after elimination insignificant terms. From the Table 6.6, it was noticed that the flank model is still significant and “lack of fit” of the model is insignificant. The “Pred R-Squared” of 0.8377 is in reasonable agreement with the “Adj R-Squared” of 0.9140. The response quadratic surface model of flank wear can be used to navigate the entire design space due to the "Adeq Precision" ratio is greater than 4.

From the normal probability plot of flank wear, it was observed that the residuals falls in a straight line as shown in Figure 6.5. Also, the plots of residuals and predicted response for tool wear revealed that they have no obvious pattern and less structure as shown in Figure 6.6. Figure 6.5 and Figure 6.6 implies that the developed regression model for flank wear is an adequate and significant to determine the relation between the independent variables and flank wear. The equation (6.10) and (6.11) indicates the final response quadratic surface model of flank wear in terms of coded and actual factors respectively.

Final equation in terms of coded factors:

$$V_b = +61.74 + 16.05 A + 36.14 B + 17.72 C + 7.54 AC + 8.68 BC + 24.88 A^2 \quad (6.10)$$

Final equation in terms of actual factors:

$$V_b = +65.931 - 1.668 v + 243.377 f - 20.817 d + 0.388 v d + 228.388 f d + 0.0105 v^2 \quad (6.11)$$

**Table 6. 5** ANOVA for response surface quadratic model (Response: Flank wear)

Source	Sum of squares	DOF	Mean square	F-value	p-value prob.>F	
Model	23466.04	9	2607.34	29.09	< 0.0001	significant
A-Cutting velocity	2577.31	1	2577.31	28.76	0.0003	
B-Feed rate	13060.27	1	13060.27	145.72	< 0.0001	
C-Depth of cut	3139.98	1	3139.98	35.03	0.0001	
AB	168.09	1	168.09	1.88	0.2008	
AC	454.96	1	454.96	5.08	0.0479	
BC	602.57	1	602.57	6.72	0.0268	
A <sup>2</sup>	1555.21	1	1555.21	17.35	0.0019	
B <sup>2</sup>	298.35	1	298.35	3.33	0.0981	
C <sup>2</sup>	202.87	1	202.87	2.26	0.1634	
Residual	896.29	10	89.63			
Lack of Fit	715.61	5	143.12	3.96	0.0786	not significant
Pure Error	180.68	5	36.14			
Cor Total	24362.33	19				
Std. Dev.	9.47		R-Squared		0.9632	
Mean	74.18		Adj R-Squared		0.9301	
C.V. %	12.76		Pred R-Squared		0.7952	
PRESS	4989.78		Adeq Precision		21.307	

**Table 6. 6** ANOVA for response surface reduced quadratic model (Response:  $V_b$ ).

Source	Sum of squares	DOF	Mean square	F-value	p-value prob.>F	
Model	22929.42	6	3821.57	34.67	< 0.0001	Significant
A-Cutting velocity	2577.31	1	2577.31	23.38	0.0003	
B-Feed rate	13060.27	1	13060.27	118.49	< 0.0001	
C-Depth of cut	3139.98	1	3139.98	28.49	0.0001	
AC	454.96	1	454.96	4.13	0.0431	
BC	602.57	1	602.57	5.47	0.0360	
A <sup>2</sup>	3094.33	1	3094.33	28.07	0.0001	
Residual	1432.90	13	110.22			
Lack of Fit	1252.23	8	156.53	4.33	0.0616	not significant
Pure Error	180.68	5	36.14			
Cor Total	24362.33	19				
Std. Dev.	10.50		R-Squared		0.9412	
Mean	74.18		Adj R-Squared		0.9140	
C.V. %	14.15		Pred R-Squared		0.8377	
PRESS	3953.97		Adeq Precision		23.691	

Design-Expert® Software  
Flank wear

Color points by value of  
Flank wear:  
182.64  
30.45

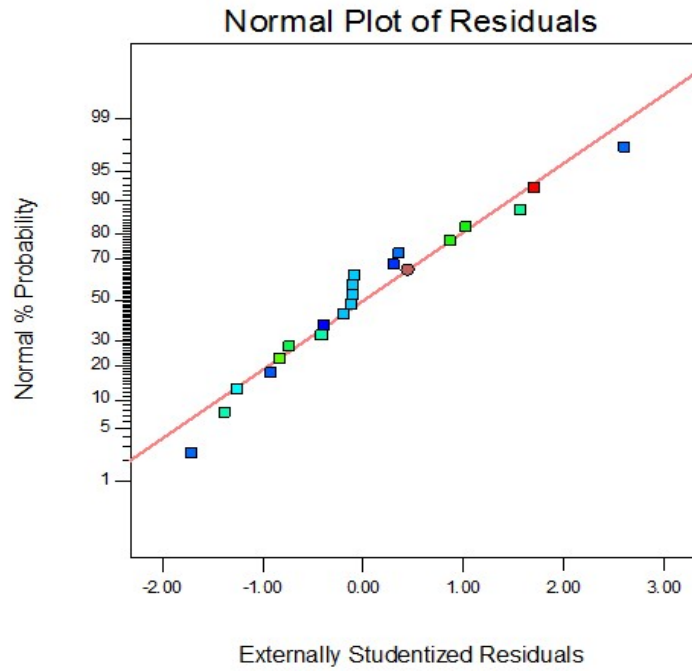


Figure 6. 5 Normal probability plot for flank wear.

Design-Expert® Software  
Flank wear

Color points by value of  
Flank wear:  
182.64  
30.45

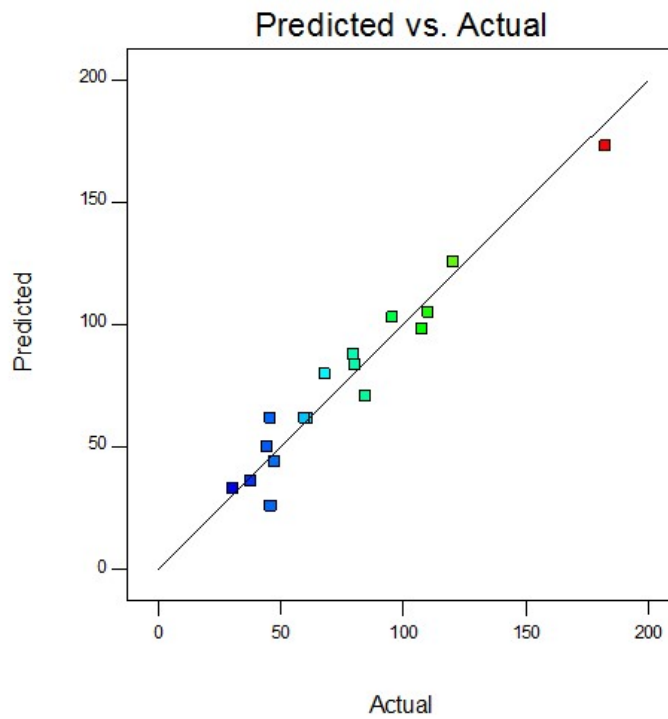


Figure 6. 6 Plot of residual Vs. predicted for flank wear.

### 6.4.2.1 Interaction effect of process variables on flank wear

Figure 6.7 depicts the combined effect of cutting velocity and depth of cut at a constant feed rate of 0.143 mm/rev respectively. At this condition, it was noticed that depth of cut is the most influenced parameter on flank wear. However, lower levels of depth of cut and cutting velocity conditions can produce low flank wear respectively. Figure 6.8 depicts the combined effect of feed rate and depth of cut at a constant cutting velocity of 83.5 m/min respectively. At this situation, the feed rate is the most effective parameter on flank wear as shown in Figure 6.8. At this condition, the respective lower levels of feed rate and depth of cut are preferable to produce low flank wear.

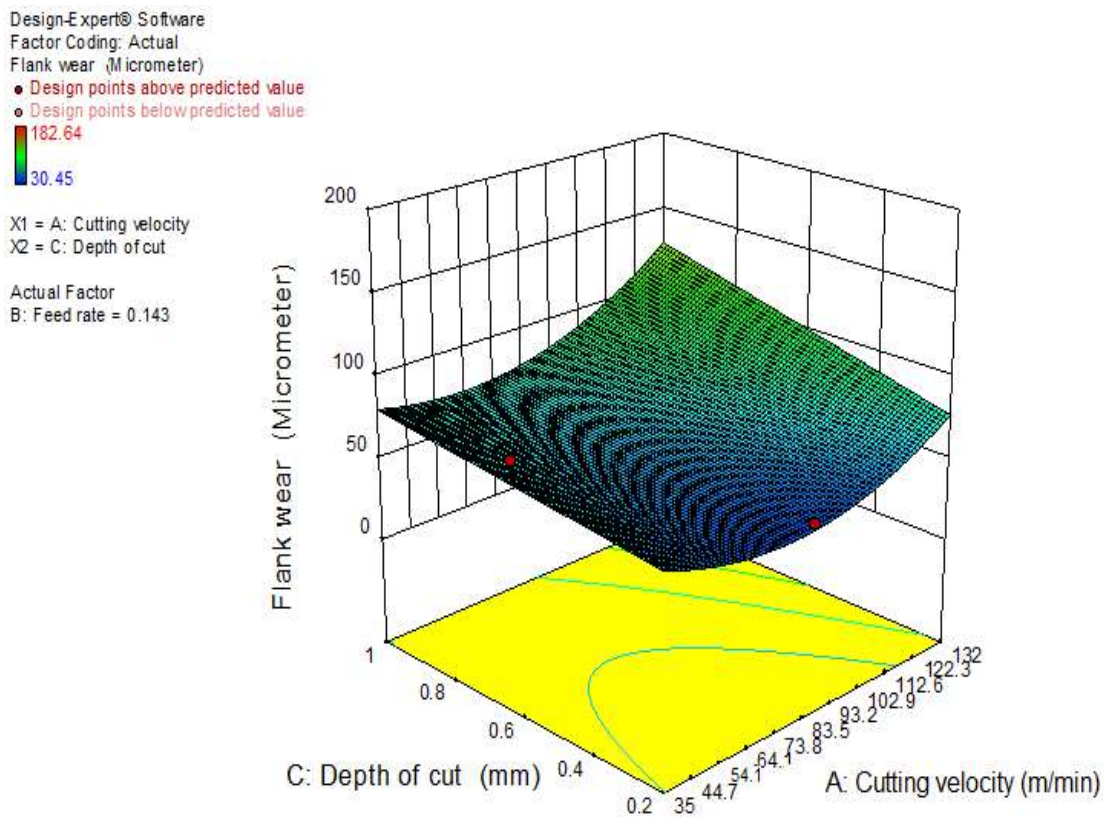
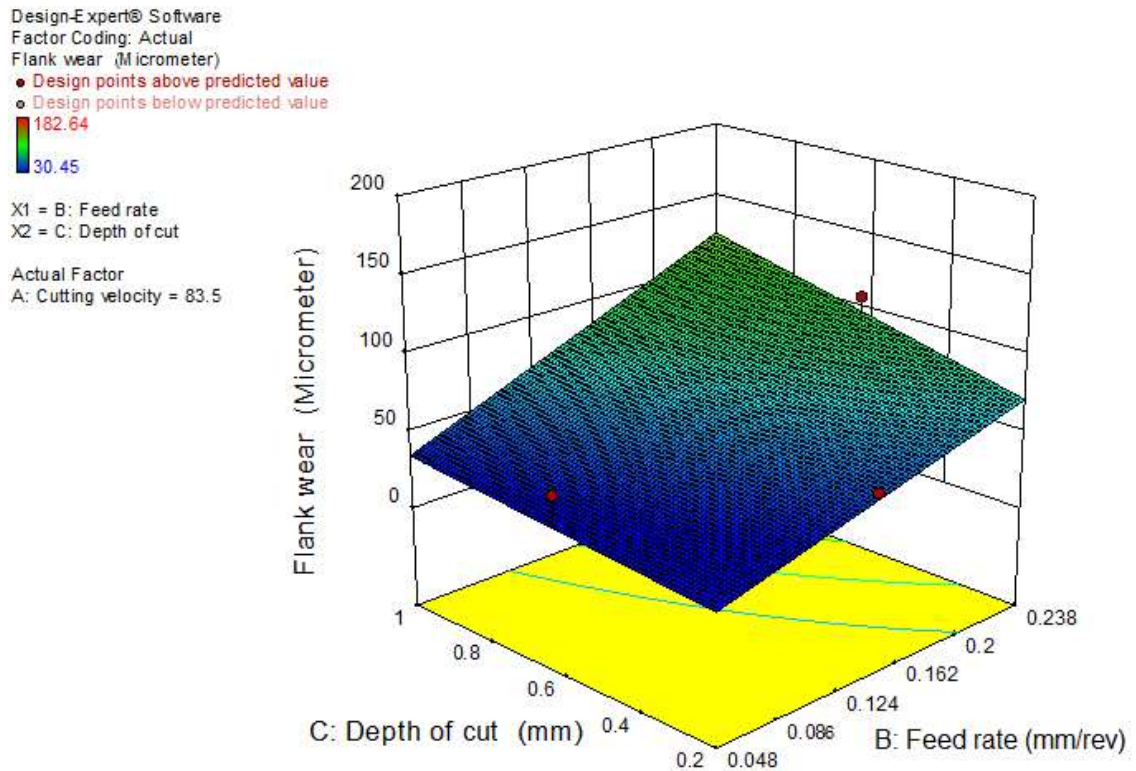


Figure 6. 7 3D surface interaction plot in depth of cut and cutting velocity for flank wear.



**Figure 6. 8** 3D surface interaction plot in depth of cut and feed rate for flank wear.

### 6.4.3 Analysis of Material removal rate (MRR)

The mathematical regression model obtained using ANOVA analysis is represented in equation (6.12).

Equation in terms of coded factors:

$$\begin{aligned} \text{MRR} = & +18.42 + 13.83 A + 15.55 B + 7.72 C + 10.31 AB + 4.14 AC + 2.98BC - 3.25 A^2 \\ & + 8.27 B^2 - 0.37 C^2 \end{aligned} \quad (6.12)$$

Table 6.7 show the ANOVA result for MRR and it was used to check the adequacy and significance of the model. From Table 6.7, it was found that the developed model is significant and “lack of fit” is insignificant due to this, the developed model is not significant relative to the pure error. Values of “Prob > F” less than 0.0500 indicate



model terms are significant. In this case, the terms A, B, C, AB, AC, BC and B<sup>2</sup> are significant model terms. From Table 6.7, the model terms A<sup>2</sup> and C<sup>2</sup> were found to be insignificant and back elimination was used to eliminate these terms from the model. After back elimination, the ANOVA result for the MRR is shown in Table 6.8 respectively. From Table 6.8, it was observed that the developed model is still significant and “lack of fit” was not significant. The “Pred R-Squared” of 0.8423 is in reasonable agreement with the “Adj R-Squared” of 0.9592. “Adeq Precision” measures the signal to noise ratio. In the present study, adequacy ratio of MRR is 32.333 indicates an adequate signal. This model can be used to navigate the design space.

From the normal probability plots of the residuals and the plots of the residuals versus the predicted response point of view, the proposed model of MRR is adequate and significant due to the residuals followed a straight line and residuals are less structured as shown in Figure 6.9 and Figure 6.10 respectively. These positive diagnostic tool test results imply that there is no reason to suspect any constant variance. The final response quadratic surface model generated for the MRR is represented in equation (6.13) and (6.14) respectively in terms of coded and actual factors.

Final equation in terms of coded factors:

$$\text{MRR} = +17.70 + 13.83 A + 15.55 B + 7.72 C + 10.31 AB + 4.14 AC + 2.98 BC + 6.10 B^2 \quad (6.13)$$

Final equation in terms of actual factors:

$$\text{MRR} = +16.86638 - 0.16294 v - 263.59566 f - 9.73745 d + 2.23806 v f + 0.21350 v d + 78.43750 f d + 675.95568 f^2 \quad (6.14)$$

**Table 6. 7** ANOVA for response surface quadratic model (Response: MRR).

Source	Sum of squares	DOF	Mean square	F-value	p-value prob.>F	
Model	6209.53	9	689.95	54.67	< 0.0001	significant
A-Cutting velocity	1913.38	1	1913.38	151.61	< 0.0001	
B-Feed rate	2417.56	1	2417.56	191.56	< 0.0001	
C-Depth of cut	596.37	1	596.37	47.25	< 0.0001	
AB	850.68	1	850.68	67.40	< 0.0001	
AC	137.24	1	137.24	10.87	0.0080	
BC	71.07	1	71.07	5.63	0.0391	
A <sup>2</sup>	29.09	1	29.09	2.31	0.1599	
B <sup>2</sup>	188.19	1	188.19	14.91	0.0032	
C <sup>2</sup>	0.37	1	0.37	0.029	0.8672	
Residual	126.21	10	12.62			
Lack of Fit	105.20	5	21.04	5.01	0.0508	not significant
Pure Error	21.00	5	4.20			
Cor Total	6335.74	19				
Std. Dev.	3.55		R-Squared		0.9801	
Mean	20.75		Adj R-Squared		0.9622	
C.V. %	17.12		Pred R-Squared		0.8311	
PRESS	1070.35		Adeq Precision		30.364	

**Table 6. 8** ANOVA for response surface reduced quadratic model (Response: MRR).

Source	Sum of squares	DOF	Mean square	F-value	p-value prob.>F	
Model	6172.38	7	881.77	64.77	< 0.0001	significant
A-Cutting velocity	1913.38	1	1913.38	140.55	< 0.0001	
B-Feed rate	2417.56	1	2417.56	177.59	< 0.0001	
C-Depth of cut	596.37	1	596.37	43.81	< 0.0001	
AB	850.68	1	850.68	62.49	< 0.0001	
AC	137.24	1	137.24	10.08	0.0080	
BC	71.07	1	71.07	5.22	0.0413	
B <sup>2</sup>	186.08	1	186.08	13.67	0.0031	
Residual	163.36	12	13.61			
Lack of Fit	142.35	7	20.34	4.84	0.0507	not significant
Pure Error	21.00	5	4.20			
Cor Total	6335.74	19				
Std. Dev.	3.69		R-Squared		0.9742	
Mean	20.75		Adj R-Squared		0.9592	
C.V. %	17.78		Pred R-Squared		0.8423	
PRESS	999.38		Adeq Precision		32.333	

Design-Expert® Software  
MRR

Color points by value of  
MRR:  
78.425  
1.93

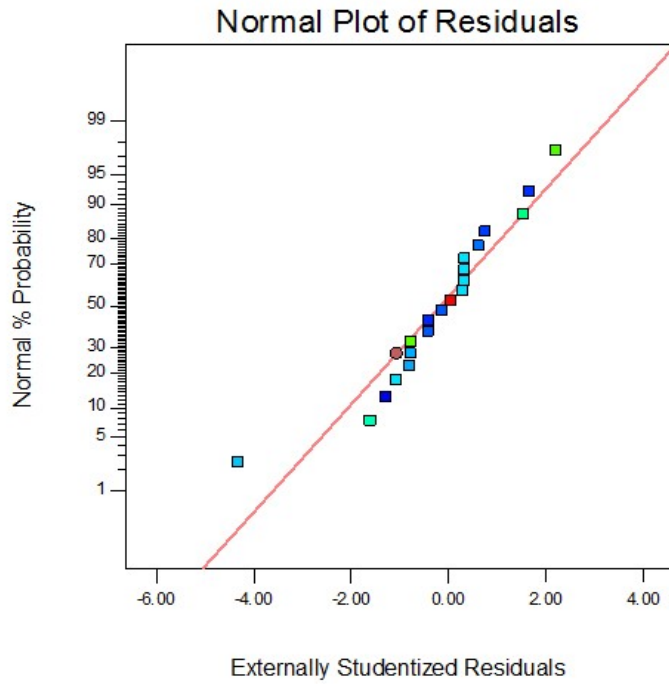


Figure 6. 9 Normal probability plot for MRR.

Design-Expert® Software  
MRR

Color points by value of  
MRR:  
78.425  
1.93

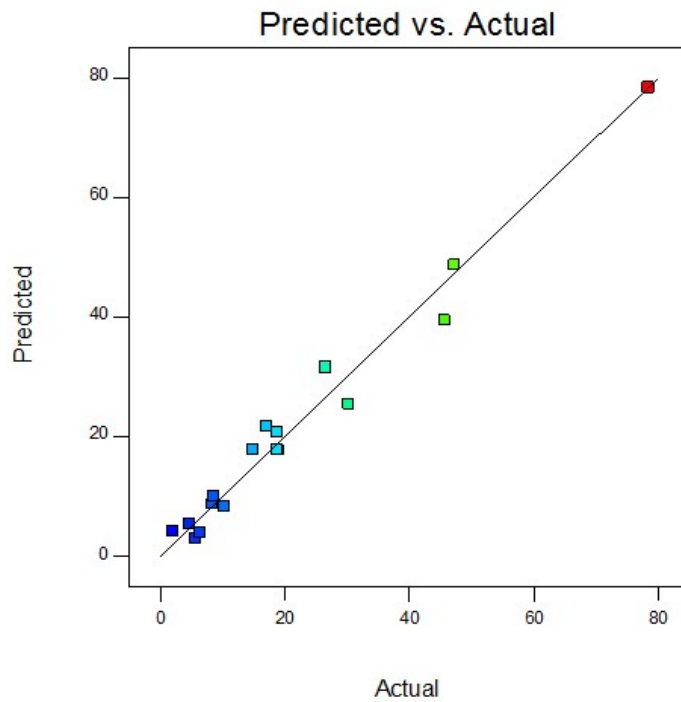
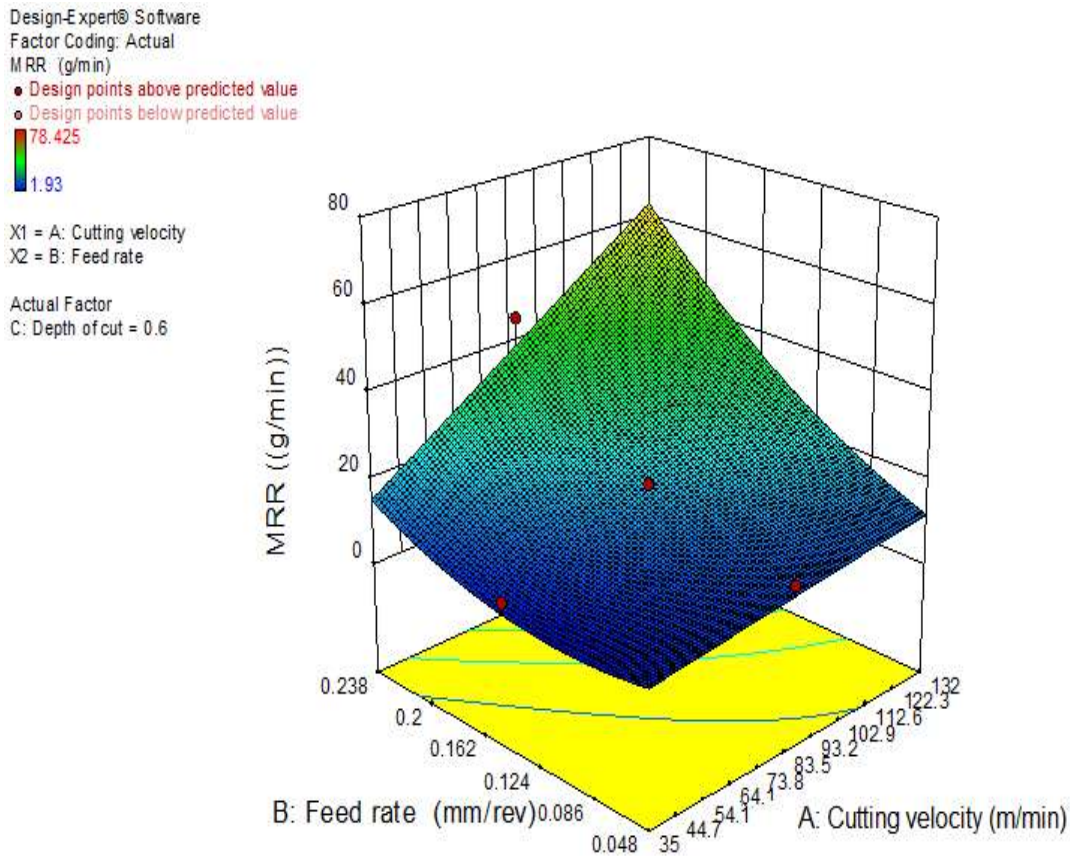


Figure 6. 10 Plot of residual Vs. predicted for MRR.

### 6.4.3.1 Interaction effect on MRR

Figure 6.11-6.13 depicts the 3D surface plots obtained for MRR. From the given conditions in Figure 6.11, it was found that the interaction effect of both cutting velocity and feed rate have almost equal on MRR. From interaction plot of cutting velocity and depth of cut as shown in Figure 6.12, it was observed that cutting velocity has most influence parameter at a constant mean feed rate condition. Whereas, Figure 6.13 shows the interaction effect of feed rate and depth of cut at constant mean cutting velocity condition. At this point, the feed rate was found as the most influence process parameter on MRR. In all the 3D surface plots related MRR shows that combination of any two cutting parameters at maximum levels can be used to obtain maximum MRR.



**Figure 6. 11** 3D surface interaction plot in feed rate and cutting velocity for MRR.

Design-Expert® Software  
 Factor Coding: Actual  
 MRR (g/min)  
 ● Design points above predicted value  
 ○ Design points below predicted value  
 78.425  
 1.93  
 X1 = A: Cutting velocity  
 X2 = C: Depth of cut  
 Actual Factor  
 B: Feed rate = 0.143

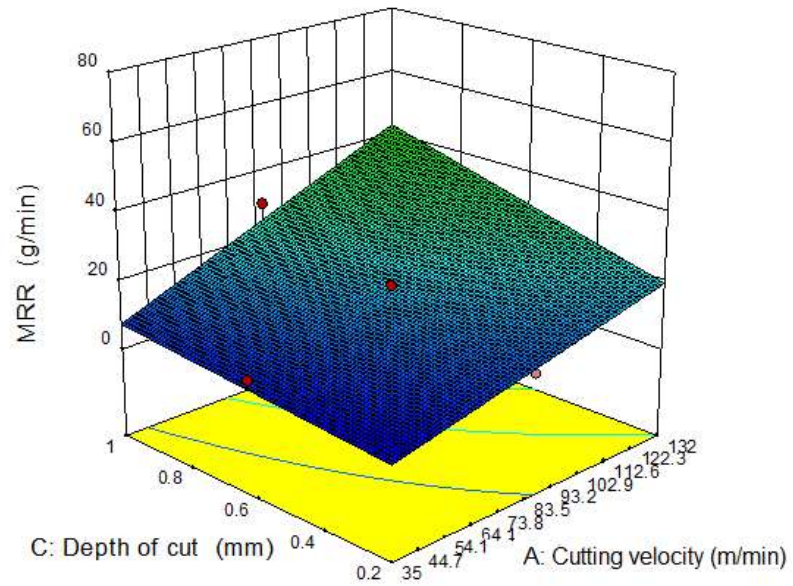


Figure 6. 12 3D surface interaction plot in depth of cut and cutting velocity for MRR.

Design-Expert® Software  
 Factor Coding: Actual  
 MRR (g/min)  
 ● Design points above predicted value  
 ○ Design points below predicted value  
 78.425  
 1.93  
 X1 = B: Feed rate  
 X2 = C: Depth of cut  
 Actual Factor  
 A: Cutting velocity = 83.5

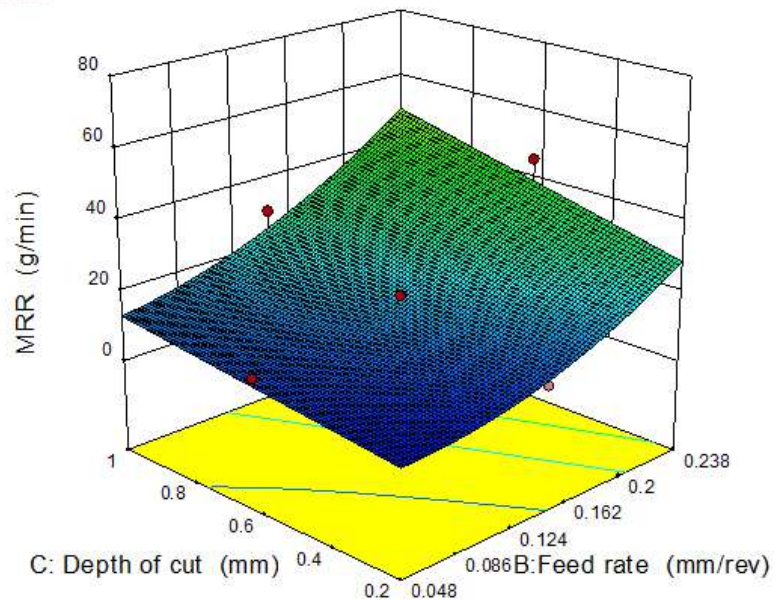


Figure 6. 13 3D surface interaction plot in depth of cut and feed rate for MRR.

## 6.5 CONFORMATION TEST FOR MODELING

In order to validate the developed models, five conformation tests were performed randomly within the previously specified range of parameters but have not been conducted previously. At the conformation test conditions, responses like surface roughness, flank wear and MRR were predicted using RSM point prediction tool. Table 6.9 show the conformation test results and predicted results from the RSM developed models. From Table 6.9, it was observed that both conformation test results and RSM predicted results were fairly close to each other for all the responses. The maximum percentage error found between the actual and predicted values for surface roughness, flank wear and MRR were 3.28 %, 4.51 % and 4.98 % respectively. From Table 6.9, it was concluded that the RSM developed models are adequate and accurate to predict the respective results with a maximum of 5 % error.

**Table 6. 9** Conformation test results for modeling.

S. No.	v (m/min)	f (mm/rev)	d (mm)	Experimental results			Predicted results			% error		
				R <sub>a</sub> ( $\mu$ m)	V <sub>b</sub> ( $\mu$ m)	MRR (g/min)	R <sub>a</sub> ( $\mu$ m)	V <sub>b</sub> ( $\mu$ m)	MRR (g/min)			
1	55	0.096	0.3	1.22	37.45	3.621	1.18	36.27	3.506	3.28	3.15	3.18
2	55	0.191	0.5	1.96	76.12	14.967	1.90	74.74	14.222	3.06	1.81	4.98
3	83.5	0.096	0.7	1.34	49.44	13.643	1.30	47.21	13.060	2.99	4.51	4.27
4	83.5	0.191	0.8	1.85	93.16	33.053	1.83	91.05	31.725	1.08	2.26	4.02
5	132	0.191	0.7	1.09	132.96	52.015	1.06	128.34	49.496	2.75	3.47	4.84

## 6.6 SUMMARY

In the present chapter, RSM has been used for modeling and analyze of responses in cryogenic turning process. From the RSM results, following conclusions were drawn.

- It was proved from the ANOVA and conformation test results that the reduced quadratic predictive models for surface roughness, flank wear and MRR are

adequate to predict the results within the investigated range of process parameters with a maximum error of 3.28 %, 4.51 % and 4.98 % respectively.

- From ANOVA, it was observed that feed rate is significantly affecting the surface roughness, flank wear, and MRR respectively under the external cryogenic cooling environment.
- From interaction plots of surface roughness, it was observed that the high level of cutting velocity and low levels of feed rate and depth of cut could be contributed to generate lower surface roughness respectively.
- From interaction plots of flank wear and MRR, it was found that the highest levels of process parameters could produce high flank wear and maximum MRR respectively.



## CHAPTER 7

### CONCLUSIONS AND SCOPE OF FUTURE WORK

#### 7.1 CONCLUSIONS

In the present thesis, cooling environments (cryogenic, minimum quantity lubrication (MQL), wet and dry) and cutting parameters (cutting velocity, feed rate and depth of cut) effect has been investigated on cutting temperature, flank wear, MRR, chip morphology and surface integrity (surface roughness, surface topography, microhardness and white layer formation) while machining of 17-4 precipitation hardenable stainless steel (PH SS). Optimization and modeling studies have been carried out for cryogenic turning process. Taguchi method was used for single response optimization and ANOVA was used to find the most influenced process parameter on each response. GRA and TOPSIS optimization techniques have been applied for multi response optimization; best multi optimization tool which suits for the current study has been selected between the GRA and TOPSIS optimization techniques through conformation tests. Response surface methodology (RSM) has been used for modeling and analyze of responses. The following conclusions were drawn from the experimental and analytical results.

- Turning performance characteristics like cutting temperature, flank wear and MRR were observed as increasing trend when the turning process parameters like cutting velocity, feed rate and depth of cut increases under all the cooling environments. Whereas, in the case of surface roughness, decreasing trend was observed at the increasing cutting velocity condition and increasing trend was found for feed rate and depth of cut increasing condition respectively. In overall, cryogenic machining attained the positive results in terms of cutting velocity, flank wear and MRR over dry, wet and MQL cooling environments.

- It was observed that cryogenic machining favorably improved performance characteristics in terms of cutting temperature, tool flank wear, MRR, chip morphology and surface integrity (surface topography, surface finish, microhardness, white layer thickness (WLT)) when compared to dry, wet and MQL machining conditions.
- From the health, environmental clean and productivity improvement point of view, cryogenic machining satisfies the requirements compared to dry, wet and MQL machining conditions.
- Taguchi determined optimum cutting conditions improved the turning performance characteristics significantly while machining of 17-4 PH SS.
- Improved turning performance characteristics results were found in TGRA technique over the Taguchi coupled TOPSIS technique. Hence, in the present work, TGRA technique is more suitable for solving the multi response optimization problem within a given range of process parameters under cryogenic cooling environment.
- From the ANOVA, it was observed that flank wear and MRR significantly affected by the cutting velocity with a contribution of 46.87 % and 53.88 % respectively, Whereas, surface roughness is highly sensitive to feed rate. From the ANOVA of gray relational grade, it was found that all the responses were significantly affected by feed rate followed by cutting velocity and depth of cut respectively.
- It was proved from the ANOVA and conformation test results that the reduced quadratic predictive models for surface roughness, flank wear and MRR are adequate to predict the results within the investigated range of process parameters with a maximum error of  $\pm 5$  % respectively.
- From interaction plots of surface roughness, it was observed that the highest level of cutting velocity and lowest levels of feed rate and depth of cut could be contributed to generate lower surface roughness respectively.

- From interaction plots of flank wear and MRR, it was found that the highest levels of process parameters could produce high flank wear and maximum MRR respectively.

## **7.2 SCOPE OF FUTURE WORK**

Although lot of work have been carried out on machinability studies of 17-4 PH SS under the cryogenic cooling environment thoroughly. Still, there is scope on machinability of 17-4 PH SS under the cryogenic cooling environment. Here some of the suggestion may useful for future investigations.

- Machinability studies can be carried out by supplying the cryogenic coolant to the rake and flank faces of the cutting tool through modified tool holder.
- Determination of optimum cryogenic turning process parameters like coolant flow rate, coolant supply angle, pressure of coolant supply and stand-off distance for coolant supply can be studied.

## REFERENCES

- Abhang, L.B. and Hameedullah, M. (2012). "Determination of optimum parameters for multi-performance characteristics in turning by using grey relational analysis". *Int. J. Adv. Manuf. Technol.*, 63 (1), 13-24.
- Aggarwal, A., Singh, H., Kumar, P. and Singh, M. (2008). "Optimization of multiple quality characteristics for CNC turning under cryogenic cutting environment using desirability function". *J. Mater. Process. Technol.*, 205 (1), 42-50.
- Ahmed, M.I., Ismail, A.F., Abakr, Y.A. and Amin, A.N. (2007). "Effectiveness of cryogenic machining with modified tool holder". *J. Mater. Process. Technol.*, 185 (1), 91-96.
- Akincioglu, S., Gökçaya, H. and Uygur, İ., 2015. A review of cryogenic treatment on cutting tools. *Int. J. Adv. Manuf. Technol.*, 9 (78), 1609-1627.
- Amini, S., Khakbaz, H. and Barani, A. (2015). "Improvement of near-dry machining and its effect on tool wear in turning of AISI 4142". *Mater. Manuf. Process.*, 30 (2), 241-247.
- Aouici, H., Yallese, M.A., Fnides, B., Chaoui, K. and Mabrouki, T. (2011). "Modeling and optimization of hard turning of X38CrMoV5-1 steel with CBN tool: Machining parameters effects on flank wear and surface roughness". *J. Mech. Sci. Technol.*, 25 (11), 2843-2851.
- Aoyama, T., Kakinuma, Y., Yamashita, M. and Aoki, M. (2008). "Development of a new lean lubrication system for near dry machining process". *CIRP Ann. - Manuf. Technol.*, 57 (1), 125-128.
- Asiltürk, I. and Akkuş, H. (2011). "Determining the effect of cutting parameters on surface roughness in hard turning using the Taguchi method". *Meas. J. Int. Meas. Confed.*, 44 (9), 1697–1704.

- Asiltürk, I., Neşeli, S. and Ince, M.A. (2016). "Optimisation of parameters affecting surface roughness of Co28Cr6Mo medical material during CNC lathe machining by using the Taguchi and RSM methods". *Meas. J. Int. Meas. Confed.*, 78, 120–128.
- Attanasio, A., Gelfi, M., Giardini, C. and Remino, C. (2006). "Minimal quantity lubrication in turning: effect on tool wear". *Wear*, 260 (3), 333-338.
- Balasubramanian, S., Gupta, M.K. and Singh, K.K. (2012). "Cryogenics and its application with reference to spice grinding: a review". *Crit. Rev. Food Sci. Nutr.*, 52 (9), 781–794.
- Baldissera, P. and Delprete, C. (2008). "Deep cryogenic treatment: a bibliographic review". *Open Mech. Eng. J.*, 2, 1–11.
- Baradie, M. A. (1996a). "Cutting fluids: Part I. Characterisation". *J. Mater. Process. Technol.*, 56 (1–4), 786–797.
- Baradie, M. A. (1996b). "Cutting fluids: Part II. Recycling and clean machining". *J. Mater. Process. Technol.*, 56 (1–4), 798–806.
- Bensely, A., Venkateswaran, S., Subisak, A.D., Mohan Lal D., Rajadurai, A., Lenkey, G.B., Paulin, P. (2012). "Influence of deep cryogenic treatment on alloy carbide precipitations and mechanical properties of AISI M2 high speed tool steel". *Cold Facts*, 28(2), 1–28.
- Birmingham, M.J., Kirsch, J., Sun, S., Palanisamy, S. and Dargusch, M.S. (2011). "New observations on tool life, cutting forces and chip morphology in cryogenic machining Ti-6Al-4V". *Int. J. Mach. Tools Manuf.*, 51 (6), 500-511.
- Bhushan, R.K. (2013). Optimization of cutting parameters for minimizing power consumption and maximizing tool life during machining of Al alloy SiC particle composites". *J. Clean. Prod.*, 39, 242–254.

- Bordin, A., Sartori, S., Bruschi, S. and Ghiotti, A. (2017). "Experimental investigation on the feasibility of dry and cryogenic machining as sustainable strategies when turning Ti6Al4V produced by Additive Manufacturing". *J. Clean. Prod.*, 142, 4142-4151.
- Bordin, A., Bruschi, S., Ghiotti, A. and Bariani, P.F. (2015). "Analysis of tool wear in cryogenic machining of additive manufactured Ti6Al4V alloy". *Wear*, 328, 89-99.
- Bosheh, S.S. and Mativenga, P.T. (2006). "White layer formation in hard turning of H13 tool steel at high cutting speeds using CBN tooling". *Int. J. Mach. Tools Manuf.*, 46 (2), 225–233.
- Bouacha, K., Yallese, M.A., Khamel, S. and Belhadi, S. (2014). "Analysis and optimization of hard turning operation using cubic boron nitride tool". *Int. J. Refract. Met. Hard Mater.*, 45, 160-178.
- Bouacha, K., Yallese, M.A., Mabrouki, T. and Rigal, J.F. (2010). "Statistical analysis of surface roughness and cutting forces using response surface methodology in hard turning of AISI 52100 bearing steel with CBN tool". *Int. J. Refract. Met. Hard Mater.*, 28 (3), 349-361.
- Brockhoff, T. and Walter, A.(1998). "Fluid minimization in cutting and grinding. *Abra.*, *J. Abra.Eng. Soc.*, 10 (11), 38-42.
- Bruschi, S., Bertolini, R., Bordin, A., Medea, F. and Ghiotti, A. (2016). "Influence of the machining parameters and cooling strategies on the wear behavior of wrought and additive manufactured Ti6Al4V for biomedical applications". *Tribol. Int.*, 102, 133-142.
- Camposeco-Negrete, C. (2013). "Optimization of cutting parameters for minimizing energy consumption in turning of AISI 6061 T6 using Taguchi methodology and ANOVA". *J. Clean. Prod.*, 53, 195–203.
- Candane, D., Alagumurthi, N. and Palaniradja, K. (2013). "Effect of Deep Cryogenic Treatment on AISI T42 High Speed Steel". *Int. J. Curr. Eng. Technol.*, 43 (1), 1164–1170.

- Cassin, C. and Boothroyd, G. (1965). Lubricating action of cutting fluids. *J. Mech. Eng. Sci.*, 7 (1), 67–81.
- Chauhan, S.R. and Dass, K. (2012). "Optimization of Machining Parameters in Turning of Titanium (Grade-5) Alloy Using Response Surface Methodology". *Mater. Manuf. Process.*, 27 (5), 531–537.
- Chetan, Ghosh, S. and Rao, P.V. (2016). "Environment friendly machining of Ni–Cr–Co based super alloy using different sustainable techniques". *Mater. Manuf. Process.*, 31 (7), 852-859.
- Ghosh, S. and Rao, P.V. (2015). "Application of sustainable techniques in metal cutting for enhanced machinability: a review". *J. Clean. Prod.*, 100, 17-34.
- Chien, W.T. and Tsai, C.S. (2003). "The investigation on the prediction of tool wear and the determination of optimum cutting conditions in machining 17-4PH stainless steel". *J. Mater. Process. Technol.*, 140 (1), 340-345.
- Chinchanikar, S. and Choudhury, S.K. (2014). "Hard turning using HiPIMS-coated carbide tools: Wear behavior under dry and minimum quantity lubrication (MQL)". *Meas. J. Int. Meas. Confed.*, 55, 536–548.
- Chinchanikar, S. and Choudhury, S.K. (2015). "Machining of hardened steel— Experimental investigations, performance modeling and cooling techniques: A review". *Int. J. Mach. Tools Manuf.*, 89, 95–109.
- Sáenz, D.C., Castillo, N.G., Romeva, C.R. and Macià, J.L. (2015). "A fuzzy approach for the selection of non-traditional sheet metal cutting processes". *Expert Syst. Appl.*, 42 (15), 6147-6154.
- Das, D., Dutta, A.K. and Ray, K.K. (2009). "Optimization of the duration of cryogenic processing to maximize wear resistance of AISI D2 steel". *Cryogenics*, 49 (5), 176–184.

Davim, J.P. (2003). "Design of optimisation of cutting parameters for turning metal matrix composites based on the orthogonal arrays". *J. Mater. Process. Technol.*, 132 (1–3), 340–344.

Debnath, S., Mohan Reddy, M. and Sok Yi, Q. (2016). "Influence of cutting fluid conditions and cutting parameters on surface roughness and tool wear in turning process using Taguchi method". *Measurement*, 78, 111–119.

Dhananchezian, M. and Kumar, M.P. (2010). "Experimental investigation of cryogenic cooling by liquid nitrogen in the orthogonal machining of aluminium 6061-T6 alloy". *Int. J. Mach. Mach. Mater.*, 7 (3-4), 274-285

Dhananchezian, M., Kumar, M.P. and Sornakumar, T. (2011). "Cryogenic Turning of AISI 304 Stainless Steel with Modified Tungsten Carbide Tool Inserts". *Mater. Manuf. Process.*, 26 (5), 781–785.

Dhananchezian, M. and Pradeep Kumar, M., 2011. "Cryogenic turning of the Ti-6Al-4V alloy with modified cutting tool inserts". *Cryogenics*, 51 (1), 34–40.

Dhar, N.R. and Kamruzzaman, M. (2007). "Cutting temperature, tool wear, surface roughness and dimensional deviation in turning AISI-4037 steel under cryogenic condition". *Int. J. Mach. Tools Manuf.*, 47 (5 SPEC. ISS.), 754–759.

Dhar, N.R., Kamruzzaman, M. and Ahmed, M., 2006. "Effect of minimum quantity lubrication (MQL) on tool wear and surface roughness in turning AISI-4340 steel". *J. Mater. Process. Technol.*, 172 (2), 299–304.

Dhar, N.R., Paul, S. and Chattopadhyay, A. B. (2001). "The influence of cryogenic cooling on tool wear, dimensional accuracy and surface finish in turning AISI 1040 and E4340C steels". *Wear*, 249 (10–11), 932–942.

Dhar, N.R., Paul, S. and Chattopadhyay, A.B. (2002). "Machining of AISI 4140 steel under cryogenic cooling—tool wear, surface roughness and dimensional deviation" *Journal of Materials Processing Technology*, 123 (3), 483-489.



Dilip Jerold, B. and Pradeep Kumar, M. (2012). "Experimental comparison of carbon-dioxide and liquid nitrogen cryogenic coolants in turning of AISI 1045 steel". *Cryogenics*, 52 (10), 569–574.

Dilip Jerold, B. and Pradeep Kumar, M. (2011). "Experimental investigation of turning AISI 1045 steel using cryogenic carbon dioxide as the cutting fluid". *J. Manuf. Process.*, 13 (2), 113–119.

Dinesh, S., Senthilkumar, V., Asokan, P. and Arulkirubakaran, D. (2015). "Effect of cryogenic cooling on machinability and surface quality of bio-degradable ZK60 Mg alloy". *Mater. Des.*, 87, 1030-1036.

Dinesh, S., Senthilkumar, V. and Asokan, P. (2017). "Experimental studies on the cryogenic machining of biodegradable ZK60 Mg alloy using micro-textured tools". *Mater. Manuf. Process.*, 32 (9),979-987.

Ding, Y. and Hong, S.Y. (1998). Improvement of Chip Breaking in Machining Low Carbon Steel by Cryogenically Precooling the Workpiece. *J. Manuf. Sci. Eng.*, 120, 76-83.

Dogra, M., Sharma, V.S., Sachdeva, A., Suri, N.M. and Dureja, J.S. (2011). "Performance evaluation of CBN, coated carbide, cryogenically treated uncoated/coated carbide inserts in finish-turning of hardened steel". *Int. J. Adv. Manuf. Technol.*, 57 (5), 541-553.

Dureja, J.S., Singh, R. and Bhatti, M.S. (2014). "Optimizing flank wear and surface roughness during hard turning of AISI D3 steel by Taguchi and RSM methods". *Prod. Manuf. Res.*, 2 (1), 767-783.

Ezugwu, E.O. (2005). Key improvements in the machining of difficult-to-cut aerospace superalloys". *Int. J. Mach. Tools Manuf.*, 45 (12–13), 1353–1367.

Ezugwu, E.O., Bonney, J. and Yamane, Y. (2003). "An overview of the machinability of aeroengine alloys". *J. Mater. Process. Technol.*, 134 (2), 233–253.

Feng, S. and Hattori, M. (2000). "Cost and Process Information Modeling for Dry Machining". In *Proc. of the International Workshop for Environment Conscious Manufacturing-ICEM-2000*, pp.1–8.

Fetecau, C. and Stan, F., (2012). "Study of cutting force and surface roughness in the turning of polytetrafluoroethylene composites with a polycrystalline diamond tool". *Meas. J. Int. Meas. Confed.*, 45 (6), 1367–1379.

Firouzdor, V., Nejati, E. and Khomamizadeh, F. (2008). "Effect of deep cryogenic treatment on wear resistance and tool life of M2 HSS drill". *J. Mater. Process. Technol.*, 206 (1), 467–472.

Gaitonde, V.N., Karnik, S.R. and Davim, J.P. (2008). "Selection of optimal MQL and cutting conditions for enhancing machinability in turning of brass". *J. Mater. Process. Technol.*, 204 (1–3), 459–464.

Gill, S.S., Singh, H., Singh, R. and Singh, J. (2010). "Cryoprocessing of cutting tool materials—a review". *Int. J. Adv. Manuf. Technol.*, 48 (1), 175-192.

Gill, S.S., Singh, J., Singh, H. and Singh, R. (2012). "Metallurgical and mechanical characteristics of cryogenically treated tungsten carbide (WC–Co)". *Int. J. Adv. Manuf. Technol.*, 58 (1), 119-131.

Gill, S.S. and Singh, H. (2013). "Cryogenic treatment of materials: cutting tools and polymers". In *Polymers at Cryogenic Temperatures (245-273)*. Springer Berlin Heidelberg.

Goel, B., Singh, S. and Sarepaka, R.V. (2015). "Optimizing single point diamond turning for mono-crystalline germanium using grey relational analysis". *Mater. Manuf. Process.*, 30 (8), 1018-1025.

Gupta, M.K., Singh, G. and Sood, P.K. (2015). Experimental investigation of machining AISI 1040 medium carbon steel under cryogenic machining: A comparison with dry machining. *J. Inst. Eng. Ser. C*, 4 (96), 373-379.

Gupta, M.K., Singh, G. and Sood, P.K. (2015). "Modelling and optimization of tool wear in machining of EN24 steel using Taguchi approach". *J. Inst. Eng. Ser. C*, 3 (96), 269-277.

Gupta, M.K., Sood, P.K. and Sharma, V.S. (2016). "Machining parameters optimization of titanium alloy using response surface methodology and particle swarm optimization under minimum-quantity lubrication environment". *Mater. Manuf. Process.*, 31 (13), 1671-1682.

Gupta, M.K., Sood, P.K. and Sharma, V.S. (2016). "Optimization of machining parameters and cutting fluids during nano-fluid based minimum quantity lubrication turning of titanium alloy by using evolutionary techniques". *J. Clean. Prod.*, 135, 1276-1288.

He, H.B., Han, W.Q., Li, H.Y., Li, D.Y., Yang, J., Gu, T. and Deng, T. (2014). "Effect of deep cryogenic treatment on machinability and wear mechanism of TiAlN coated tools during dry turning". *Int. J. Precis. Eng. Manuf.*, 4 (15), 655-660.

Hong, S.Y. (1995), Advancement of economical cryogenic machining technology. In *Proceedings of 3rd International Conference on Manufacturing*, 12, 86-92.

Hong, S.Y. (2006). "Lubrication Mechanisms of  $\text{LN}_2$  in Ecological Cryogenic Machining". *Mach. Sci. Technol.*, 10 (1), 133–155.

Hong, S.Y. and Broomer, M. (2000). "Economical and ecological cryogenic machining of AISI 304 austenitic stainless steel". *Clean Prod. Process.*, 2 (3), 0157–0166.

Hong, S.Y. and Ding, Y. (2001). "Cooling approaches and cutting temperatures in cryogenic machining of Ti-6Al-4V". *Int. J. Mach. Tools Manuf.*, 41 (10), 1417–1437.

Hong, S.Y. and Ding, Y. (2001). "Micro-temperature manipulation in cryogenic machining of low carbon steel". *J. Mater. Process. Technol.*, 116 (1), 22–30.

- Hong, S.Y., Ding, Y. and Ekkens, R.G. (1999). "Improving low carbon steel chip breakability by cryogenic chip cooling". *Int. J. Mach. Tools Manuf.*, 39 (7), 1065–1085.
- Hong, S.Y., Ding, Y. and Jeong, J. (2002a). "Experimental Evaluation of Friction Coefficient and Liquid Nitrogen Lubrication Effect in Cryogenic Machining". *Mach. Sci. Technol.*, 6 (2), 235–250.
- Hong, S.Y., Ding, Y. and Jeong, J. (2002b). "Experimental Evaluation of Friction Coefficient and Liquid Nitrogen Lubrication Effect in Cryogenic Machining". *Mach. Sci. Technol.*, 6 (2), 235-250.
- Hu, Y., Chang, X., Wang, Y., Wang, Z., Shi, C. and Wu, L. (2017). "Cloud manufacturing resources fuzzy classification based on genetic simulated annealing algorithm". *Mater. Manuf. Process.*, (Just accepted ) 1-7.
- Hwang, C.L. and Yoon, K. (1981). *Multiple Attribute Decision Making Methods and Applications*, Springer. *New York*.
- Hwang, Y.K. and Lee, C.M. (2010). "Surface roughness and cutting force prediction in MQL and wet turning process of AISI 1045 using design of experiments". *J. Mech. Sci. Technol.*, 24 (8),1669–1677.
- Indumathi, J., Bijwe, J., Ghosh, A.K., Fahim, M. and Krishnaraj, N. (1999). "Wear of cryo-treated engineering polymers and composites". *Wear*, 225, 343-353.
- Jawahir, I.S., Attia, H., Biermann, D., Duflou, J., Klocke, F., Meyer, D., Newman, S.T., Pusavec, F., Putz, M., Rech, J. and Schulze, V. (2016). "Cryogenic manufacturing processes". *CIRP Ann. - Manuf. Technol.*, 65 (2), 713-736.
- Jawahir, I.S. (1988). "The chip control factor in machinability assessments: recent trends". *J. Mech. Work. Technol.*, 17, 213–224.
- Jerold, B.D. and Kumar, M.P. (2012). "Machining of AISI 316 Stainless Steel under Carbon-Di-Oxide Cooling". *Mater. Manuf. Process.*, 27 (10), 1059–1065.

Jerold, B.D. and Kumar, M.P. (2013). "The Influence of Cryogenic Coolants in Machining of Ti-6Al-4V". *J. Manuf. Sci. Eng.*, 135 (3), 31005, 1-8.

Jeyakumar, S., Marimuthu, K. and Ramachandran, T. (2013). "Prediction of cutting force , tool wear and surface roughness of Al6061 / SiC composite for end milling operations using RSM". *J. Mech. Sci. Technol.*, 27 (9), 2813–2822.

Deng, L. L. (1982). "Control problems of grey systems". *Syst. Control Lett.*, 1 (5), 288–294.

Jun, S.C. (2005). "Lubrication effect of liquid nitrogen in cryogenic machining friction on the tool-chip interface". *J. Mech. Sci. Technol.*, 19 (4), 936–946.

Kalyan Kumar, K.V.B.S. and Choudhury, S.K. (2008). "Investigation of tool wear and cutting force in cryogenic machining using design of experiments". *J. Mater. Process. Technol.*, 203 (1–3), 95–101.

Kaynak, Y. (2014). "Evaluation of machining performance in cryogenic machining of Inconel 718 and comparison with dry and MQL machining". *Int. J. Adv. Manuf. Technol.*, 72 (5–8), 919–933.

Kaynak, Y., Robertson, S.W., Karaca, H.E. and Jawahir, I.S. (2015). "Progressive tool-wear in machining of room-temperature austenitic NiTi alloys: The influence of cooling/lubricating, melting, and heat treatment conditions". *J. Mater. Process. Technol.*, 215, 95-104.

Kaynak, Y., Karaca, H.E. and Jawahir, I.S. (2014) "Cutting Speed Dependent Microstructure and Transformation Behavior of NiTi Alloy in Dry and Cryogenic Machining". *J. Mater. Eng. Perform.*, 24 (1), 452–460.

Kaynak, Y., Lu, T. and Jawahir, I.S. (2014). "Cryogenic Machining-Induced Surface Integrity: A Review and Comparison with Dry, MQL, and Flood-Cooled Machining". *Mach. Sci. Technol.*, 18 (2), 149–198.

- Kenda, J., Pusavec, F. and Kopac, J. (2011). "Analysis of Residual Stresses in Sustainable Cryogenic Machining of Nickel Based Alloy—Inconel 718". *J. Manuf. Sci. Eng.*, 133 (4), 41009.
- Khan, A.A. and Ahmed, M.I. (2008). "Improving tool life using cryogenic cooling". *J. Mater. Process. Technol.*, 196 (1–3), 149–154.
- Khan, A. A., Ali, M.Y. and Haque, M.M. (2010). A new approach of applying cryogenic coolant in turning AISI 304 stainless steel. *Int. J. Mech. Mater. Eng.*, 5 (2), 171–174.
- Khan, M.M. A, Mithu, M. a H. and Dhar, N.R. (2009). "Effects of minimum quantity lubrication on turning AISI 9310 alloy steel using vegetable oil-based cutting fluid". *J. Mater. Process. Technol.*, 209 (15–16), 5573–5583.
- Khandey, U., Ghosh, S. & Hariharan, K. (2017). "Optimization of Machining Parameters for Satisfying the Multiple Objectives in Machining of MMCs". *Mater. Manuf. Process.*, Just accepted.
- Kibria, G., Doloi, B. & Bhattacharyya, B. (2013). "Experimental investigation and multi-objective optimization of Nd : YAG laser micro-turning process of alumina ceramic using orthogonal array and grey relational analysis". *Opt. Laser Technol.*, 48, 16–27.
- Kirby, E.D., Zhang, Z., Chen, J.C. and Chen, J. (2006). "Optimizing surface finish in a turning operation using the Taguchi parameter design method". *Int. J. Adv. Manuf. Technol.*, 30 (11), 1021-1029.
- Klocke, F., Settineri, L., Lung, D., Priarone, P.C. and Arft, M. (2013). "High performance cutting of gamma titanium aluminides: Influence of lubricoolant strategy on tool wear and surface integrity". *Wear*, 302 (1), 1136-1144.
- Klocke, F. and Eisenblätter, G. (1998). Dry cutting - State of research. *VDI Berichte*, 46 (1399), 159–188.

- Kochmański, P. and Nowacki, J. (2006). "Activated gas nitriding of 17-4 PH stainless steel". *Surf. Coatings Technol.*, 200 (22–23), 6558–6562.
- Kouam, J., Songmene, V., Balazinski, M. and Hendrick, P. (2015). "Effects of minimum quantity lubricating (MQL) conditions on machining of 7075-T6 aluminum alloy". *Int. J. Adv. Manuf. Technol.*, 79, 45-55.
- Kumar, A., Balaji, Y., Prasad, N.E., Gouda, G. and Tamilmani, K. (2013). "Indigenous development and airworthiness certification of 15–5 PH precipitation hardenable stainless steel for aircraft applications". *Sadhana*, 38 (1), 3-23.
- Kumar, V. and Kumar, P. (2014). "Optimization of cryogenic cooled EDM process parameters using grey relational analysis". *J. Mech. Sci. Technol.*, 28 (9), 37-42.
- Kuzu, A.T., Bijanzad, A. and Bakkal, M. (2015). "Experimental Investigations of Machinability in the Turning of Compacted Graphite Iron using Minimum Quantity Lubrication". *Mach. Sci. Technol.*, 19 (4), 559–576.
- Lahiri, S. (2014). "Robust growth for metalworking fluids" 32–35.
- Lawal, S. A., Choudhury, I. A. and Nukman, Y. (2012). "Application of vegetable oil-based metalworking fluids in machining ferrous metals - A review". *Int. J. Mach. Tools Manuf.*, 52 (1), 1–12.
- Li, L., Li, Z.Y., Wei, X.T. and Cheng, X. (2015). "Machining characteristics of Inconel 718 by sinking-EDM and wire-EDM". *Mater. Manuf. Process.*, 30 (8), 968-973.
- Lin, C.L. (2004). "Use of the Taguchi method and grey relational analysis to optimize turning operations with multiple performance characteristics". *Mater. Manuf. Process.*, 19 (2), 209-220.
- Liu, Z., Nouraei, H., Spelt, J.K. and Papini, M. (2015). "Electrochemical slurry jet micro-machining of tungsten carbide with a sodium chloride solution". *Precis. Eng.*, 40, 189-198.

- MacHai, C. and Biermann, D. (2011). "Machining of  $\beta$ -titanium-alloy Ti-10V-2Fe-3Al under cryogenic conditions: Cooling with carbon dioxide snow". *J. Mater. Process. Technol.*, 211 (6), 1175–1183.
- Maity, K.P. and Swain, P.K. (2008). "An experimental investigation of hot-machining to predict tool life". *J. Mater. Process. Technol.*, 198 (1–3), 344–349.
- Makadia, A.J. and Nanavati, J.I. (2013). "Optimisation of machining parameters for turning operations based on response surface methodology". *Meas. J. Int. Meas. Confed.*, 46 (4), 1521–1529.
- Mandal, N., Doloi, B. and Mondal, B. (2011). "Development of flank wear prediction model of Zirconia Toughened Alumina (ZTA) cutting tool using response surface methodology". *Int. J. Refract. Met. Hard Mater.*, 29 (2), 273–280.
- Mandal, N., Doloi, B. and Mondal, B. (2012). "Force prediction model of zirconia toughened alumina (ZTA) inserts in hard turning of AISI 4340 steel using response surface methodology". *Int. J. Precis. Eng. Manuf.*, 13 (9), 1589–1599.
- Mandal, N., Doloi, B. and Mondal, B. (2013). "Predictive modeling of surface roughness in high speed machining of AISI 4340 steel using yttria stabilized zirconia toughened alumina turning insert". *Int. J. Refract. Met. Hard Mater.*, 38, 40–46.
- Manimaran, G. and Kumar, M.P. (2013). "Multiresponse optimization of grinding AISI 316 stainless steel using grey relational analysis". *Mater. Manuf. Process.*, 28 (4), 418-423.
- Manivannan, R. and Kumar, M.P. (2017). "Multi-attribute decision-making of cryogenically cooled micro-EDM drilling process parameters using TOPSIS method". *Mater. Manuf. Process.*, 32 (2), 209-215.
- Manivel, D. and Gandhinathan, R., 2016. Optimization of surface roughness and tool wear in hard turning of austempered ductile iron (grade 3) using Taguchi method. *Meas. J. Int. Meas. Confed.*, 93, 108–116.



- Manjaiah, M., Narendranath, S. and Basavarajappa, S. (2016). "Wire Electro Discharge Machining Performance of TiNiCu Shape Memory Alloy". *Silicon*, 8 (3), 467–475.
- Manna, A. (2013). "Multi-response optimisation of machining parameters during drilling LM6Mg15SiC-Al-MMC based on Grey relational analysis". *Int. J. Mach. Mach. Mater.*, 14 (3), 275–294.
- Marksberry, P.W. (2007). "Micro-flood (MF) technology for sustainable manufacturing operations that are coolant less and occupationally friendly". *J. Clean. Prod.*, 15 (10), 958–971.
- Mohanty, A., Gangopadhyay, S. and Thakur, A. (201)6. "On applicability of multilayer coated tool in dry machining of aerospace grade stainless steel". *Mater. Manuf. Process.*, 31 (7), 869-879.
- Montgomery, D.C. (1987). "Design and analysis of experiments-second edition". *Quality and Reliability Engineering International*, 3 (3), 212–212.
- Obikawa, T., Kamata, Y. and Shinozuka, J. (2006). "High-speed grooving with applying MQL". *Int. J. Mach. Tools Manuf.*, 46 (14), 1854–1861.
- Palanikumar, K. (2008). "Application of Taguchi and response surface methodologies for surface roughness in machining glass fiber reinforced plastics by PCD tooling". *Int. J. Adv. Manuf. Technol.*, 36 (1–2), 19–27.
- Palanikumar, K. and Karthikeyan, R. (2006). "Optimal Machining Conditions for Turning of Particulate Metal Matrix Composites Using Taguchi and Response Surface Methodologies". *Mach. Sci. Technol.*, 10 (4), 417–433.
- Paul, S. and Chattopadhyay, A. B. (2006). "Environmentally Conscious Machining and Grinding With Cryogenic Cooling". *Mach. Sci. Technol.*, 10 (1), 87–131.

- Paul, S., Dhar, N.R. and Chattopadhyay, A. B. (2001). "Beneficial effects of cryogenic cooling over dry and wet machining on tool wear and surface finish in turning AISI 1060 steel". *J. Mater. Process. Technol.*, 116 (1), 44–48.
- Pawade, R.S., Joshi, S.S., Brahmankar, P.K. and Rahman, M. (2007). "An investigation of cutting forces and surface damage in high-speed turning of Inconel 718". *J. Mater. Process. Technol.*, 192,139-146.
- Pereira, O., Rodríguez, A., Fernández-Abia, A.I., Barreiro, J. and de Lacalle, L.L. (2016). "Cryogenic and minimum quantity lubrication for an eco-efficiency turning of AISI 304". *J. Clean. Prod.*, 139, 440-449.
- Philip Selvaraj, D., Chandramohan, P. and Mohanraj, M. (2014). "Optimization of surface roughness, cutting force and tool wear of nitrogen alloyed duplex stainless steel in a dry turning process using Taguchi method". *Meas. J. Int. Meas. Confed.*, 49 (1), 205–215.
- Podgornik, B., Leskovšek, V. and Vižintin, J. (2009). "Influence of deep-cryogenic treatment on tribological properties of P/M high-speed steel". *Mater. Manuf. Process.*, 24 (7–8), 734–738.
- Poulachon, G., Albert, A., Schluraff, M. and Jawahir, I.S. (2005). "An experimental investigation of work material microstructure effects on white layer formation in PCBN hard turning". *Int. J. Mach. Tools Manuf.*, 45 (2), 211-218.
- Priyadarshi, D. and Sharma, R.K. (2016). "Optimization for turning of Al-6061-SiC-Gr hybrid nanocomposites using response surface methodologies". *Mater. Manuf. Process.*, 31 (10), 1342-1350.
- Pu, Z., Outeiro, J.C., Batista, A.C., Dillon, O.W., Puleo, D.A. and Jawahir, I.S. (2012). "Enhanced surface integrity of AZ31B Mg alloy by cryogenic machining towards improved functional performance of machined components". *Int. J. Mach. Tools Manuf.*, 56, 17-27.

Pusavec, F., Hamdi, H., Kopac, J. and Jawahir, I.S. (2011). "Surface integrity in cryogenic machining of nickel based alloy—Inconel 718". *J. Mater. Process. Technol.*, 211 (4), 773-783.

Pusavec, F., Kramar, D., Krajnik, P. and Kopac, J. (2010). Transitioning to sustainable production—part II: evaluation of sustainable machining technologies. *J. Clean. Prod.*, 18 (12), 1211-1221.

Rajyalakshmi, G. and Ramaiah, P.V. (2013). "Multiple process parameter optimization of wire electrical discharge machining on Inconel 825 using Taguchi grey relational analysis". *Int J Adv Manuf Technol*, 69 ( 5-8), 1249-1262.

Ramanujam, R., Muthukrishnan, N. and Raju, R. (2011). "Optimization of cutting parameters for turning Al-SiC (10p) MMC using ANOVA and grey relational analysis". *International Journal of Precision Engineering and Manufacturing*, 12 (4), 651-656.

Ramesh, S., Viswanathan, R. and Ambika, S., 2016. "Measurement and optimization of surface roughness and tool wear via grey relational analysis, TOPSIS and RSA techniques". *Meas. J. Int. Meas. Confed.*, 78, 63–72.

Ranganathan, S. and Senthilvelan, T. (2011). "Multi-response optimization of machining parameters in hot turning using grey analysis". *Int. J. Adv. Manuf. Technol.*, 56 (5), 455-462.

Rao, R.V. (2010). "*Advanced modeling and optimization of manufacturing processes: international research and development*". Springer Science & Business Media.

Rao, R. V. and Davim, J.P. (2008). "A decision-making framework model for material selection using a combined multiple attribute decision-making method". *Int. J. Adv. Manuf. Technol.*, 35 (7–8), 751–760.

- Rao, R.V., Patel, B.K. and Parnichkun, M. (2011). "Industrial robot selection using a novel decision making method considering objective and subjective preferences". *Rob. Auton. Syst.*, 59 (6), 367–375.
- Raza, S.W., Pervaiz, S. and Deiab, I. (2014). "Tool wear patterns when turning of titanium alloy using sustainable lubrication strategies". *Int. J. Precis. Eng. Manuf.*, 15 (9), 1979–1985.
- Reddy, T.S., Sornakumar, T., Reddy, M.V., Venkatram, R. and Senthilkumar, A. (2009). "Turning studies of deep cryogenic treated p-40 tungsten carbide cutting tool inserts– Technical communication". *Mach. Sci. Technol.*, 13 (2), 269-281.
- Rotella, G., Dillon, O.W., Umbrello, D., Settineri, L. and Jawahir, I.S. (2013). "The effects of cooling conditions on surface integrity in machining of Ti6Al4V alloy". *Int. J. Adv. Manuf. Technol.*, 71 (1–4), 47–55.
- Routara, B.C., Bandyopadhyay, A. and Sahoo, P. (2009). "Roughness modeling and optimization in CNC end milling using response surface method: Effect of workpiece material variation". *Int. J. Adv. Manuf. Technol.*, 40 (11–12), 1166–1180.
- Rozzi, J.C., Sanders, J.K. and Chen, W. (2011). "The Experimental and Theoretical Evaluation of an Indirect Cooling System for Machining". *Journal of Heat Transfer*, 133 (3), 31006.
- Sahoo, A.K. and Pradhan, S. (2013). "Modeling and optimization of Al/SiCp MMC machining using Taguchi approach". *Meas. J. Int. Meas. Confed.*, 46 (9), 3064–3072.
- Sánchez-Lozano, J.M., Antunes, C.H., García-Cascales, M.S. and Dias, L.C. (2014). "GIS-based photovoltaic solar farms site selection using ELECTRE-TRI: Evaluating the case for Torre Pacheco, Murcia, Southeast of Spain". *Renew. Energy*, 66, 478-494.
- Sarikaya, M. and Güllü, A. (2014). "Taguchi design and response surface methodology based analysis of machining parameters in CNC turning under MQL". *J. Clean. Prod.*, 65, 604-616.

Sarıkaya, M. and Güllü, A. (2015). "Multi-response optimization of minimum quantity lubrication parameters using Taguchi-based grey relational analysis in turning of difficult-to-cut alloy Haynes 25". *J. Clean. Prod.*, 91, 347–357.

Sarıkaya, M., Yılmaz, V. and Güllü, A. (2016). "Analysis of cutting parameters and cooling/lubrication methods for sustainable machining in turning of Haynes 25 superalloy". *J. Clean. Prod.*, 133, 172–181.

Sartori, S., Moro, L., Ghiotti, A. and Bruschi, S. (2017). "On the tool wear mechanisms in dry and cryogenic turning Additive Manufactured titanium alloys". *Tribol. Int.*, 105, 264-273.

Schoop, J., Ambrosy, F., Zanger, F., Schulze, V., Balk, T.J. and Jawahir, I.S. (2016). "Cryogenic machining of porous tungsten for enhanced surface integrity". *J. Mater. Process. Technol.*, 229, 614-621.

Schoop, J., Ambrosy, F., Zanger, F., Schulze, V., Jawahir, I.S. and Balk, T.J. (2016). "Increased surface integrity in porous tungsten from cryogenic machining with cermet cutting tool". *Mater. Manuf. Process.*, 31 (7), 823-831.

Seeman, M., Ganesan, G., Karthikeyan, R. and Velayudham, A. (2010). "Study on tool wear and surface roughness in machining of particulate aluminum metal matrix composite-response surface methodology approach". *Int. J. Adv. Manuf. Technol.*, 48 (5), 613-624.

Senthilkumar, D. and Rajendran, I. (2011). "Influence of shallow and deep cryogenic treatment on tribological behavior of En 19 steel". *J. Iron Steel Res. Int.*, 18 (9), 53–59.

Senthilkumar, N., Ganapathy, T. and Tamizharasan, T. (2016). "Optimisation of machining and geometrical parameters in turning process using Taguchi method". *Aust. J. Mech. Eng.*, 12 (2), 232–246.

- Senthilkumar, N., Tamizharasan, T. & Anandakrishnan, V. (2014). "Experimental investigation and performance analysis of cemented carbide inserts of different geometries using Taguchi based grey relational analysis". *Measurement*, 58, 520–536.
- Sharma, J. and Sidhu, B.S. (2014). "Investigation of effects of dry and near dry machining on AISI D2 steel using vegetable oil". *J. Clean. Prod.*, 66, 619–623.
- Sharma, P., Chakradhar, D. and Narendranath, S. (2015). "Evaluation of WEDM performance characteristics of Inconel 706 for turbine disk application". *Jmade*, 88, 558–566.
- Sharma, V.S., Dogra, M. and Suri, N.M. (2009). "Cooling techniques for improved productivity in turning". *Int. J. Mach. Tools Manuf.*, 49 (6), 435–453.
- Shaw, M.C. (1984). "*Metal Cutting Principles*", Clarendon Press. U.S
- Shaw, M.C., Pigott, J.D. & Richardson, L.P. (1951). "Effect of cutting fluid upon chip–tool interface temperature". *Trans. ASME*, 71 (2), 45–56.
- Shokrani, A., Dhokia, V. and Newman, S.T. (2012). "Environmentally conscious machining of difficult-to-machine materials with regard to cutting fluids". *Int. J. Mach. Tools Manuf.*, 57, 83–101.
- Siddiquee, A.N., Khan, Z.A. and Tomar, J.S. (2013). "Investigation and optimisation of machining parameters for micro-countersinking of AISI 420 stainless steel". *Int. J. Mach. Mach. Mater.*, 14 (3), 230–256.
- Şimşek, B. and Uygunoğlu, T. (2016). "Multi-response optimization of polymer blended concrete: A TOPSIS based Taguchi application". *Constr. Build. Mater.*, 117, 251–262.
- Singh, A., Datta, S. and Mahapatra, S.S. (2011). "Application of TOPSIS in the Taguchi Method for Optimal Machining Parameter Selection". *J. Manuf. Sci. Prod.*, 11(1–3), 49–60.

Singh, H. and Kumar, P. (2006). "Optimizing feed force for turned parts through the Taguchi technique". *Sadhana*, 31 (6), 671-681.

Sri Siva, R., Mohan Lal, D. and Jaswin, M.A. (2012). "Optimization of Deep Cryogenic Treatment Process for 100Cr6 Bearing Steel Using the Grey-Taguchi Method". *Tri. Trans.*, 55 (6), 854-862.

Sivapirakasam, S.P., Mathew, J. and Surianarayanan, M. (2011). "Multi-attribute decision making for green electrical discharge machining". *Expert Syst. Appl.*, 38 (7), 8370–8374.

Sohrabpoor, H., Khanghah, S.P. and Teimouri, R. (2014)." Investigation of lubricant condition and machining parameters while turning of AISI 4340". *Int. J. Adv. Manuf. Technol.*, 76 (9–12),2099–2116.

Sornakumar, T., Krishnamurthy, R. and Gokularathnam, C. V. (1993). "Machining performance of phase transformation toughened alumina and partially stabilised zirconia composite cutting tools". *J. Eur. Ceram. Soc.*, 12 (6), 455–460.

Stephan, D.D., Werner, J. and Yeater, R.P. (1998). Essential regression and experimental design for chemists and engineers. *MS Excel add Softw. Packag.*, 2001.

Strano, M., Albertelli, P., Chiappini, E. and Tirelli, S. (2015). "Wear behaviour of PVD coated and cryogenically treated tools for Ti-6Al-4V turning". *Int J Mater Form*, 8, 601-611.

Sun, S., Brandt, M., Palanisamy, S. and Dargusch, M.S. (2015). "Effect of cryogenic compressed air on the evolution of cutting force and tool wear during machining of Ti–6Al–4V alloy". *J. Mater. Process. Technol.*, 221, 243-254.

Suresh, R., Basavarajappa, S., Gaitonde, V.N. and Samuel, G.L. (2012). "Machinability investigations on hardened AISI 4340 steel using coated carbide insert". *Int. J. Refract. Met. Hard Mater.*, 33, 75-86.

- Taguchi, G. (1987). *System of experimental design: engineering methods to optimize quality and minimize costs*, UNIPUB/Kraus International Publications.
- Tang, L. and Du, Y.T. (2014). "Multi-objective optimization of green electrical discharge machining Ti-6Al-4V in tap water via Grey-Taguchi method". *Mater. Manuf. Process.*, 29 (5), 507-513.
- Thakur, D., Ramamoorthy, B. and Vijayaraghavan, L. (2008). "Influence of different post treatments on tungsten carbide-cobalt inserts". *Mater. Lett.*, 62 (28), 4403-4406.
- Thakur, D.G., Ramamoorthy, B. and Vijayaraghavan, L. (2012). "Effect of cutting parameters on the degree of work hardening and tool life during high-speed machining of Inconel 718". *Int. J. Adv. Manuf. Technol.*, 59 (5-8), 483-489.
- Thakur, D.G., Ramamoorthy, B. and Vijayaraghavan, L. (2014). "Effect of posttreatments on the performance of tungsten carbide (K20) tool while machining (turning) of Inconel 718". *The Int. J. Adv. Manuf. Technol.*, 76 (1-4), 587-596.
- Thakur, D.G., Ramamoorthy, B. and Vijayaraghavan, L. (2010). "Investigation and optimization of lubrication parameters in high speed turning of superalloy Inconel 718". *Int. J. Adv. Manuf. Technol.*, 50 (5-8), 471-478.
- Thornton, R., Slatter, T. and Ghadbeigi, H. (2013). "Effects of deep cryogenic treatment on the dry sliding wear performance of ferrous alloys". *Wear*, 305 (1-2), 177-191.
- Tiwary, A.P., Pradhan, B.B. and Bhattacharyya, B. (2014). "Study on the influence of micro-EDM process parameters during machining of Ti-6Al-4V superalloy. *Int. J. Adv. Manuf. Technol.*, 76 (1-4), 151-160.
- Tzeng, C.J., Lin, Y.H., Yang, Y.K. and Jeng, M.C. (2009). "Optimization of turning operations with multiple performance characteristics using the Taguchi method and Grey relational analysis". *J. Mater. Process. Technol.*, 209 (6), 2753-2759.



Uehara, K. and Kumagai, S. (1970). "Characteristics of tool wear in cryogenic machining". *Ann. CIRP*, 19, 273-285.

Uehara, K. and Kumagai, S. (1968). "Chip formation, surface roughness and cutting force in cryogenic machining". *Ann. CIRP*, 17 (1), 409–416.

Uehara, K. and Kumagai, S. (1969). "Mechanism of tool wear in the cryogenic machining". *J Japan Soc Precis Eng*, 35 (416), 593–599.

Umbrello, D. and Filice, L. (2009). "Improving surface integrity in orthogonal machining of hardened AISI 52100 steel by modeling white and dark layers formation". *CIRP Ann. - Manuf. Technol.*, 58 (1), 73–76.

Umbrello, D., Micari, F. and Jawahir, I.S. (2012). "The effects of cryogenic cooling on surface integrity in hard machining: A comparison with dry machining". *CIRP Ann. - Manuf. Technol.*, 61 (1), 103–106.

Venugopal, K. A., Paul, S. and Chattopadhyay, A. B. (2007a). "Growth of tool wear in turning of Ti-6Al-4V alloy under cryogenic cooling". *Wear*, 262 (9–10), 1071–1078.

Venugopal, K. A., Paul, S. and Chattopadhyay, A. B. (2007b). "Tool wear in cryogenic turning of Ti-6Al-4V alloy". *Cryogenics*, 47 (1), 12–18.

Wang, P., Zhu, Z. and Wang, Y. (2016). "A novel hybrid MCDM model combining the SAW, TOPSIS and GRA methods based on experimental design". *Inf. Sci. (Ny)*, 345, 27–45.

Wang, Z.Y. and Rajurkar, K.P. (2000). "Cryogenic machining of hard-to-cut materials". *Wear*, 239 (2), 168–175.

Wu, H.H. (2002). "A comparative study of using grey relational analysis in multiple attribute decision making problems". *Qual. Eng.*, 15 (2), 209-217.

- Xuan, F.Z., Huang, X. and Tu, S.T. (2008). "Comparisons of 30Cr2Ni4MoV rotor steel with different treatments on corrosion resistance in high temperature water". *Mater. Des.*, 29 (8), 1533–1539.
- Yap, T.C., El-Tayeb, N.S.M. and Von Brevern, P. (2013). "Cutting forces, friction coefficient and surface roughness in machining Ti-5Al-4V-0.6Mo-0.4Fe using carbide tool K313 under low pressure liquid nitrogen". *J. Brazilian Soc. Mech. Sci. Eng.*, 35 (1), 11–15.
- Yildiz, Y. and Nalbant, M. (2008). "A review of cryogenic cooling in machining processes". *Int. J. Mach. Tools Manuf.*, 48 (9), 947–964.
- Yuvaraj, N. and Pradeep Kumar, M. (2015). "Multiresponse optimization of abrasive water jet cutting process parameters using TOPSIS approach". *Mater. Manuf. Process.*, 30 (7), 882-889.
- Zhang, S., Li, J.F. and Wang, Y.W. (2012). "Tool life and cutting forces in end milling Inconel 718 under dry and minimum quantity cooling lubrication cutting conditions". *J. Clean. Prod.*, 32, 81–87.
- Zhao, H., Barber, G.C. and Zou, Q. (2002). "A study of flank wear in orthogonal cutting with internal cooling". *Wear*, 253 (9), 957-962.

**LIST OF PUBLICATIONS BASED ON PHD RESEARCH WORK**

<b>S. No.</b>	<b>Title of the paper</b>	<b>Authors</b>	<b>Name of the Journal/ Conference/ Symposium, Vol., No., Pages</b>	<b>Month &amp; Year of Publication</b>	<b>Category *</b>
1	Influence of cryogenic coolant on turning performance characteristics: A comparison with wet machining	<b>P. Sivaiah,</b> D. Chakradhar	Materials and Manufacturing Processes, <a href="http://dx.doi.org/10.1080/10426914.2016.1269920">http://dx.doi.org/10.1080/10426914.2016.1269920</a>	January, 2017	1
2	Experimental investigation on feasibility of cryogenic, MQL, wet and dry machining environments in turning of 17-4 PH stainless steel	<b>P. Sivaiah,</b> D. Chakradhar	Materials and Manufacturing Processes, <a href="http://dx.doi.org/10.1080/10426914.2017.1339317">http://dx.doi.org/10.1080/10426914.2017.1339317</a>	May, 2017	1
3	Comparative evaluations of machining performance during turning of 17-4 PH stainless steel under cryogenic and wet machining conditions	<b>P. Sivaiah,</b> D. Chakradhar	Machining Science and Technology. <a href="http://dx.doi.org/10.1080/10910344.2017.1337129">http://dx.doi.org/10.1080/10910344.2017.1337129</a> (Accepted)	----	1
4	Multi objective optimization of cryogenic turning process using Taguchi based grey relational analysis	<b>P. Sivaiah,</b> D. Chakradhar	International Journal of Machining and Machinability of Materials (Accepted)	----	1
5	Multi performance characteristics optimization in cryogenic turning of 17-4 PH stainless steel using Taguchi coupled grey relational analysis	<b>P. Sivaiah,</b> D. Chakradhar	Advances in Materials and Processing Technologies (Under review)	----	1

NATIONAL INSTITUTE OF TECHNOLOGY KARNATAKA, SURATHKAL

6	Performance investigation during machining of 17-4 ph stainless steel using different sustainable machining techniques	<b>P. Sivaiah,</b> D. Chakradhar	Machining Science and Technology (Under review)	----	1
7	Effect of cryogenic coolant on turning performance characteristics during machining of 17-4 PH stainless steel: A comparison with MQL, wet, dry machining	<b>P. Sivaiah,</b> D. Chakradhar	International Journal of Machining and Machinability of Materials (Under review)	----	1
8	Performance improvement of green manufacturing process using Taguchi integrated grey relational analysis	<b>P. Sivaiah,</b> D. Chakradhar	Arabian Journal for Science and Engineering (Under review)	----	1
9	Modeling and optimization of sustainable manufacturing process in machining of 17-4 PH stainless steel	<b>P. Sivaiah,</b> D. Chakradhar	Measurement (Under review)	----	1
10	Multi objective optimization of sustainable turning process using TOPSIS method	<b>P. Sivaiah,</b> D. Chakradhar	Emerging Materials Research (Under review)	----	1

\* Category: 1 : Journal paper, full paper reviewed  
 2 : Journal paper, Abstract reviewed  
 3 : Conference/Symposium paper, full paper reviewed  
 4 : Conference/Symposium paper, abstract reviewed  
 5 : Others (including papers in Workshops, NITK Research Bulletins, Short notes etc.)  
 ( If the paper has been accepted for publication but yet to be published, the supporting documents must be attached.)

**Research Scholar**  
Name & Signature, with Date

**Research Guide**  
Name & Signature, with Date

## BIODATA

1. **Name:** Potta Sivaiah  
2. **Father's Name:** Chinna sankaraiah  
3. **Date of Birth:** 05/06/1987  
4. **Nationality:** Indian  
5. **Address:**

**Permanent Address**

S/o. Chinna sankaraiah,  
House No.6/453,  
New Boyanapalli (P&V), Rajampet (M)  
Kadapa (Dist),  
Andhra Pradesh (State)-516126, India.

**Present Address**

Department of Mechanical Engineering,  
National Institute of Technology Karnataka,  
Surathkal-575025, Srinivasanagar,  
Dhakshina Kannada (Dist),  
Karnataka, India.

6. **Mobile Number:** +91-77353668949, +91-8147951043.  
7. **E-mail id.:** sivaiah.337@gmail.com, sivaiah.me14f21@nitk.edu.in

**8. Educational Qualification:**

Qualification	University/Board	Year of Passing	Percentage
Ph.D. (Mechanical Engineering)	National Institute of Technology Karnataka, Surathkal, India	Pursuing	-----
M. Tech (Production Engineering)	Sri Venkateswara University, Tirupathi, India.	2011	80 %
B. Tech (Mechanical Engineering)	JNTU Hyderabad, India	2008	74.86 %
Intermediate (12 <sup>th</sup> )	Board of Intermediate Education, A.P, India	2004	77.50 %
Secondary School Education (10 <sup>th</sup> )	Board of Secondary Education, A.P, India	2002	79.85 %

I declare that the above information is true and correct to best of my knowledge.

*(Potta Sivaiah)*